"Model-based multi-scale performance assessment and experimental validation of different states of lithium ion based e-mobility batteries under different operating condition"

A thesis submitted to the

UPES

For the award of

Doctor of Philosophy

in

Engineering

By

Kaushik Das

SUPERVISOR

Dr. Roushan Kumar

May 2024

UPES
UNIVERSITY OF TOMORROW

Research and Development

School of Advanced Engineering

UPES, Dehradun-248007, Uttarakhand, India

"Model-based multi-scale performance assessment and experimental validation of different states of lithium ion based e-mobility batteries under different operating condition"

A thesis submitted to the

UPES

For the award of

Doctor of Philosophy

in

Engineering

By

Kaushik Das

SAP ID: 500080551

May 2024

SUPERVISOR

Dr. Roushan Kumar

Sr. Associate Professor

Mechanical Cluster (Mechanical & Aerospace Engineering), UPES

Mechanical Cluster

School of Advanced Engineering

UPES, Dehradun-248007, Uttarakhand, India

DECLARATION

I declare that the thesis entitled **"Model-based multi-scale performance assessment and experimental validation of different states of lithium ion based e-mobility batteries under different operating condition"** has been prepared by me under the guidance of Dr. Roushan Kumar, Sr. Associate Professor, School of Advanced Engineering, UPES, Dehradun. No part of this thesis has formed the basis for the award of any degree or fellowship previously.

Kaushik Das

School of Engineering

UPES, Dehradun-248007

Uttarakhand, India

CERTIFICATE

I confirm that Kaushik Das has completed his thesis titled "**Model-based Multi-Scale Performance Assessment and Experimental Validation of Different States of Lithium-Ion-Based E-Mobility Batteries Under Various Operating Conditions**" under my supervision for the fulfilment of the Ph.D. degree at UPES. The research was conducted at the Electrical and Mechanical Cluster, School of Advanced Engineering, UPES, Dehradun, India.

I can confidently affirm that Mr. Das's thesis represents a significant contribution to the field of e-mobility batteries. His comprehensive examination of different states of lithium-ion-based batteries under varying operating conditions is both innovative and methodologically sound. In conclusion, I wholeheartedly endorse Kaushik Das's eligibility for the Ph.D. degree from UPES, recognizing his exemplary research efforts and scholarly achievements in advancing our understanding of e-mobility battery performance.

Supervisor

Dr. Roushan Kumar

Sr. Associate Professor

Mechanical Cluster (Mechanical & Aerospace Engg.)

School of Advanced Engineering

UPES, Dehradun- 248007 Uttarakhand, India

Date: 06/09/2024

ABSTRACT

Effectual understanding of lithium-ion cell and battery pack (LIB) level performance assessment and capacity degradation mechanism is essential for development of fossil free mobility segment in future. LIBs, being a thermo- electro- mechanical device undergoes several performance degradation mechanisms, which are still not fully understood and decoded. Methodologies based on machine learning (ML) is fast gaining popularities but still a lot of work is needed. As the degradation is due to electrochemical main and side reactions, causing component level decay, only physics based or ML based modeling is not sufficient, as they are complementary to each other's but have their own challenges and limitations. Hybridization of ML with physics-based methodologies are current flavor and only limited work has been carried out.

Several important internal & external factors influence the design of LIBs suitable for e-mobility applications, which are unique and widely differentiated from stationery applications. The complex interaction of cell to design of battery, design of vehicle, operational and environmental aspects play an active role than interplay of electrochemistry of various components of cell like chemical composition of electrodes and electrolyte, size & distributions of active material particles, thickness of electrodes, porosity of the electrodes, foam factor, cell dimensions, tab placement etc.

This dissertation explores from identifying cell electro chemistries suitable for different types of widely used e mobility applications, namely e-2V and e-3V, which uses 1-5KWh battery packs predominantly made with NMC cylindrical cells for e-2V and LFP prismatic cells for e-3V applications along with basic to semi smart battery management system, which also estimates state of charge (SOC) and state of health (SOH), which are two intertwined characteristics of the states of LIBs. The survey also revealed that SOC & SOH are mostly done through high error open circuit voltage or Coulomb count method. A thorough review of available research also revealed that the majority of the experimental studies are either done on cell level or under a narrow band of environmental or operational conditions.

With identified gaps, this study is further divided into two parts; in the first part, capacity degradation of NMC cells are experimentally derived under distinguished environmental (15℃,

25℃, 35℃) and operational conditions (1C & 2C discharge rate) and results are derived for both charging and discharging capacity with 0-100% SOC. Full capacity degradation is used as input feature for SOC estimation using multiple ML algorithms, namely, , Decision trees (DT), K-Nearest Neighbor (KNN), Random forest (RF) are employed for estimating multiple error metrics, namely, Mean Absolute Error (MAE), Mean Squared Error (MSE), Root Mean Squared Error (RMSE) and Mean Absolute Percentage Error (MAPE). The results obtained outclasses several other ML methods under wide spectrum of environmental and operational conditions.

In the second part, a battery pack (4.4kWh) with LFP prismatic cell is made for experimental analysis. A thorough analysis has been carried out on its capacity- open circuit voltage variance and a novel and executable methodology is proposed on making battery pack by way of cell capacity and voltage making over full discharge voltage profile, highlighting the complexity of LFP cell's knee- plateau- elbow region analysis. The battery pack was made successfully tested for several charge- discharge cycles and SOC estimation was carried out using full voltage profile with Linear Regression (LR) algorithm. The error metrics of the battery pack are not in confirmatory to the results of cell, which is a clear indication that performance assessment methodology via cell is not a robust method and that; battery pack level performance assessment is a necessity.

The scientific innovation of this paper is to introduce an optimized ML technique for SOC and SOH evaluation towards the advancement of sustainable EV technologies, which shall have huge attention for their enhanced learning capability, generalization performance, convergence speed, and high accuracy, hence it can be ideal to address the complex and nonlinear characteristics of LIBs, which shall have a proper combination of ML algorithm and optimization technique not only resolves the computational complexity of ML algorithms but also achieves excellent solutions.

The proposed ML-based state estimation methods are validated by multiple experiments under different operational and environmental conditions in order to prove the adaptability and generalization capability. In addition, the accuracy and robustness of the KNN and DT model are further verified with similar results reported by researchers. The proposed method is suitable for online BMS since the execution of state estimations in real-time is easy, effective, and fast due to low mathematical complications in the testing and training stage.

Acknowledgment

I extend my heartfelt gratitude to the Almighty for blessing me with the opportunity to embark on this enriching academic journey.

Foremost, I am deeply indebted to my supervisor, Dr. Roushan Kumar, for his unwavering guidance, insightful criticism, and invaluable suggestions which have immensely contributed to the advancement of my research. His continuous support has been instrumental in shaping my academic endeavors.

I am also grateful to the vice chancellor Dr. Ram Sharam, cluster head Dr. Piyush Kuchhal and Dr. Asish Karn, faculty members, staff, and fellow students at the UPES Dehradun who generously extended their assistance and expertise, thereby enriching my academic experience.

Lastly, I express my profound appreciation to my beloved family members, Subrata, Sipra, Paushali, Sangita, Anurup, and Shreyaa. Their boundless love, unwavering encouragement, and unwavering support have been the cornerstone of my journey. Without their steadfast belief in me, this accomplishment would not have been possible. I am forever grateful for their unwavering support and encouragement.

Kaushik Das

TABLE OF CONTENTS

LIST OF FIGURES

LIST OF TABLES

LIST OF ABBREVIATION

ACRONYM **DEFINITION**

A	Ampere
Ah	Ampere-hours
AI	Artificial intelligence
BMS	Battery management systems
BOL	Beginning of life
CC-CV	Constant current- constant voltage
CCT	Continuous charge test
CDT	Continuous discharge test
CE	Coulombic efficiency
DT	Decision trees
°C	Degree centigrade
DOD	Depth of discharge
EVs	Electric vehicles
EOL	End of life
EFC	Equivalent full cycles
FOM	Figures of merit
ICE	Internal combustion engines
KNN	K-nearest neighbor
LR	Linear regression
Li+	Lithium ion
LFP	Lithium iron phosphate
NMC	Lithium nickel manganese cobalt oxide
LIBs	Lithium-ion batteries
ML	Machine learning

MAE	Mean absolute error
MAPE	Mean absolute percentage error
MSE	Mean square error
NCA	Nickel cobalt aluminum oxide
C	Nominal capacity
OCV	Open circuit voltage
RF	Random forests
RPT	Reference performance test
RUL	Remaining useful life
RMSE	Root mean square error
SEI	Solid electrolyte interphase
SOC	State of charge
SOH	State of health
SVR	Support vector regression
TC	Test case
V	Voltage
Wh	Watt-hours

CHAPTER 1

INTRODUCTION

1.1   CHAPTER OVERVIEW

The chapter overview outlines the structure of the document, beginning with a foundational exploration in the background section, which provides context and introduces the topic of electrochemical energy storage systems with and particular emphasis on lithium-ion batteries (LIB) and their applications in e-mobility. The electrochemical energy storage system section delves into the fundamental principles and mechanisms underlying such systems, laying the groundwork for further discussion. Subsequently, the document shifts focus to the use of LIB in electric mobility, examining their current usage and impact in the transportation industry. Moving forward, the lithium-ion batteries figure of merits section explores the various performance metrics and characteristics that are crucial for evaluating their effectiveness. The research objectives section outlines the specific goals and aims of the study providing insight into the intended contributions of the research. Finally, the chapter summary succinctly summarizes the key findings and conclusions discussed in the preceding sections, offering a comprehensive overview of the chapter.

1.2   BACKGROUND

In the contemporary world, marked by a burgeoning global population and an unprecedented surge in technological advancement, the insatiable appetite for energy remains far from satiated. To quench this unyielding thirst for energy, humanity continues to deplete our finite natural resources. A staggering statistic reveals that 70.45% of the world's energy generation still hinges on the combustion

of fossil fuels and nuclear [1] , as graphically depicted in Fig. 1.1. While numerous alternatives have been tabled to address our present and future energy requirements, only a select few can truly rival fossil fuels in terms of both cost-efficiency and energy density [2]. The dual nature of efficiency improvements asserts that while innovation is crucial for reducing energy usage and improves greenhouse gas productions, the situation paradoxically tends to enable the growth and heightened resource consumption within civilization, at the same time, it challenges the conventional view linking global population growth directly to increased energy consumption, suggesting that population expansion could be a consequence of past efficiency gains, making it more feasible for societies to support larger populations [3]. Notwithstanding the substantial allocation towards clean energy, with investments surpassing 70%, amounting to $1740 billion as opposed to $1050 billion in fossil fuel during 2023, the global consumption of primary energy continues to exhibit an upward trajectory. The domain of renewables, particularly spearheaded by solar energy, which attracted investments totaling $659 billion, along with EVs securing $129 billion in investments during the same period, are at the forefront of propelling the anticipated augmentation in clean energy funding in the forthcoming years. The momentum behind investments in clean energy emanates from a synergistic array of drivers, encompassing economic feasibility, ambitions pertaining to climate change mitigation and energy sovereignty, as well as blueprints for industrial advancement.
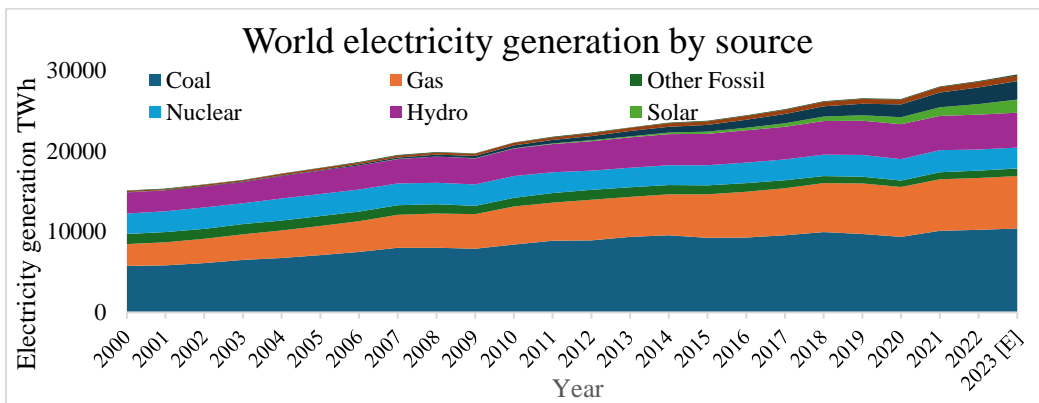
Fig. 1.1   Global electricity generation by source.

This predicament catapults humanity into the midst of an urgent challenge: climate change, an outcome of the insidious "greenhouse effect" triggered by the widespread emission of CO_2, primarily, and other greenhouse gases into our atmosphere. Climate change has evolved into a worldwide menace, demanding a comprehensive international initiative to address it. According to datasets presenting global monthly mean surface temperature from Berkeley Earth [4], the alarming conditions have already manifested as shown below in Fig. 1.2, and despite numerous endeavors, the situation remains elusive to control.
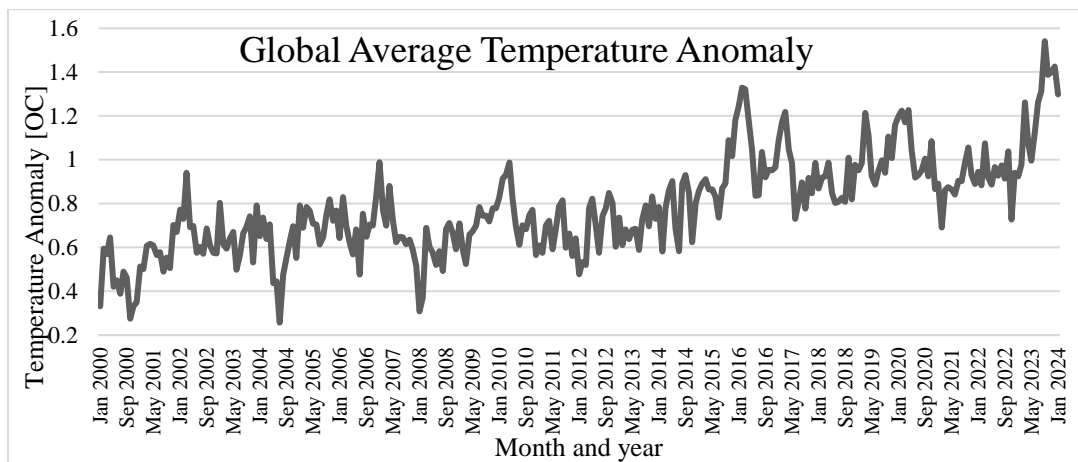
Fig. 1.2   Raw land-surface average results through the Berkeley averaging method.

It is within this context that the Paris Climate Agreement was conceived, representing a collective pledge to combat global warming. This historic accord unites the most influential countries worldwide, which also happen to be the foremost energy consumers, in a concerted mission to curtail the emission of "greenhouse gases". Global warming caused by human activity has increased by about 1.0 °C cover pre-industrial levels, most likely within a range of 0.8 to 1.2 °C. Between 2030 and 2052, global warming is forecasted to touch 1.5 °C if the current rate continues [5]. In different scenarios, the projected global warming under different initiatives based on pledges and current policies are as below and at alarming conditions as shown below in Fig. 1.3.
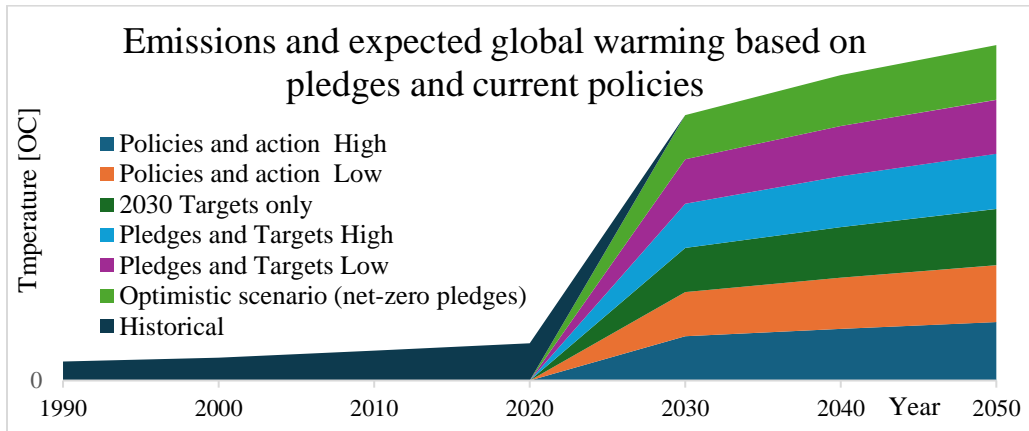
Fig. 1.3   Year 2050 Warming Projections: Emissions and expected warming.

Lithium-ion based e-mobilities are increasingly recognized as a pivotal solution to combat global warming and address climate change. The performance of e-mobilities is intricately linked to the characteristics of their energy storage systems, which exert a significant influence on both e-mobilities safety and consumer acceptance [6],[7]. In the current landscape, the LIBs industry stands as the dominant force meeting the energy storage demands of e-mobilities. However, the longevity and efficiency within lithium-ion batteries components are vital for sustaining optimal performance. Over time, degradation of these parts contribute to a decline in performance, resulting in loss of rated capacity due to an increase in internal impedance. This intricate process is influenced by a myriad of interconnected factors such as stress, temperature, chemical factor [8]. Understanding and addressing these factors is imperative for mitigating performance degradation, ensuring the sustained efficiency of LIB, and consequently, improving the overall performance and viability of e-mobilities.

To effectively implement the action plan, it is imperative that various sectors outlined in Fig. 1.4 as shown below instigate the necessary transformations. At the same time, the growth in emissions by different sectors revealed that the electricity and heat, transport sectors are the largest contributors. Within these sectors, the transportation industry stands out as a significant contributor to greenhouse gas emissions, primarily due to its continued reliance on conventional vehicles powered

by fossil fuels, which often present notable advantages when compared to more environmentally friendly alternatives.
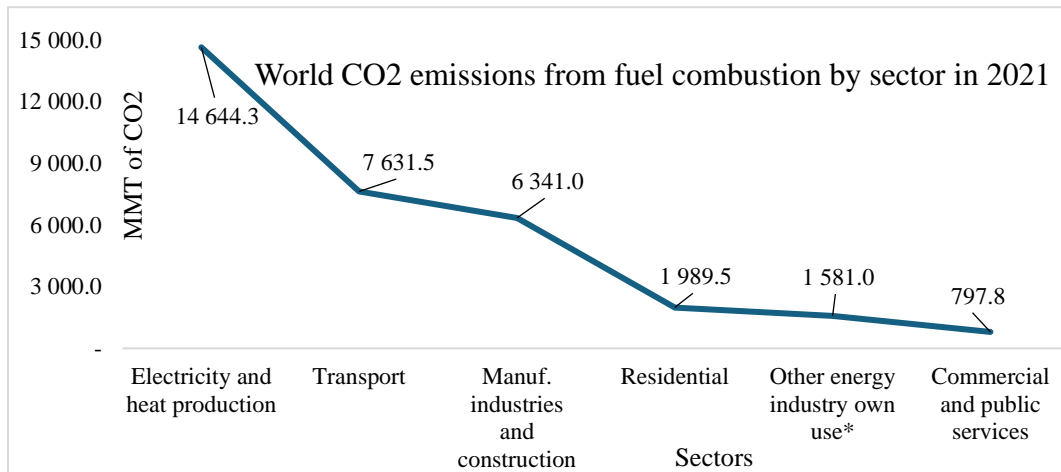
Fig. 1.4   Greenhouse gas emissions by different sectors.

During the past decade, e-mobility has emerged as a considerably more sustainable solution for surface transportation [9], significantly contributing to the reduction of our reliance on fossil fuels. While the automotive sector's shift away from internal combustion engine vehicles is well underway, it is important to acknowledge the existing challenges and barriers that need to be addressed to achieve our sustainability goals. The imperative to advance the electrification of transportation as shown in Fig. 1.5, bolster centralized and decentralized energy storage, and harness the dynamic strides in emerging technologies has never been more crucial.
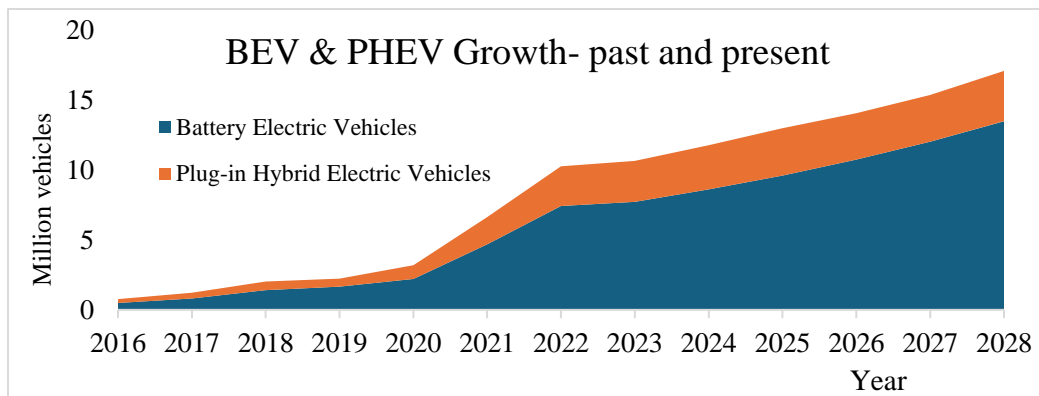
Fig. 1.5   Growth of e-mobility from 2016 till 2028.

This urgency is a direct response to the escalating levels of carbon emissions and the pressing need to address the resulting climate change and energy shortages. Electric mobility emits the least CO_2, boasts the lowest maintenance expenses is ideal for higher adaptation of renewable energy sources, and has achieved significantly favorable total cost of ownership and the adaptation by leading countries and their advantages. Within this context, the significance of developing electrochemical energy storage systems that are emissions-free and the concurrent need for meticulous performance monitoring and optimization cannot be overstated. Among the array of energy storage solutions, LIBs unequivocally emerge as a standout choice [10]. Their prominence derives from a constellation of remarkable attributes, including exceptionally good energy & power densities, a commendably low self-discharge, and a significantly extended operational lifespan. These exceptional qualities have not only facilitated the widespread proliferation of portable electronic devices but have also catalyzed the remarkable growth observed in the e-mobility market [11].

It becomes evident that the automotive industry is embracing the transition towards e-mobility. 14% of all new cars sold in 2022 were electric, 9% in 2021 and 5% in 2020, but till now e-mobility comprises only a minute fraction, around 1% or even less, of the global vehicle fleet. However, there are optimistic expectations that this figure will surge to approximately 31% by the year 2040. This signifies a significant transformation in the composition of the global vehicle fleet, reflecting the growing acceptance and adoption of e-mobility [12]. The advantages of e-mobility are several as it is energy efficient, environmentally friendly, has performance benefits, and reduces conventional energy dependencies. To meet the expectations, significant research attention from the scientific community in recent years has arisen for addressing concerns related to vehicles and especially towards LIB trustworthiness, safety, prognostics, and diagnostics in e-mobility and its charging infrastructure [13].

Pure e-mobility was first demonstrated in 1828 and showed a clear advantage over competing steam and petroleum-powered vehicles, making them the earliest technology to demonstrate such an advantage [14]. However, until 1980 petroleum-powered vehicles dominated the market, and e-mobility was grossly ignored [15]. The last few decades have brought e-mobility into focus because of several opportunities and developments [16],[17]. From a requirement of 550 GWh in e-mobility LIB requirement in 2022 [18], it is expected to reach over 900 GWh in 2023. LIB consumes 65% of total global lithium production and demand is expected to soar to 188,000 MT by 2027. Among all vehicles, hardly 20% of all 2 and 3-wheelers (which is 90% of the total vehicular population) are electric, which contributes to significant vehicular pollution [19],[20]. With the maturity in application and learning across different aspects, the demand from different perspectives has multi-folded [21]. From a consumer perspective, the classifications are different and are centered around uses for long-distance travel, mass transportation, performance vehicles, etc. [22]. From different points of view, the e-mobility ecosystem is categorized differently, but in meeting those expectations, serious techno-commercial objectives are to be achieved in a very short period [23].

As highlighted by United Nations and World Economic Forum's publications [24] the rapid urbanization of cities shall add over 2.5 billion by 2050 and crucial role of e-mobility in reducing carbon emissions, and the integration of cutting-edge technologies in energy systems collectively underpin the assertion that these developments are integral to the Fourth Industrial Revolution [25]. The multi-objective oriented approach for the development of e-mobility batteries is centered on different aspects of cell and pack performance [26], [27], life, reliability, safety enhancement [28], futuristic BMS with cloud computing, better and precision estimation, connected etc., BOS meeting requirement of high current/ high voltage applications [29],[30] and other safety feature [31]. LIBs are true water-free batteries, and work on rocking chair mechanisms [32],[33] at present are 100 times

less than different petroleum-based fuels on different energy and power criteria [34],[35] as shown in Fig.1.6.
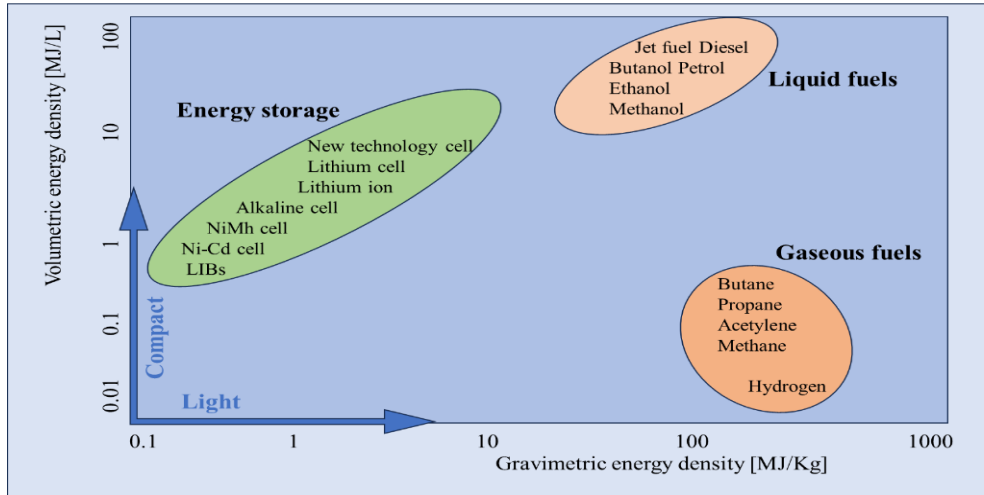
Fig. 1.6   Comparison of volumetric and gravimetric energy density of different fuels with batteries.

The future requirements from e-mobility and possibilities with LIB are to bring interesting features like hybridization [36],[37], high speed-high power-high capacity [38], integration of EV with grid [39], wireless charging, smart charging for a reliable and resilient grid, demand-charge mitigation via stationary storage [40], automated EV in ride-hailing fleets [41], charging technology validation and demonstration, managed charging by building loads or with multiple commercial buildings [42],[43], behind-the-meter energy storage [44],[45], wireless charging [46],[47], performing predictive analysis [48],[49], security and privacy threats associated with the e-mobility ecosystem [50]. Numerous researchers and engineers are working on component-level enhancement for low-temperature and high-temperature application-oriented cathode, anode, electrolyte, separators, and multiple combinations with and without the help of artificial intelligence and coming up with novel cell chemistry [51]. At the same time, different national and international organizations had set ambitious targets for achieving petroleum performance parity within the next decade [52].
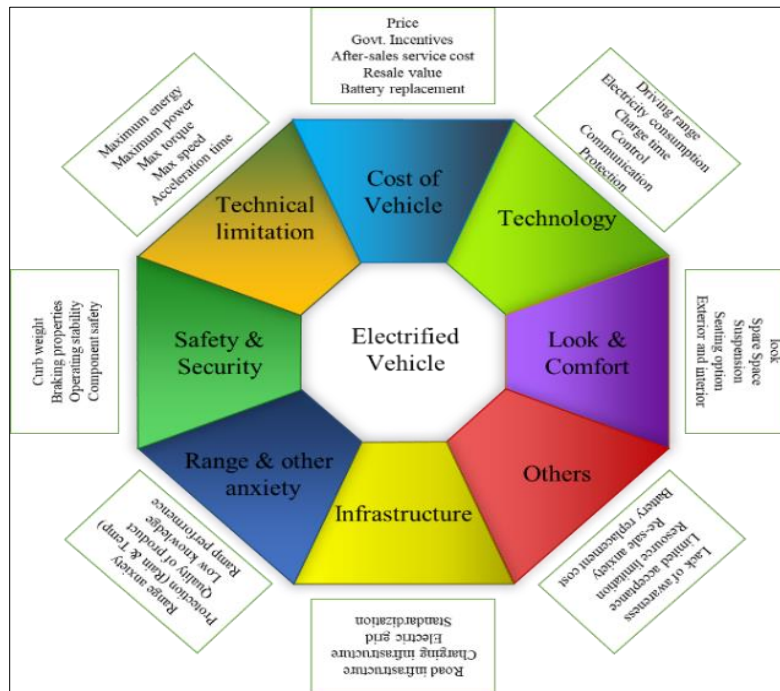
Fig. 1.7   Perception towards EV & impact on consumers' preference.

As the use of LIB continues to expand at an unprecedented rate, it is anticipated that the cost of batteries will drop to below $100 per kilowatt-hour very shortly, under different perspectives on technological learning, expert elicitation, etc. E-mobility will be economically competitive with internal combustion engine (ICE) alternatives because of the predicted cost decrease. The transition from an electromechanically heavy to an information-intensive vehicle is another benefit of e-mobility. It provides an essentially blank canvas on which to quickly design safe, software-defined vehicles, with computing and related electronics serving as the primary enablers of these vehicles' features, functions, and value. The software, which has LIB at its core, also makes it possible to decouple the internal mechanical connections required in an ICE car, enabling remote or autonomous operation of e-mobility [53].

Policymakers promoting the shift to e-mobility are underestimating how messy, expensive, and time-consuming it will be and it is represented in Fig. 1.7. It clearly explains the general perception towards it and influences buyer's preferences. The

shift to e-mobility is a complicated web of technological innovation, uncertainty, and complexity mixed with equal parts of hope and dysfunction in policymaking [54]. Buyer expectations are fairly resigned to the significant disruptions that will unavoidably transpire over the next several years and decades.

1.3   ELECTROCHEMICAL ENERGY STORAGE SYSTEM

The energy ecosystem relies on three fundamental components: generation, transmission, and distribution, followed by consumption. A fourth essential pillar is emerging in the form of energy storage. As energy generation resources shift from centralized systems to a more distributed setup, the critical demand for electrical energy storage across various applications is becoming increasingly pronounced [55]. The growing imperatives for optimizing the amount of energy generated and its effective utilization underscore the necessity for energy storage solutions. Energy can be stored in various forms, but major types of energy storage can be categorized as shown in Fig. 1.8.
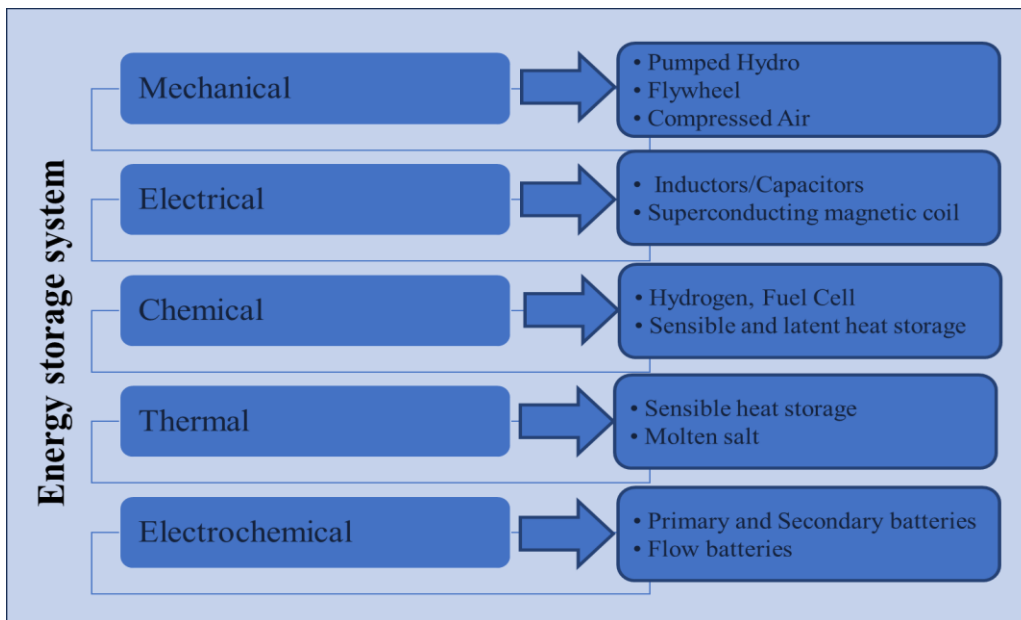
Fig. 1.8   Different types of energy storage systems.

Storage systems harness the power of reversible chemical reactions to store electrical energy in the guise of chemical potential. Batteries stand as the

predominant example of electrochemical storage, finding utility across a wide array of applications within power systems. Diverse battery chemistries exist, each showcasing unique performance characteristics, setting them apart from one another. Over time, the field of electrochemical energy conversion technology has undergone significant advancements. The primary focus now revolves around addressing the challenges related to effectively integrating these electrochemical energy storage systems into emerging application domains of the modern era [56]. Despite being invented in the 19th century, even before the advent of grid electricity, lead-acid batteries are still widely utilized across various applications, such as stationary energy storage systems and automotive starter batteries, due to their reliability, cost-effectiveness, and well-established manufacturing infrastructure. Those earliest batteries were charged by applying a reverse current through the battery, a process that involves forcing electrical energy into the battery to reverse the chemical reactions that occurred during discharge. This reverse current was typically provided by a DC power source, such as a hand-cranked generator, dynamo, or another battery. However low energy and power densities with lesser cyclic life, the need for better batteries has arisen in the last two decades because of the development of various telecommunication, space, military, portable electronics, etc. LIB, since its invention in 1980 and commercialization in 1990, then we have witnessed large increases in energy & power density and huge reductions in the cost of production [57],[58]. These advances have brought EVs to the center of plans of vehicle manufacturers and created a boom in LIB manufacturing. To further advance these technologies, and properly manage them, there is a clear need to develop our quantitative and qualitative understanding of LIB.

In general, a battery is an array of similar cells, either connected in series, parallel, or both, and in reality; these modules of cell (or battery) are in true use as in its elementary form, because of its low energy and power densities and in reality several cells (in series-parallel combination) with a battery management system,

connectors, wires and cables, holders, packing, etc. are housed in a casing of suitable size, making batteries, as physio -electro- chemical- mechanical device of suitable voltage and ampere- hours. The most popular commercially available LIB comes in the four foam factors: coil cell, pouch cell, prismatic cell, and cylindrical cell [59]. Cell design can be approached in multi-directional ways and can be built into different simulation models to accomplish its behavioral theme for chemical, electrical, or hybrid points of view with or without temperature or other mechanical stresses. Applying a probabilistic data-driven machine learning (ML) approach allows for quantification of uncertainty to support decisions in design and control more effectively, even though complex behavioral, operational, and environmental phenomena limit the value of classical deterministic modelling techniques and are a foremost tailback in design iterations.

1.4   STATUS OF LIB IN E-MOBILITY

In the year 2023, the landscape of demand within the realm of emerging EV technology witnessed a remarkable transformation. Approximately 60% of the coveted lithium resources, 30% of the sought-after cobalt reservoirs, and 10% of the precious nickel stores were fervently allocated to satiate the insatiable hunger for EV batteries. Notably, in the year of 2017, these shares were a mere fraction of their present stature, constituting a mere 15%, 10%, and 2%, respectively [60],[61]. The appetite for LIBs within the automotive sector surged dramatically in 2023, experiencing a remarkable 65% upswing, culminating in a robust demand of 550 GWh, up from the 330 GWh recorded in the previous year.
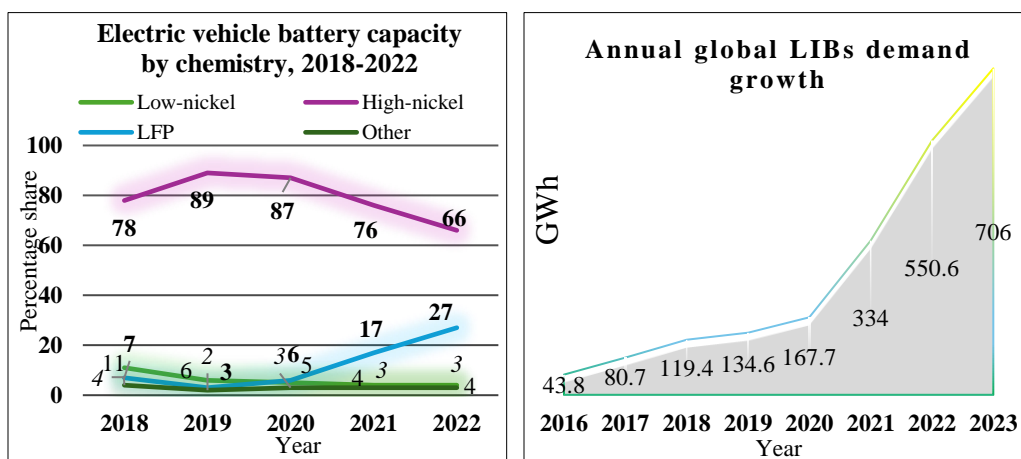
Fig. 1.9 (a) Global market share of different cell chemistry (b) Global LIBs demand growth.

This formidable expansion can be attributed predominantly to the electric passenger car segment, which witnessed a meteoric 55% surge in new registrations throughout 2022 compared to its 2021 counterpart. Lithium nickel manganese cobalt oxide (NMC) has a significant market of 60% in 2023, lithium iron phosphate (LFP) are under 30% and nickel cobalt aluminum oxide (NCA) at roughly 8%, as Fig. 1.9 (a) illustrates. In their report unveiled by the McKinsey battery insights team, a tantalizing projection unfurls as shown below Fig. 1.9 (b), foretells the luminous trajectory of the complete LIBs continuum suggests an annual growth rate exceeding 30 percent, from the year 2022 through 2030. By that time, it shall have a valuation of over $400 billion and a market of 4.7 terawatt-hours [62].

Future advancement of LIB technology relies heavily on material science advancements and the precise control of operational parameters. Understanding the multi-level degradation process is crucial for devising strategies to extend battery lifespan, enhance performance, and ensure the continued progress of this indispensable technology. State of charge and cycle bandwidth, overcharging with high voltage and current region, over-discharge and temperature (high and low) during storage and operation, internal and external short circuits in the cell, overheating on the cell and battery, and accelerated degradation are the main causes

of LIB health degradation [63]. To ensure that LIB operates dependably, safely, and for a longer period, a battery management system (BMS) is necessary because of some inherited properties and limitations. Battery data collecting, battery condition prediction and determination, charge and discharge control, safety protection, thermal management, balancing, control, and communication are just a few of the multiple processing features that an all-inclusive BMS should have [64].
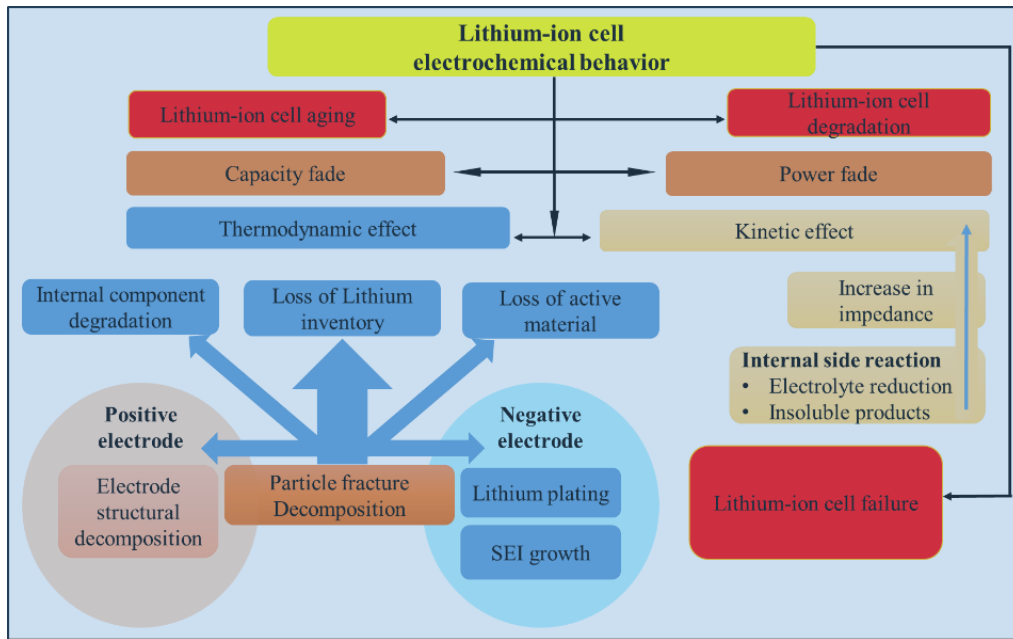
Fig. 1.10   Influence factors responsible for main and side reactions.

The various influence factors, as seen in Fig. 1.10, are ultimately in charge of capacity and power fading. These factors originate at the design stage and continue through usage, giving rise to a multitude of primary and secondary reactions within the cell. Numerous studies have been conducted in this area of academic interest: the physics of reaction modes and consequences, degradation modes, and the impacts that follow. The indirect indices, which are various dynamic states of charge, power, energy, health, remaining useful life, and temperature are crucial for recognizing and keeping an eye on the battery system, just as the measurable indices of LIB are voltage, current, internal resistance, impedance, and temperature [65]. State of charge (SOC) and state of health (SOH) are two of the most crucial

parameters and accurately determining SOH is needed to continue the service life and guaranteeing the secure and dependable operation of the system. When comparing a battery's capacity or impedance to its unused state, SOH is a metric that assesses the battery's overall health and capacity to meet performance requirements.

1.5   LIBs DIFFERENT FIGURE OF MERITS

A figure of merit (FOM) in the context of LIBs is a specific quantitative metric used to evaluate the performance or efficiency of the battery in a particular aspect and serves as a benchmark to compare different batteries or to assess how well a battery meets certain performance criteria. FOMs are routinely established to evaluate the specific suitability of materials or devices for a given application [66]. These metrics are instrumental in assessing the relative effectiveness and practicality of various options within the field of engineering applications [67]. In the context of engineering applications, particularly in the domains of e-mobility, energy storage systems, backup power, and decentralized systems, LIB is extensively employed, and this widespread usage necessitates a tailored set of FOM to address the diverse objectives associated with LIB [68],[69]. Collectively, these FOM ensure the effectiveness of energy storage systems and provide a comprehensive indication of their performance (energy/ power), lifespan, reliability, safety aspects, and more [70]. Essentially, these metrics quantify the aging and degradation processes in various components such as electrodes (anode/cathode), current collectors, separators, and other critical elements of the system [71]. The FOM used to characterize the performance of LIB varies on the specific application or use case, but some commonly used FOM for LIB include:

1. Energy density: The FOM measures the volume of energy stored with respect to the weight of the battery. Batteries with a higher energy density are preferred because they can provide longer run times for portable devices or increase the range of e-mobility [72].

2. Power density: The FOM measures the rate at which energy can be delivered from the battery. Higher power density batteries are desirable because they can provide more power for high-performance applications such as EVs or power tools [73].

3. Cycle life: The number of charge-discharge cycles the battery can withstand before its capacity declines to a predetermined level is measured by the FOM. High cycle LIB are desirable because they can last longer and require less frequent replacement [74].

4. Safety: The FOM measures the risk of the battery causing fires, explosions, or other safety hazards. Safer batteries are desirable because they can reduce the risk of accidents and increase user confidence [75],[76].

5. Cost: The FOM measures the cost of the battery per unit of energy or power. Lower-cost batteries are desirable because they can make energy storage inexpensive and welcoming to large applications [17].

6. Weight: Weight can be used as an FOM for LIBs, specifically through the specific energy or specific power metrics [77].

7. Thermal stability: Thermal stability is an important FOM for LIB because it can affect the safety, performance, and lifetime of the battery. When a LIB experiences thermal runaway, it can lead to fires or explosions, which can be dangerous and can cause property damage. Therefore, LIBs with high thermal stability are desirable because they can reduce the risk of thermal runaway and improve overall safety [78],[79].

8. Lifespan: lifespan is another commonly used FOM as it implies to length of time that the LIB be used before it dies [80].

The establishment and evaluation of these FOMs are pivotal in guiding the development and optimization of energy storage technologies for diverse applications as shown in Fig. 1.11. State is a type of information that is linked to the item it characterizes and the time context in which both the information and the object are defined [81]. State is defined as information about a thing at a certain

moment inside of a context. The complex electrochemical behavior in any specific LIB occurs singularly as well as simultaneously. The pattern of degradation, which is invariably nonlinear, is chemistry as well as foam factor specific, which results in typical behavior & recommendation to a particular application by a particular cell chemistry [82].
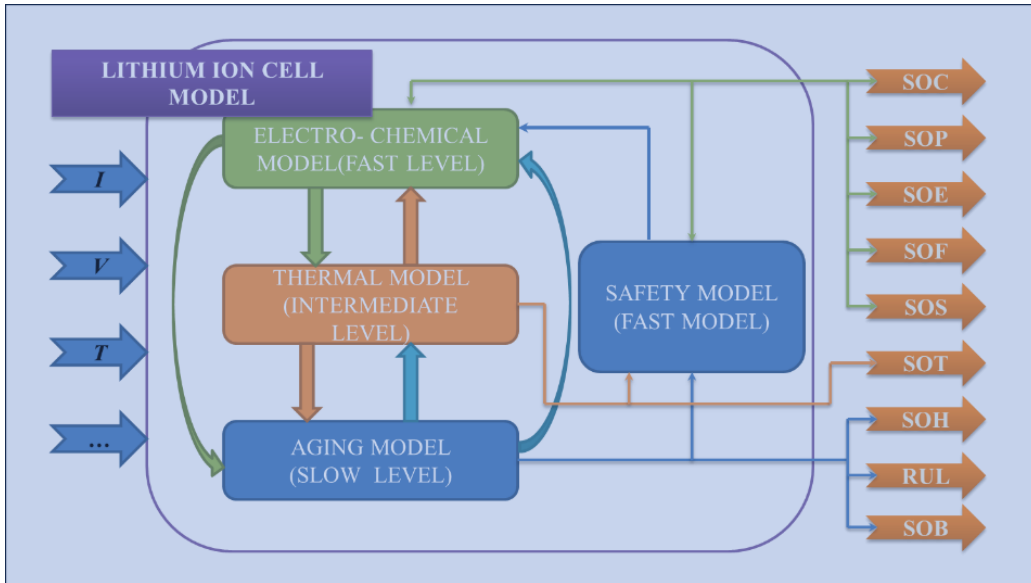
Fig. 1.11   Relationship between different models and different states of LIB.

1.6   RESEARCH OBJECTIVES

Performance assessment, state estimation, and correlating its findings with LIB in multi-scale levels of capacity deterioration on health and charge level is an intriguing research subject with practical implications in diagnostics and prognostics. At the same time, it has a complex web of implications on life, reliability, and safety aspects. The LIB is highly nonlinear, and it is problematic to precisely model, the inner states of LIB cannot be directly measured by physical sensors, and the states are easily influenced by the operational and external environment, the efficiency of the battery pack is impacted by the cell irregularities, which raises in the battery pack. Several methods from different approaches, objectives, datasets, and cell chemistries are proposed, which added confusion in

its universality in applications. From the point of data bias, interpretability, and scalability the suitability of a particular model is highly uncertain, and state monitoring point of view, advanced methods need to be applicable from size, cost, ease of implementation ability, and durability.

The focus and overall objectives are to achieve a novel, accurately developed, lower complexities, lower cost or less error and tested through experimentation of cell performance and state estimation models leading towards performance assessment for multiple applications in energy management strategies, battery sizing, and state prediction for e-mobility based LIB in real life application is based on using full charge and discharge capacity.

1.   Development of a model-based strategy for accurate different state estimation in lithium-ion batteries for e-mobility applications.

2.   Comprehensive evaluation and analysis of lithium-ion batteries state estimation methods under various operating and environmental conditions for assessment of state of health and state of charge.

3.   Development, analysis, and experimental validation of novel computational models for state estimation under different operating and environmental conditions.

1.7   CHAPTER SUMMARY

This chapter offers a comprehensive overview of the current global energy landscape, underscoring the formidable challenges arising from escalating energy demand, dependence on finite natural resources, and the escalating environmental repercussions, particularly concerning climate change. It introduces the Paris Climate Agreement as a concerted initiative to confront greenhouse gas emissions, spotlighting the pivotal role of the transportation sector particularly e-mobility in combating climate change. Emphasizing the necessity of electrochemical energy storage systems, specifically LIB, in the transition to e-mobility, this chapter explores the advancements and challenges within LIB technology. Key factors such as energy & power density, cycle index, safety, cost, weight, thermal stability, and

lifespan are discussed as essential FOM. This chapter delves into the intricate dynamics of battery degradation, highlighting the imperative for cutting-edge monitoring and estimation techniques. Key focal points include the exponential surge in e-mobility adoption, the dominance of LIB in steering this transition, the hurdles in addressing climate change, and the pivotal role of evolving LIB technology.

This thesis is composed of six chapters. The overview of each chapter is briefly described below,

• Chapter 1 "introduction" is overview of the subject research, which emphasis how energy storage is essential in modern day. This chapter also provides information on various electrochemical energy storage systems. Finally, this chapter outlines the status of LIB in e-mobility and discusses the function of different figures of merits.

• Chapter 2 "literature survey" contains an extensive review of related literatures on various aspects of capacity degradation factors of battery in e-mobility, as well as different states analysis, the scope of the research, research gap, problem definition, the research objectives. This chapter gives details of research that was conducted on various performance aspects of LIBs.

• Chapter 3 "fundamentals of lithium-ion batteries" details about the fundamental, working principles, types of lithium-ion batteries and their comparison on different aspects. Different degradation mechanisms, different states and their modeling aspects of LIBs are outlined in this chapter.

• Chapter 4 "methodology and experimental setup" represents the first step in the development of methodology and experiments related to different states, experimental setups, and cell selection protocols. The chapter also includes capacity measurement, assembly of battery packs, BMS, and cell selection.

• Chapter 5 "results and discussions" outlines the results and discussion of experiments carried out during the experimentation related to cell and battery

performance under various stresses of various temperature and at different discharging current. Results are graphically analyzed.

• Chapter 6 "conclusions and future scope" presents the conclusion of the whole research and future work are discussed.

CHAPTER 2   LITERATURE SURVEY

2.1   CHAPTER OVERVIEW

This chapter overview outlines the structure of a document or report focusing on lithium-ion batteries and related research work. The background section provides introductory information about the topic being discussed, which could include an overview of battery technology, its importance, and any relevant background information. The Capacity degradation section explores the various factors that contribute to the degradation of the capacity of LIB over time, such as cycling, temperature, overcharging, and other environmental or operational conditions. The different modeling approach section discusses different methodologies or techniques used for modeling and simulating LIB for electric vehicle applications. Different states in the LIB section elaborate on the different states or conditions that LIBs can exhibit, including parameters like SOC, SOH, SOF, SOP, SOB, SOE, SOT, and RUL. The gaps identified section covers different areas where further research is needed or where existing research may be lacking, providing direction for future studies. Finally, the chapter summary section provides a concise summary of the key points discussed in the chapter, highlighting the main findings and conclusions.

2.2   BACKGROUND

Over the last thirty years, significant strides in LIB have yielded materials capable of reversibly storing lithium-ion, encompassing anodes, cathodes, separators, electrolytes, current collectors, and mechanical casings. Despite claims of enhanced performance, increased lifespan, reliability, and safety, only a select few innovations have found commercial use. The primary hindrance is the absence of long-term indices like SOC and SOH, derived from direct performance indices

voltage, current, temperature, and resistance [83]. Traditional testing methods and field trials, crucial for validation, are hindered by their time-consuming nature and the susceptibility of LIB to operational and environmental variations. Throughout their lifespan, LIBs exhibit capacity and power fade trajectories, including super-linear fades termed knee points, rollover failures, or sudden deaths [84]. Applying machine learning to LIB is challenging due to its intricate nature and involvement of variables like performance, lifespan, safety, cost, and environmental impact. The entire battery circular economy, from mining to recycling, adds further complexity. Current research relies heavily on a material-centric trial-and-error approach, involving synthesis, manufacturing, assembly, and performance evaluation. Initiating a literature survey entails thoroughly investigating the existing body of knowledge regarding the state estimation of LIB [85]. This exploration aims to uncover the diverse methodologies, recent advancements, and existing challenges that shape the field of predicting and managing the operational state of these vital energy storage devices.

The process adopted for the literature survey is outlined and shown in Fig. 2.1. The selection of "n" in the bibliographic study is aligned with the study's scope to ensure comprehensive coverage to achieve literature saturation, prioritize quality over quantity, relevant sources that align with research objectives. From the five-year bibliographic study, only high impact factored peer previewed original research journals with high cited articles in the research field with the goal on SOC and SOH estimation through ML are considered for selection of "n".
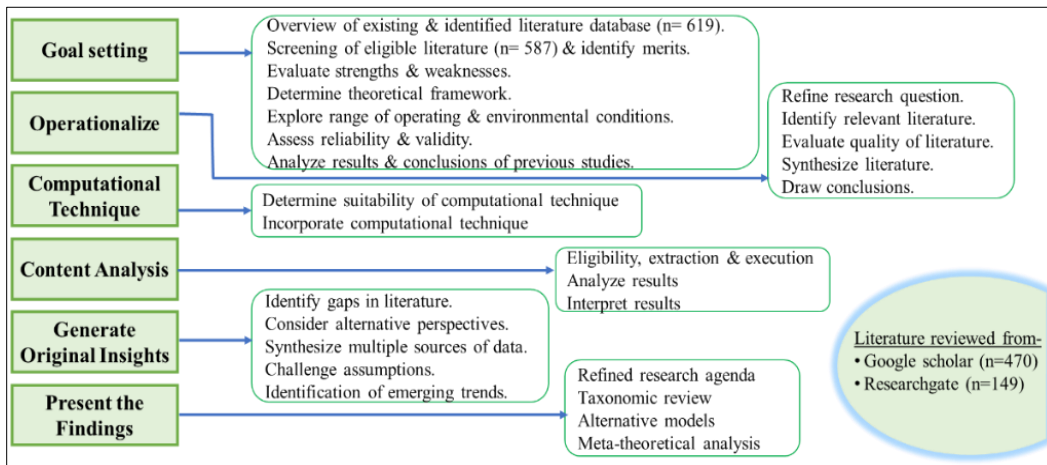
Fig. 2.1   Process of literature survey.

A bibliographic study on annual publications on keywords such as "state of charge", "state of health", "SOC", "SOH", "ML", "supervised learning" and "machine learning", in Google Scholar from 2018 till 2024 has been carried out and the outcome is as in Fig. 2.2. which displays the novelty of the subject and possibilities of future work in this direction.
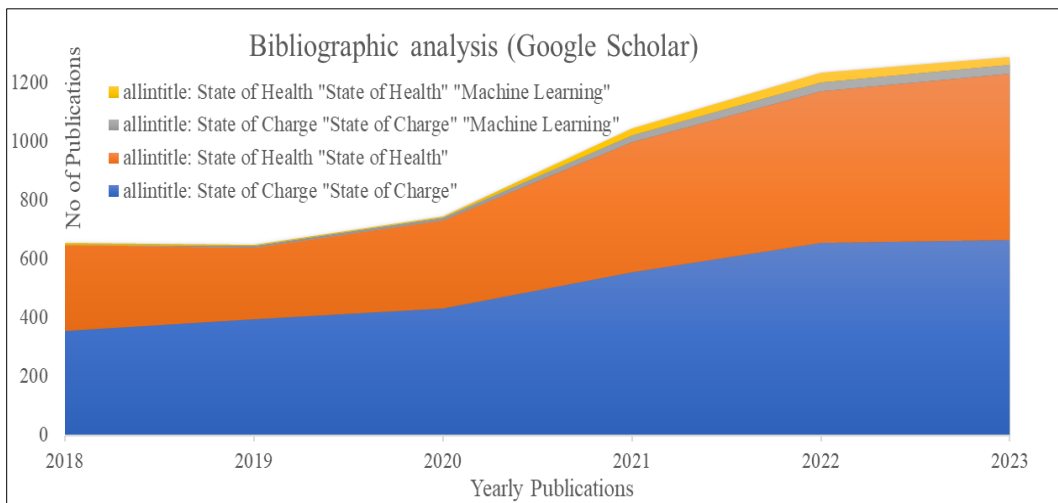
Fig. 2.2   Annual bibliographic analysis of available literature 2018- 2023.

The origins of state estimation can be arguably linked to the efforts of astronomers in the early nineteenth century, when in 1801, Gauss developed what might be considered the inaugural state estimation algorithm by employing Kepler's laws and

ordinary least squares exclusively, successfully calculated the orbit of the asteroid Ceres with precision, despite having to work with limited and noisy observations [86]. The earliest evidence of state estimation of any electrochemical devices used in e-mobility is in 1939 [87]. The pace for state estimation gathered after the invention and commercialization of LIB in 1990 because of dynamic and patio–temporal behavior with several publications on methods and methodologies researched. Over the past three decades, there has been extensive research and development on LIB, resulting in numerous materials capable of storing lithium ions reversibly, as either an anode or cathode [88]. Various components such as separators, electrolytes, current collectors, mechanical casings, and others have also been developed with claims of improved performance, life, reliability, safety, and other parameters [89]. However, despite these developments, only a few have found commercial use due to the non-availability of long-term indirect indices like SOC, SOH, etc. from direct performance indices like voltage, current, temperature, and internal resistance (IR) over time [90].

A typical electrochemical cell only stores (charges) energy and releases (discharges) it on demand and in a controlled manner. This stored energy is determined by the intrinsic properties of individual electrode materials and design characteristics. The energy content of any battery is divided into three sections namely, available energy that can instantly be retrieved, zone that can be refilled, unusable part, or rock content that becomes inactive as part of capacity degradation. In general, all cells fade over time due to some ratio of irreversible chemical reaction on storage (calendar aging) or during operation (degradation), but this fade is not linear [91]. LIBs also follow somehow similar trends but have distinct characteristics and fading parameters because of their electrochemistry, operating conditions, and application. The key stumbling block for the advancement of LIB is the unpredictability of fade and thus accurate prediction of battery states is needed to know its exact status and whether a battery is suitable to a particular application, should be replaced, and avoid unexpected life fade.

LIB capacity and power fading are cumulative effects of degradation on active components like electrodes (anode and cathode), electrolytes, or passive components like separators, current collectors, etc. Aging in LIB is a linear process of becoming older as a decline or loss of capacity and other vital characteristics with increasing age is caused by a time-progressive decline, called calendar fade. Rates of aging are non-controllable and are mostly a function of cycle count (already used status) and age, apart from storage SOC, storage temperature, etc. Degradation in LIB is the non-linear process of becoming older as a decline or loss of capacity and other vital characteristics with chemical and mechanical degradation caused by different operational and environmental conditions, maintenance, upkeeping, etc. This has to do with the various forms of mechanical, thermal, and electrochemical deterioration that cells encounter in application settings [92]. The magnitude of degradation is affected by operating and environmental elements include charge/discharge rates, electrochemical working windows, and temperatures. The degradation mechanism triggers anode and cathode degradation, inactive material degradation, and higher-order degradation. Aging and degradation occur simultaneously in any electrochemical cell or battery including LIB.

Unlike stationary applications, LIBs used in e-mobility behave differently as the industry progressively moves towards electrification. LIBs are an important component in an EV and thereby require accurate real-time supervising, monitoring, prognostics, and diagnostics to keep updated. Weather and climatic conditions like temperature, etc. are vital and play a significant role in its performance, life, and reliability. On vehicles, energy and power needs are directly related to the propulsive force $F_{Propulsion}$, which itself depends upon several factors as represented through equation 1 and propulsive power P_{Prop} through equation 2. The equation calculates the power required for propulsion, where P_{Prop} represents the propulsion power, μ is the coefficient of rolling resistance, and v is the velocity of the vehicle.

$$F_{Propulsion} = F_{rolling\ resistance} + F_{Aerodynamic\ drag} + F_{Road\ slop} + F_{Acceleration} \qquad (1)$$

$$P_{Prop} = \mu v F_{Propulsion} \qquad (2)$$

Total auxiliary power consumption, where P_{Aux} is the total auxiliary power. P_{Base} represents the base power consumption that includes the power required for essential functions of the system and $P_{Climate}$ represents the additional power consumption related to control systems and is represented through equation 3. The total power consumption is represented through equation 4 and the variability in total power is dependent on P_{Prop} and $P_{Climate}$.

$$P_{Aux} = P_{Base} + P_{Climate} \qquad (3)$$

$$P_{Total} = P_{Prop} + P_{Aux} \qquad (4)$$

LIB concerns about performance, safety, and trust ability remain major hindrances, which necessities be addressed to improve recognition of energy storage chemistry [49]. The nonlinearity and, complexity in the degradation of LIB over time scale lie at the center of this challenge [93]. Time duration of charge/ discharge, operational, and environmental conditions lead towards performance deterioration at the cell level leading to battery pack failures, which, in certain cases, can be catastrophic due to fires, because of thermal runaway.
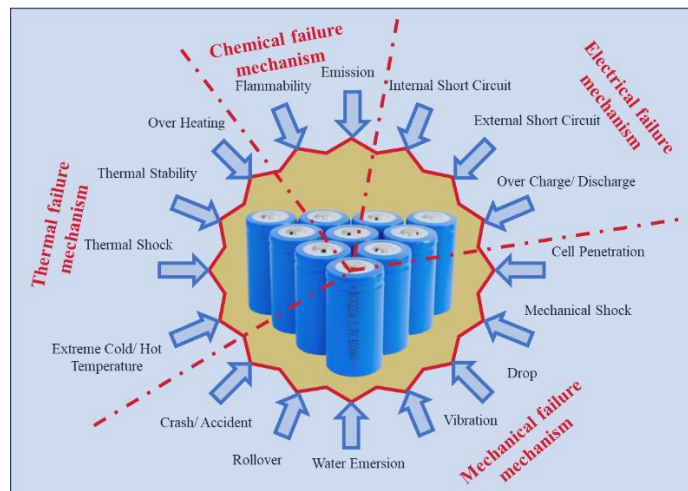
Fig. 2.3 lithium-ion battery failure mechanism.

There are four main ways to approach the process of diagnosing and detecting capacity and power degradation: boundary and movement checking on inputs and outputs is used by temporal redundancy, which use expert and knowledge-based techniques. This strategy is arguably the most popular in business today. Hardware redundancy that detects trends in capacity decline using majority vote governing logic [94]. Despite being widely used in mission-critical and safety systems, this scheme's high cost prevents it from being used in many other applications. Analytical redundancy is a model-based technique that creates software quantities known as residuals by utilizing data and the system's model. The residuals are treated for detection, isolation, estimate, and accommodation; they are sensitive to the degradation pattern. Combining many algorithms from the same or different classes results in algorithmic or hybrid redundancy [95], [96]. Cell level failures are either chemical level, electrical level, mechanical level, or thermal level failure, which solemnly occurs singularly, but in actual operation, it is always a combination of multiple factors. Understanding the interplay between this failure mechanism is crucial for designing robust and resilient systems and is outlined in Fig. 2.3.

Multiple types of faults occur inside a LIB which are classified as shown in Fig. 2.4 which leads towards ultimate failure as well as creating safety hazards. This happens alongside aging and degradation in a cell. Understanding of capacity and power degradation and failure is still very limited and more limited yet dependable and real-world models & techniques for prediction of these diverse facts. Capacity degradation and its accurate estimation & reliable fault diagnosis technique are decisive in the assurance of safety, stability, and reliable operation of LIB-based e-mobility batteries.
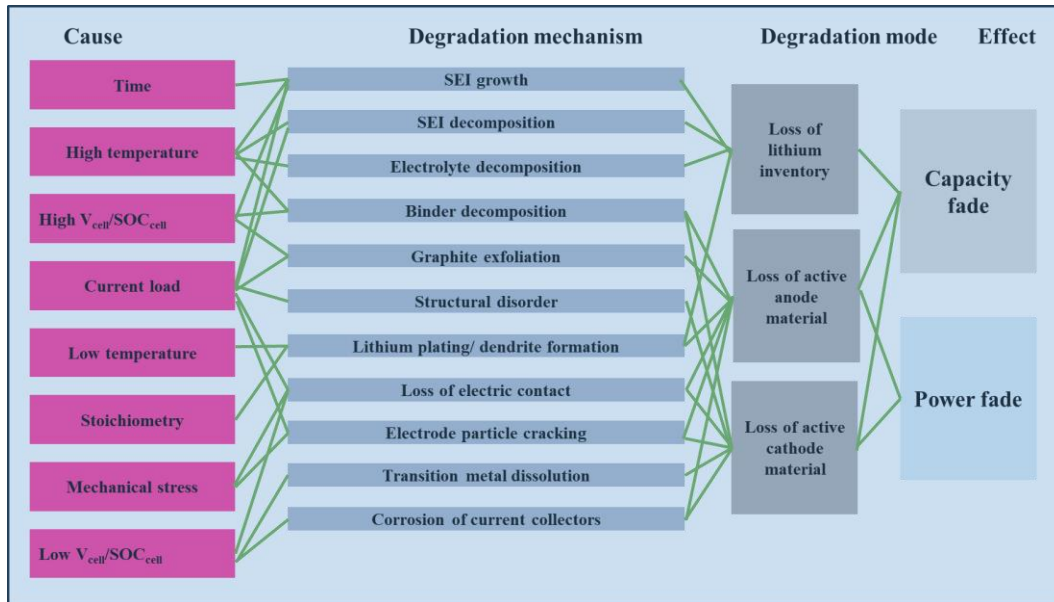
Fig. 2.4   Types of faults and their effect in LIB.

While material science takes care of enhancing energy and power densities, safety concerns, increasing life, reliability, safety concerns, and multi-disciplinary approach [97] towards decoding cells from different approaches, monitoring, estimation of various dynamic states- charge, health, function, etc. are employed for higher deployability, understanding remaining useful life, end of life prediction, and warranty prediction [98],[99]. A drawback of LIBs is that for appropriate, safe, and durable applications with optimum life, they demand persistent investigation to operate in a constricted band of voltage, temperature, and other mechanical conditions [100],[101]. The ability of LIBs to alter their mechanical values while operating is another crucial feature and it operates on a rocking chair mechanism, as proposed by Armand in the 1970 [102]. The active materials in LIB expand and contract throughout various operations, along with a portion of non-reversible physical changes that partially represent the SOH [80]. Mechanical instabilities such as plastic bend, destruction, fragmentation, and shattering are caused by this strain. These effects are closely related to the SOH or RUL since they are recognized as a primary cause of performance fading during the course of the cycle [103].

LIBs, as an electrochemical entity with multifaceted planetary of constituents (electrodes, electrolytes, binders, and separators) at the cell level and different electrical, mechanical, and electronic components at the battery pack level with large design space subjected to wide variation in operational & environmental conditions [104],[105]. Cell design parameters can be approached in multidirectional ways and can be built into different simulation models to accomplish and analyze its behavioral theme for chemical, electrical, or hybrid points of view with or without temperature or other mechanical stresses [106]. While complex behavioral, operational & environmental phenomenon restricts the value of classical deterministic modeling techniques [107],[108]. This poses a significant challenge for further design iterations, to shorten test durations and test numbers while maintaining accuracy, future state prediction is required. Applying a probabilistic data-driven machine learning approach which enables the quantification of uncertainty to inform design and control decisions more effectively. LIBs, when stored or charge-discharged, exhibit a two-phase degradation behavior characterized by first, a linear phase and second a nonlinear phase where degradation is comparatively rapid [109]. The multitude of degradation phenomena occurring in LIB complicates the understanding of the two-phase degradation pattern.

2.3   CAPACITY DEGRADATION FACTORS

LIB's capacity degradation is dominated by different mechanisms during each phase in its lifetime. LIB in operation are characterized by two phenomena: thermodynamics (equilibrium) and kinetics (non-equilibrium) [110]. The primary cause of capacity degradation is exothermic chemical processes, which also result in the loss of active material. The ineffective byproducts that are produced obstruct the current migration pathways, raise internal resistance, and reduce power capabilities. Numerous factors influence the degradation, both at the level of individual cells and the battery, and their effects are frequently connected [111].

Although the factors that cause degradation at the single cell level are both thermodynamic and kinetic, the environment (such as temperature, pressure, or mechanical effect) and the duty cycle (such as voltage and current intensity) have an effect on properties of the cell, and batteries deteriorate even in storage situations [112]. The degradation can be coarsely estimated through increasing internal resistance and gradual capacity loss resulting in a drop in the amount of power provided. These factors collectively contribute to active and inactive material degradation. The primary contributors to degradation include excessive charging in both high current and high voltage conditions, frequent over-discharging and cycling, temperature extremes during storage and operation (both low and high), SOC and cycle bandwidth, internal short circuits within cells, external short circuits in batteries, cell and battery overheating, accelerated degradation, and thermal runaway.

2.4 DIFFERENT MODELING APPROACH

Different modeling approaches follow different methodologies that are used to create mathematical or computational models for studying and simulating systems, processes, or phenomena [113]. The analytical modeling approach involves deriving mathematical equations that describe the behavior of a system based on fundamental principles and assumptions. Analytical models often provide insights into system behavior but may be limited to simple or idealized scenarios due to the need for mathematical tractability [114]. Empirical modeling relies on data and observations to develop relationships or patterns that describe the behavior of a system. Statistical techniques, regression analysis, and machine learning algorithms are commonly used to create empirical models [115]. These models may lack physical interpretability but can capture complex behaviors and patterns from real-world data. Numerical modeling involves solving mathematical equations or simulations using computational techniques [116]. Finite element analysis and computational dynamics used in numerical modeling techniques. Numerical

models can provide detailed insights into complex systems but require computational resources and involve simplifying assumptions.

Agent-based modeling approaches are represented as collections of autonomous agents that interact with each other and their environment according to predefined rules. Especially helpful for analyzing complex systems with emergent behaviors are agent-based models, such as social systems, ecological systems, and traffic flow. Systems dynamics modeling focuses on understanding the behavior of complex systems over time by representing feedback loops, delays, and nonlinear relationships [117]. These models are often used to simulate dynamic systems such as supply chains, economic systems, and environmental systems. Hybrid modeling combines multiple modeling approaches to capture different aspects of a system [118]. A hybrid model may integrate analytical, empirical, and numerical components to simulate a system's behavior more accurately. Each modeling approach has its own merits and flaws with selection of approach lies on the specific characteristics of the system being studied, the available data and resources, and the research objectives. Fig. 2.5 illustrates different modeling approaches used for state evaluation in LIB.
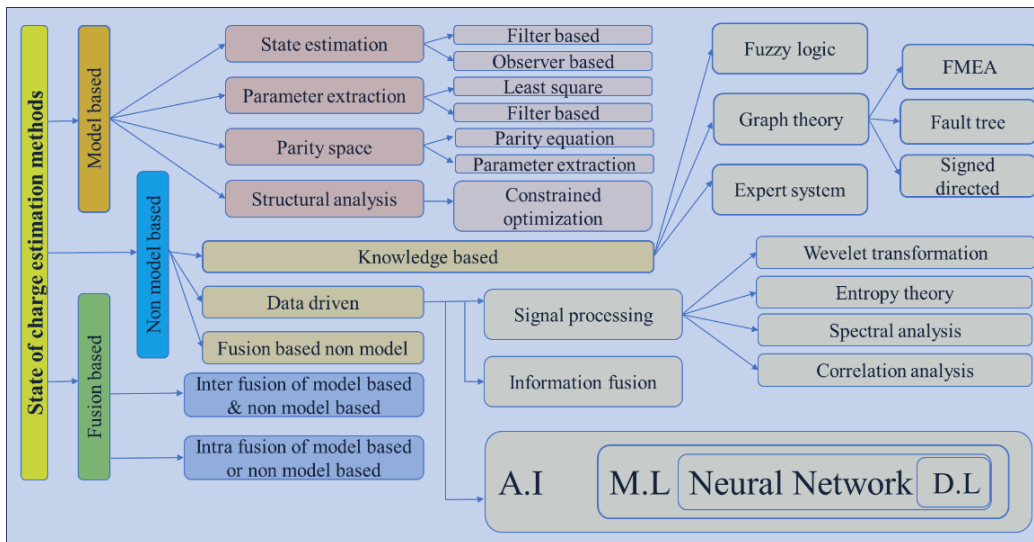
Fig. 2.5   Different state estimation approaches are used in the lithium-ion battery.

2.5   DIFFERENT STATES IN LIB

The state parameters are crucial for monitoring and managing the performance, safety, and reliability of LIB in different applications, including EVs, movable devices, energy storage systems, and grid stabilization. Effective battery management systems utilize measurements and algorithms related to SOC, SOH, SOS, RUL, SOP, and SOF to optimize battery operation, extend service life, and ensure safe and reliable performance. The state of charge in LIB signifies the presently available capacity concerning its present maximum available capacity. This relative value, which varies between 0 or 0% (fully discharged) to 1 or 100% (fully charged) is influenced by the LIB's electrochemistry, operational conditions, and SOH affected by environmental factors [119]. Thus, the relationship between SOC_{min}, SOC_{max}, and SOC_t must satisfy equation 5. Precise determination of SOC with other indirectly derived indices like SOH, etc. is essential for extending cell lifespan and guaranteeing secure operation [120],[121].

$$SOC_{min} \leq SOC_t \leq SOC_{max} \tag{5}$$

Among several FOMs that define LIB inherited characteristics that determine performance, safety, and economic viability, SOC is a crucial factor, and it indicates the capacity of the LIB, and it is frequently utilized to optimize the regulation of charging and discharging processes. Hence, an accurate SOC estimation method is of utmost importance to manage more efficiently [122]. Numerous reasons that affect the accuracy of SOC include temperature, age, discharge rate, battery history, cell chemistry, and measurement method [123]. Categorized into several SOC estimation methods are generally defined as the ratio of the remaining charge in a battery to its maximum capacity, expressed as a percentage. Nonetheless, accurate SOC evaluation of LIBs is still difficult because of their variable properties in various operating conditions and is commonly estimated using three distinct approaches, non-model based [124],[125], model based [126],[127] and fusion-based [128],[129].
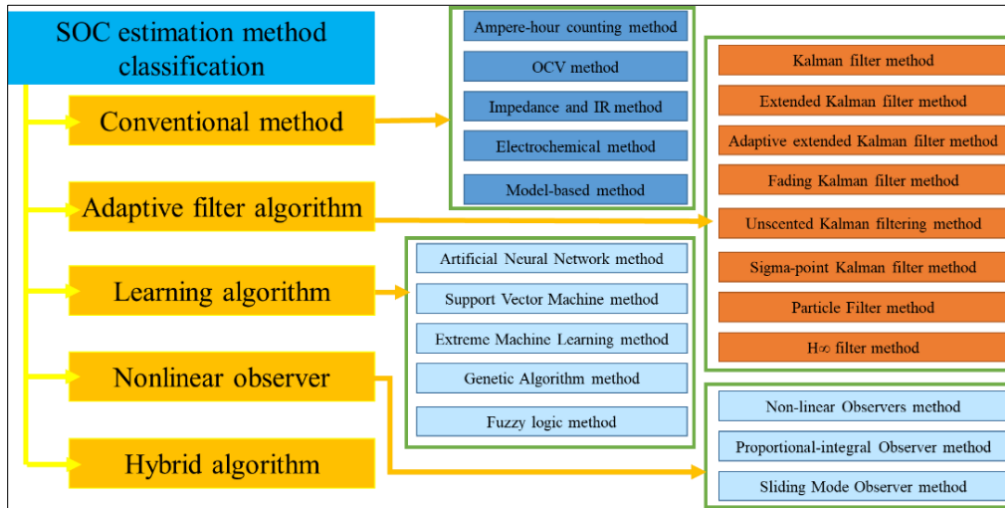
Fig. 2.6   Different types of SOC estimation methods.

The filter algorithm, nonlinear observer, hybrid algorithm, and conventional method are the five classes into which SOC estimation methodologies can be divided [130]. The frequently used approaches for SOC prediction are direct measurement with model-based and data-driven approaches or in combination of two or more of these methods [131], [132]. Open-circuit voltage (OCV) and coulomb counting (CC) are examples of direct measurement-based techniques. To simulate SOC, the model-based approach makes use of in-depth knowledge of the electrochemistry domain, including internal electrochemical reactions, the electrical properties of the components employed in the model, and intricate mathematical equations. The Luenberger observer, Kalman filters, sliding mode observer, electrochemical model, equivalent circuit model, and electrochemical impedance model [133],[134], which is illustrated in Fig. 2.6 are notable examples of model-based approaches.

SOH is commonly defined as the current state of the battery as compared to its ideal state and its fresh state. Its estimation techniques are applied to various indirect health indicators (iHI) and can be broadly classified into four categories: model-based, data-driven, hybrid, and differential analysis methods, each of which is further subdivided. The mathematical description of SOH is in terms of LIB

capacity decrease or impedance increase over the time horizon. State of health based on the ratio of the actual capacity of the aged LIB Q_{aged} to its rated capacity Q_{rated} and represented through equation 6 and SOH based on the impedance of the battery represented through equation 7.

$$\text{SOH} = \frac{Q_{aged}}{Q_{rated}} \text{x } 100\% \qquad (6)$$

$$\text{SOH} = \frac{R_{eol}-R}{R_{eol}-R_{new}} \text{x } 100\% \qquad (7)$$

Except for ML-based approaches, all others are effective in accurately modeling the behavior of LIBs; however, they are not suitable for online operations and are difficult to design due to both practical and theoretical concerns. Practically, these methods require extensive research, experimentation, and time to develop an accurate SOH estimation model [84],[135]. Theoretically, they rely on complex mathematical equations based on thorough understanding of cell chemistry, physics, and chemical properties, leading to challenges in battery model development and parameter estimation.

On the other hand, SOH can be estimated using data and strong processors in ML-based SOH estimation algorithms with little to no prior knowledge of internal properties and chemical interactions. However, the caliber and volume of the accessible data have a significant impact on the performance and accuracy of ML techniques. Since SOH is essentially regarded as a multi-physics and multiscale system due to the complicated interplay between various physical processes at various length scales, imbalanced data may result in issues with overfitting or underfitting. A persistent scientific issue is to predict this behavior of multi-physics and multiscale systems through modelling and forecasting [136]. The processes that take place in the LIBs on a physical, chemical, and electrochemical level are intricately linked and can span many spatiotemporal scales [137]. Lithium ions travel through an intricate web of components, including the electrode, electrolyte, and separator, at the molecular level. Numerous physical and chemical processes,

such as diffusion, intercalation, and phase changes, control its movement [138]. At the same time, the overall behavior of the battery is affected by a variety of external factors, such as environmental and operational [139],[140]. These external factors can influence the internal processes of the battery and can lead to complex feedback loops that can affect the LIB working, safety, and cycle index [141],[142]. Given the complexity of LIBs, it is important to have a detailed understanding of the underlying physics and chemistry to optimize their design and operation. This requires a multidisciplinary approach that combines expertise in materials science, electrochemistry, and systems engineering [143].

Electrochemical reactions and failure mechanisms are not taken into account by data-driven techniques and work on two main steps: first, identify one or more elements from the measured battery data (such as temperature, voltage, and current, which are generally called direct health indicators) or iHI that can characterize the degradation [144], which are then used to establish a relationship between these health indicators to SOH, using different machine learning methods [145]. Feature extraction plays a significant role and is a critical step and the iHI will significantly affect the performance of SOH estimation [146],[147]. Several researchers have developed different iHI at the cell level and employed different SOH estimation methodologies like [148] estimated charge storage for the kth cycle and internal resistance and number of cycles and used particle filter algorithm [149],[150]. The investigation of SOH [151] using ohmic internal resistance and polarized internal resistance employed ELM-based FF-NN. LSTM-based NN has been used by [152] and initial discharge voltage drop and time interval to equal discharging voltage difference have been employed as iHIs. Investigated SOH [153] employing ELM and RVFL network and employed duration of an equal charging voltage difference as iHIs.

The battery's unique capacity for continuous or instantaneous power output throughout time is known as the state of function, or SOF. It shows how the battery performs in relation to the actual load needs and can be expressed as

battery peak output power, which is constrained by SOC, voltage, and current constraints, among other criteria. SOF reflects the deterioration in performance (power fading) and calculation involves parameters such as SOC, voltage, current, and temperature [154]. As batteries age and environmental conditions change, the safe operating area undergoes alterations, leading to a decline in battery performance. The estimation of SOF relies on the simultaneous assessment of SOC and SOH, derived from SOP.

The available power that a battery can supply to or absorb over a time horizon is known as the state of power (SOP), which is determined by the product of the corresponding voltage and the threshold current. Various operational constraints must be explicitly considered and adhered to. It has significant importance in the context of dynamic driving scenarios for e-mobility, such as ascending ramps, accelerating, overtaking, cruising, and sudden braking [134],[155]. This information about dynamic driving conditions is relayed to the vehicle control unit to regulate the power distribution from the battery. Within battery energy management, SOC and SOP are identified as pivotal factors and SOP specifically represents the accessible power that the battery can either absorb from or deliver to the electric vehicle's powertrain [156], [157].

The remaining energy in the battery, crucial for predicting the driving mileage in e-mobility through the BMS, is determined by state of energy (SOE). As the battery discharges, the voltage declines, while during charging, voltage increases at distinct SOC levels, leading to corresponding variations in energy levels. High discharge rates result in significant internal energy losses with minimal capacity changes. Notably, SOC signifies residual battery capacity in ampere-hours (Ah) rather than the available energy in watt-hours (Wh). In [158] it delves into the disparity between SOC and SOE, emphasizing it as a parameter for SOH estimation. The widening of this difference is linked to decreasing temperature and increasing aging. The mathematical expression for SOE is presented with equation 8 where SOE_{in} is the initial SOE of the battery, E_{rated} is the rated energy

of the battery, and P(τ) is battery power at time interval τ.

$$SOE_t = = SOE_{in} + \frac{1}{Erated} \int_0^t P(\tau) \, d\tau \tag{8}$$

The temperature distribution, which results from heat production and degeneracy inside a battery cell or battery pack during regular operations, is the macroscopically manifested thermal dynamics of a battery and is known as the state of temperature (SOT). The surface, average, and core temperatures of a battery are frequently indicative of SOT for control and convenience of use. LIB exhibits dynamic and non-linear behavior, being particularly sensitive to fluctuations in temperature. Their widespread use in both stationary and portable applications is attributed to their compact size and high energy density [159]. However, the thermal management of high energy density LIBs poses challenges during charging and discharging processes. Elevated battery temperatures can lead to capacity degradation and increased resistance. Thermal runaway, resulting from thermal, mechanical, and electrical stresses, is a critical concern. Understanding the changes in battery characteristics during thermal impact is crucial and implementing safety techniques becomes essential to minimize stress factors in the battery. The research focused on the heat distribution and flow within the battery emphasizes the significance of SOT. Achieving an exact thermal model and precise limits is essential for obtaining a thorough understanding of the battery thermal dynamic characteristics [160].

Remaining useful life (RUL) of LIB represents the remaining life of the battery before it degrades to a point where it becomes unusable. Predicting RUL is crucial to prevent unexpected battery failure or complete shutdown in a controlled manner, facilitating proper maintenance. Despite the vital role RUL prediction plays in battery technology, literature is scarce on this subject, as noted in [161]. The prediction of RUL not only contributes to extending battery life but also assists in assessing the current health status of the battery based on historical data, thereby enabling the detection of potential failure risks. In [103], a diagnostic model is

developed to identify health indicators for online SOH estimation. It addresses [150] various issues related to the safety and reliability of batteries, emphasizing that battery malfunctions can lead to fire explosions and an increased risk of system failure. Historical incidents, such as the 1999 US Space Research Laboratory failure due to nonstandard internal impedance and the 2013 Boeing 787 fire caused by abnormal battery behavior, underscore the critical importance of battery health. The continuous overcharging of the battery led to the failure of NASA's MARS probe, emphasizing the need for effective RUL management and it extends the application of RUL to electronic devices for predictive maintenance [162]. The paper introduces a RUL model developed using the Unscented Kalman Filter and Bayesian Progression neural network, showcasing the diverse approaches employed in RUL prediction across different technological domains.

2.6   GAPS IDENTIFIED

While there has been considerable research on SOC estimation in LIB using different ML techniques [70],[154] there are still some research gaps that need to be addressed in physics-inspired SOC estimation using supervised learning [163]. Some of these research gaps include:

1. LiFePO$_4$ batteries often encounter difficulties in accurately estimating their SOC because of the plateaus that exist in the mid-range of the OCV- SOC curve, which is not in existence in other LIBs. Traditional SOC estimation techniques are generally inadequate in accurately determining the SOC in this range [164].

2. Most of the research was centered around the experimental analysis of cells, whereas cells are seldom used in any application, the truth is in real life, only battery packs of different configurations are used, which consist of series-parallel configured cells, battery management system, electrical & mechanical balance of system, etc.

3. Limited research on the use of physics-inspired features: While the use of physics-inspired features has shown promise in improving SOC estimation

accuracy, there is still limited research on the selection and optimization of these features for different supervised learning algorithms [160]. Further research is needed to investigate the optimal set of physics-inspired features and their impact on SOC estimation accuracy [165],[166].

4. Lack of research on the impact of experimental conditions: SOC estimation accuracy can be affected by various experimental conditions, such as temperature, cycling rate, and aging [167],[168]. However, there is limited research on the impact of these conditions on the performance of different supervised learning algorithms in physics-inspired SOC estimation[169],[170]. Further research is needed to investigate the robustness of different supervised learning algorithms under different experimental conditions.

5. Limited research on the use of multi-scale modeling: SOC estimation in LIBs involves modeling at multiple scales [171],[172] including cell-level and battery-level modeling [173]. However, there is limited research on the use of multi-scale modeling in physics-inspired SOC estimation using supervised learning algorithms [174],[175]. Further research is needed to investigate the potential benefits of using multi-scale modeling in physics-inspired SOC estimation [176].

6. Lack of comparative studies: There is a lack of comparative studies that evaluate the performance of different supervised learning algorithms for physics-inspired SOC estimation in LIB [177]. Further research is needed to conduct comparative studies to evaluate the strengths and weaknesses of different supervised learning algorithms for SOC estimation in LIB [178],[179].

2.7   CHAPTER SUMMARY

This chapter explores the evolutionary trajectory of state estimation of LIB, giving insights into the formidable challenges and influential elements that contribute to capacity degradation, with a specific emphasis on SOC, RUL, SOT, SOP, SOE, SOF, and SOH, which encompasses a spectrum of degradation mechanisms. It underscores the paramount importance of precisely predicting battery states,

particularly in the dynamic and spatiotemporal context of LIB powering e-mobility. The intricate nature of LIB degradation, dissecting factors such as aging, impedance fluctuations, and electrode slippage, and exploration extended to the nonlinear facets of degradation, encapsulating both calendar aging and degradation during operational phases are the main purpose of this chapter. Furthermore, this chapter investigates the hurdles faced in the electrification of vehicles, where LIB serves as linchpins, necessitating real-time monitoring and diagnostics. Environmental factors, particularly temperature, emerge as pivotal influencers on LIB performance, lifespan, and reliability.

The concept of capacity degradation factors takes center stage, accentuating the prevalence of distinct mechanisms throughout various stages of a battery's lifespan. Emphasis is placed on comprehending and predicting SOC and SOH to ensure the safety, stability, and dependable operation of LIB. This chapter identifies limitations in current research, highlighting gaps in SOC estimation through supervised learning. A need for further exploration into multi-scale modeling, physics-inspired features, and the impact of experimental conditions on the accuracy of state estimation. Additionally, there is a call for comparative studies evaluating different supervised learning algorithms for SOC estimation in LIB. At the core, this chapter carries a thorough panorama of the obstacles, mechanisms, and factors influencing the state estimation and degradation of LIBs, with a specific focus on SOC and SOH. It underscores the indispensable role of precise prediction in ensuring the secure and efficient functioning of LIB across e-mobility.

CHAPTER 3

FUNDAMENTALS OF LITHIUM-ION BATTERIES

3.1   CHAPTER OVERVIEW

This chapter provides a thorough overview of lithium-ion batteries and their research advancements, focusing on fundamental principles. The introduction section begins with detailing the evolution from lithium metal to different LIB classifications, discussing on cell-level working principles and highlighting research progress. Furthermore, it presents an overview of the current state of research, encompassing advancements in LIB technology, modeling methodologies, and characterization techniques. The effects of capacity degradation mechanisms on battery performance, such as electrode material degradation and electrolyte decomposition, are covered in considerable detail. The chapter also explores diverse modeling techniques for LIB, crucial for understanding dynamics and optimizing performance. The chapter culminates with a succinct summary encapsulating the key insights and conclusions drawn from the preceding discussions and serves as a consolidation of the main findings, highlighting the significance of the concepts in advancing LIB technology.

3.2   INTRODUCTION

Lithium also known as "lithion" or "lithina," was initially identified in 1817 by Arfwedson and Berzelius during their analysis of petalite ore ($LiAlSi_4O_{10}$) [180]. Lithium has a lot of potential as a battery anode because of its exceptional physical properties, which include its low density, high specific capacity, and low redox potential [181]. Since the late 1960, non-aqueous 3V LIB primary batteries have been available in the market with simultaneous research on advances to create rechargeable (secondary) LIB, when in the early 1970s, a resurgence of interest in

intercalation reactions, where ions, atoms, or molecules are inserted into a crystalline lattice of a host material without disrupting its structure. Adhering to the aforementioned criteria, groundbreaking research on intercalation was initiated by multiple teams in 1972, employing Prussian-blue materials like iron cyanide bronzes $M_{0.5}Fe(CN)_3$ [132]. During the same time, at a NATO conference, it was suggested to use transition metal disulfides as intercalation electrode materials for energy storage devices [182], [183]. A decade later, Li//TiS$_2$ cells were commercialized in various sizes by different companies [184]. Another successful metal disulfide was MoS$_2$, with MOLICEL batteries manufactured by Moli Energy. Among the various metal chalcogenides studied at that time, only NbSe$_3$ emerged as a commercialized cathode material by AT&T in 1989.

Additionally, V_2O_5 was used as a cathode material in commercialized LIB in the 1990s. In 1979 [185] replaced sodium with lithium ion Na_xCoO_2, patenting $LiCoO_2$ as a new cathode material with improved stability and excellent electrochemical properties. This marked the beginning of research into solid-solution materials, particularly $Li(Ni_xMn_yCo_z)O_2$ (NMC) in the 1990s. In 1984, conducted early work on spinel $LiMn_2O_4$, which offered cost advantages and better thermal stability than $LiCoO_2$. The issue of manganese dissolution into electrolytes at high temperatures was later addressed using an effective salt, LiFNFSI. Olivine-based cathodes, especially $LiFePO_4$, gained significant attention, with Goodenough's group pioneering its development while a crucial breakthrough was the discovery of a carbon-coating process. While $LiFePO_4$ is thermally stable, its redox potential is relatively small (3.5 V vs. Li+/Li). LIBs comprise an array of electrochemical devices, encompassing various cathode types, while predominantly employing carbon as the anode material. Dissimilar to other branches of electrochemistry, it operates through an intercalation mechanism.

3.3   TYPES OF LITHIUM-ION BATTERIES

The selection of cathode material is a key factor in defining the performance characteristics of LIBs, which are often employed in a variety of applications. LTO (Lithium Titanate Oxide), which is well-known for its outstanding cycle life and safety, is one of the frequently utilized cathode materials and is ideal for applications demanding durability and quick charging. NMC is widely used in consumer electronics and e-mobility because it provides a balanced combination of energy density, power capability, and cycle life. The safety and extended cycle life of LFP makes it perfect for power tools and stationary energy storage. LMO is preferred because of its thermal stability, whereas LCO, which is frequently used in portable devices and offers high energy density but has a short cycle life, is less durable. High energy density NCA is preferred in high-performance applications like some e-mobility. These cathode materials are chosen based on the requirements of each application, weighing aspects including energy density, cycle life, safety, and cost. NMC with a 60% market share [186] is the most popular LIBs cell chemistry for e-mobility itself and has several variants.
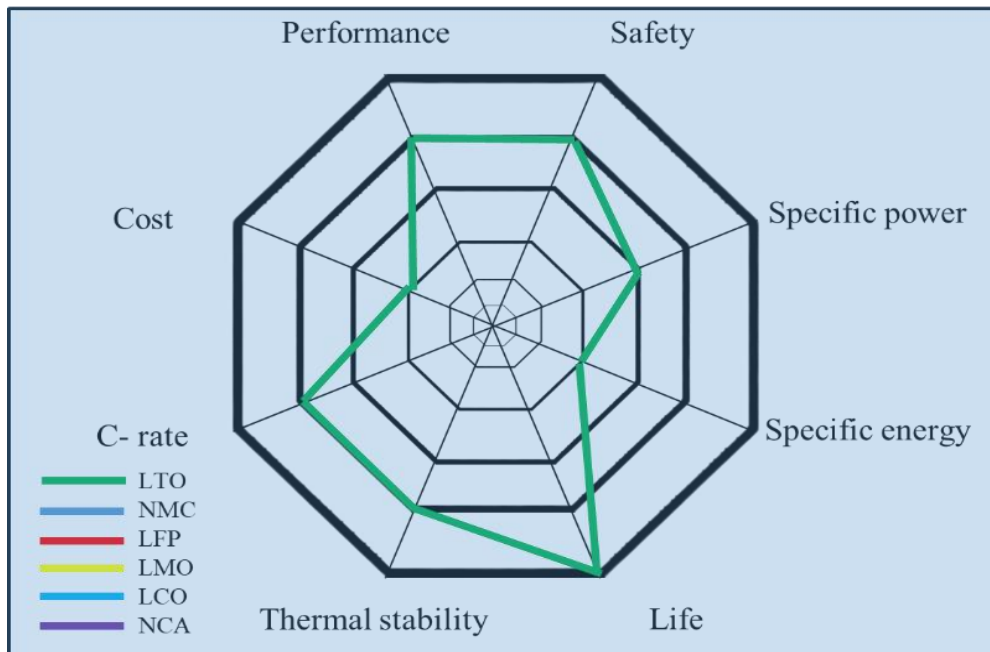
Fig. 3.1   Performance attributes of different lithium-ion cells.

Several important internal & external factors influence the design of LIBs suitable for e-mobility. The complex interaction of the cell to the design of the battery, design of the vehicle, operational aspects, and environmental aspects plays an active role in the interplay of electrochemistry of various components of the cell like chemical composition of electrodes and electrolyte, size & distributions of active material particles, the thickness of electrodes, porosity of the electrodes, foam factor, cell dimensions, and tab placement. Within different LIBs cell electrochemistry, numerous performance attributes come into play, encompassing electrical performance, safety, specific power and energy, lifespan, thermal stability, C rate for both charging and discharging, and cost, etc. as explained in Fig. 3.1. Various electrochemical compositions in LIBs showcase distinct characteristics, and the choice of a specific cell for a particular application relies on finding a balance among these diverse attributes.

3.3.1   NMC CELL

NMC based cells which can produce 3.6V to 3.7V and are available in different foam factors and configurations are most popular among high-energy, high-power density applications such as electric vehicles. John B. Goodenough's work during 1980 on LiCoO2 and is conceptualized as a combination of a layered $NaFeO_2$-type oxide and a closely related lithium-rich Li_2MnO_3 oxide, with the amount of the latter linked to the initial lithium excess and this development was carried out by four different four research teams during 2000. Among different NMC cells, $LiNi_xMn_yCo_zO_2$, NMC, where $x + y + z = 1$ is a highly promising material class, attention is now turning to Ni-rich NMCs with $x > 0.5$. Increasing the nickel content allows for more lithium extraction from the layered NMC structure within a given upper potential limit, thereby enhancing specific energies.

3.3.2   LFP CELL

LFP cells can produce 3.2V are also available in different foam factors and configurations are most popular among moderate energy and moderate power

density applications. Due to its affordability, lack of toxicity, abundant iron resources, non-usage of Ni and Co materials, exceptional thermal stability, safety features, electrochemical performance, and specific capacity, considerably longer cycle life than other LIB it has garnered significant market adoption.

3.3.3 COMPARISION

Globally for e-mobility applications, NMC maintained its lead with 70% and above market share, followed by LFP at nearly 27% and above. Whereas NCA ($LiNi_{0.8}Co_{0.15}Al_{0.05}O_2$) at around 3% among all LIB cell electrochemistry, among them LFP are rising fast whereas Ni rich NMC are losing market constantly. Many techniques are used to enhance technology. For example, silicon has been used to replace all or part of the graphite in the anode, making it lighter and increasing the energy density. Currently, silicon makes up around 30% of anodes. When innovative lithium metal anodes are commercially accessible, they may produce even higher energy densities.

NCA cathodes display a high specific capacity and excellent calendar life. This capacity contribution primarily hinges on the cobalt element, while the doped aluminum element exhibits minimal electrochemical activity. Integrating aluminum with reduced cobalt content can enhance thermal stability and reduce costs. Despite NCA cathode materials being approximately 50% more expensive than LFP due to the latter's abundant elements (Fe and P), NCA offers around 30% higher capacity and operates at a higher voltage of 3.6V equated to 3.2V for LFP, positioning NCA as a promising commercial cathode material in the LIB domain. However, NCA cathodes exhibit notable rapid capacity degradation and inferior thermal performance when operated at high voltages or elevated temperatures beyond room temperature.

3.4 WORKING PRINCIPLE

LIBs represent a category of rechargeable energy storage devices renowned for their ability to undergo multiple charging and discharging cycles. Nonetheless, their

delicate nature necessitates careful handling to prevent potential failures. The charging process involves the migration of lithium ions from the cathode to the anode through the electrolyte, with concurrent electron flow through the external circuit in the same direction. Conversely, during discharge, the stored lithium ions move back from the anode to the cathode. In both processes, lithium-ion is extracted from and inserted into host materials, a phenomenon referred to as intercalation [187],[188]. It is worth emphasizing that every constituent component plays a crucial role in determining battery performance and safety. The pursuit of the optimal combination of these components is pivotal for advancing battery technology. LIB makes use of charged particles of lithium to convert chemical energy into electrical energy. LIBs initiate their lifecycle in a fully discharged state, with all their lithium ions integrated into the cathode, lacking the capability to generate electricity. Before usage, the cell must undergo a charging process. During this charging phase, an oxidation reaction transpires at the cathode, resulting in the loss of negatively charged electrons [189].
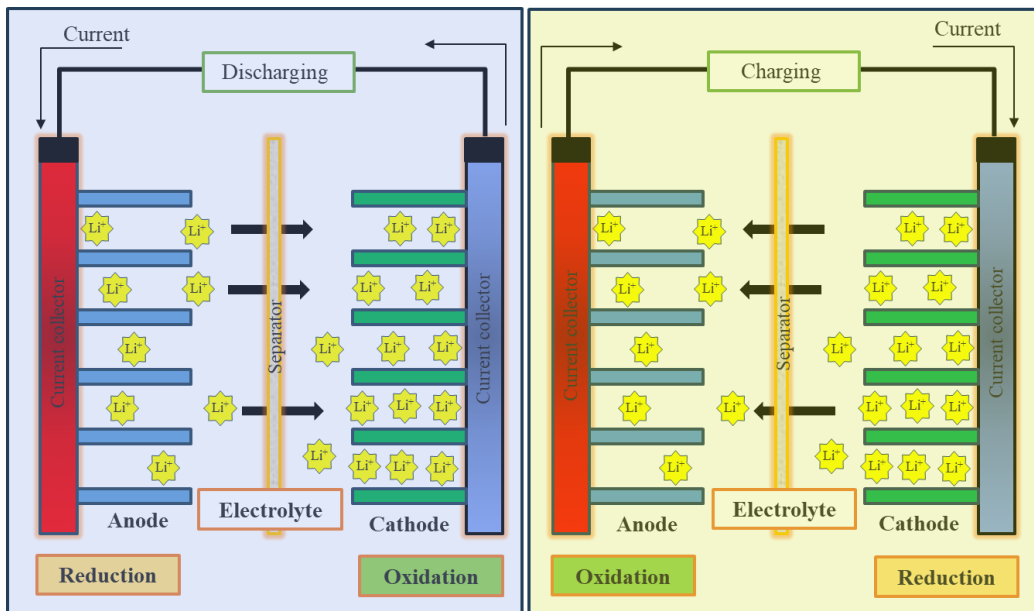
Fig. 3.2   Illustration depicting the operational concept of a lithium-ion battery.

To preserve charge equilibrium in the cathode, a corresponding quantity of positively charged intercalated lithium ions dissolves into the electrolyte solution. These ions then migrate to the anode, where they become integrated into the graphite structure. Simultaneously, this intercalation reaction introduces electrons into the graphite anode, effectively 'binding' the lithium ions. LIBs operate based on the "rocking chair principle", where chemical energy is converted into electrical energy through redox reactions. During charging, lithium-ion migrates towards the negative electrode (anode), and during discharge, lithium-ion returns to the positive electrode (cathode). This back-and-forth movement- insertion (intercalation) or extraction (deintercalation) of lithium-ion between the electrodes defines the working principle of LIB [190]. The schematic of the working principle of LIB is shown in Fig. 3.2.

The reversibility in any LIBs is an important criterion and is defined as Coulombic efficiency (CE) which is the ratio of its discharge capacity to the preceding charge capacity, considering specific operational conditions. These metrics gauge the reversibility of electrochemical energy storage reactions, with a value below one indicating the presence of non-productive, often irreversible reactions. Non-productive reactions, while some may be reversible and only lead to self-discharge, others pose more severe consequences due to their irreversibility. Recognizing the significance of CE operating as closed chemical systems with a finite supply of reactants (lithium-ion and anode/cathode active materials). Meeting such demands necessitates nearly flawless chemical reactions [191]. While CE stands as a crucial feature, the inevitable decline in CE is attributed to variations in diverse environmental and operational conditions [192].

3.5   PRESENT STATUS

LIBs have become increasingly popular for use in e-mobility due to their energy density, and long life. The major push towards LIBs in e-mobility is partially due to governmental support [193], lower cost, improved durability [73], increased

range [194], and faster charging. In any LIB the primary components are cells, BMS, and other components, like casing, thermal management, wires, connectors, packing materials, and sensors form part of the balance of the system [195]. Most of the research is centered on cells & BMS. From the first LIB commercialized by SONY, with galvanic and volumetric capacities of 80 Wh/kg and 200 Wh/L, the cell today has achieved more than tripled within 30 years [32], with maximum growth in development coming in last a decade. Cell electro-chemistries are several in the LIB family with comparable advantages and disadvantages with certain criteria like higher energy and power densities, driving range per charge, safety, temperature range, life, etc. fit with NMC, NCA, and LFP and are presently commercialized [196], apart from this, several other electrochemistry is in different level of demonstration and at R&D stage.

According to current research in materials chemistry, LIBs are projected to achieve a total initial cell galvanic energy density of 350-400Wh/kg, which falls short of meeting the energy requirements for e-mobility applications. The experiments have prompted the exploration of beyond LIB initiatives, which began around a decade ago. The initial beyond lithium-ion efforts focused on three main technologies relevant to the automotive industry: lithium-air, lithium-sulfur, and lithium-metal. Lithium air has faced challenges related to life and energy efficiency, limiting its practical application to research labs [197],[198]. Although sulfur chemistries have shown more promise than lithium-air, their low densities have limited their use in niche market applications such as unmanned aerial vehicles [199]. Among the future technologies, lithium metal has made the most progress in the past decade, and its potential impact is reflected in the recent issuance of automotive lithium metal cell targets by the USABC. The recent development of novel liquid electrolytes compatible with lithium metal, along with the discovery of solid lithium superionic conductors, has renewed the viability of solid-state batteries [89].

Recent investigations have been concentrated on augmenting energy and energy density, power, and power density, enhancing safety measures, reducing charging times, and cutting costs. Additionally, specialized studies tailored to specific application domains of LIBs have garnered increasing attention to maximize performance while minimizing limitations [200],[201]. Manufacturing of LIB is a multifaceted process that encompasses a range of activities from the initial preparation of electrodes using diverse chemical compositions to the assembly of cells with specific configurations and form factors [14],[202]. This progression extends from the cellular level to modules and ultimately to the construction of battery packs, each stage demanding distinct methodologies. Integral to this process is the application of multiscale modeling, which is essential for the development of an effective battery pack.

Material science and the rigorous monitoring of various factors play a crucial role in shaping the future trajectory of this technology. LIB technology has already achieved significant milestones in the past, and its continued advancement hinges on the unwavering pursuit of superior materials and the precise management of operational parameters. As delineated in Figure 3.3, this battery-making comprises a spectrum of engineering disciplines, highlighting the necessity for modeling at various scales, from the material science domain to the comprehensive design of a functional battery pack.
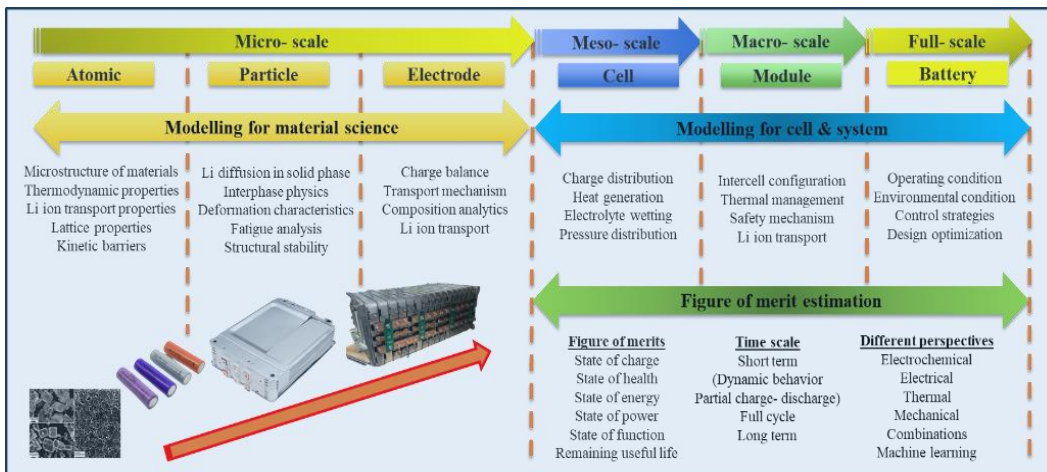
Fig. 3.3   Multiscale modeling from atomic level to battery pack level.

Energy and power density a critical metrics for LIB, especially in applications where high peak energy or power is required for short periods [203]. LIBs with high power density can deliver more power per unit mass or volume, which makes them ideal for such applications and represents the rate capabilities at which a LIB can supply energy, essentially indicating the maximum current that a LIB of a specific size can discharge [204]. This metric is determined by dividing the power output of the battery ($V_o \times I_o$) by its mass (kg) or volume (m^3), maximizing the power density of LIB is central to the success and widespread adoption of e-mobility. Higher power density translates into increased range, improved performance, and faster charging, all of which are essential for the growth of this sustainable mode of transportation.

Scientists and researchers have dedicated substantial efforts towards enhancing the energy and power density of LIB through two primary approaches: internal structure optimization-focused design: The approach involves refining the physical arrangement and configuration of components within the battery pack itself. Researchers explore ways to improve the geometry and organization of the battery's internal elements, such as the cell, BMS, partitions, thermal management, ware & harnesses, and battery box [205], [206] by optimizing the internal structure, they aim to enhance efficiency, and this results in more efficient and powerful battery power densities [207]. Another option is materials-oriented design: In this approach, the emphasis is on developing and utilizing advanced materials for various components of the cell. Researchers work on creating new materials for the anode [208] ,[209] cathode [210], [211] and electrolyte [212], [213] that offer higher energy density, better conductivity, and improved thermal stability.

In other words, the primary challenge that must be addressed to usher in the era of e-mobility is the extension of energy storage systems. Within the realm of electrochemical devices, LIBs have emerged as a pivotal rechargeable battery technology [214]. They have found widespread application in the realm of portable electronics and are increasingly being adopted by the e-mobility industry [215].

LIB technology presents a significant potential to displace traditional fossil fuels in powering vehicles, owing to its exceptional energy density and scalability for large-scale production. Furthermore, there is still room for further cost reduction in the production of LIBs.

Over the past decade, a range of cutting-edge characterization tools has become essential for the comprehensive study, optimization, characterization, and modeling of LIB across diverse and specialized applications [216]. The diagnostic and detection process for capacity and power degradation is typically categorized into four overarching approaches. To detect degradation trends, temporal redundancy depends on expert and knowledge-based techniques that use limit, and trend checks on inputs and outputs based on historical system information. This method is widely employed in various industries today and is considered a standard approach. Hardware redundancy employs a majority vote ruling logic to detect capacity degradation trends [217]. While this approach is popular and widespread adoption is hindered by significant costs, making it less feasible for various applications. This approach aims to leverage the strengths of diverse algorithms to enhance the overall effectiveness of the diagnostic and detection process. Details of cell-level performance degradation modes are as follows:

- Conductivity loss: It refers to a reduction in the capacity of a material to direct electrical current and it implies a decline in the efficient flow of electric charge within the battery components. It reported damage of current collectors peeling and degradation of binder as potential degradation mechanisms in LIB, whereas [218] researched that peeling and degradation of binder are other potential degradation mechanisms.

- Loss of lithium inventory: A significant phenomenon in the context of LIB, particularly when considering the intricacies of the solid electrolyte interphase (SEI). Loss of lithium inventory occurs when certain compounds within the SEI structure tend to trap lithium ions, making them unavailable for participation in the electrochemical reactions crucial for charge storage. Essentially, these

trapped lithium ions are sequestered and cannot contribute to the flow of electrical current, leading to a reduction in the overall capacity and performance of the battery [92]. It is concluded that lithium-ion is consumed by parasitic reactions, such as growth and decomposition of solid electrolyte interface, another phenomenon that occurs due to electrolyte decomposition as researched by [101],[219] concluded that formation is another significant potential failure mechanism.

- Loss of active material at anode: The degradation mechanism is responsible for a decrease in the LIB capacity, efficiency, and overall performance and contributes to a shorter lifespan. Various research on physical damage [220], chemical reaction, binder decomposition [33], contact isolation, graphite exfoliation, lithium plating and dendrite formation [221], electrode particle cracking [203], corrosion in current collector [222] are found to be significant in addressing this potential degradation mechanism.

- Loss of active material at the cathode: The degradation mechanism is due to physical damage, chemical reaction, binder decomposition, contact isolation, electrode particle cracking, transitional metal dissolution, and corrosion in the current collector.

- Impedance change- It is observed that change in impedance is also due to the depletion of electrolytes of free lithium-ion [223].

- Electrode slippage or stoichiometric drift is a potential degradation mechanism, as researched by and is due to the reduction in the lithium-ion from the negative electrode will decrease SOC whilst the positive electrode remains the same [224].

Understanding of capacity and power degradation and subsequent failures are still very limited and more limited yet dependable and real-world models and methods for the detection and prediction of these diverse phenomena. Capacity degradation and its accurate estimation & reliable fault diagnosis technique are decisive in the assurance of safety, stability, and reliable operation of the LIB e-mobility batteries

[224],[225]. Material science takes care of enhancing energy & power densities, safety concerns, increasing life, reliability, and safety concerns. Multidisciplinary approaches towards decoding cells from different approaches, monitoring, and estimation of various dynamic states such as charge, health, function, etc., are employed for higher deployability, understanding remaining useful life, end-of-life prediction, and warranty prediction.

As manufacturers and end users seek enhanced performance and safety, thorough characterization becomes crucial for detecting manufacturing and design flaws. Evaluating LIBs through both in-situ and destructive testing is essential to optimize performance and safety. This involves identifying effective materials and processes that improve these aspects without inflating battery costs. Nonlinearity and aperiodicity of data originating from short- and long-term dynamical behavior are two of the main difficulties in multivariate time series forecasting. Research on modelling this long-term dependence information in time sequence series jobs has always been focused on the fact that a long-term relationship's memory can more accurately forecast the time series' next step. Multivariable time series modeling and prediction are used in engineering, energy, meteorology, earthquake, business, and transportation for desired forecasting accuracy through various methodologies like statistical and ML [226].

The accurate modeling & estimation of states guarantee the safety, usability, and performance of LIB and avoid over-charge and over-discharge [227]. State estimation methods are divided into three categories, the first category is traditional methods, the second category is model-based methods, and the last is data-driven algorithms [228],[229]. Traditional methods include the integral method and open-circuit-voltage method, model-based methods, particle filtering algorithms [230]. Data-driven algorithms include fuzzy control, ML-based, and neural network methods [231],[232]. Co-estimation of states is possible only with model and data-driven methods [233].

As the demand for higher performance and enhanced safety grows among both battery manufacturers and end users, the importance of characterization becomes increasingly pronounced for identifying manufacturing and design defects. To enhance performance and safety, batteries require evaluation through a combination of in-situ and destructive testing. This involves identifying effective materials and processes without significantly increasing the cost of the batteries. The choice of a suitable characterization technique is contingent on the required information, the desired accuracy level, and the budget allocated for qualification and testing. Nondestructive testing offers the advantage of avoiding battery disassembly, although the information extracted may be limited [234]. The most precise techniques typically involve the use of expensive instruments and extended time, but they are essential at times to comprehend failure mechanisms and refine battery design. A comprehensive characterization methodology comprises different measurements of cell electrical parameters in Fig. 3.4.
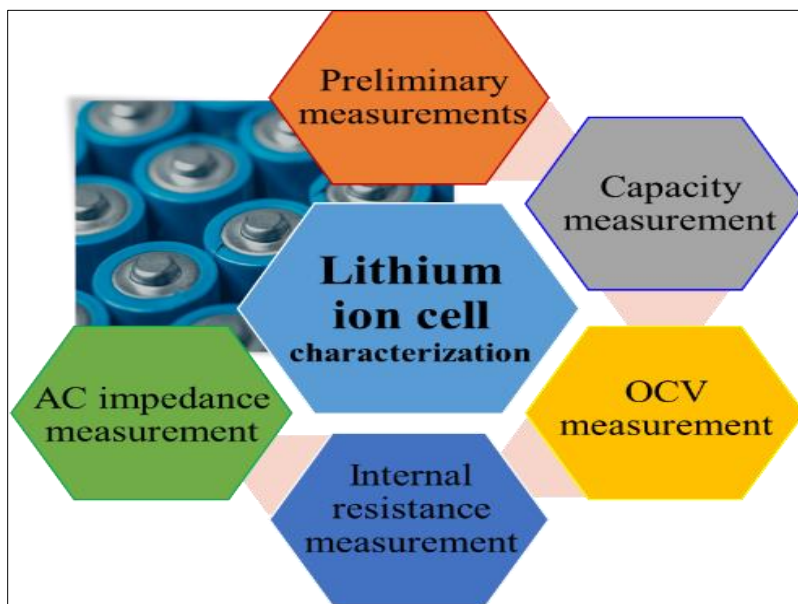
Fig. 3.4   Measurement procedure for LIB's cell characterization.

A drawback of LIBs is that for appropriate, safe, and durable applications with optimum life, they require constant surveillance to operate in a constricted band of

voltage, temperature, and other mechanical conditions. Another important LIB property is that its mechanical values can change during operation, as it operates on a rocking chair mechanism, as proposed by Armand in 1970. Over various operations, LIB active materials swell and contract with a proportion of non-reversible physical changes, which partially reflects the SOH. Mechanical instabilities such as plastic deformation, fragmentation, disintegration, and fracturing are caused by this strain. These effects are closely related to the SOH or RUL since they are recognized as a primary cause of performance fading during the course of the cycle [112],[235].

Batteries, as an electrochemical entity with a intricate planetary of materials (electrodes, electrolytes, binders, and separators) at the cell level and different electrical, mechanical, and electronic components at the battery pack level with large design space subjected to wide variation in operational & environmental conditions. Cell design parameters can be approached in multidirectional ways and can be built into different simulation models to accomplish and analyze its behavioral theme for chemical, electrical, or hybrid points of view with or without temperature or other mechanical stresses [236]. While intricate operational, behavioral, and environmental phenomena limit the usefulness of traditional deterministic modelling techniques and pose a significant obstacle to further design iterations, precise future state prediction is required to shorten test durations and the number of cells tested. This can be accomplished by using a probabilistic data-driven machine learning approach, which enables quantification of uncertainty to more effectively support design and control decisions [237]. LIB when stored or charged- discharged, exhibits a two-phase degradation behavior characterized by first, a linear phase and second a nonlinear phase where degradation is comparatively rapid. The multitude of degradation phenomena occurring in LIB complicates understanding of the two-phase degradation pattern.

3.6   CAPACITY DEGRADATION

LIBs being an electrochemical component, the overall degradation is a reality and the factors affecting are several based on operating and environmental factors [238],[239]. A summary of all degradation-causing mechanisms [240],[241] on different electrodes. Capacity fade refers to a reduction in the cell's usable capacity, whereas power fade is the dip in the cell's deliverable power after degradation. Capacity decline and power fade are thus two typical and useful markers of cell ageing. The usable capacity of LIB decreases, and internal resistance rises with time-scaled ageing and uses induced deterioration. This is because a variety of the previously listed degradation mechanisms, some of which happen simultaneously, cause further degradation mechanisms to be triggered. Among all the degradation types, the directly observable effects during operation or storage are collectively induced electrochemical behavior change and capacity and power fade [242].
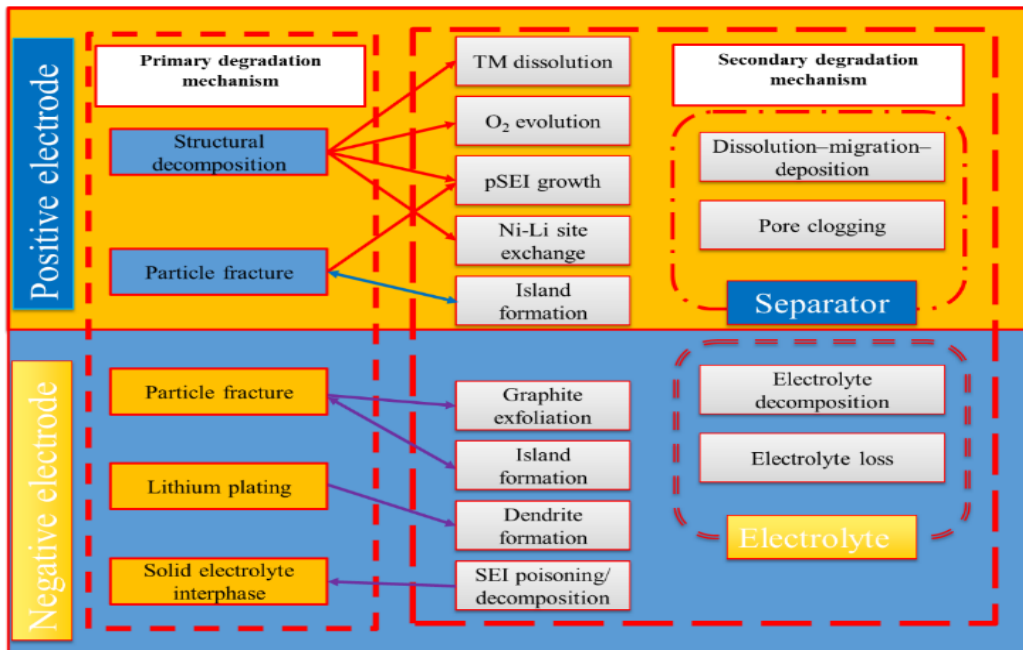
Fig. 3.5   Active material degradation as a primary and secondary mechanism at cell level.

The detailed positive and negative electrode degradations are several, which solemnly occur singularly, but are primary degradation in positive electrodes as structural decomposition, and particle fracture whereas in negative electrodes, it is particle fracture, lithium plating, and SEI. The secondary degradation mechanism involves TM dissolution, O_2 evolution, pSEI growth, Ni-Li site exchange, and island formation in the positive electrode and graphite exfoliation, island formation, dendrite formation, and SEI poisoning in the negative electrode, as shown in Fig. 3.5.

In the context of LIBs, the deterioration of inactive materials is a significant factor influencing cell performance. The control systems governing capacity decline and impedance increase in LIBs exhibit a high level of sophistication. The intricacies involved in the degradation mechanisms and their interactions underscore the complexity inherent in LIB. The dynamic interplay among various subcomponents within LIBs unveils an aging mechanism that encompasses both mechanical and chemical factors, intricately interconnected. It contributes to several critical failures and instances of heat-induced malfunctions [243]. The resulting heat generation inside a cell is a combination of reversible processes responsible for electrochemical reactions and irreversible processes which in turn are a combination of enthalpy change, active polarization, ohmic heating, and heating from mixing.

3.7   BATTERY MODELS

The operational performance and behavior of LIBs hinge on the integrity of their intricate internal structure. Currently, gauging the SOH directly poses challenges, given the expense and potential disruption associated with embedding sensors within the structure. Instead, employing battery models that precisely forecast long-term behavior serves as a digital twin, which operates alongside the actual battery, synchronizing intermittently using data from limited measurable factors like cell voltage, temperature, and current. At the same time, determining SOC, crucial for

intelligent charging and range determination also proves challenging, necessitating estimation by the digital twin [244].

While different battery models play a crucial role in forecasting future performance, it is equally important to focus on the parameterization and validation processes. In many studies, the foundational aspect of characterization relies on electrochemical measurements, where galvanostatic methods serve as a vital tool for establishing metrics such as capacity, resistance, and coulombic efficiency. Despite their apparent simplicity, these measurements offer substantial insights. Broadly, there are two primary methodologies for modeling: empirical and physics based. The empirical approach entails a step-by-step process of applying equations and parameters to attain the optimal alignment with experimental data where the underlying equations may lack intrinsic significance, merely aiming to replicate the behavior of the battery treated as a mysterious system. This can be further subdivided into the electrochemical model, thermal model, aging model, and safety model, which in turn gives vital states of a LIB like SOC, SOH, RUL, etc.

In the realm of monitoring multiple states like SOC and SOH, simulations must be both rapid and accurate, delivering real-time results. By anticipating vital performance parameters such as capacity and lifespan, these models emerge as valuable tools in electrode, cell, and pack design. They empower exploration within the battery design space, allowing for variation and combination of constituent materials, electrode structures, thermal management, and other factors. This eliminates the need for constructing costly and potentially risky prototypes. A diverse range of battery models has been created, each exhibiting varying levels of intricacy, thereby proving valuable across a spectrum of application domains [245]. The physical process inside a cell results in multi-scale physical modeling either through electrochemical, aging, stress, or thermal modeling, which in turn uses empirical modeling, equivalent circuit modeling, or data-driven modeling techniques as explained and shown in Fig. 3.6.
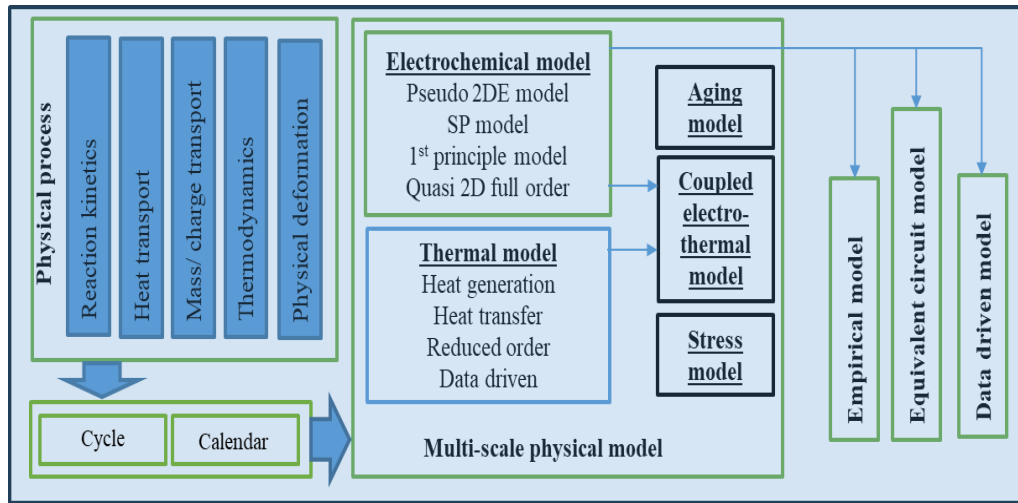
Fig. 3.6   Different modeling techniques for battery packs.

Empirical modeling of LIB involves the development of models based on observed data and experimental results rather than relying solely on theoretical principles, which are particularly useful for predicting battery performance, optimizing charging, and discharging strategies, and understanding the impact of external factors on battery behavior. High-quality electrochemical battery models stand out as exceptionally accurate within the realm of battery modeling. Their advantage comes from their capacity to quantitatively explain important behaviors of a battery at the minuscule level; this is dependent on their comprehension of the chemical reactions occurring in the battery in both the liquid phase and the electrode. Because data-driven modelling can handle nonlinearity, it performs better than other approaches in parameter prediction [246]. A general machine learning system for battery state monitoring can mimic the nonlinear relationship between input and output variables by putting a learning model into practice. On the other hand, the hybrid approach derives simulated behavior from equations recognized to accurately represent the genuine physical processes at play.

3.8   CHAPTER SUMMARY

In the ambit of electrochemical energy storage, LIBs have emerged as a leading choice, surpassing other electrochemical storage options like lead acid or Ni-

cadmium batteries, owing to their promising applications in e-mobility and grid-level energy storage. Their superiority is underpinned by a suite of advantageous characteristics, including remarkable energy density, robust power capabilities, high efficiency, and minimal self-discharge, thus positioning them as highly sought-after solutions across various domains. Capitalizing on advancements in electrode and electrolyte material manipulation, researchers have adeptly tailored LIB to accommodate diverse operational settings and objectives. This chapter presents a comprehensive exploration of the historical evolution and developmental phases of LIB, illuminating the formidable challenges encountered in electrode fabrication, cell assembly, characterization, and understanding the different operational states, particularly concerning e-mobility applications. It introduces various electrode types, discusses the performance attributes of distinct cell configurations, researches their working principles, assesses their present status, and examines multiscale modeling techniques and cell-level performance degradation modes. Through this comprehensive exploration, the chapter aims to provide valuable insights into the advancements, challenges, and methodologies shaping the current landscape of LIB technology.

CHAPTER 4

METHODOLOGY AND EXPERIMENTAL SETUP

4.1   CHAPTER OVERVIEW

The chapter overview outlines the contents of the document, which primarily focuses on machine-learning applications in lithium-ion batteries. It covers different ML methods utilized in experiments, covers support vector regression, decision trees, k-nearest neighbor, random forest, and linear regression. Additionally, it discusses performance evaluation and error metrics such as mean absolute error, mean square error, root mean square error, and mean absolute percentage error. The document also details experiments related to the state of health and charge, along with experimental setups, capacity aging equipment, SOH experimentation, and cell selection protocols. Physics-inspired feature engineering is pivotal to this research, from cell selection process through meticulous evaluation of performance attributes- capacity from CCT/ CDT, and OCV variance, post-testing at various temperatures (25°C, 35°C, etc.) and discharge rates (1C, 2C, etc.), essential for assembling battery packs tailored for detailed experimentation and gives appropriate input to the application of ML to a refined accuracy of performance predictions and ensures reliability and robustness of experimental outcomes, which ultimately advancing the understanding and management of LIBs diverse conditions. The chapter also includes cell capacity measurement, SOC experimentation, assembly of battery packs, battery management systems, and measurement of capacity and cell selection, concluding with a chapter summary.

4.2   MACHINE LEARNING IN LIB

Starting in early 1943, efforts were dedicated to exploring concepts inherent in nervous activity, giving rise to the initial mathematical model of neural networks.

Additionally, in 1949, there was a focus on developing theories that elucidate the connection between behavior and the workings of neural networks and brain activity. The foundational work of the Turing test, which was introduced in 1950, further contributed to these advancements. The future development gained momentum thanks to various hardware and software innovations in computing. Currently, machine learning stands at the forefront of research and innovation across diverse fields and is extensively employed in chemistry, physics, biology, engineering, and materials science [247]. ML is employed to improve the estimation accuracy of LIBs by reducing the calculation burden. ML can be characterized as the creation of computer algorithms that acquire knowledge from examples, make predictions, and improve performance based on data inputs rather than being explicitly programmed to execute a specific task.

The concept of multiscale modelling has emerged in recent decades, using data from computational models at finer scales to simulate continuum-scale behavior instead of depending on empirical constitutive models. Various methods have been developed to bridge across multiple length and time scales. While the fundamental ideas of multiscale modeling have historical roots dating back to da Vinci, the recent surge in its development is attributed to advancements in parallel computing, experimental techniques for atomic-level characterization of structure-property relations, and theories accommodating multiple length scales [248],[249]. Artificial intelligence (AI) and its subset, machine learning (ML), are useful tools to help researchers effectively solve the parameterization and data difficulties on the user and production side. Managing, monitoring, understanding, and assimilation of the large amounts of data generated for LIB is a big task. It takes a significant team effort from experimentalists, modelling experts, and AI/ML specialists. ML and multiscale modeling are two distinct yet interconnected fields that play vital roles in diverse scientific and technological domains. The integration of ML with multiscale modeling has become increasingly prevalent. ML techniques can enhance the predictive capabilities and efficiency of multiscale models by learning

complex relationships within the data, optimizing simulations, and aiding in the interpretation of large datasets.

ML methods are extensively employed to characterize LIB performance, lifetime, reliability, and safety, apart from accelerating the understanding of new materials, chemistries, cell designs, and beyond. At this stage, there are four main categories for data-driven approaches: supervised, unsupervised, semi-supervised, and reinforced learning. These are further divided into subcategories based on the variations in data-mining techniques, such as support vector machines (SVM), relevance vector machines (RVM), long short-term memory (LSTM), Gaussian process regression (GPR), and deep learning [250],[251].

ML algorithms are broadly categorized into four main types based on the type of data they use, and the type of learning involved as in Fig. 4.1. The training process of a supervised learning algorithm involves the provision of both the input data and their associated outputs, as it is trained on labelled data. By reducing the error between its expected and actual outputs, the algorithm gains the ability to map input data to output labels. An unsupervised learning algorithm is trained on unlabeled data, which means that it doesn't have any predefined output labels. By combining related data points, the objective is to find patterns and organization in the data. Combining supervised and unsupervised learning results in semi-supervised learning. To train the algorithm, a small amount of labelled data is combined with a larger amount of unlabeled data. This method works well when it is difficult or costly to acquire labelled data. Through interaction with its surroundings, an agent that uses reinforcement learning learns to carry out specific behaviors in response to rewards or penalties from the environment. The goal is to maximize the total reward received over time by learning a policy that maps states to actions.
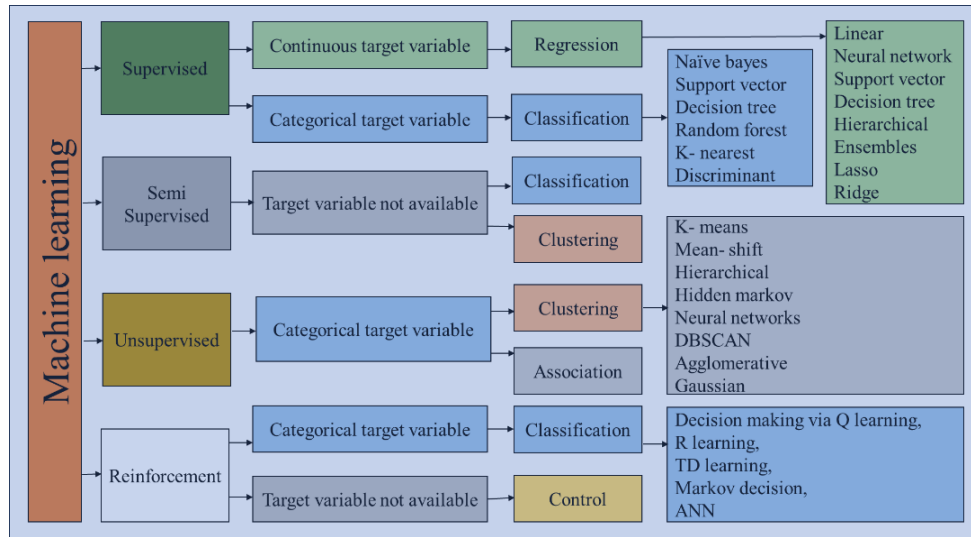
Fig. 4.1　　　　　Different ML methods employed in LIB state estimation.

Among different types of ML methods, there are several advantages and disadvantages associated with them for creating battery models. The ageing data collecting, and SOH data extraction are supported by the supervised learning models, which also help with the optimization of performance measures that are based on past performance. Long computation times, inefficient data downtime, challenging pre-processing, and an ongoing need for updates are some of its disadvantages. The selection of training data in semi-supervised learning models is expensive and time-consuming, and the consistency of the classes may not match spectral classifications. Its shortcomings include unstable iteration results and low precision when applied to network-level data. The expense and time associated with choosing training material is a drawback for unsupervised learning methods [252]. Although varying consistency in classes may not match spectral classifications, there are benefits such as the potential to minimize human mistake that can be achieved quickly and easily. The use of reinforced learning techniques can yield long-term benefits for SOH and has a great capacity to address complicated issues. In nonlinear health profiles, it is particularly helpful for reaching perfection. It is only helpful, nevertheless, in complex situations like SOH where operational and

environmental factors are involved. The approach requires a large amount of computation labor and old data [198].

Multiscale supervised learning methods offer a promising alternative to traditional approaches for solving challenging physical problems, particularly those involving partial differential equations (PDE) and multiscale phenomena [253]. These leverages supervised learning techniques to approximate PDE solutions while incorporating the governing physical laws as constraints during model training. This enables the model to learn from limited data and achieve accurate predictions even in the presence of missing or noisy information. It can also be applied to inverse problems, where the aim is to estimate the underlying properties or parameters of a system from limited measurements. By incorporating physical laws as constraints, it can provide efficient and precise solutions to inverse problems, without requiring complicated formulations or extensive computational resources.

4.3   ML METHODS USED IN EXPERIMENTS

There are various ML methods employed in state estimation for LIBs in e-mobility, and the choice of method often depends on the nature of the data, the research question, and the specific goals of the experiment. The following algorithms are used as the ML methods in experiments.

4.3.1   SUPPORT VECTOR REGRESSION

In 1995, Vapnik introduced Support Vector Machines (SVM) by leveraging the concept of minimizing systemic risk in mathematical learning theory [254]. SVM, in its fundamental configuration, acquires both linear and nonlinear decisions and essentially, it identifies the hyperplane with the maximum soft margin. For the nonlinear SVM regression dual formula, a Lagrangian function from the primal function by introducing nonnegative multipliers α_n and α_n^* for each observation x_n which leads to the dual formula, where we minimize the coefficients as per equation 9.

$$L(\alpha) = \frac{1}{2}\sum_{i=1}^{N}\sum_{j=1}^{N}(\alpha_i - \alpha_i^*)(\alpha_j - \alpha_j^*)\,G(x_i, x_j) + \varepsilon\sum_{i=1}^{N}(\alpha_i + \alpha_i^*) - \sum_{i=1}^{N}y_i(\alpha_i + \alpha_i^*) \tag{9}$$

Subject with following conditions:

$$\sum_{i=1}^{N}(\alpha_n + \alpha_n^*) = 0$$

$$\forall_n : 0 \leq \alpha_n \leq C$$

$$\forall_n : 0 \leq \alpha_n^* \leq C$$

The function used to predict new values is equal and presented through equation 10.

$$f(x) = \sum_{n=1}^{N}(\alpha_n - \alpha_n^*)\,G(x_n, x) + b. \tag{10}$$

The goal of supporting vector machines (SVR) is to find a function that minimizes the prediction error and roughly captures the relationship between the input variables and a continuous target variable. Utilizing a kernel function to translate the data into a higher-dimensional space, SVR can manage non-linear interactions between the input variables and the goal variable. Because of this, it's an effective tool for regression problems where the goal and input variables may have intricate interactions. SVR's reliance on kernel functions makes it a nonparametric approach.

4.3.2   DECISION TREES

Developed as early as 1963, the modern form of Decision trees took place during 1986 by John Ross Quinlan proposed a tree concept with multiple answers. Well-liked machine learning methods, DTs are applied to both regression and classification problems. They are a great option for those new to machine learning because they are simple to comprehend, interpret, and use. It is a predictive model that bases its choices on incoming data and has a flowchart structure. Data is split into branches, and leaf nodes are assigned results. Regression and classification tasks are handled by decision trees, which yield models that are simple to comprehend.

4.3.3   K-NEAREST NEIGHBOR

The K closest neighbours algorithm (KNN) is a non-parametric supervised learning technique in statistics that was initially created in 1951 by Evelyn Fix and Joseph Hodges. Thomas Cover further refined the approach. The KNN algorithm is a popular machine learning technique for applications involving regression and classification. Its foundation is the idea that similar data points usually have similar labels or values. During the training phase, the KNN algorithm refers to the entire training dataset. Before making predictions, it calculates the distance between each training example and the input data point using a chosen distance metric, such as Euclidean distance. The system then calculates the K nearest neighbours of the input data point based on their respective distances. Regarding categorization, the method forecasts the label of the incoming data point by utilizing the most common class label among the K closest neighbours. Regression uses the average, or weighted average, of the goal values of the K to estimate the value for the input data point.

4.3.4   RANDOM FOREST

In 1995, random forests (RF), a tree-based ML algorithm leveraging the power of multiple decision trees was created in 1995 by Tin Kam Ho [255]. An ensemble of several decision trees is used by the flexible RF machine learning method to produce predictions or classifications. Through the amalgamation of various trees' outputs, the RF algorithm yields a more refined and precise outcome. Its versatility and simplicity of usage, which enable it to tackle regression and classification problems with ease, are the reasons for its widespread acceptance. Because of the method's ability to handle complex datasets and mitigate overfitting, it can be used to a wide range of machine learning predictive applications. One of the most important features of the RF Algorithm is its ability to handle data sets with continuous variables; this is useful for regression and classification if the variables are categorical. It functions better on tasks that include regression and classification.

4.3.5   LINEAR REGRESSION

Linear regression (LR) is a type of statistical analysis that is used to predict the relationship between two variables. Assuming a linear relationship between the independent and dependent variables, the objective is to find the best-fitting line to depict their relationship. By minimizing the total squared discrepancies between the expected and actual values, the line is found. The advantages of using these ML methods for LIB's state estimation are several, ML methods are advanced with lower errors over the existing CC or OCV method currently employed in the majority of BMS for state estimation. It can produce accurate and interpretable predictions if you have enough relevant data. These methods usually result in higher accuracy, as they incorporate the user's domain knowledge. It has a feedback mechanism to check whether predictions are correct or not. It is sufficient to retain the decision boundary as a mathematical formula once the entire training process is over, rather than retaining the training data in memory. For smaller BMS, these are advantageous as to keep the computational power and cost at a minimum with a fair degree of errors in control.

4. 4   PERFORMANCE EVALUATION AND ERROR METRICS

The process of constructing ML, AI, or DL models revolves around the principle of constructive feedback. The iterative cycle involves creating a model, receiving feedback through metrics, implementing enhancements, and repeating the process until a satisfactory level of classification accuracy is attained. Error metrics and performance evaluation are essential components of many fields' evaluation frameworks. The most important and widely used metrics, as determined by the surveys, are scale-dependent metrics like Mean absolute error (MAE), Root mean square error (RMSE), and Mean square error (MSE), or metrics based on percentage errors like Mean absolute percentage error (MAPE). Metrics for evaluation are essential for understanding how well the model performs. One important aspect of these metrics is their capacity to distinguish between the model's outputs in an efficient manner. Performance error measures play a crucial

role in evaluation frameworks across diverse fields. These metrics can be characterized as logical and mathematical constructs specifically crafted to gauge the proximity of actual outcomes to the anticipated or predicted values. Academic literature encompasses a wide array of performance metrics and similar measures, being frequently cited in research studies. These metrics serve as valuable tools for assessing the accuracy and reliability of predictions or expectations in various applications [256]. Among different aspects of LIB state estimation, for evaluating the performance of individual ML models for predicting different states, these below performance metrics are used extensively [257],[258]. For this experiment, we carried out MAE, MSE, RMSE, and MAPE. We had considered y_i as the estimated target output and y is the corresponding correct target output.

4.4.1 Mean absolute error

The Mean absolute error (MAE) serves as a statistical metric for assessing the precision of a forecasting model, be it a regression model or a time series model. It gauges the typical magnitude of errors between the anticipated values and the actual values, all within the units of the response variable. Computed as the average of the absolute disparities between predicted and actual values, the MAE represents the meaning of these absolute errors. A lower value is preferable, the optimal score is 0 and the permissible range is (0 to infinity). Mathematically MAE is presented through equation 11.

$$\text{MAE}(y, \hat{y}) = \frac{\sum_{i=0}^{N-1} |y_i - \hat{y}_i|}{N} \tag{11}$$

4.4.2 Mean square error

The Mean square error (MSE) is the mean squared difference between the observed values in a statistical study and the values predicted by a model are calculated by squaring the discrepancies. It is crucial to square the differences between the observed and expected values when comparing them since some data values may fall short of the expectations and result in negative differences, while other data

values may exceed them and result in positive differences. Squaring the differences eliminates the chance that the observations will add up to zero, so addressing the equally common scenario of observations being higher or lower than the projected values and equation 12 mathematically represents the mean square error (MSE).

$$\text{MSE}(y, \hat{y}) = \frac{\sum_{i=0}^{N-1}(y_i - \hat{y}_i)^2}{N} \tag{12}$$

4.4.3   Root mean square error

The Root mean square error (RMSE) serves as a statistical metric commonly employed to assess the precision of forecasting models, such as regression or time series models. It gauges the disparity between predicted and actual values, expressed in the units of the response variable. The square root of the average of the squared variances between the expected and actual values is used to calculate the root mean square error, or RMSE. In essence, it is the square root of the mean of squared errors; a smaller number indicates a more accurate forecast. The optimal score is 0.0, and a smaller value is considered more favorable, with the range being (0 to infinity). Despite its widespread use for evaluating forecast accuracy, the RMSE has a limitation in that it lacks normalization. This implies that its interpretation is influenced by the scale of the response variable, making comparisons challenging across diverse datasets with varying scales. The mathematical presentation of RMSE is presented through equation 13.

$$\text{RMSE}(y, \hat{y}) = \sqrt{\frac{\sum_{i=0}^{N-1}(y_i - \hat{y}_i)^2}{N}}, \text{ or RMSE} = \sqrt{\text{MSE}} \tag{13}$$

4.4.4   Mean absolute percentage error

The Mean absolute percentage error (MAPE) is a statistical metric that assesses the precision of a forecasting model, frequently applied in engineering, business, economics, etc. It calculates the average percentage variance between the projected

and actual values, with a reduced MAPE signifying improved forecast accuracy. The mathematical presentation of MAPE is presented through equation 14.

$$\text{MAPE}(y, \hat{y}) = \frac{100\%}{N} \sum_{i=0}^{N-1} \frac{|y_i - \hat{y}_i|}{|y_i|} \tag{14}$$

4.5 EXPERIMENTS FOR STATE OF HEALTH AND STATE OF CHARGE

To cover the maximum identified research gaps and their potential applications, this research's experiments were devised in such a way that it covers both cell and battery packs of different cell electrochemistry for different applications and at the same time uses various environmental and operating conditions and uses different ML methods. In this chain of experiments, different cell electrochemistry was used having different foam factors, and were experimented under different operational and environmental conditions. Different ML methods were employed to arrive at different error metrics. The experiment plan brief is outlined in Fig. 4.2 below for both cell electrochemistry and different states.
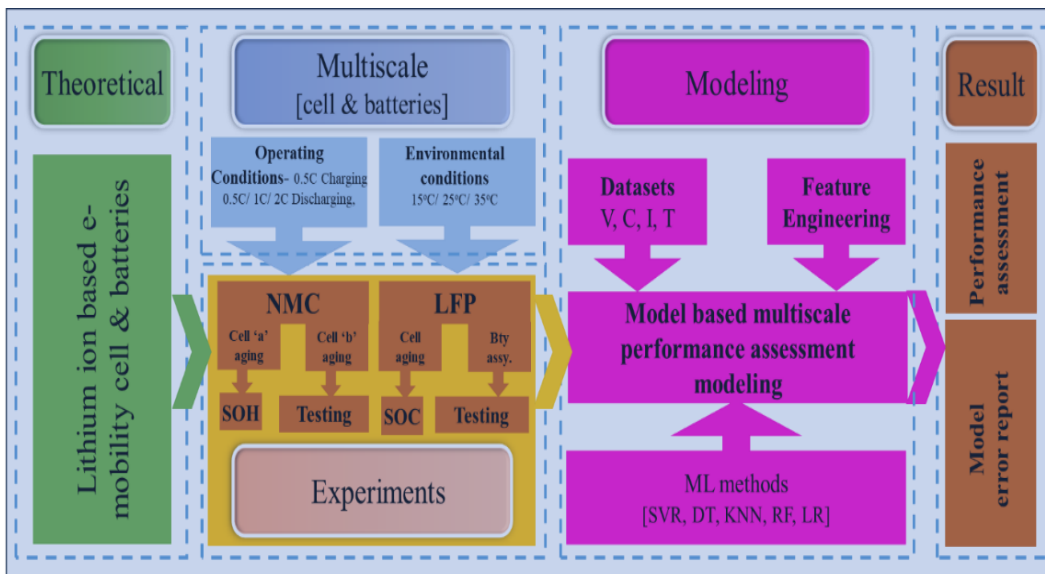
Fig. 4.2 Experimental flowchart for SOC and SOH for cell and battery.

4.5.1 EXPERIMENTAL SETUP FOR STATE OF HEALTH

The experimental procedure and applicability of various ML-based modeling have been done through defining and elaborating the research objectives. The information provided by different manufacturers varies based on the specific battery cell and is typically presented in tables and graphs which generally include nominal, electrical, mechanical, and safety specifications. As an illustration, the table below highlights the nominal characteristics of LG Chem and Fareast lithium-ion cells, as found in the datasheet information. In the research work, high-power NMC cells with cylindrical foam factor with details are listed in Table 4.1, and the parameters used are tested and analyzed for SOH modeling. The NMC cells are widely used as they have high power- high energy densities, which are essentially needed in e mobility applications. This enables the suitability in application and maintained its lead with 70[+]% market share, followed by LFP at nearly 27[+]% and NCA at around 3[+]% among all LIBs cell electro-chemistries for e mobility applications.

Table 4.1   Types of NMC cells used in SOH experimentation.

Cell description	NMC CELL (NMC 811, 18650 [Cylindrical])		
	Dataset cell "a"	Experiment cell b"	
Manufacturer	LG Chem	Fareast	
Cathode	$Ni_{0.84}Mn_{0.06}Co_{0.1}$	$Ni_{0.84}Mn_{0.06}Co_{0.1}$	Photograph of cells
Anode	Graphite +SiO	Graphite +SiO	
Nom. Voltage(V)	3.6 V	3.6 V	
Nominal Capacity	3.0 Ah	2.6 Ah	
Voltage Range under extreme conditions	2.50V~3.65V [25°C＜T≤60°C] 2.00V~3.65V [-20°C≤T≤0°C]	2.50V~3.65V [25°C＜T≤60°C] 2.00V~3.65V [-20°C≤T≤0°C]	

Max Dis. Current	20 A	7.8 A	
Acceptable Temp.	−5 to 50°C	−5 to 50°C	
Nominal Mass	47 g	44 g	

At the start, these commercially available cells were subjected to a cell sorting machine in Fig. 4.3 and initial sorting was carried out based on grouping end cell voltage and cell internal resistance. A total of 181 cells were selected based on the set of acceptable criteria. Following the cell selection, a preconditioning test is conducted under IEC 62660–1. The secondary lithium-ion cells for the propulsion of electric road vehicles – Part 1: Performance testing [1] in 512 channel cell grading machines as per Fig. 4. 3 to ensure cell stabilization. This test consists of one cycle at the manufacturer-specified current, followed by a 30-minute rest period. Following the preconditioning test, a reference performance test (RPT) is carried out at the beginning of life (BOL). Subsequently, the cells of each test case (TC) undergo cycling based on the conditions before the periodic RPT is conducted.

Cell sorting machine is an important aspect for battery assembly, as it systematically sorts cells based on specific parameters of voltage, internal resistance, and capacity, ensuring that only cells meeting the desired criteria progress to the next stage of assembly. By accurately categorizing cells, the sorting machine enhances the consistency and reliability of battery packs, reducing the risk of performance variations or failures. This process is essential for applications requiring high precision and uniformity, such as electric vehicles and energy storage systems.

Fig. 4.3   Cell sorting machine for voltage and internal resistance.

4.5.2 CAPACITY AGING EQUIPMENT FOR SOH EXPERIMENTATION

Experimental cells as shown in Fig. 4.4 (a) are capacity cycle aging was carried out using a Raunik SCTS and a Raunik high-precision Model: LBT21084 is a multichannel battery testing system as shown in Fig. 4.4 (b). This 5V 3A / 6A 512-channel Battery Grading Machine is primarily designed for the formation and capacity grading of incoming cylindrical lithium-ion batteries. Formation involves the initial low-current charging of a newly manufactured lithium-ion battery to develop a passivation layer on the negative electrode, known as the solid electrolyte interphase (SEI) film. Upon receipt of the cells, capacity grading assesses the cell's capacity through a charge-discharge cycle and categorizes the cells based on this capacity value. This process ensures proper balance during battery pack assembly.

LBT21084 is a multichannel battery testing system that consists of a computer system, control software, communication interface, and a battery detection cabinet. The detection cabinet includes a clamp and a board for supporting the clamp, a constant current and voltage charging source, a constant current discharging source, a storage control circuit, current and voltage sampling circuits, a main control CPU, data memory, a microcontroller program, and a control panel.

Fig. 4.4   (a) Experimental cells (b) 512 cell grading machine for cell preconditioning test.

Single cells were inserted into 18650 battery holders (memory protection devices) that were sold commercially. To reduce voltage, drop an 18-gauge wire was used to link the holders, and cable lengths were maintained under eight feet. The SPX Tenney Model T10C-1.5 environmental chambers, which have temperature controls ranging from -73°C to 200°C, were used to house the cells during the cycling process.

4.5.3 SOH EXPERIMENTATION AND CELL SELECTION

While complete elimination of inconsistency resulting from the production process may not be achievable, employing screening methods proves effective in identifying batteries with satisfactory consistency. This, in turn, enhances the reliability, safety, and overall lifespan performance of packs. Utilizing criteria such as capacity, internal resistance, and self-discharge rate in screening methods can notably enhance the overall performance of the pack. Finally, among sorted cells, the selection of TC was carried out as per Fig. 4.5 for capacity selection through from continuous charge test/ continuous discharge test (CCT/CDT), and as per Fig. 4.6 selection of cell according to OCV (mV) variance for different cell after full charge from continuous charge test (CCT) and as per Fig. 4.7 selection of cell according to OCV (mV) variance for different cell after full discharge (CDT). In selecting cells based on capacity from CCT or CDT data, a systematic approach is followed. Initially, data from CCT or CDT experiments is collected, wherein batteries undergo continuous charging or discharging at a constant rate. Subsequently, the capacity of each cell is calculated based on the obtained charge or discharge profiles, typically measured in ampere-hours (Ah) or watt-hours (Wh). These cells are then sorted according to their capacities, allowing for the identification of cells with similar capacity levels. Finally, selected cells meet the quality standards to ensure reliability and consistency in battery performance.
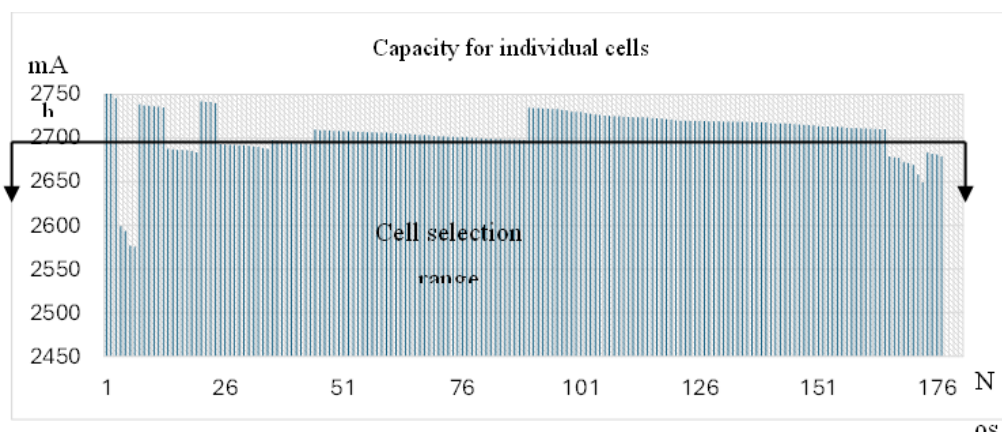
Fig. 4. 5   Selection of cell according to capacity from CCT/ CDT.
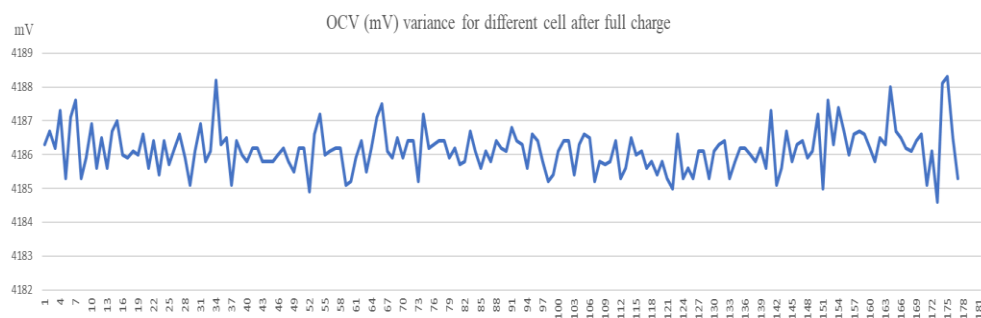
Fig. 4.6   Selection of cell according to OCV (mV) variance for different

cells after CCT.
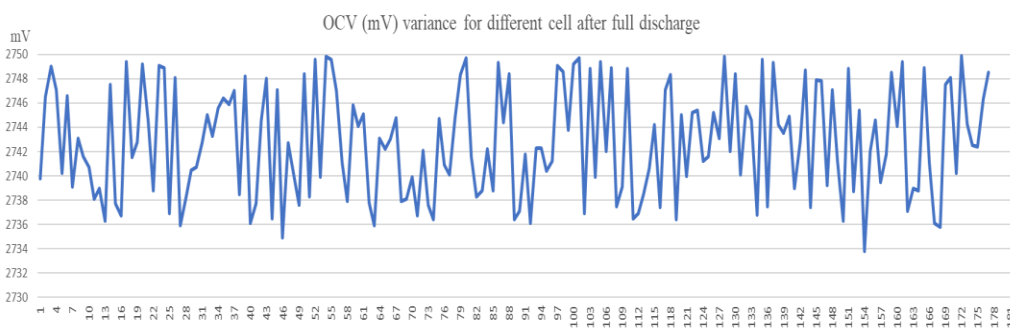
Fig. 4.7   Selection of cells according to OCV (mV) variance for different

cells after CDT.

The whole process of aging as per the experimental plan is presented in Fig. 4.8
and in conducting cycle life tests for NMC cells using CCT/CDT methods an

77

experimental approach is essential. After preparing the cells and setting up the experimental environment with precise instrumentation, the test protocol is defined, specifying parameters such as charging/discharging rates, cut-off voltages, and cycling conditions. Throughout the test, data on voltage, current, temperature, and time are meticulously recorded and analyzed to assess key performance indicators like capacity retention and voltage fade.
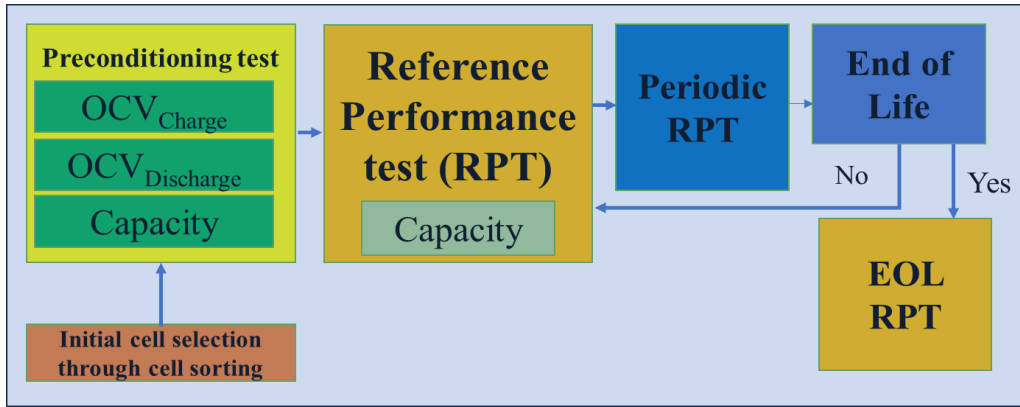
Fig. 4.8　　　Experimental methodology for NMC cell cycle life test (CCT/CDT).

The equivalent full cycles (EFC), which represent a cell's total charge throughput, are utilized to analyze the real SOH of the cells. One EFC is equal to one full charge and one full discharge over the cell's rated capacity multiplied by two and as per the rain flow method [2] and it is presented through equation 15.

$$\text{EFC} = \frac{1}{2}[\int I_{cycle}.dt]/C_{nom} \tag{15}$$

In this rain flow method employed, half-cycles are tallied exclusively after the data and in this study, as each cell charging and discharging dataset attains a maximum value of 100% during analysis, the half-charge and discharge cycles are independently incremented. The determination of an equivalent full cycle involves calculating the average battery charge and discharge cycles over a specified period. This approach allows the estimation of the number of full equivalent cycles during the analysis rather than waiting until the conclusion of the dataset. Consequently,

calculating the remaining useful life between load points becomes a straightforward process.

Data from machine	
	Extraction of capacity at defined temperature and C rate (Cell "a") at 100% DOD
	Continuous cycling till Capacity reaches 60% of rated capacity
	$SOH_r = CAP_{max(aged)}/CAP_{max(fresh)}$

Training data (80%) ← Data pre processing → Testing data (20%)

Calculating aging parameter & feature engineering

Modeling through different ML methods (SVR, DT, KNN, RF)

Trained Model ← Extraction of capacity at defined temperature and C rate (Cell "b") at 100% DOD

Model accuracy (MAE, MAPE, RMSE, MSE) of Cell 'a' & Cell 'b' datasets at defined temperature and C rate at 100% DOD

Fig. 4.9   Flowchart for SOH model development.

4.5.4 CELL CAPACITY MEASUREMENT

Capacity is the most important aspect, and its measurement is performed on a fully charged cell in two steps: constant current charging at 0.5C with upper cutoff voltage at 4.2 V with limiting current and temperature is always kept at 25°C. After a 15-minute rest period, the cell is discharged at 1C or 2C (as the case may be) to the end-of-discharge voltage (2.5V) at different temperatures maintained at 15°C, 25°C & 35°C. For ML-based model development and analysis, all three capacity measurements are performed, and the third discharging capacity measurement is used in the validation analysis. Raw data is directly fetched from the computer system, and it comprises following parameters-

Cycle_Index	Start_Time	End_Time	Test_Time (s)	Min_Current (A)	Max_Current (A)	Min_Voltage (V)	Max_Voltage (V)	Charge_Capacity (Ah)	Discharge_Capacity (Ah)	Capacity Loss (Ah)	Charge_Energy (Wh)	Discharge_Energy (Wh)	Energy Loss (Wh)

This set of parameters is used to describe the performance and characteristics of a battery during a cycle test. Cycle_Index is a unique identifier for each test cycle performed on the battery. It helps in tracking and differentiating multiple test cycles. Start_Time is the timestamp when the battery test cycle begins. This marks the start of data collection for the cycle. End_Time is the timestamp when the battery test cycle concludes. This marks the end of data collection for the cycle. Test_Time (s) is the total duration of the test cycle, measured in seconds. It is calculated as the difference between the End_Time and Start_Time. Min_Current (A) is the minimum current measured during the test cycle, expressed in amperes (A). This represents the lowest current drawn from or supplied to the battery during the test. Max_Current (A) is the maximum current measured during the test cycle, expressed in amperes (A). This indicates the highest current drawn from or supplied to the battery during the test. Min_Voltage (V) is the minimum voltage recorded during the test cycle, expressed in volts (V). It represents the lowest voltage the battery reached during the test. Max_Voltage (V) is the maximum voltage recorded during the test cycle, expressed in volts (V). It shows the highest voltage the battery reached during the test. Charge_Capacity (Ah) is the total amount of charge the battery can store during the charging phase of the cycle, measured in ampere-hours (Ah). It indicates the battery's capacity to hold energy. Discharge_Capacity (Ah) is the total amount of charge the battery delivers during the discharging phase of the cycle, measured in ampere-hours (Ah). It shows how much energy the battery can

provide. Capacity Loss (Ah) is the difference between the Charge_Capacity and Discharge_Capacity, measured in ampere-hours (Ah). This value represents the loss of capacity during the test cycle, which can indicate battery degradation. Charge_Energy (Wh) is the total amount of energy supplied to the battery during the charging phase, measured in watt-hours (Wh). It reflects the energy input into the battery. Discharge_Energy (Wh) is the total amount of energy delivered by the battery during the discharging phase, measured in watt-hours (Wh). It represents the energy output from the battery. Energy Loss (Wh) is the difference between Charge_Energy and Discharge_Energy, measured in watt-hours (Wh). This value indicates the energy lost during the cycle, which can be due to inefficiencies such as internal resistance or heat. These parameters provide a comprehensive overview of the battery's performance and efficiency during a test cycle, helping to assess its health, capacity, and energy efficiency.

This experiment concentrates on cycle index, Charge_Capacity (Ah)and Discharge_Capacity (Ah) only. consecutive charge/ discharge of cell and to investigate the capacity evolution over the lifetime, different operational stress factors (1C, 2C), and environmental stress factors ($15℃, 25℃,$ and $35℃$) were investigated. For a better comparison, all values were normalized using a reference value measured at the beginning of life under the respective test conditions. The flowchart for the development of a model for SOH is shown in Fig. 4.9.

Uncertainty regression analysis has been carried out for different cells, working under different operating parameters. Table 4.2 provided summarizes the regression analysis results for the NMC battery under various cycling conditions across different temperatures ($15℃, 25℃,$ and $35℃$). The metrics include R Square, Adjusted R Square, and P-value, which are key indicators in evaluating the model's performance and statistical significance. The calculation steps of uncertainty in results have been presented in Appendix 2.

Table 4.2   Regression analysis for cells used in SOH experimentation.

Regression Statistics	15C_0-100_0.5-1C_a_cycle	15C_0-100_0.5-1C_b_cycle	25C_0-100_0.5-1C_a_cycle	25C_0-100_0.5-1C_b_cycle	35C_0-100_0.5-1C_a_cycle	35C_0-100_0.5-1C_b_cycle
R Square	6.23E-01	6.32E-01	2.04E-01	1.67E-01	1.70E-01	1.53E-01
Adjusted R Square	6.22E-01	6.31E-01	2.02E-01	1.66E-01	1.69E-01	1.51E-01
P-value	4.33E-110	1.04E-112	1.88E-27	5.26E-33	1.21E-33	5.15E-30

It is observed that for the 15°C cycling conditions, the R² values are approximately 0.62-0.63, indicating that around 62-63% of the variance in the battery's performance which suggests a moderately strong relationship between the cycling conditions and battery performance. For the 25°C and 35°C conditions, the R² values are significantly lower (ranging from 0.15 to 0.20), indicating that the model explains only 15-20% of the variance, which indicates relative weaker relationship under these conditions, implying that other unaccounted factors may influence battery performance more heavily at these temperatures. The Adjusted R² values are very close to the R² values for all conditions, indicating that the number of predictors has little impact on the overall explanatory power of the model. This stability suggests that the model's complexity is appropriate and not overly reliant on the number of predictors. The p-values for all conditions are extremely small (e.g., 4.33E-110, 1.04E-112), far below the conventional significance level of 0.05. This indicates that the results are statistically significant, meaning there is a very low probability that the observed relationships occurred by chance. Thus, the regression models can be considered reliable for understanding the relationships between cycling conditions and battery performance. The regression analysis reveals that the models for the 15°C conditions are more robust in explaining the variance in battery performance compared to the 25°C and 35°C conditions. The

consistently low p-values across all conditions confirm the statistical significance of the models. However, the lower R^2 values at higher temperatures suggest the need to consider additional factors that might affect battery performance under those conditions.

The uncertainty analysis of experimental data has been carried out on the basis of [259], who developed a practical approach to conducting uncertainty analysis using Excel macros and highlighted the importance of uncertainty analysis in engineering and scientific research, where accurately quantifying uncertainties is crucial for reliable data interpretation. Table 4.3 lists the different calculations for measurement uncertainty of experimental data.

Table 4.3   Calculating measurement uncertainty of experimental data.

Readings	DC Voltage V	Ampere I	Temperature °C
1	3.21	1.25	28.00
2	3.21	1.25	28.10
3	3.22	1.25	28.00
4	3.20	1.24	28.05
5	3.20	1.25	28.10
6	3.21	1.24	28.00
7	3.20	1.25	28.00
8	3.21	1.25	28.15
9	3.21	1.24	28.00
10	3.20	1.24	28.10
11	3.20	1.25	28.10
12	3.21	1.22	28.00
Calculation uncertainty analysis of experimental data			
Average	3.21	1.24	28.05
Number of measurements	12	12	12

DOF (n-1) of average	11	11	11
Standard Deviation	6.51E-03	9.00E-03	5.64E-02
Random Uncertainty	1.88E-03	2.60E-03	1.63E-02
Readability	0.01	0.01	0.01
Synthetic Uncertainty	5.77E-03	5.77E-03	5.77E-03
Combined Uncertainty	8.75E-02	9.15E-02	1.49E-01
Expanded Uncertainty [from calibration report]	1.90E-05	4.00E-04	3.40E-04

The data comprises twelve readings for each parameter, followed by a calculation section that aggregates these readings to assess the uncertainty. The average values are 3.21 for Voltage, 1.24 for Ampere, and 28.05 for Temperature, calculated across the twelve measurements. The standard deviations for these parameters—0.00651 for Voltage, 0.00900 for Ampere, and 0.0564 for Temperature—reflect the dispersion of the data around the mean, with the Temperature showing the highest variability. Key contributors to measurement uncertainty include random uncertainty, synthetic uncertainty, and the instrument's readability, with a combined uncertainty calculated for each parameter. The expanded uncertainty, derived from the calibration report, is also provided, highlighting the importance of calibration in minimizing overall uncertainty. The calculation of combined uncertainty, which encompasses various error sources, ensures that the final measurement is not just a single value but a range within which the true value is likely to lie, thereby enhancing the robustness and credibility of the results.

The expanded uncertainty, derived from the calibration report as per Appendix 2, provides a more comprehensive view by incorporating a coverage factor (typically to achieve a confidence level, often 95%). The Voltage measurement has a very low expanded uncertainty of 1.90E-05, indicating a high level of confidence in the calibration of the instrument used for this measurement. The expanded uncertainty for Ampere and Temperature are 4.00E-04 and 3.40E-04, respectively, reflecting

slightly higher but still low levels of uncertainty compared to the combined uncertainty.

Further to the results arrived on capacity, the process of consolidated ML model development method is followed as per the flowchart as shown below Fig. 4.10. In the process of developing ML models, a streamlined approach involves several key stages that involve collecting and preprocessing data, ensuring its quality and suitability for analysis. Appropriate models (SVR, DT, KNN, and RF) are selected based on the problem and data characteristics, followed by training and optimization. Model performance is then evaluated using testing data, and if satisfactory, the model is deployed into production. This consolidated flow enables the development of robust and efficient machine-learning solutions tailored to specific needs.
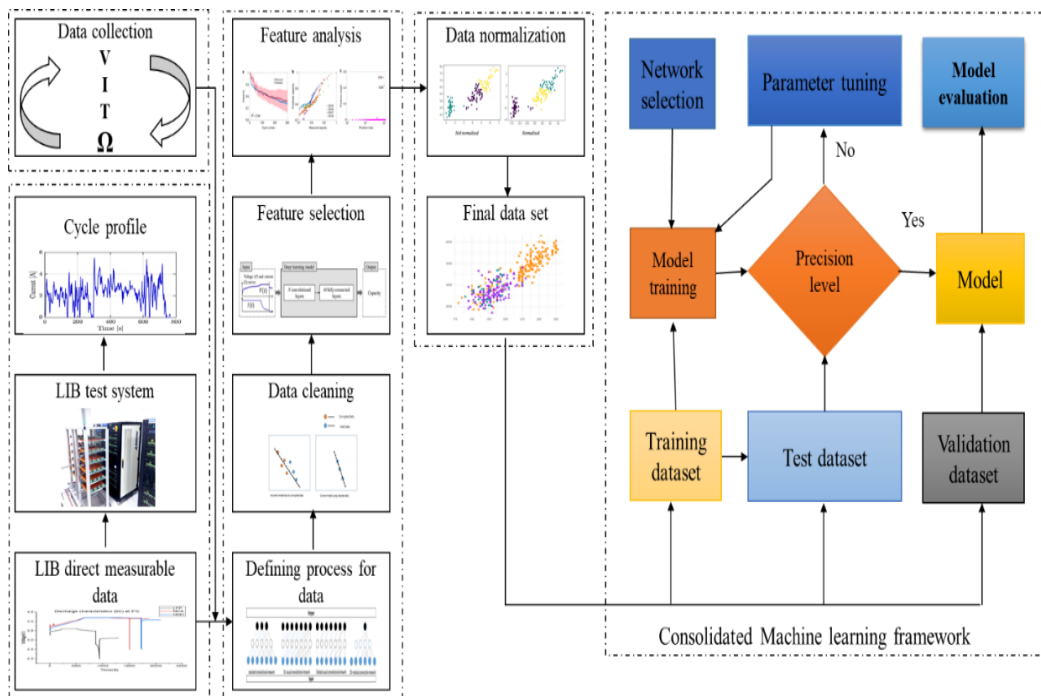
Fig. 4.10   Consolidated common ML model development algorithm flowchart.

4.5.5   CELL CYCLE AGING PROTOCOL FOR SOH ESTIMATION

Cell cycle aging protocol covers several steps, as cells were placed in thermal chambers to adjust to the desired cycling temperatures. This is important because the performance of batteries can vary depending on temperature. After this step, the cells were discharged to 0% SOC before the start of each round of cycling. This is to ensure that the cells are starting from a consistent SOC. The capacity of the cells was checked after each round of cycling. This is done by performing three charge/discharge cycles from 0% to 100% SOC at a current of 0.5C. The capacity check allows us to track the degradation of the cells over time. The cells were cycled at the designated conditions for that cell. The conditions could vary depending on the cell type, the desired cycling profile, and the goals of the study. The capacity of the cells was checked again at the end of each round of cycling. This allows us to compare the capacity of the cells before and after cycling. Every cell in the study underwent an identical capacity assessment procedure. This ensures that the results are comparable between cells. This ensures that the results are comparable between cells. The test matrix for experiments is detailed in Table 4.4.

Table 4.4   Test matrix for NMC cell.

DOD, Temperature, Discharge Rate	
0%–100%, 15℃, 1C	0%–100%, 15℃, 2C
0%–100%, 25℃, 1C	0%–100%, 25℃, 2C
0%–100%, 35℃, 1C	0%–100%, 35℃, 2C

4.5.6   CELL CAPACITY FADING ANALYSIS

In addition to the cell manufacturing process which causes cell-level inconsistency, the assembly techniques for modules and packs are equally crucial for ensuring consistency which widens with aging and in operation. For efficient management of the battery through BMS, the inconsistency must be low at any point of operation and any point of age. The fading inconsistency of individual cells is an important

aspect of making a good battery pack. The equivalent full cycles (EFC) capacity graph for Fareast makes cells no 1, 2, 3, and 4 and it is represented through Fig. 4.11. It is evident that significant capacity increases up to the first hundred cycles and gradually starts depleting in a nonlinear manner.
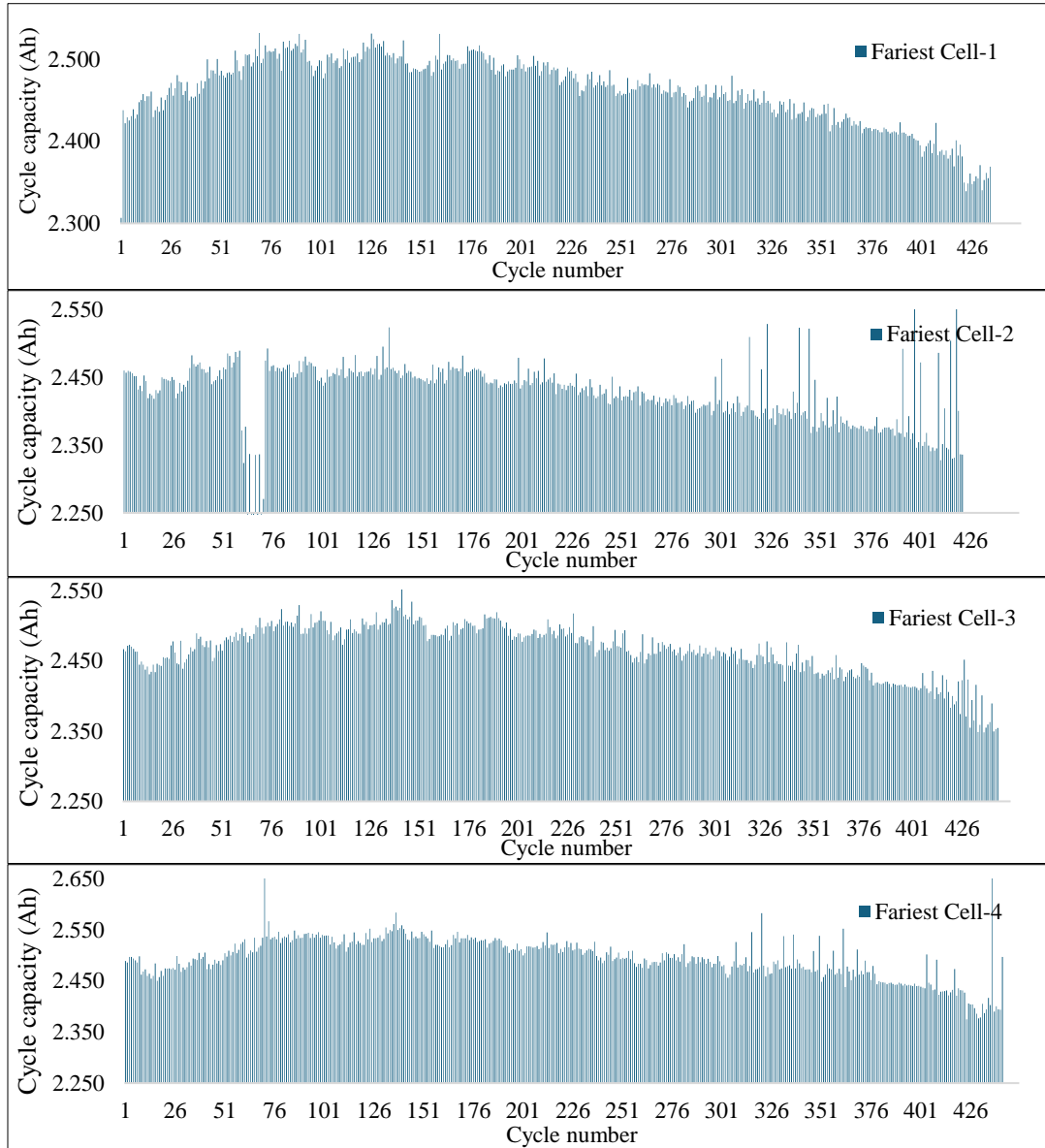
Fig. 4.11   Equivalent full cycles capacity graph for Fareast make cell no 1, 2, 3, and 4.

Figure 4.12 illustrating the percentage loss in capacity over electric field control capacity for Fareast make cells 1, 2, 3, and 4 provide valuable insights into the relative performance and degradation of each cell. By plotting the calculated percentage loss values against the respective cell numbers, the graph enables quick comparison and analysis of capacity loss trends across the cells. This information is essential for identifying potential issues, optimizing maintenance strategies, and ensuring efficient management of battery performance and longevity.
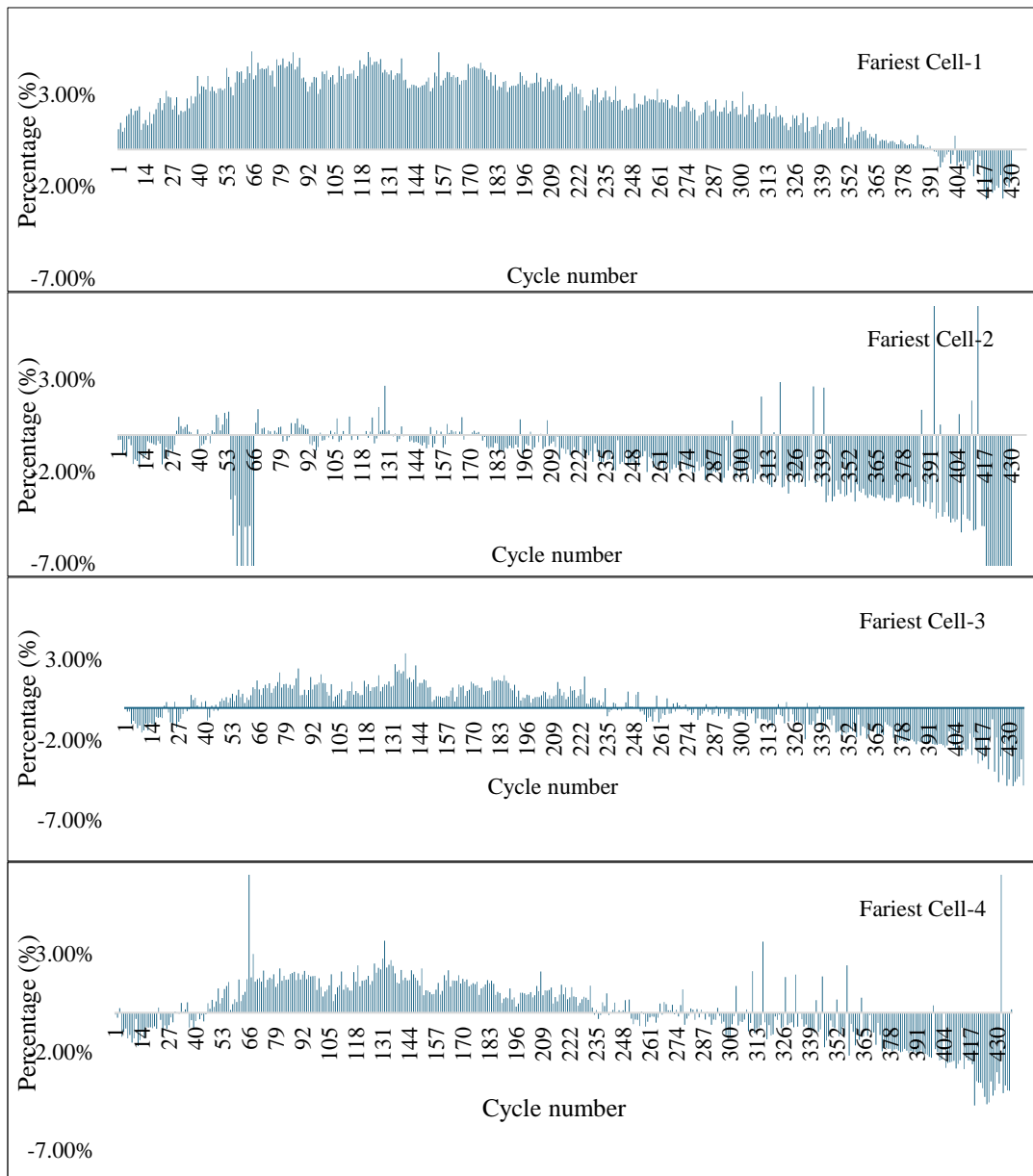
Fig. 4.12   Percentage loss in capacity over EFC capacity graph for Fareast make cell no 1, 2, 3, 4.

4.6   SOC EXPERIMENTATION AND CELL SELECTION

The primary objective of LIBs testing is to ensure proper function and safety in any environment by creating similar environmental conditions in which these batteries will operate. Several series of tests are according to industry standards from UL, SAE, IEC, and others with specific objectives including capacity checking and degradation, thermal abuse, heat resistance, temperature cycling, and short-circuiting under heat.

4.6.1   CELL AND BATTERY CAPACITY MEASUREMENT

Cell and battery packs either at individual cell level or entire battery pack level are undergoing the testing process. The process allows researchers to understand how individual cells degrade and how that translates to the overall performance of the battery pack. EFC is a standardized unit used to represent the cumulative wear and tear of a battery pack and EFC represents a complete discharge and recharge cycle of the battery. Fig. 4.13 shows the capacity loss compared to the initial capacity after a certain number of EFC and cell and battery packs are being tested as per details.

Cell & battery aging test plan

Cell	Battery	Step No	Step Type	Step Time	Oneset Date	End Date	Capacity (Ah)
CC Charge, I_j=43A Till V_t= 3.63V	CC Charge, I_j=43A Till V_t= 58.08V	1	CC Chg	00:56:28	2023-02-23 15:14:50	2023-02-23 16:11:19	28.2356
		2	Rest	00:05:00	2023-02-23 16:11:19	2023-02-23 16:16:19	0.0000
CV Charge, I_j= 43A Till V_t= 3.65V	CV Charge, I_j= 43A Till V_t= 51.20V	3	CV Chg	00:01:14	2023-02-23 16:16:19	2023-02-23 16:17:33	0.6175
		4	Rest	00:60:00	2023-02-23 16:17:33	2023-02-23 17:17:33	0.0000
Rest for 60 min	Rest for 60 min	5	CC DChg	02:02:19	2023-02-23 17:17:33	2023-02-23 19:19:52	91.9270
		6	Rest	00:15:00	2023-02-23 19:19:52	2023-02-23 19:34:52	0.0000
CC Discharge I_j=43A until V_t=2.50V	CC Discharge I_j=43A until V_t=40.00V	7	CC Chg	01:00:00	2023-02-23 19:34:52	2023-02-23 20:34:52	49.9993

Cell assembly

Fig. 4.13   (a) Cell and battery aging plan (b) schedule of LFP cell aging.

A complete schematic of an LFP battery pack experimental setup resembles a controlled environment for testing the battery's performance and characteristics. LFP battery pack comprises multiple lithium iron cells configured in series or parallel to achieve the desired voltage and capacity. A DC power source acts as a conductor, providing controlled voltage or current to the pack, simulating charging, discharging, or other operating conditions. The experimental setup covers a battery tester unit, host computer, software unit, data logger, and developed battery pack. The complete test setup is presented in Fig. 4.14, and it comprises of BK-3080 E/60 cycler equipped with proprietary software for test process programming, and a primary computer attached with transmission control protocol/internet protocol. With sixty-four separate channels, the BK-3080 E/60 can independently charge or discharge up to sixty-four cells based on the intended profile. The system can achieve a maximum voltage of 5 V and a maximum current of 100 A across multiple ranges from 1 A to 100 A. The current and voltage sensors exhibit measurement inaccuracies of less than 0.1%.
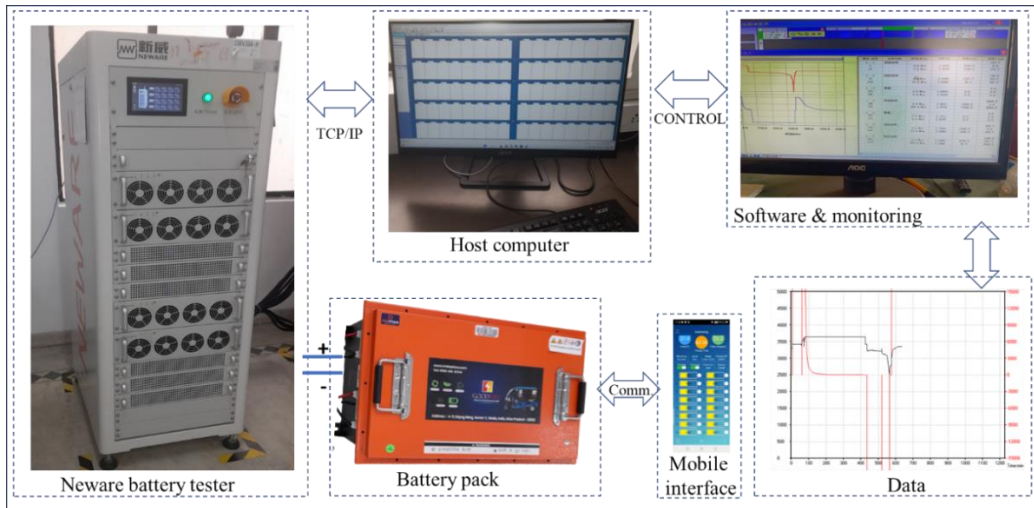
Fig. 4.14   Complete schematic of LFP battery pack experimental setup.

The BK-3080 E/60 Cycler was used to conduct individual testing of these cells. Table 4.5 depicts the test schedules devised to produce varied stimuli for these twenty cells. This study concentrates on the datasets obtained at 25℃ and a specific

stage of aging. At first, all cell discharge data were sorted for the first 0.18 minutes and documented for sorting for accepted/ rejected criteria.

Table 4.5   Individual LFP cell test plan.

Description	Details
Input voltage	AC200V~265V, 50Hz
Max DC battery Voltage range	5V
Min DC battery Voltage range	2V
Charging Current	43A
Discharging current	43A

4.6.2   CELL AND BATTERY PACK SPECIFICATION

In the investigation process, the experiments were carried out as per the plan for the LFP prismatic cell, a total of 20 fresh sample cells of the same batch, make and model were selected for experimentation and were marked as serial numbers 1 to 20. The vital characteristics of the cell were retrieved from manufacturer datasets and important parameters are listed in Table 4.6. An LFP cell is safe, has a long cycle life, and high-power density. It utilizes lithium iron phosphate as the cathode material, which provides excellent thermal stability and reduces the risk of thermal runaway. Proper thermal management is essential to optimize their performance and ensure longevity.

Table 4.6   Detail description of LFP cell.

Description	Details	Photograph
Manufacturer	Ganfung LiEnergy Part no: 48174133-086Ah	
Typical capacity	86.0Ah at C1 discharge rating	
Operating voltage	2.50V~3.65V [0°C<T≤60°C] 2.00V~3.65V [-20°C≤T≤0°C]	
Impedance (1KHz)	≤0.40mΩ	
Operating temperature	0~60℃	
Weight	≤2.30Kg	
Standard charge current	C/2 at 25±2℃ upto 3.65V	
Self-discharge	≤3.5%/month at 25±2℃	

Month of manufacturing	12/2022

All cells were put on initial constant current- constant voltage (CC-CV) charging at C/2 rate as per details of BK3080E/60 and technical specification along with a description of LFP aging machine are presented in Table 4.7. After fully charging and resting as per the charging plan, the cells were put into constant discharging at a C/2 rate. At the time scale, response voltage against charging and discharging current was measured through the host computer and recorded on a .CSV file.

Table 4.7   Description of LFP aging machine.

Description	Details
Input voltage	AC200V~265V, 50Hz
DC cell Voltage measurement range	0-5V
Charging Current	0-100A
Discharging current	0-100A
Data transmission	via RS232 port or network
Measurement Capacity	64 cells

4.7   ASSEMBLY OF BATTERY PACK

Within the realm of e-mobility, the vulnerability of LIBs to diverse environmental stressors such as thermal runaway, vibrations, and impacts from vehicle collisions poses a considerable risk to their overall integrity. This heightened sensitivity arises from the LIB responsiveness to ambient temperature fluctuations, external pressure variations, and dynamic mechanical loads. In the complex landscape of EVs, the safety and reliability of LIBs emerge as paramount concerns. These challenges constitute significant hurdles that must be surmounted for the widespread electrification of both public and private transportation sectors. The potential for failures induced by thermal runaways, vibrational forces, or impacts underscores the critical importance of addressing safety and reliability issues to ensure the successful and secure integration of electric vehicles into mainstream transportation infrastructure. Tackling these challenges head-on is essential for instilling confidence in technology and facilitating the large-scale adoption of e-mobility.

Accordingly, the LFP 51.2V86Ah (16S1P) Battery pack design & development of its BOM for the development of the experiment sample are carried out.

A resilient and dependable battery packaging design requires a comprehensive approach to tackle various design considerations, particularly focusing on thermal runaway, vibration isolation, and crash safety both at the individual cell level and within the modular structure. Addressing these critical issues is essential to ensure the integrity and functionality of the battery system. At the cell level, careful attention must be given to preventing thermal runaway events, as they can have detrimental effects on the overall performance and safety of the battery. The design should incorporate measures to manage and dissipate heat effectively, safeguarding against potential thermal issues. Additionally, vibration isolation measures are crucial to minimize the impact of external vibrations on the battery cells.

One common thread across these levels is the need to restrict relative motion between cells. This is vital to eliminate any potential points of failure within the battery pack. By minimizing movement between cells, the risk of mechanical stress, thermal inconsistencies, and other potential issues is mitigated, contributing to the overall robustness and reliability of the battery packaging design. In summary, a well-thought-out battery packaging design should holistically address thermal management, vibration isolation, and crash safety considerations at both the cell and modular levels, emphasizing the importance of restricting relative motion to enhance the overall reliability and durability of the battery system. Fig. 4.15 illustrates the LFP battery pack actual view with top cover opened and pack assembly for e-mobility.

Fig. 4.15   LFP battery pack actual view (a) battery pack with top cover opened, (b) battery pack ready for assembly with e-mobility.

4.8   BATTERY MANAGEMENT SYSTEM

A battery management system (BMS) serves as a crucial control unit designed to ensure the safe and efficient operation of a battery pack [2,3,4]. Its core function revolves around safeguarding the battery, with a primary focus on addressing safety concerns, managing cell balancing, and mitigating aging-related issues. The indispensable supervision of each cell is a critical aspect, driven by safety considerations and the need for optimal performance. Furthermore, the BMS plays a pivotal role in implementing preset corrective measures to address any abnormal conditions within the system infrastructure. This proactive approach not only enhances the overall safety of the battery pack but also contributes to its longevity and reliability. Beyond safety considerations, the BMS is also responsible for regulating the system temperature. Recognizing the significant impact of temperature on the power consumption profile, the BMS ensures the implementation of proper procedures to control and maintain the system temperature within optimal ranges. This multifaceted role underscores the BMS's comprehensive contribution to the overall health, safety, and performance of Li-ion battery systems. Looking at these aspects, the BMS (Model: JBD-SP25S003-L23S-80A-B-U) for LFP battery is used in the battery pack having the following specifications in Table 4.8.

Table 4.8   Specification of digital BMS.

Description	Parameter
Cell compatibility	LiFePO$_4$
Cell in series	13-25
Operating voltage	32.50- 86.25V
Operating current limit	100Amp
Cell charge protection	3.75VPC
Cell discharge protection	2.50VPC
Cell equalizing function	3.40VPC
Cell discharge protection	2.50VPC
Battery pack overcurrent protection	90V
Battery pack temperature operating range	-15-70°C
Battery pack short circuit protection	100A
RS485 & UART functionality	Yes
Charger type	CC-CV
Charging current	40A

4.9   MEASUREMENT OF CAPACITY AND CELL SELECTION

Batteries are created by connecting various cells in parallel or series arrangements. The requirement for stable batteries in electric vehicles cannot be met by the voltage, current, and capacity/energy levels of individual cells. Every cell has unique properties that set it apart from other comparable cells. These differences are amplified in battery packs that contain linked cells. Therefore, changes in battery performance degradation would be made worse by differences in cell state. Accordingly, individual LFP cells were capacity graded as per details and the measurement of values are as given in Table 4.9.

Table 4.9   Individual LFP cell test results and selection.

Final cell selection according to BMS setting (43A discharge)						
Cell no.	V_{OC} (mV) at 0.00 Min	V_{OC} (mV) at 0.18 Min	% variance	Total Dis$_{time}$ (minutes)	V_{EC} (mili V)	Dis$_{current}$ (milli A)	Remark
1	3601.40	3327.40	7.61%	129.75	2500.00	-43000.00	Reject
2	3363.80	3260.60	3.07%	128.50	2500.00		Accept
3	3334.20	3255.20	2.37%	127.93	2499.60		Accept
4	3405.40	3278.70	3.72%	128.62	2499.50		Accept

5	3472.30	3288.70	5.29%	128.58	2498.90		Accept
6	3371.80	3258.80	3.35%	129.33	2498.60		Accept
7	3411.60	3266.10	4.26%	128.32	2498.50		Accept
8	3367.30	3254.00	3.36%	129.57	2499.70		Accept
9	3583.70	3311.80	7.59%	130.90	2499.20		Accept
10	3331.00	3247.70	2.50%	128.37	2498.90		Accept
11	3423.80	3267.30	4.57%	130.17	2499.10		Accept
12	3646.40	3327.20	8.75%	129.78	2499.10		Reject
13	3432.90	3277.00	4.54%	129.13	2498.60		Accept
14	3628.50	3325.80	8.34%	127.77	2499.80		Reject
15	3590.30	3311.60	7.76%	129.32	2499.20		Reject
16	3332.90	3253.40	2.39%	127.37	2500.00		Accept
17	3583.70	3306.10	7.75%	130.10	2499.40		Accept
18	3441.90	3271.20	4.96%	130.22	2499.60		Accept
19	3405.50	3267.70	4.05%	130.95	2499.80		Accept
20	3561.30	3302.40	7.27%	129.82	2499.90		Accept

It is the battery operating environment that disperses variances in cell performance degradation to individual cells, and variations in cell performance degradation led to supply chain interactions. Since a non-uniform feature would result in a variation in the battery state, it is challenging to completely ensure the uniformity of the initial performance characteristics as well as the extrinsic or intrinsic process conditions of battery packs. Accordingly, cell numbers marked as 2-11, 13, 16-20 are selected for making battery packs. This assembled battery pack is put on a charging/ discharging cycle at the NEWARE battery pack testing machine, which is capable of undertaking up to 100V and 50A charging/ discharging. The battery pack was put into the charging (C/2) and discharging (C/2) test as per the details given in Table 4.10.

Table 4.10   Individual LFP battery pack test plan.

Description	Details
Input voltage	AC200V~265V, 50Hz
Max DC battery Voltage range	60V
Min DC battery Voltage range	40V
Charging Current	43A
Discharging current	43A

The test plan for an individual LFP battery pack involves defining objectives, specifying test conditions, ensuring safety measures, setting up equipment, conducting performance and safety tests, analyzing data, and preparing a comprehensive report. Performance tests assess capacity, energy efficiency, and cycle life, while safety tests evaluate responses to adverse conditions. The results inform design decisions, ensure compliance, and enhance product quality and reliability. Data on charging and discharging are stored in a PC hard drive for further analysis. The battery pack full cycle recipe (charge- rest-discharge- rest-charge) is as per Table 4.11.

Table 4.11   Battery pack single cycle aging log.

Step number	Step type	Step time	Onset date	End date	Capacity (Ah)
1	CC Chg	00:56:28	2023-02-23 15:14:50	2023-02-23 16:11:19	28.2356
2	Rest	00:05:00	2023-02-23 16:11:19	2023-02-23 16:16:19	0.0000
3	CV Chg	00:01:14	2023-02-23 16:16:19	2023-02-23 16:17:33	0.6175
4	Rest	00:60:00	2023-02-23 16:17:33	2023-02-23 17:17:33	0.0000
5	CC DChg	02:02:19	2023-02-23 17:17:33	2023-02-23 19:19:52	91.9270
6	Rest	00:15:00	2023-02-23 19:19:52	2023-02-23 19:34:52	0.0000
7	CC Chg	01:00:00	2023-02-23 19:34:52	2023-02-23 20:34:52	49.9993

4.10   CHAPTER SUMMARY

The integration of ML modeling in the domain of LIB, particularly in the context of e-mobility, marks a significant advancement. This integration is rooted in the historical development of MLs, and its pivotal role is highlighted across various scientific and technological domains. ML-based modeling serves the purpose of simulating continuum-scale behavior by incorporating information from

computational models at finer scales. ML methods are extensively employed to characterize various aspects of LIB, including performance, lifetime, reliability, and safety. A range of ML categories, such as supervised, unsupervised, semi-supervised, and reinforcement learning, along with specific methods like SVM, RVM, LSTM, GPR, and DL, are applied for data-driven approaches. The challenges in LIB especially within the context of e-mobility, are outlined, which include variables related to performance, lifespan, safety, cost, environmental impact, and resource management. ML emerges as a valuable tool in addressing the trial-and-error approach prevalent in LIB research, offering a data-driven alternative for predicting battery component properties. The chapter also emphasizes the necessity of battery aging data for ML methods and addresses challenges in bridging the gap between laboratory and practical applications. Performance metrics, including MAE, MSE, RMSE, and MAPE, are proposed to be utilized for evaluating the accuracy of ML models in predicting different states of LIBs.

The chapter emphasizes the continuous need for improvement in ML-based state estimation methods, considering factors like computational cost and real-world applicability. This chapter provides an in-depth examination of experimental procedures and outcomes related to SOH and SOC estimation in batteries. It encompasses a meticulous investigation into various cell types, specifically NMC and LFP cells, focusing on estimating their capacities through diverse protocols. Additionally, it delves into the intricacies of cell selection, matching, and grading processes, elucidating the methodologies employed for battery pack assembly in detail. Moreover, the chapter offers a thorough analysis of the phenomenon of cell fading, emphasizing its significance in the context of SOH estimation. By elucidating the mechanisms underlying cell degradation over time, the narrative underscores the necessity of factoring in such degradation phenomena when assessing the health of battery cells. Furthermore, the chapter presents a specialized investigation into SOC estimation, utilizing a battery pack comprising LFP

prismatic cells. This segment encompasses an exhaustive exploration and experimentation regarding capacity estimation methodologies, alongside an assessment of cell matching to ensure optimal performance in the construction of a robust battery pack. Additionally, the chapter discusses the implementation of a battery management system to monitor and regulate the SOC of the battery pack effectively.

CHAPTER 5

RESULTS AND DISCUSSIONS

5.1   CHAPTER OVERVIEW

For the estimation of the state of health of NMC cylindrical cells, we propose the implementation of three simplistic, data-driven modeling techniques and unique estimation methodologies. This novel estimation method utilizes both the charge and discharge capacities employs multiple ambient temperatures with two distinct discharging cycles for data analysis and reports the model's performance on four error techniques. The validity of the results is further corroborated through the results of cells from various manufacturers having the same electrochemical composition, to ensure the generalizability of the outcomes. For the estimation of the state of charge of LFP prismatic cells and battery packs, we propose the implementation of simplistic, data-driven modeling techniques utilizing linear regression algorithms. This approach encompasses the selection of appropriate LFP cells, the assembly of battery packs, and the undertaking of experimental and analytical work. We aim to contribute meaningful insights that will guide both commercial technology strategies and academic research initiatives, promoting progress in data-driven state estimation methodologies of both NMC and LFP cell chemistries for SOH and SOC estimation for e-mobility applications.

5.2   STATE OF HEALTH ESTIMATION

In the context of SOH estimation, DT, KNN, and RF algorithms were utilized for estimating and predicting the performance of LIB, highlighting the model's performance on MAPE, RMSE, MSE, and MAE. The experimental setup is designed to conduct an extensive analysis, encompassing the thorough characterization of multiple discharge cycles at both 1C and 2C rates, along with a

meticulously controlled 0.5C charging process. A noteworthy aspect of this experimentation is the variation of temperature conditions, 15℃, 25℃, and 35℃, to comprehensively assess the battery performance under different operational and thermal stresses.

The primary focus during this experimentation lies in scrutinizing key parameters, with a particular emphasis on the discharge capacity and charge capacity. By subjecting the LIBs to diverse discharge rates and temperature environments, the research aims to gain a nuanced understanding of how these factors influence the overall performance and durability of the batteries. This approach enhances the robustness and reliability of the findings, providing valuable insights into the intricate dynamics of LIB behavior under varying operational conditions. For data analytics, a rigorous approach is employed, where 80% of the acquired data is dedicated to training the analytical models, while the remaining 20% is reserved for robust testing and validation. It's crucial to emphasize that the entire dataset, encompassing full capacity values, is utilized in each case. This approach ensures a comprehensive and representative dataset, enhancing the reliability and applicability of the ensuing analytics. The general flowchart of experiments with ultimate research goals is given in Fig. 5.1.
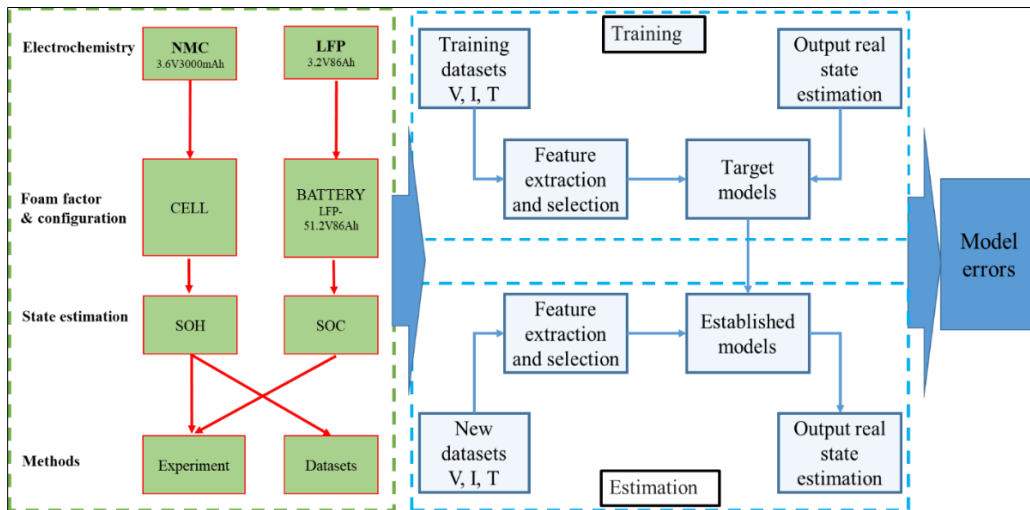
Fig. 5.1　　　　Experiment plan cell and battery.

101

By systematically examining discharge and charge capacities across different temperatures and employing a meticulous division of data for training and testing, this experimental design aims to yield insights that can contribute to a nuanced understanding of battery performance under diverse conditions. This approach not only bolsters the accuracy of the data-driven models but also enhances their generalizability and utility across various operational scenarios. Experimental verification in an ML algorithm refers to the process of testing the performance of an ML model on a specific dataset or task. In this process, the dataset is divided into training and testing sets, the model is trained on the training set, and its performance is assessed on the testing set [260]. The DT, KNN, and RF algorithm helps to determine the system performance generate new unseen data, and provide insights into areas where the system needs improvement [261]. Additionally, experimental verification involves comparing the performance of different models to identify the best approach for a given task. Table 5.1 lists different test metrics for lithium-ion cell 'a' and cell 'b' with different charge and discharge rates at 1C and 2C for DOD of 0-100% at a different temperature range of 15℃, 25℃, and 35℃.

Table 5.1   Test matrix for lithium-ion cell 'a' and cell 'b' with different charges and discharge rates.

DOD	Temperature	Discharge rate	Charging rate	Charge capacity	Discharge capacity
0%–100%	15°C	1C & 2C	0.5C	Cell 'a' and 'b'	Cell 'a' and 'b'
0%–100%	25°C	1C & 2C	0.5C	Cell 'a' and 'b'	Cell 'a' and 'b'
0%–100%	35°C	1C & 2C	0.5C	Cell 'a' and 'b'	Cell 'a' and 'b'

The modeling is executed with Google Colaboratory programming which allows writing and executing Python code. This is a cloud-based platform that provides free access to graphics processing units and tensor processing units for running

Python code. In the experiment, the aging data of cell 'a' is used to validate the generalization and accuracy of the model through DT, KNN, and RF algorithms. First, 80% of the data is used for training, and the remaining 20% are utilized to assess the model's fundamental functionality. The model is next evaluated using all the data in cell 'b' to determine its generalizability and robustness. At last, the model is utilized to estimate SOH at various temperatures to further confirm its effectiveness.

5.2.1 HEALTH ESTIMATION THROUGH CHARGE CAPACITY

Figures 5.2 (a) and 5.2 (b) illustrate the expected against actual charge capacity health estimation using the decision tree algorithm for cells 'a' and 'b' at 15℃ for a discharge rate of 1C and 2C along with LIBs cycle index. Charge capacity health prediction of LIB involves measuring the battery's capability to store and deliver power over time and assessing its remaining capacity relative to its original capacity. Using the decision tree algorithm, the charge capacity of the lithium-ion cell exhibits 2.8 Ah at the beginning of the cycle index and falls to 2.0 Ah after 400 cycles at 1C and 2C discharge rates. Cell 'b' exhibits similar characteristics but at 2C discharge rate predicted and actual behavior are identical whereas at 1C minor deviation is observed.
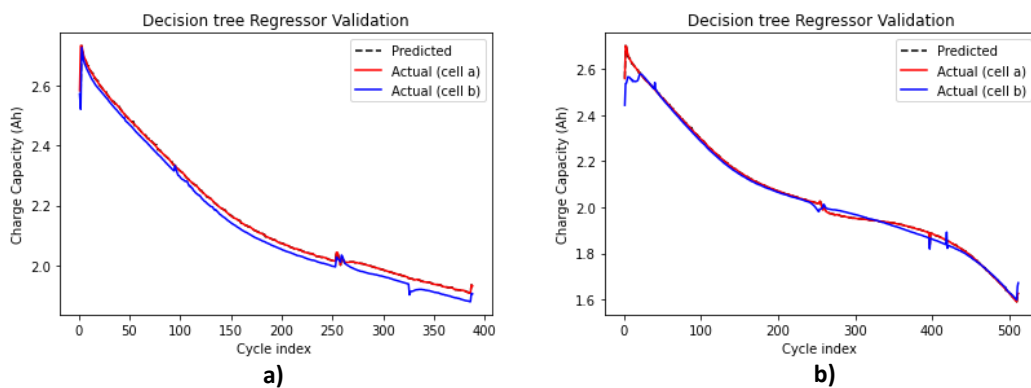
Fig. 5.2   Predicted versus actual charge capacity health estimation using decision tree algorithm for cells 'a' and 'b' at 15℃ for (a) 1C discharge rate and (b) 2C discharge rate with cycle index.

Figures 5.3 (a) and 5.3 (b) illustrate the expected against actual charge capacity health estimation using the decision tree algorithm for cells 'a' and 'b' at 25℃ for a discharge rate of 1C and 2C along with LIBs cycle index. Using the DT algorithm, the charge capacity of the lithium-ion cell exhibits 3.0 Ah at the beginning of the cycle index and falls to 2.35 Ah after 530 cycles at 1C and 2C discharge rate cell exhibit 3.0 Ah at the beginning of the cycle index and falls to 2.2 Ah after 650 cycles at 25℃. This is typically done by measuring the battery's voltage and current output during charge and discharge rate and analyzing the data using mathematical models to estimate the battery's SOH. Accurate SOH prediction of LIB is an important attribute for ensuring the dependable and secure operation of the system, as well as optimizing battery performance and minimizing costs associated with battery replacement.
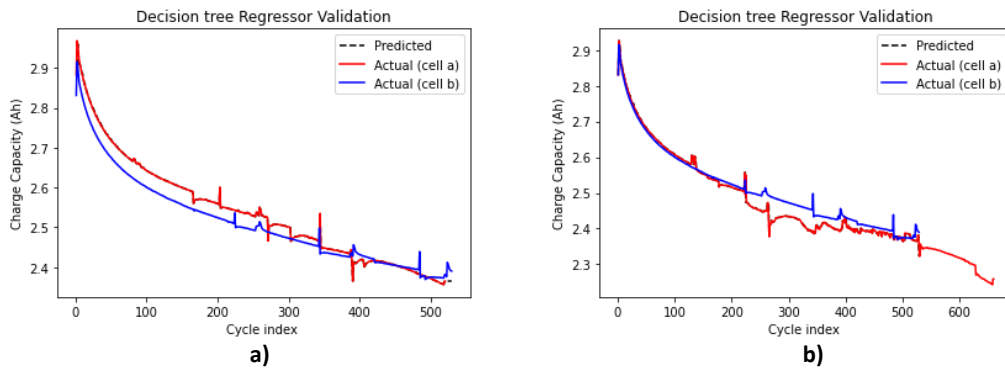
Fig. 5.3   Predicted versus actual charge capacity health estimation using decision tree algorithm for cells 'a' and 'b' at 25℃ for (a) 1C discharge rate and (b) 2C discharge rate with cycle index.

Figures 5.4 (a) and 5.4 (b) illustrate the predicted against actual charge capacity health estimation using the decision tree algorithm for cells 'a' and 'b' at 35℃ for a discharge rate of 1C and 2C along with LIBs cycle index. Using the DT algorithm, the charge capacity of the lithium-ion cell exhibits 3.0 Ah at the beginning of the cycle index and falls to 2.4 Ah after 800 cycles at 1C, and at 2C discharge rate cell exhibits 3.0 Ah at the beginning of the cycle index and falls to 2.2 Ah after 800

cycles at 35°C. Cell 'b' exhibits wide variation against predicted and actual behavior at 2C discharge rate whereas identical behavior at 1C is observed.
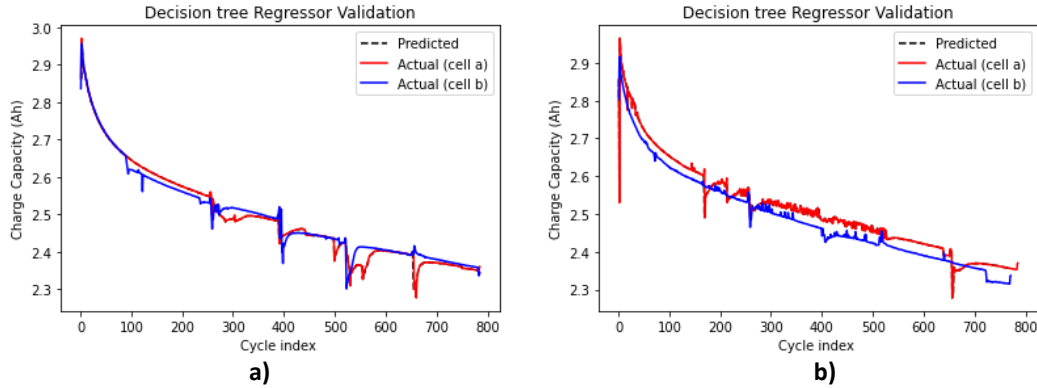
Fig. 5.4   Predicted versus actual charge capacity health estimation using decision tree algorithm for cells 'a' and 'b' at 35℃ for a) 1C discharge rate and b) 2C discharge rate with cycle index.

Figures 5.5 (a) and 5.5 (b) illustrate the predicted against actual charge capacity health estimation using the K-nearest neighbor algorithm for cells 'a' and 'b' at 15℃ for a discharge rate of 1C and 2C along with LIBs cycle index. This is done by measuring the battery's voltage and current output during charge cycles and analyzing the data using mathematical models to estimate the battery's SOH. Accurate estimation of battery SOH ensures the safe and reliable operation of battery-powered systems, as well as optimizing battery performance and minimizing costs associated with battery replacement. Using the KNN algorithm, the charge capacity of the lithium-ion cell exhibits 2.7 Ah in the beginning and falls to 1.6 Ah after 510 cycles at 1C, and at 2C discharge rate cell exhibits 2.6 Ah at the beginning of the cycle index and falls to 1.8 Ah after 380 cycles at 15℃.
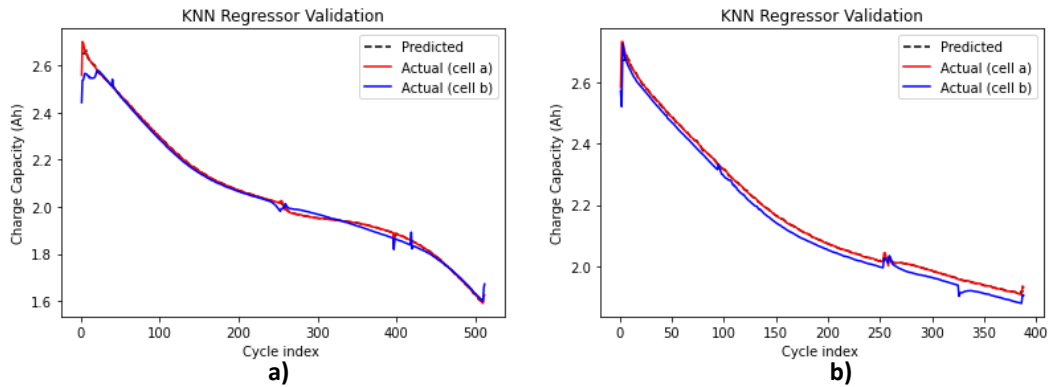
Fig. 5.5   Predicted versus actual charge capacity health estimation using KNN regressor algorithm for cells 'a' and 'b' at 15℃ for a) 1C discharge rate and b) 2C discharge rate with cycle index.

Figures 5.6 (a) and 5.6 (b) illustrate the predicted against actual charge capacity health estimation using the K-nearest neighbor algorithm for cells 'a' and 'b' at 25℃ for a discharge rate of 1C and 2C along with LIBs cycle index. Using the KNN algorithm, the charge capacity of the lithium-ion cell exhibits 3.0 Ah at the beginning of the cycle index and falls to 2.3 Ah after 550 cycles at 1C, and at 2C discharge rate cell exhibits 2.9 Ah at the beginning of the cycle index and falls to 2.4 Ah after 650 cycles at 25℃.
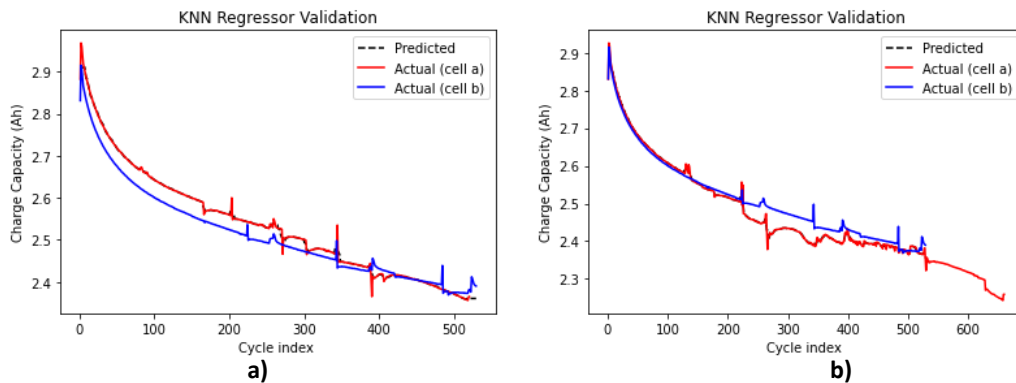
Fig. 5.6   Predicted versus actual charge capacity health estimation using KNN regressor algorithm for cells 'a' and 'b' at 25℃ for a) 1C discharge rate and b) 2C discharge rate with cycle index.

106

Figures 5.7 (a) and 5.7 (b) illustrate the predicted against actual charge capacity health estimation using the K-nearest neighbor algorithm for cells 'a' and 'b' at 35℃ for a discharge rate of 1C and 2C along with LIBs cycle index. Using the KNN algorithm, the charge capacity of the lithium-ion cell exhibits 2.95 Ah at the beginning of the cycle index and falls to 2.4 Ah after 800 cycles at 1C and 2C discharge rate cell exhibits 2.9 Ah at the beginning of the cycle index and falls to 2.35 Ah after 780 cycles at 35℃.
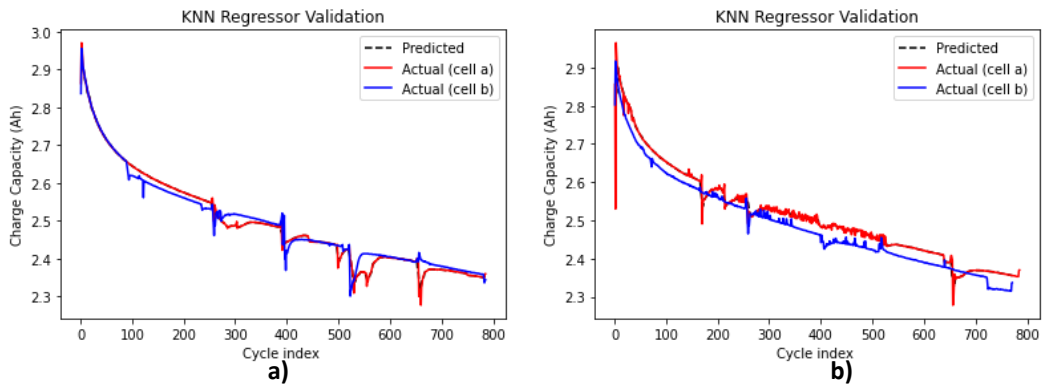
Fig. 5.7   Predicted versus actual charge capacity health estimation using KNN regressor algorithm for cells 'a' and 'b' at 35℃ for a) 1C discharge rate and b) 2C discharge rate with cycle index.

Figures 5.8 (a) and 5.8 (b) illustrate the predicted against actual charge capacity health estimation using a random forest algorithm for cells 'a' and 'b' at 15℃ for a discharge rate of 1C and 2C along with LIBs cycle index. This is done by examining the battery's voltage and current output data during charge cycles and analyzing the data using random forest ML models to estimate the battery's SOH. Using the random forest algorithm, the charge capacity of the lithium-ion cell exhibits 2.6 Ah at the beginning of the cycle index and falls to 1.6 Ah after 510 cycles at 1C, and at 2C discharge rate cell exhibits 2.7 Ah at the beginning of the cycle index and falls to 1.8 Ah after 380 cycles at 15℃.
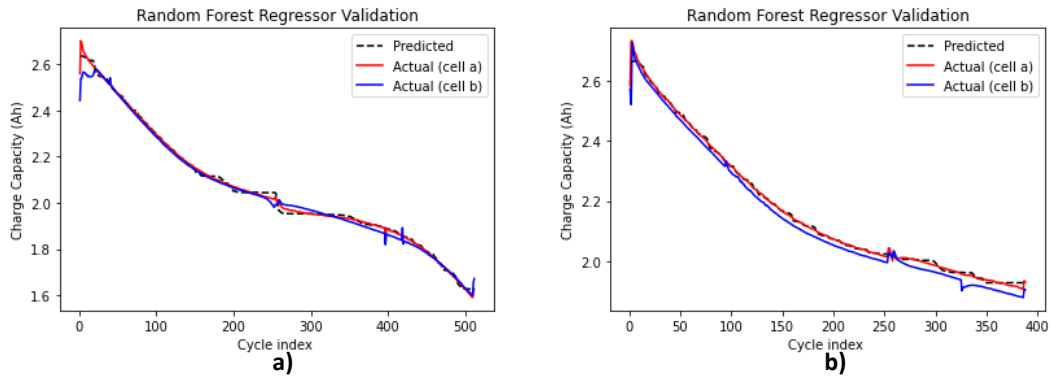
Fig. 5.8   Predicted versus actual charge capacity health estimation using random forest regressor algorithm for cells 'a' and 'b' at 15℃ for a) 1C discharge rate and b) 2C discharge rate with cycle index.

Figures 5.9 (a) and 5.9 (b) illustrate the predicted against actual charge capacity health estimation using a random forest algorithm for cells 'a' and 'b' at 25℃ for a discharge rate of 1C and 2C along with LIBs cycle index. Using the random forest algorithm, the charge capacity of the lithium-ion cell exhibits 3.0 Ah at the beginning of the cycle index and falls to 2.4 Ah after 520 cycles at 1C and at 2C discharge rate cell exhibits 2.9 Ah at the beginning of the cycle index and falls to 2.4 Ah after 530 cycles at 25℃.
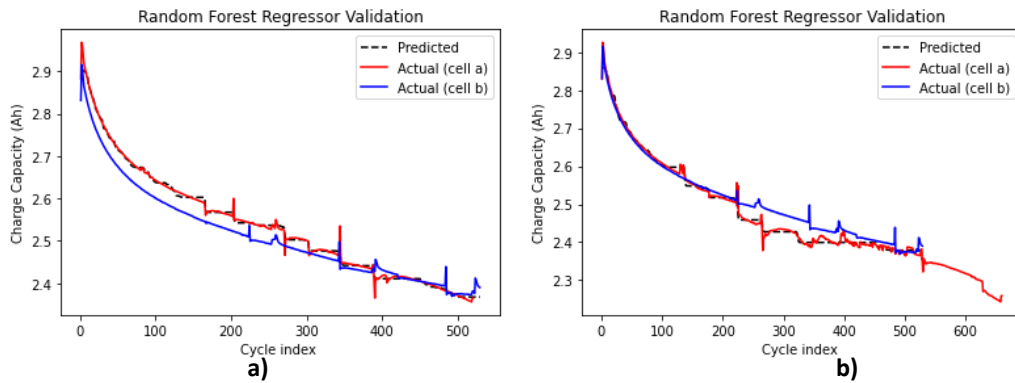
Fig. 5.9   Predicted versus actual charge capacity health estimation using random forest regressor algorithm for cells 'a' and 'b' at 25℃ for a) 1C discharge rate and b) 2C discharge rate with cycle index.

Figures 5.10 (a) and 5. 10 (b) illustrate the predicted against actual charge capacity health estimation using a random forest algorithm for cells 'a' and 'b' at 35℃ for a discharge rate of 1C and 2C along with LIBs cycle index. Using the random forest algorithm, the charge capacity of the lithium-ion cell exhibits 3.0 Ah at the beginning of the cycle index and falls to 2.4 Ah after 800 cycles at 1C and at 2C discharge rate cell exhibits 3.0 Ah at the beginning of the cycle index and falls to 2.4 Ah after 800 cycles at 35℃.
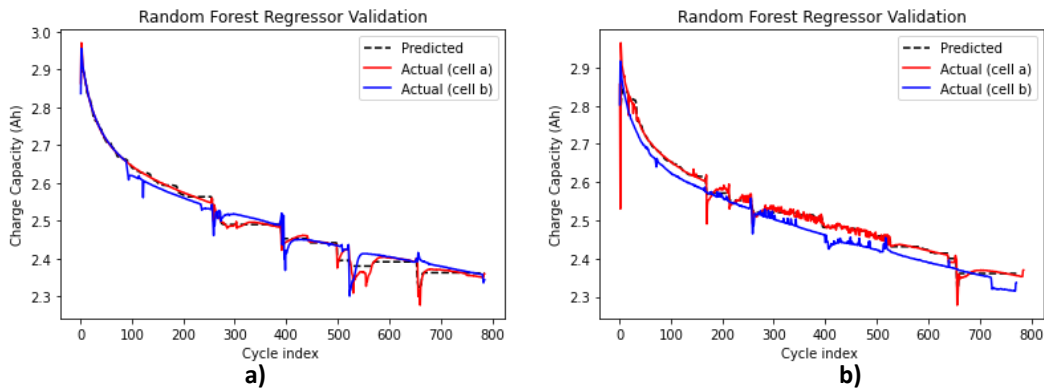
Fig. 5.10   Predicted versus actual charge capacity health estimation using random forest regressor algorithm for cells 'a' and 'b' at 35℃ for a) 1C discharge rate and b) 2C discharge rate with cycle index.

5.2.2   HEALTH ESTIMATION THROUGH DISCHARGE CAPACITY

The discharge characteristics of a LIB represent the quantity of electrical charge that can be delivered by the battery before it needs to be recharged. State of health estimation of a LIB typically involves monitoring the battery's discharge capacity and other performance metrics over time to determine its remaining useful life and predict when it will need to be replaced. Factors that can affect the health of a LIB include the number of discharge cycles it has undergone, operating temperature, and usage patterns. Figures 5.11 (a) and 5.11 (b) illustrate the predicted against actual discharge capacity health estimation using the decision tree algorithm for cells 'a' and 'b' at 15℃ for a discharge rate of 1C and 2C along with LIBs cycle index. Using the decision tree algorithm, the discharge capacity of the lithium-ion

cell exhibits 2.6 Ah at the beginning of the cycle index and falls to 1.6 Ah after 510 cycles at 1C, and at 2C discharge rate, the discharge capacity of the lithium-ion cell exhibits 2.7 Ah at the beginning of cycle index and falls to 1.8 Ah after 380 cycles.
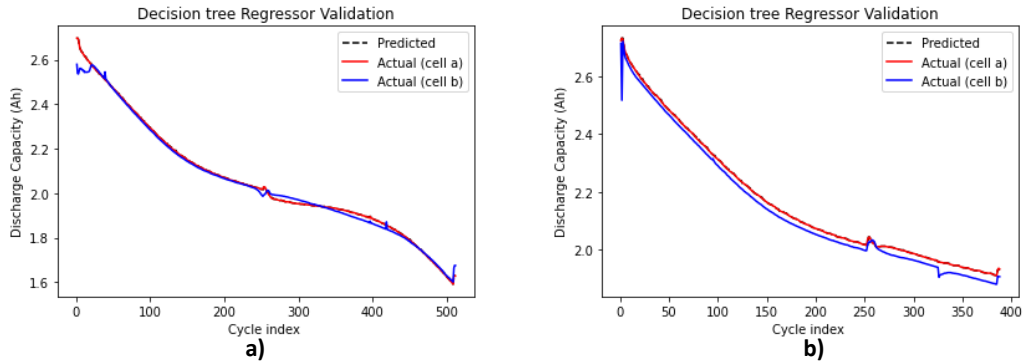
Fig. 5.11 Predicted versus actual discharge capacity health estimation using decision tree regressor algorithm for cells 'a' and 'b' at 15℃ for a) 1C discharge rate and b) 2C discharge rate with cycle index.

Figures 5.12 (a) and 5.12 (b) illustrate the predicted against actual discharge capacity health estimation using the decision tree algorithm for cells 'a' and 'b' at 25℃ for a discharge rate of 1C and 2C along with LIBs cycle index. Using the DT algorithm, the discharge capacity of the lithium-ion cell exhibits 2.9 Ah at the beginning of the cycle index and falls to 2.4 Ah after 510 cycles at 1C, and at 2C discharge rate cell exhibits 2.9 Ah at the beginning of the cycle index and falls to 2.3 Ah after 680 cycles at 25℃.
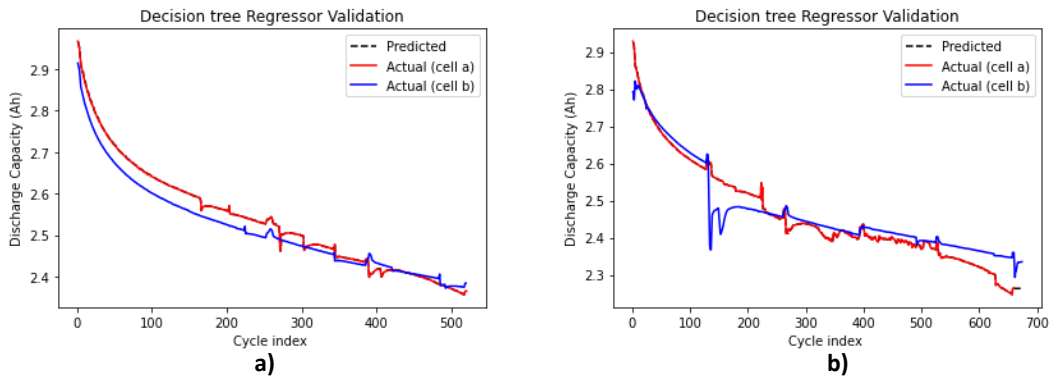
Fig. 5.12   Predicted versus actual discharge capacity health estimation using decision tree regressor algorithm for cells 'a' and 'b' at 25℃ for a) 1C discharge rate and b) 2C discharge rate with cycle index.

Figures 5.13 (a) and 5.13 (b) illustrate the predicted against actual discharge capacity health estimation using the decision tree algorithm for cells 'a' and 'b' at 35℃ for a discharge rate of 1C and 2C along with LIBs cycle index. Using the DT algorithm, the discharge capacity of the lithium-ion cell exhibits 3.0 Ah at the beginning of the cycle index and falls to 2.35 Ah after 800 cycles at 1C, and at 2C discharge rate cell exhibits 3.0 Ah at the beginning of the cycle index and falls to 2.4 Ah after 780 cycles at 35℃.
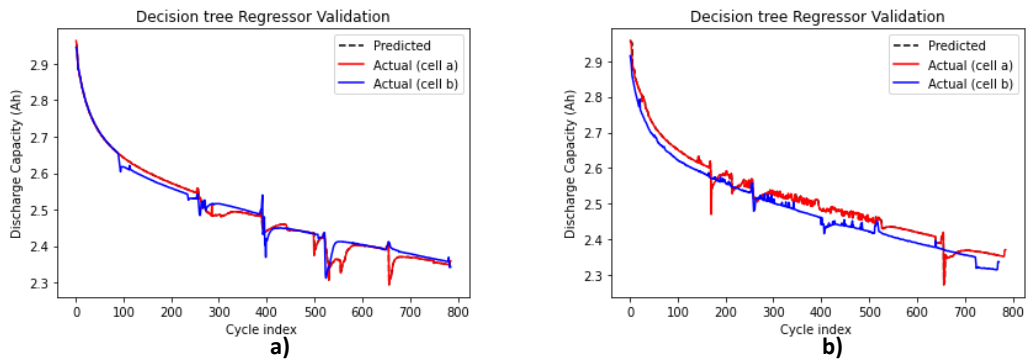
Fig. 5.13   Predicted versus actual discharge capacity health estimation using decision tree regressor algorithm for cells 'a' and 'b' at 35℃ for a) 1C discharge rate and b) 2C discharge rate with cycle index.

Figures 5.14 (a) and 5.14 (b) illustrate the predicted against actual discharge capacity health estimation using the K-nearest neighbor algorithm for cells 'a' and 'b' at 15℃ for a discharge rate of 1C and 2C along with LIBs cycle index. Using the KNN algorithm, the discharge capacity of the lithium-ion cell exhibits 2.60 Ah at the beginning of the cycle index and falls to 1.6 Ah after 510 cycles at 1C, and at 2C discharge rate cell exhibits 2.7 Ah at the beginning of the cycle index and falls to 1.8 Ah after 380 cycles at 15℃.
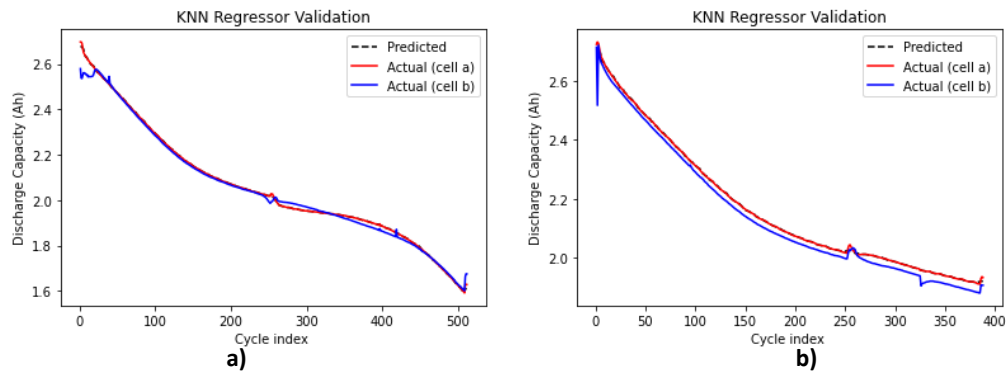
Fig. 5.14   Predicted versus actual discharge capacity health estimation using KNN regressor algorithm for cells 'a' and 'b' at 15℃ for a) 1C discharge rate and b) 2C discharge rate with cycle index.

Figures 5.15 (a) and 5.15 (b) illustrate the predicted against actual discharge capacity health estimation using the K-nearest neighbor algorithm for cells 'a' and 'b' at 25℃ for a discharge rate of 1C and 2C along with LIBs cycle index. Using the KNN algorithm, the discharge capacity of the lithium-ion cell exhibits 3.0 Ah at the beginning of the cycle index and falls to 2.35 Ah after 530 cycles at 1C and 2C discharge rate cell exhibits 3.0 Ah at the beginning of the cycle index and falls to 2.2 Ah after 650 cycles at 25℃.
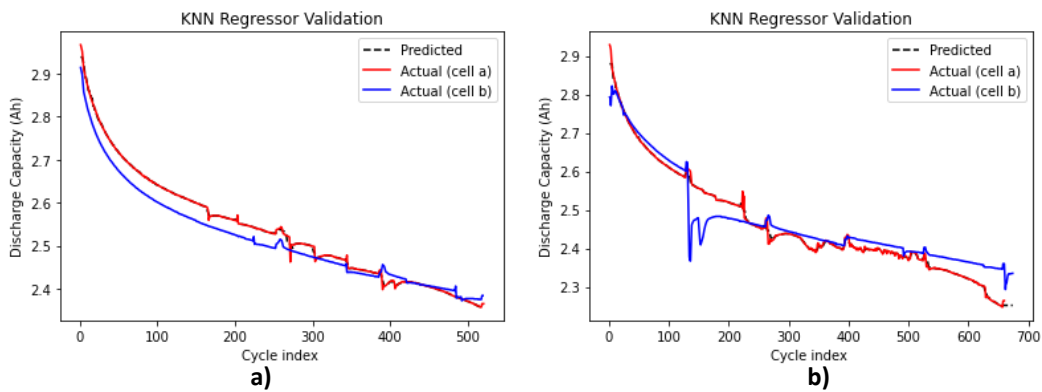
Fig. 5.15   Predicted versus actual discharge capacity health estimation using KNN regressor algorithm for cells 'a' and 'b' at 25℃ for a) 1C discharge rate and b) 2C discharge rate with cycle index.

Figures 5.16 (a) and 5.16 (b) illustrate the predicted against actual discharge capacity health estimation using the K-nearest neighbor algorithm for cells 'a' and 'b' at 35℃ for a discharge rate of 1C and 2C along with LIBs cycle index. Using the KNN algorithm, the discharge capacity of the lithium-ion cell exhibits 3.0 Ah at the beginning of the cycle index and falls to 2.35 Ah after 800 cycles at 1C and 2C discharge rate cell exhibits 3.0 Ah at the beginning of the cycle index and falls to 2.3 Ah after 760 cycles at 35℃.
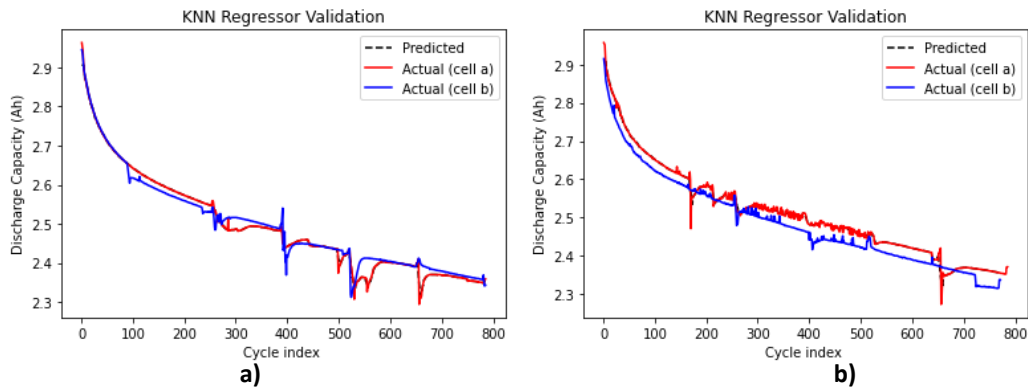
Fig. 5.16   Predicted versus actual discharge capacity health estimation using KNN regressor algorithm for cells 'a' and 'b' at 35℃ for a) 1C discharge rate and b) 2C discharge rate with LIBs cycle index.

Figures 5.17 (a) and 5.17 (b) illustrate the predicted against actual discharge capacity health estimation using a random forest algorithm for cells 'a' and 'b' at 15℃ for a discharge rate of 1C and 2C along with LIBs cycle index. Using the random forest algorithm, the discharge capacity of the lithium-ion cell exhibits 2.6 Ah at the beginning of the cycle index and falls to 1.6 Ah after 520 cycles at 1C, and at 2C discharge rate cell exhibits 2.7 Ah at the beginning of the cycle index and falls to 1.8 Ah after 380 cycles at 15℃.
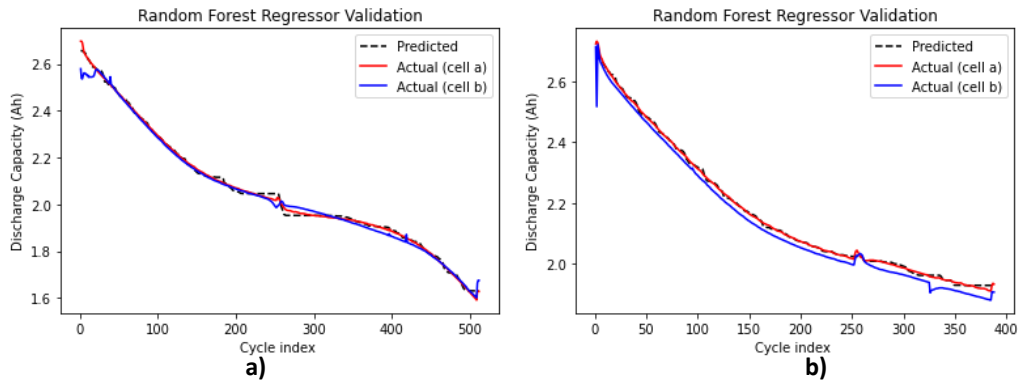
Fig. 5.17 Predicted versus actual discharge capacity health estimation using random forest regressor algorithm for cells 'a' and 'b' at 15℃ for a) 1C discharge rate and b) 2C discharge rate with cycle index.

Figures 5.18 (a) and 5.18 (b) illustrate the predicted against actual discharge capacity health estimation using a random forest algorithm for cells 'a' and 'b' at 25℃ for a discharge rate of 1C and 2C along with LIBs cycle index. Using the random forest algorithm, the discharge capacity of the lithium-ion cell exhibits 3.0 Ah at the beginning of the cycle index and falls to 2.35 Ah after 530 cycles at 1C and at 2C discharge rate cell exhibits 3.0 Ah at the beginning of the cycle index and falls to 2.3 Ah after 680 cycles at 25℃.
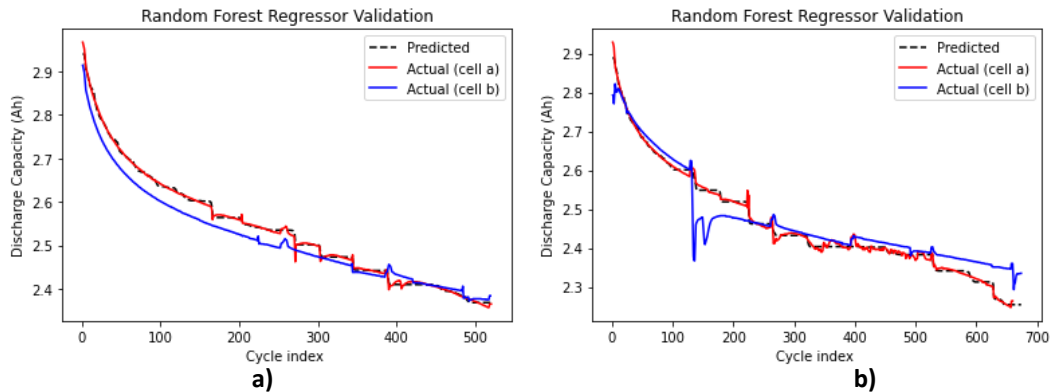
Fig. 5.18 Predicted versus actual discharge capacity health estimation using random forest regressor algorithm for cells 'a' and 'b' at 25℃ for a) 1C discharge rate and b) 2C discharge rate with cycle index.

Figures 5.19 (a) and 5.19 (b) illustrate the predicted against actual discharge capacity health estimation using a random forest algorithm for cells 'a' and 'b' at 35℃ for a discharge rate of 1C and 2C along with LIBs cycle index. Using the random forest algorithm, the discharge capacity of the lithium-ion cell exhibits 3.0 Ah at the beginning of the cycle index and falls to 2.35 Ah after 800 cycles at 1C and at 2C discharge rate cell exhibits 3.0 Ah at the beginning of the cycle index and falls to 2.3 Ah after 800 cycles at 35℃.
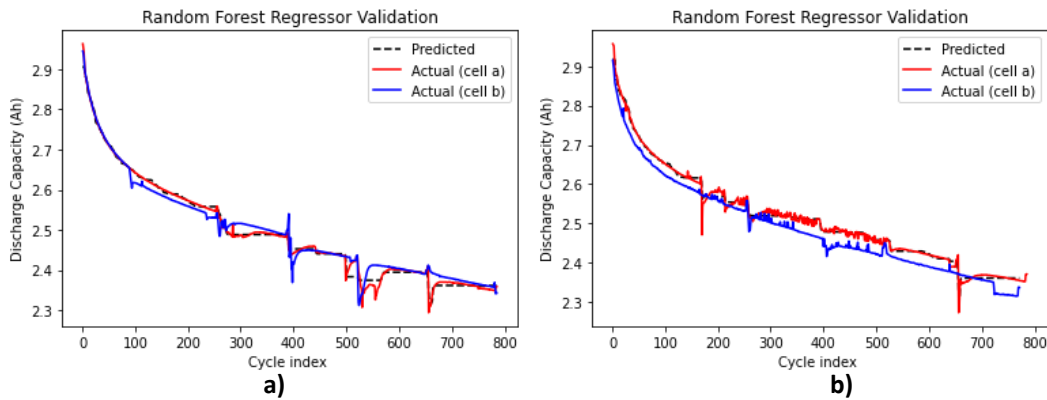
Fig. 5.19   Predicted versus actual discharge capacity health estimation using random forest regressor algorithm for cells 'a' and 'b' at 35℃ for a) 1C discharge rate and b) 2C discharge rate with cycle index.

For charging capacity estimation, at 35℃, KNN and DT have the best result of SOH prediction for both 1C and 2C discharge rates. For discharging capacity estimation, at 35℃, KNN & DT have the best result of SOH prediction for a 2C discharge rate. A similar result has been predicted for KNN on similar parameters. For charging capacity estimation at 25℃, DT has achieved a better result in comparison with both RF and KNN. For discharging capacity estimation at 25℃, KNN & DT achieved a better result in 2C, in comparison with both RF in similar parameters. For charging capacity estimation, at 15℃, both KNN and DT have achieved a better result in comparison with RF. At all temperatures, the output of the KNN and DT model is closer to the measured value than the RF model. At 15℃ at 2C, the RF model's output is also optimal, although some of the individual points differ from

the values that were measured. The correctness of the KNN and DT models is significantly higher than the RF model. Verifications are made because the model's generalizability is crucial, 100% data of cell 'b' is used to test and train the model to verify the generalizability of different models. The output of RF, KNN, and DT when using 80% training data, shows that errors increase after different datasets of cell 'b' are used, but the errors of KNN and DT methods are significantly smaller than those of RF. It is important to note that the KNN and DT model enhances the model's generalizability and can still demonstrate strong estimation capabilities.

It is demonstrated from the model's training data results that the proposed features can help the model achieve accurate estimation using KNN and DT. Compared with RF, KNN, and DT, the KNN model has the highest accuracy and lowest error. Hence, even after training with only 100% of the data from cell 'b' the KNN model can still produce accurate SOH estimates. Different temperatures over the nominal significantly influence the cycle life of LIB and impact SOH prediction. Therefore, all these models are to be further verified at high temperature and low temperature respectively for all cells 'a' and cell 'b' with similar discharge and charge conditions. The results signify that a suitable selection of a data-driven method is very important. The result signifies that further development of a fault-tolerant mechanism of BMS requires higher learning with the incremental value being required to be used.

5.2.3   ERROR COMPARISON WITH DIFFERENT METHODS

Error comparisons obtained with different methods are important to consider the nature of the error for charge and discharge characteristics for the SOH prediction. Error metrics are calculated through different methods to evaluate the quality of their SOH prediction results. Mean absolute error, mean absolute percentage error, mean squared error, and root mean squared error are used in the regression problems, while the classification problem covers the accuracy score. The scale of the error metrics also affects how errors are compared, and it is difficult to compare

these methods directly, so normalizations are done to make the comparison more meaningful. Statistical significance is observed to ensure that any differences in error through MAE, MAPE, MSE, and RMSE between methods are significant. Table 5.2, Table 5.3, and Table 5.4 list out a comparison of testing and training dataset results for cell 'a' using the MAPE, RMSE, MSE, and MAE error techniques for the three supervised learning algorithms DT, KNN, and RF regressors at 15℃, 25℃, and 35℃ respectively.

Table 5.2   Comparison of testing dataset results using the MAPE, RMSE, MSE, and MAE error techniques for the three supervised learning algorithms DT, KNN, and RF regressors at 15℃.

Test and Training Dataset (80% Training + 20% Testing for cell 'a') NMC cell at 15℃			
Model	DT	KNN	RF
	Error Value	Error Value	Error Value
MAE	2.63725E-03	1.91569E-03	8.22488E-03
MAPE	1.32111E-03	9.85191E-04	4.19216E-03
RMSE	5.60724E-03	3.13331E-03	1.11461E-02
MSE	3.14412E-05	9.81765E-06	1.24236E-04

Table 5.3   Comparison of testing dataset results using the MAPE, RMSE, MSE, and MAE error techniques for the three supervised learning algorithms DT, KNN, and RF regressors at 25℃.

Test and Training Dataset (80% Training + 20% Testing for cell 'a') NMC cell at 25℃			
Model	DT	KNN	RF
	Error Value	Error Value	Error Value
MAE	3.78641E-03	3.62524E-03	6.16931E-03
MAPE	1.48921E-03	1.40631E-03	2.40260E-03
RMSE	1.26813E-02	9.73320E-03	1.17238E-02
MSE	1.60816E-04	9.47351E-05	1.37448E-04

Table 5.4   Comparison of testing dataset results using the MAPE, RMSE, MSE, and MAE error techniques for the three supervised learning algorithms DT, KNN, and RF regressors at 35℃

Test and Training Dataset (80% Training + 20% Testing for cell 'a') NMC cell at 35℃			
Model	DT	KNN	RF
	Error Value	Error Value	Error Value
MAE	3.65806E-03	3.35097E-03	8.80143E-03
MAPE	1.43534E-03	1.33972E-03	3.56308E-03
RMSE	1.14894E-02	1.01762E-02	1.46577E-02
MSE	1.32006E-04	1.03555E-04	2.14847E-04

Table 5.5, Table 5.6, and Table 5.7 list out a comparison of validation dataset results for cell 'b' using the MAPE, RMSE, MSE, and MAE error techniques for the three supervised learning algorithms DT, KNN, and RF regressors at 15℃, 25℃, and 35℃ respectively.

Table 5.5   Comparison of validation dataset results for cell 'b' using the MAPE, RMSE, MSE, and MAE error techniques for the three supervised learning algorithms DT, KNN, and RF at 15℃.

Validation Dataset (100% for validation for cell 'b') NMC cell 'b' at 15℃			
Model	DT	KNN	RF
	Error Value	Error Value	Error Value
MAE	1.30118E-02	1.29728E-02	1.67570E-02
MAPE	6.24932E-03	6.24155E-03	8.18244E-03
RMSE	2.06257E-02	2.10567E-02	2.38013E-02
MSE	4.25421E-04	4.43384E-04	5.66503E-04

Table 5.6   Comparison of validation dataset results for cell 'b' using the MAPE, RMSE, MSE, and MAE error techniques for the three supervised learning algorithms DT, KNN, and RF at 25℃.

Validation Dataset (100% for validation for cell 'b') NMC cell 'b' at 25℃			
Model	DT	KNN	RF
	Error Value	Error Value	Error Value
MAE	2.72706E-02	2.70127E-02	2.71204E-02
MAPE	1.06377E-02	1.05432E-02	1.05881E-02
RMSE	3.22903E-02	3.16871E-02	3.19584E-02
MSE	1.04266E-03	1.00408E-03	1.02134E-03

Table 5.7   Comparison of validation dataset results for cell 'b' using the MAPE, RMSE, MSE, and MAE error techniques for the three supervised learning algorithms DT, KNN, and RF at 35℃.

Validation Dataset (100% for validation for cell 'b') NMC cell 'b' at 35℃			
Model	DT	KNN	RF
	Error Value	Error Value	Error Value
MAE	1.37012E-02	1.37321E-02	1.48082E-02
MAPE	5.52650E-03	5.53572E-03	5.96257E-03
RMSE	2.05500E-02	2.00694E-02	1.96755E-02
MSE	4.22301E-04	4.02780E-04	3.87124E-04

Further examination of model error unveils that the developed methodology and algorithms exhibit superiority over those presented in prior investigations reported across several academic journals. The subsequent comparison is delineated in Table 5.8, it is observed that DT and KNN scores better than other supervised as well as non-supervised learning methods. As different researchers adopted their strategies, the wide variance in results indicates a need for standardization of methods and parameter extraction. As AI methods are dependent on data and its quality, it is also imperative that for universalizing the process, BMS and battery manufacturers should come forward and allow researchers and engineers to create algorithms and design a suitable system.

Table 5.8   Comparison of developed methodology and models with other methods employed by researchers.

Ref	ML MODELS	15ºC				25ºC				35ºC			
		MAE	MAPE	RMSE	MSE	MAE	MAPE	RMSE	MSE	MAE	MAPE	RMSE	MSE
Experimental	DT	2.64E-03	1.32E-03	5.61E-03	3.00E-05	3.79E-03	1.49E-03	1.27E-02	1.60E-04	3.66E-03	1.44E-03	1.15E-02	1.30E-04

Ref	Model												
	KNN	1.92E-03	9.90E-04	3.13E-03	1.00E-05	3.63E-03	1.41E-03	9.73E-03	9.00E-05	3.35E-03	1.34E-03	1.02E-02	1.00E-04
	RF	8.22E-03	4.19E-03	1.11E-02	1.20E-04	6.17E-03	2.40E-03	1.17E-02	1.40E-04	8.80E-03	3.56E-03	1.47E-02	2.20E-04
[128]	RF	Results not reported				9.70E-03	1.67E-02	1.12E-02	Results not reported				
	DT					1.56E-02	1.77E-02	1.83E-02					
	Adaboost					1.22E-02	1.19E-02	1.34E-02					
	FNN					1.27E-02	1.22E-02	1.48E-02					
	BiLSTM					1.16E-02	1.20E-02	1.43E-02					
	1DCNN					7.00E-03	9.10E-02	1.01E-02					
	DSMTNet					6.30E-03	7.20E-01	8.90E-03					
[129]	LSTM					2.09E-01	Results not	2.59E-01	6.70E-02				

Encoder–decoder		1.72E-01		2.21E-01	4.90E-02
CNN-LSTM		1.95E-01		2.47E-01	6.10E-02
ConvLSTM		1.51E-01		2.05E-01	4.20E-02

Based on the test and training datasets for Cell "a" and the validation dataset for Cell "b," the performance of DT, KNN, and RF models across various temperature conditions (15℃, 25℃, 35℃) was evaluated using multiple error metrics: MAE, MAPE, RMSE, and MSE.

During test and training dataset of Cell "a", at 15℃, it is observed that KNN emerged as the most accurate model with the lowest error metrics (MAE: 0.19%, MAPE: 0.10%, RMSE: 0.31%, MSE: 0.00%), where as DT also performed well but with slightly higher error values compared to KNN. RF showed the highest errors (MAE: 0.82%, RMSE: 1.11%). At 25℃, KNN maintained superior performance (MAE: 0.36%, MAPE: 0.14%, RMSE: 0.97%, MSE: 0.01%), followed closely by DT. RF again exhibited the highest error values. At 35℃, KNN continued to outperform the other models (MAE: 0.34%, MAPE: 0.13%, RMSE: 1.02%, MSE: 0.01%). DT remained competitive, while RF had the highest errors (MAE: 0.88%, RMSE: 1.47%).

During validation with dataset Cell "b", at 15℃, it is observed that DT and KNN both demonstrated similar performance (MAE: 1.30%, MAPE: 0.62%), with RF having the highest errors (RMSE: 2.38%). At 25℃, KNN slightly outperformed DT and RF, although the error values were higher in this condition (MAE: 2.70%, RMSE: 3.17%) with RF exhibited errors comparable to DT but was slightly higher.

At 35℃, KNN and DT performed similarly, with KNN having a marginal advantage in RMSE (2.01%). RF had slightly higher errors, particularly in MAPE (0.60%).

Overall, KNN consistently showed the best performance across both the training and validation datasets, making it the most reliable model for state estimation in the provided scenarios. DT was a close second, particularly effective in the validation dataset where it matched KNN's performance. RF generally had higher errors, suggesting it may not be as well-suited for this task, especially under validation conditions. The results indicate that KNN might be the preferred model for state estimation in similar datasets, but the effectiveness of the models can vary depending on specific operating conditions.

At the same time, models like Adaboost, FNN, BiLSTM, 1DCNN, and DSMTNet were reported in other references, with varying performance. Adaboost and BiLSTM showed relatively low errors, compared to KNN and DT. LSTM, Encoder–decoder, and CNN-LSTM models were reported to have significantly higher errors, especially in the MAPE metric, indicating potential issues in accuracy or overfitting. DSMTNet had the lowest errors among the newer models but still didn't outperform the traditional KNN model. The overall results suggest that while newer models offer potential, traditional methods like KNN still provide robust and accurate results in this specific application.

5.3   STATE OF CHARGE ESTIMATION

A comprehensive analysis was conducted on 20 LFP prismatic cells to assess their voltage variations under varying discharging times. Notably, significant voltage discrepancies were observed among individual cells, aligning with distinct capacities. To initiate the battery pack assembly process, a crucial initial step involves aligning and matching the capacity and voltage responses against different discharging rates. This meticulous matching process ensures the harmonization of individual cell characteristics, enabling a more coherent and efficient performance

when integrated into a battery pack. By addressing voltage variations and capacity discrepancies at this early stage, the subsequent battery pack is poised to exhibit enhanced overall stability and reliability in its discharge characteristics. The individual cell's OCV at the start of discharge after rest (OCV relaxation period for LFP for SOC investigations) and just after the start of discharge (with C/2 discharge rating, current- 43A) is graphically represented at 5.20 (a), whereas the duration of discharge after full charge and rest are plotted at Fig. 5.20 (b). In both cases, it is observed that even for the same manufacturing code and similar test setup, individual cell exhibits wide variance and necessitate the process of cell selection.
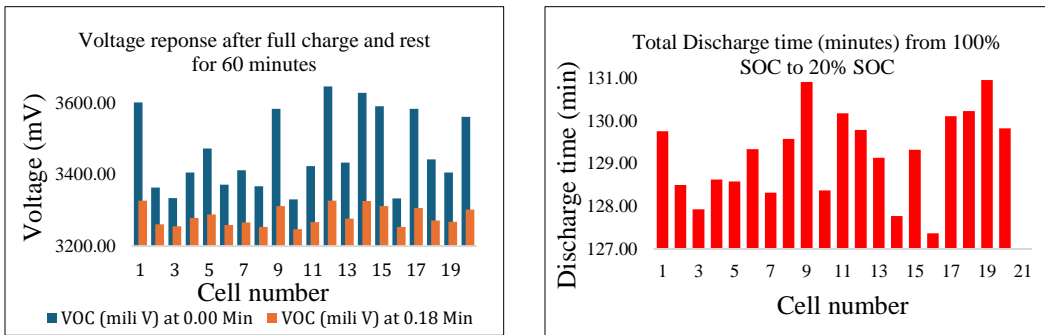
Fig. 5.20   Bar chart analysis of (a) the first 40 minutes and (b) the last 40 minutes for individual LFP cells.

The voltage after rest returns to its stable OCV state through a relaxation mechanism. This process occurs due to the presence of a Li^+ gradient across the positive electrode, which seeks to reach a state of minimum energy following a partial charge or discharge cycle. As voltage is contingent upon the surface concentration of lithium-ion within the electrode, this gradient gradually diminishes over time, thereby impacting the voltage observed at the terminals of LIBs.

Further, the discharging voltage of individual cells was analyzed at 10-minute intervals during continuous discharge until complete charging using a CC-CV charger, followed by a 30-minute resting period. The graph depicting this data over time for each cell is presented in Figure 5.21. It was recorded that following an initial 10-minute discharge period, cells exhibited a rather linear discharge trend

until reaching the discharge threshold limit. As every LIB consists of a BMS, it is essential to make the cells behave within a closed voltage window across a full discharge period.
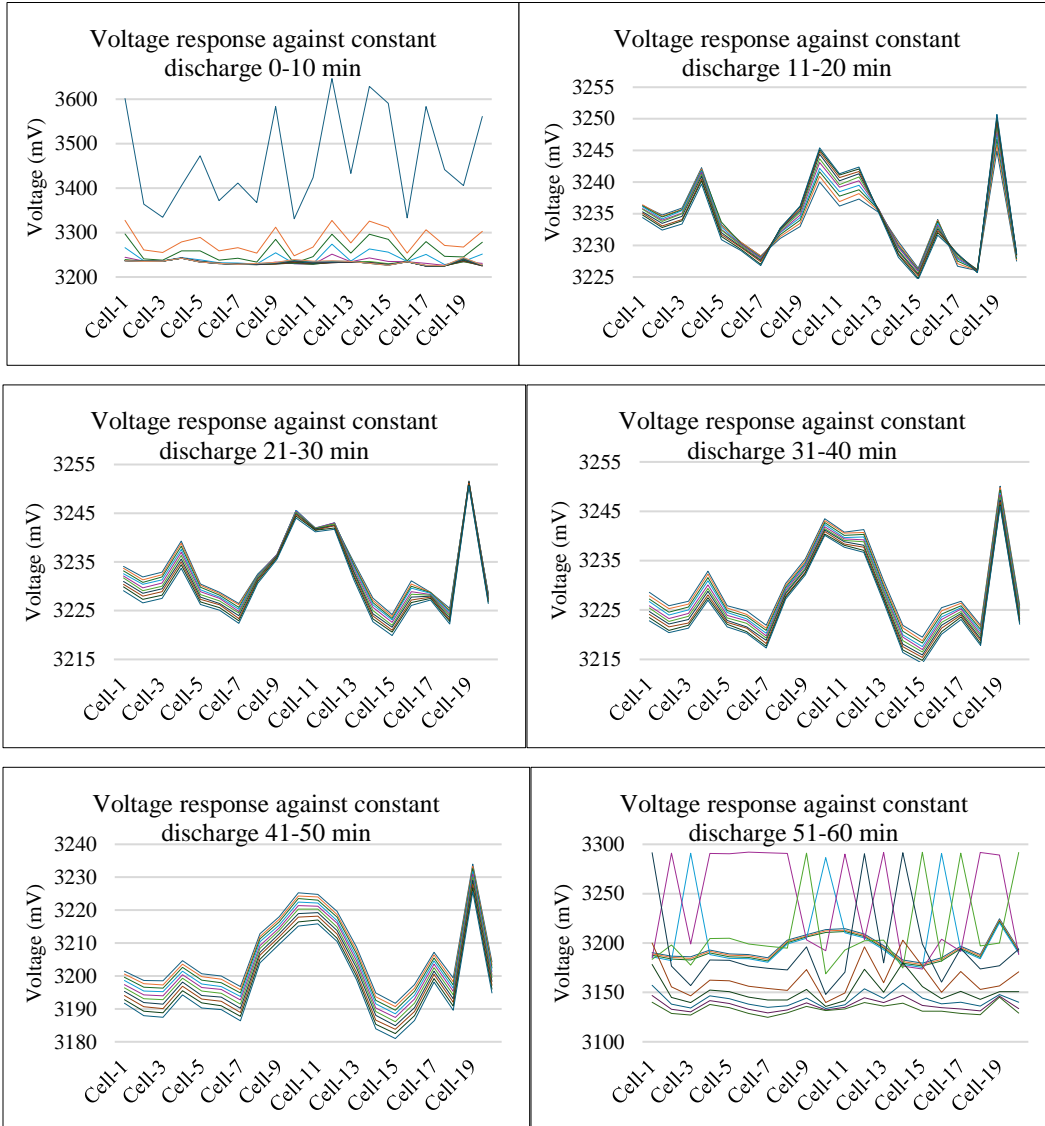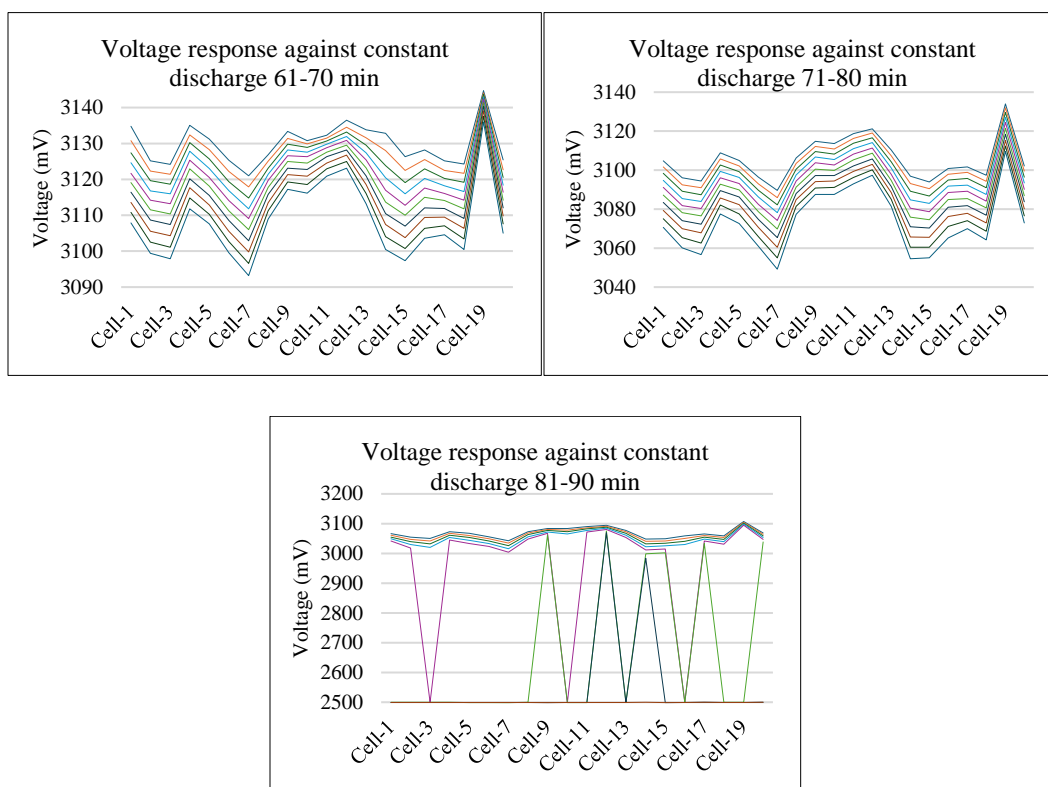
Fig. 5.21   Voltage response for individual LFP cells for every 10 minutes until full discharge.

It is observed that LFP cells exhibit a flat plateau range and are found to be from the first 3 minutes to 80 minutes of constant discharge at 43A. This is due to the lithiation process of LFP exhibiting a direct pathway characterized by a prolonged phase transition between the Li-poor (α) and Li-rich (β) phases. This transition is substantiated by the extended plateau observed in the OCV curve, depicted in Fig. 5.22, which covers nearly the entire SOC range. It is reported that LFP has a cubic crystal structure, which expands almost isotopically as lithium-ion are intercalated and the expansion of LFP is linear in the whole stoichiometric window.
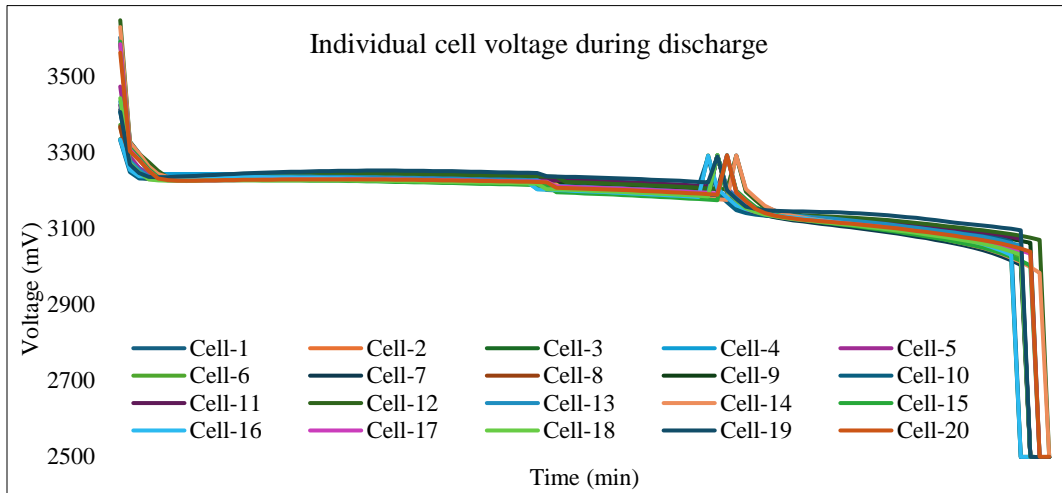
Fig. 5.22   Elbow, plateau, and knee analysis for individual LFP cells until full discharge.

Individual cells results were further analyzed using statistical tools and graphs were plotted for standard deviation with individual cell voltage difference at 0.00 min, standard deviation with individual cell voltage difference at 0.18 min, standard deviation and normal distribution for individual cell capacity difference, standard deviation for voltage between 0.00 min and 0.18 min at C/2 discharge rate for all 20 cell and presented in Fig. 5.23.
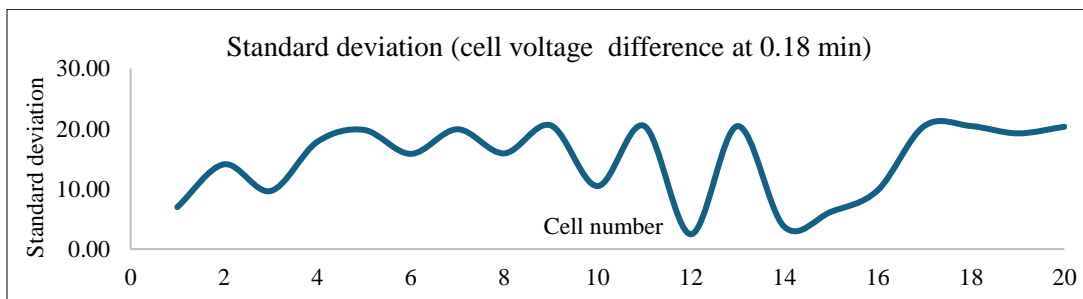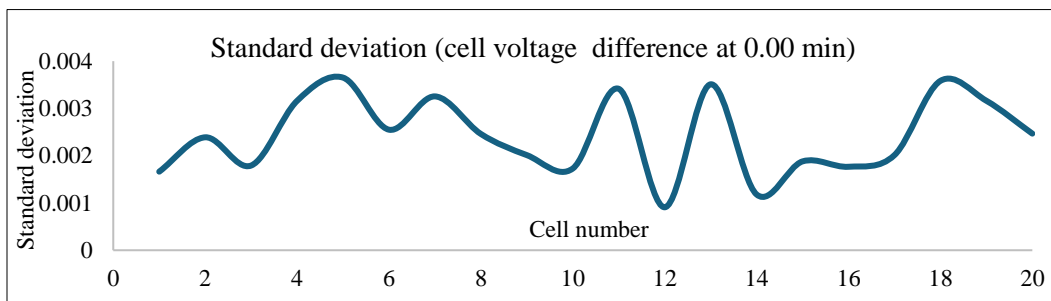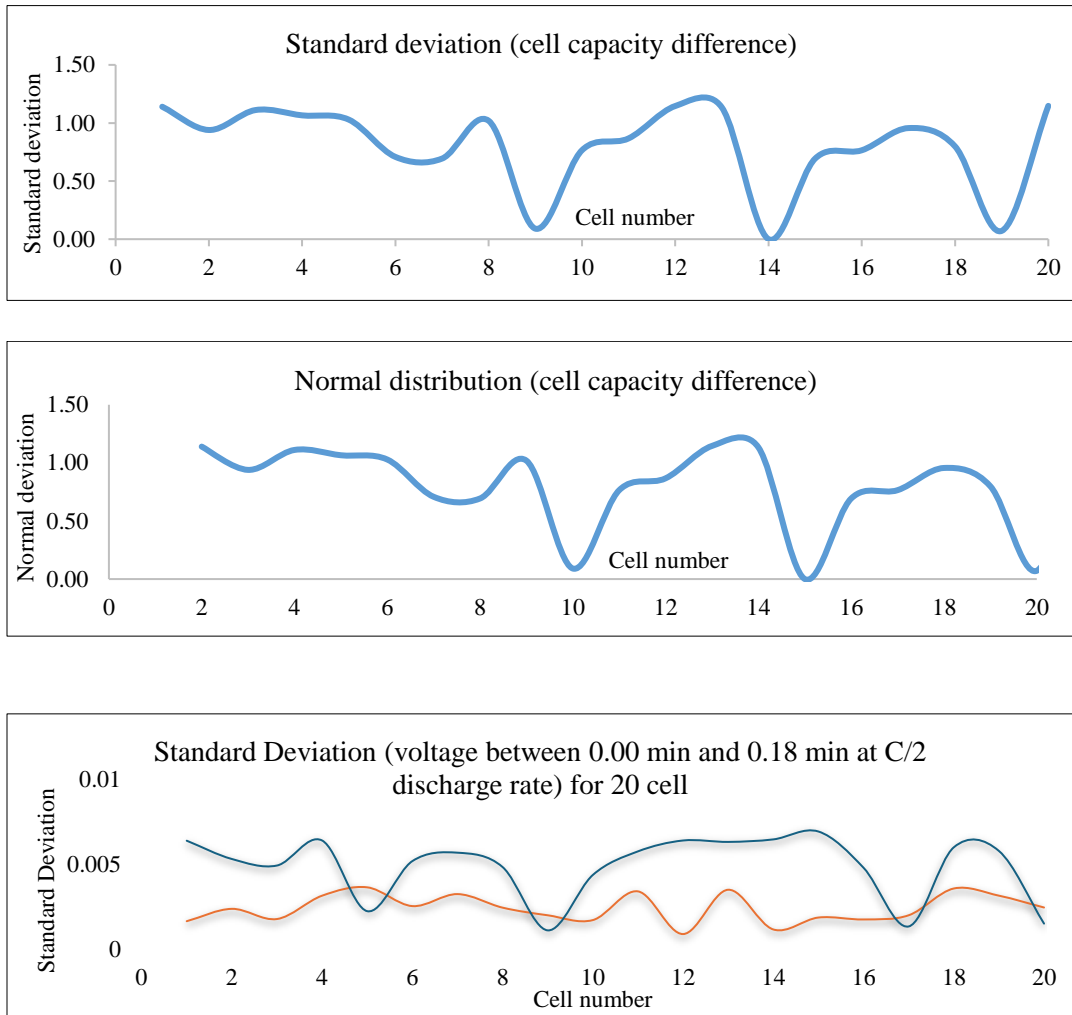
Fig. 5.23   Graphs on standard deviation ($\Delta V_{0.00}$, $\Delta V_{0.18}$, Δ_{Cap}) and normal distribution of Δ_{Cap}.

With the aid of this information, the final decision on the suitable cells was carried out and is analyzed as Fig. 5.24 for making a battery pack.
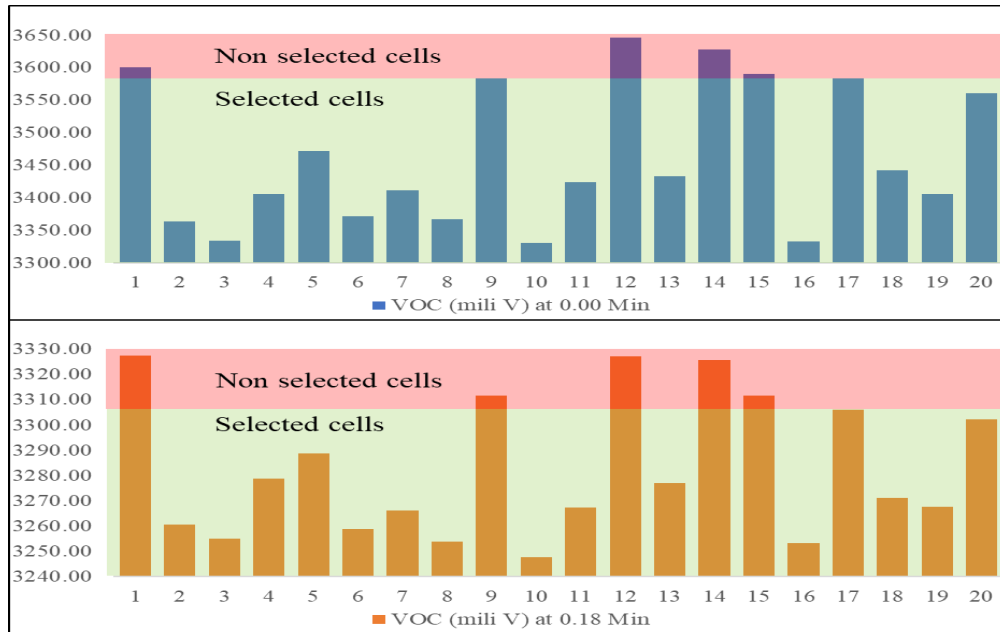
Fig. 5.24   Final cell selection for LFP battery pack.

Following the assembly of the battery pack, a comprehensive discharge process was conducted. The resulting graph as in Fig. 5.25 illustrates the voltage response to the discharge current, observed after the batteries reach their full charge capacity. This data provides a detailed representation of how the battery pack's voltage varies under different discharge currents, shedding light on its performance characteristics and aiding in the assessment of its overall efficiency and stability during discharge cycles.
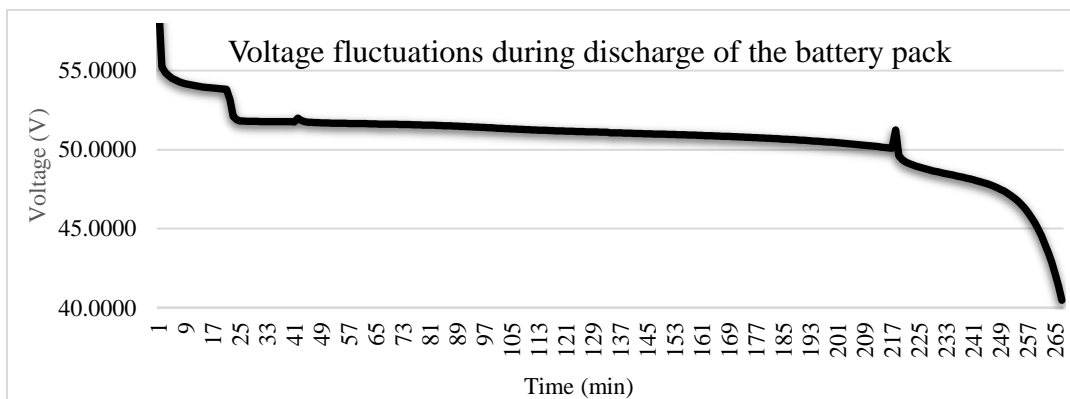
Fig. 5.25   Voltage response for LFP battery pack until full discharge.

The dataset of individual cells is split into training, validation, and testing sets and is split into training and validation in the ratio of 80% to 20%, respectively. The training set data is used to train the model, and finally, the testing set of the battery pack is used to test the performance. The analysis and result of the application of the linear regression algorithm are as per Fig. 5.26.
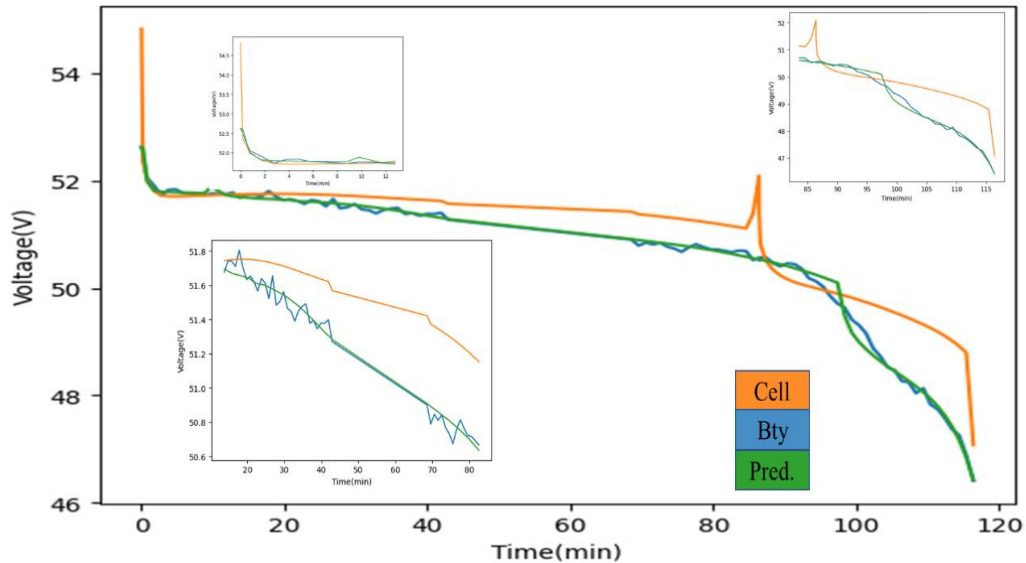
Fig. 5.26   LFP battery pack voltage prediction.

5.4   CHAPTER SUMMARY

It is of high importance to accurately predict the SOH for e-mobility applications. This paper presents multiple data-driven SOH prediction methods based on supervised learning. After investigating the aging attributes through datasets at different discharge rates and temperatures. The performance of these models is extracted and compared on different model accuracies and validated through experiments on similar conditions. The experimental model demonstrates a good prediction performance using KNN and DT methods and outperforms in terms of accuracy and generalizability. The outcome of battery health indices and their usage in BMS development, cloud technology, and further development of various application-oriented equipment and devices are provided by this method, which can significantly lower the cost and complexity.

At the temperature range from 15℃ to 35℃ which is below the critical threshold and recommended temperature by the manufacturer, the fade rate of SOH decreases, indicating unique nonlinear degradation mechanisms. KNN has been used for battery health estimation of e-mobility under different charge, discharge, and temperature conditions. KNN is effective in estimating battery health, but its performance is affected by the size of the training data. In general, when comparing errors obtained with different methods, it is important to carefully consider the error metric being used, the scale of the error, the context in which the methods are being applied, and whether any observed differences in error are statistically significant. The degradation of battery pack capacity is not considered in this study, even though a trustworthy battery pack SOH estimate method is suggested, and its ML model parameters are updated continually via the KNN, RF, and DT learning methods.

SOH and SOC serve as critical indicators pivotal for monitoring LIBs deployed in e-mobilities. While laboratory environments have established standard performance tests for state estimation, such tests are impractical to conduct onboard vehicles. At the same time, heavy and costly state estimation methods that require higher computing power or costly hardware also make it impractical to implement or conduct on-board estimation. To address these challenges, we developed novel data-driven approaches that can be virtually applied to LIB. Leveraging real-time variables accessible during ordinary e-mobility operation including battery current, voltage, and temperature, our data-driven models are designed to accurately estimate different states. This study presents comprehensive experimental validation of our method, introducing novel features such as SOH and SOC estimation. By subjecting typical LIB usage data to our proposed method, we successfully estimate SOH and SOC, comparing results to direct measurements obtained from standard tests. Our findings demonstrate high accuracy in estimation for typical EV operating conditions, facilitating online detection of battery degradation and energy storage.

CHAPTER 6

CONCLUSIONS AND FUTURE SCOPE

This chapter offers a comprehensive overview of the research efforts in creating innovative data-driven models for analyzing the critical states (SOC and SOH) of LIB in e-mobility. Specifically, the focus is on batteries made with different electro chemistries, such as NMC and LFP, operating under various conditions (1C and 2C discharging with 0.5C charging) at different temperatures (15℃, 25℃, and 35℃). The emphasis lies on experimental validation, involving the creation of real batteries through standardized manufacturing processes and subsequent testing under diverse conditions. The chapter not only outlines the procedures for cell testing, matching, and the selection process for battery production but also conducts a comparative review of different model-based data-driven methods. This includes an exploration of their limitations and shortcomings, providing valuable insights for further advancements in the field.

6.1   CONCLUSIONS

Achieving carbon neutrality is essential for mitigating global warming and reducing greenhouse gas emissions. The widespread adoption of lithium-ion batteries (LIBs) in the mobility sector is a key driver in this transition to cleaner energy solutions. LIBs are characterized by a broad spectrum of performance and failure metrics-such as performance, efficiency, lifespan, reliability, and safety- especially under the varied operational and environmental conditions typical of e-mobility applications. Understanding the behavior and failure modes of LIBs, however, is inherently complex and not directly measurable, leading to the characterization of various figures of merit (FOMs). These FOMs are typically derived through various modeling methods, each with its own set of strengths and limitations. Among these, machine learning (ML) methods have emerged as particularly effective for rapid

estimation. ML approaches themselves are diverse, offering multiple categorizations based on their underlying techniques and applications.

This thesis underscores the critical need for a cleaner and more sustainable world by analyzing the relationship between global electricity generation, population growth, and their impact on emissions and global warming, with a particular emphasis on the transportation sector. The expansion and increasing demand for e-mobility, with a particular focus on LIBs are comprehensively examined from production to usage perspectives. Given the diverse performance metrics inherent to LIBs, this research meticulously explores and critically analyzes various modeling techniques through an extensive literature review, which serves to outline and establish the foundational framework for the study, ensuring a rigorous approach to understanding and advancing the application of LIBs in the e-mobility sector.

The experimental results on charging and discharging LIBs revealed that individual cells exhibit varied behavior under different operating conditions. This variability is attributed to factors such as manufacturing differences and storage conditions. Within the same batch, NMC cells demonstrated significant variation in equivalent full cycle capacity and percentage loss in capacity, highlighting the need for voltage and capacity grading when assembling battery packs. Similar is the case where LFP cells from the same batch also showed discrepancies in capacity and aging characteristics, underscoring the importance of stringent quality control and accurate modeling for battery pack assembly and an intelligent BMS that monitor and balance individual cells. Additionally, some cells exhibited higher voltages even after identical full charges and resting periods. Different models for charge and discharge capacities yielded varied results, and various machine learning algorithms demonstrated the least error across different error metrics.

Within this thesis, an investigation explores the consideration of four distinct model-based data-driven estimation methods for the LIB state. The primary focus

is on decoding two pivotal parameters of battery state: SOC and SOH. The development and validation of these estimators are thoroughly carried out through multiple data-driven modeling iterations, leveraging the capabilities of the Google Colaboratory environment. This specialized environment is chosen to facilitate the actual cell-level experiments, specifically tailored to different electrochemistry, such as the NMC-based cylindrical foam factor and the LFP-based prismatic foam factor. The experimental framework involves a comprehensive testing regimen employing diverse charger-discharger setups, tactically chosen to closely mimic real-world target systems. This meticulous approach ensures the robustness and applicability of the proposed model-based data-driven estimation methods across various electrochemical scenarios, laying a solid foundation for advancing battery state estimation in both research and practical applications.

Experimental time series data, reflecting different battery ages, consist of measurements (sampled at 1 second) of battery capacity, voltage, current, and temperature. In comparing the different estimation approaches, it can be concluded that the ML-based technique proves to be a more effective approach for addressing the problem, achieving superior estimation results with a relatively minor development effort. A potential avenue for future work could involve testing these proposed techniques on experimental data or exploring alternative estimation strategies. The present study can provide guidelines to accurately estimate the SOH and SOC for different LIBs cell chemistries. The environmental and operational conditions incorporated in the experiment are robust enough to give decent forecasting over the complete lifecycle or charge cycle, which is the novelty of the research work. There is a direct influence of environmental and operational conditions on SOC and SOH and accuracy varies accordingly.

The outcomes of experimental investigation done on NMC cells for SOH with different operating conditions (1C and 2C) with different environmental conditions (15℃, 25℃, and 35℃) suggest that KN and DT are better ML methods than other ML-based methods. At the same time, the outcomes of the experimental

investigation done on the LFP battery pack for SOC suggest that LR is comparable to ML methods among several other ML-based methods. The current study and test plan may also be utilized to investigate alternative cell electrochemistry at different operating and environmental conditions, which is the project's future focus.

6.2   FUTURE SCOPE

The study highlights several future research directions for ML-based fault diagnosis in LIBs used in e-mobility. Future research should address the limitations of ML-based fault diagnosis in LIBs used in e mobility, including overcoming the lengthy training processes and the challenge of acquiring extensive fault data, which is often restricted due to manufacturer confidentiality. There is a need for improved access to comprehensive and realistic datasets, particularly for high-energy applications with complex cell configurations. Given the high risks and costs associated with real fault simulations, future work should focus on simulation studies to obtain relevant data. Additionally, research should explore methods to capture insights into internal electrochemical dynamics, addressing challenges related to distinguishing faults with similar external characteristics and sensor faults versus battery faults. Research should target advancements in sensing technology, processors, and rapid data analysis to enhance early fault detection and model accuracy. Emphasis should be placed on developing sensor-less or minimal-sensor approaches to improve fault diagnosis in practical applications such as e-mobility and grid power storage. Cloud-based fault diagnosis, leveraging cloud computing and parallel processing, represents a promising avenue for future exploration, aiming to support effective BMS over the lifespan of LIBs.

References

[1] I.-I. E. Agency, "World Energy Outlook 2023 Executive Summary." 2023. [Online]. Available: www.iea.org/terms

[2] M. Mądziel and T. Campisi, "Energy Consumption of Electric Vehicles: Analysis of Selected Parameters Based on Created Database," *Energies*, vol. 16, no. 3, 2023, doi: 10.3390/en16031437.

[3] T. J. Garrett, M. Grasselli, and S. Keen, "Past world economic production constrains current energy demands: Persistent scaling with implications for economic growth and climate change mitigation," *PLoS One*, vol. 15, no. 8 August, 2020, doi: 10.1371/journal.pone.0237672.

[4] "Berkeley Earth high-resolution land time series data and gridded temperature data," *www.berkeleyearth.org*. 2023.

[5] IPCC, *Global Warming of 1.5°C*. Cambridge University Press, 2022. doi: 10.1017/9781009157940.

[6] H. Yu *et al.*, "Sandwich structured ultra-strong-heat-shielding aerogel/copper composite insulation board for safe lithium-ion batteries modules," *J. Energy Chem.*, vol. 76, pp. 438–447, 2023, doi: 10.1016/J.JECHEM.2022.10.009.

[7] S. Shaheen *et al.*, "Mobility on Demand Planning and Implementation: Current Practices, Innovations, and Emerging Mobility Futures."

[8] E. Sadeghi, M. H. Zand, M. Hamzeh, M. Saif, and S. M. M. Alavi, "Controllable Electrochemical Impedance Spectroscopy: From Circuit Design to Control and Data Analysis," *IEEE Trans. Power Electron.*, vol. 35, no. 9, pp. 9935–9944, 2020, doi: 10.1109/TPEL.2020.2977274.

[9] A. Babaei, M. Khedmati, M. R. A. Jokar, and E. B. Tirkolaee, "Sustainable transportation planning considering traffic congestion and uncertain conditions," *Expert Syst. Appl.*, vol. 227, p. 119792, 2023, doi: 10.1016/J.ESWA.2023.119792.

[10] A. G. Li, A. C. West, and M. Preindl, "Towards unified machine learning characterization of lithium-ion battery degradation across multiple levels: A critical review," *Appl. Energy*, vol. 316, 2022, doi: 10.1016/j.apenergy.2022.119030.

[11] M. M. Kumbure, C. Lohrmann, P. Luukka, and J. Porras, "Machine learning techniques and data for stock market forecasting: A literature review," *Expert Syst. Appl.*, vol. 197, p. 116659, 2022, doi: 10.1016/J.ESWA.2022.116659.

[12] I.-I. E. Agency, "Global EV Outlook 2023: Catching up with climate ambitions." 2023. [Online]. Available: www.iea.org

[13] K. Buchholz, "Electric Vehicles Go Big," *https://www.forbes.com/sites/katharinabuchholz/2023/05/05/electric-vehicles-go-big-infographic/?sh=78ad782341fc*, 2023.

[14] M. Fichtner, "Recent Research and Progress in Batteries for Electric Vehicles," *Batter. Supercaps*, vol. 5, no. 2, 2022, doi: 10.1002/batt.202100224.

[15] A. Dall-Orsoletta, P. Ferreira, and G. Gilson Dranka, "Low-carbon technologies and just energy transition: Prospects for electric vehicles," *Energy Convers. Manag. X*, vol. 16, p. 100271, Dec. 2022, doi: 10.1016/J.ECMX.2022.100271.

[16] C. Xu *et al.*, "Electric vehicle batteries alone could satisfy short-term grid storage demand by as early as 2030," *Nat. Commun.*, vol. 14, no. 1, 2023, doi: 10.1038/s41467-022-35393-0.

[17] W. Zhou, C. J. Cleaver, C. F. Dunant, J. M. Allwood, and J. Lin, "Cost, range anxiety and future electricity supply: A review of how today's technology trends may influence the future uptake of BEVs," *Renew. Sustain. Energy Rev.*, vol. 173, 2023, doi: 10.1016/j.rser.2022.113074.

[18] I. E. Agengy, "Global EV Outlook 2015," *Geo*, no. Geo, pp. 9–10, 2015.

[19] B. K. Chaturvedi, A. Nautiyal, T. C. Kandpal, and M. Yaqoot, "Projected transition to electric vehicles in India and its impact on stakeholders," *Energy Sustain. Dev.*, vol. 66, pp. 189–200, Feb. 2022, doi: 10.1016/J.ESD.2021.12.006.

[20] D. Singh, U. K. Paul, and N. Pandey, "Does electric vehicle adoption (EVA) contribute to clean energy? Bibliometric insights and future research agenda," *Clean. Responsible Consum.*, vol. 8, p. 100099, Mar. 2023, doi: 10.1016/J.CLRC.2022.100099.

[21] M. MineSpan, "McKinsey and Global Battery Alliance," 2023.

[22] M. S. H. Lipu *et al.*, "Battery Management, Key Technologies, Methods, Issues, and Future Trends of Electric Vehicles: A Pathway toward Achieving Sustainable Development Goals," *Batteries*, vol. 8, no. 9, 2022, doi: 10.3390/batteries8090119.

[23] M. S. Hossain, L. Kumar, M. El Haj Assad, and R. Alayi, "Advancements and Future Prospects of Electric Vehicle Technologies: A Comprehensive Review," *Complexity*, vol. 2022, 2022, doi: 10.1155/2022/3304796.

[24] U. Nations, D. of Economic, S. Affairs, and P. Division, "World

Urbanization Prospects The 2018 Revision." 2018.

[25]   P. Ross and K. Maynard, "Towards a 4th industrial revolution," *Intelligent Buildings International*, vol. 13, no. 3. Taylor and Francis Ltd., pp. 159–161, 2021. doi: 10.1080/17508975.2021.1873625.

[26]   H. Dai, B. Jiang, X. Hu, X. Lin, X. Wei, and M. Pecht, "Advanced battery management strategies for a sustainable energy future: Multilayer design concepts and research trends," *Renew. Sustain. Energy Rev.*, vol. 138, p. 110480, 2021, doi: 10.1016/J.RSER.2020.110480.

[27]   F. Mohammadi and M. Saif, "A comprehensive overview of electric vehicle batteries market," *e-Prime - Adv. Electr. Eng. Electron. Energy*, vol. 3, p. 100127, Mar. 2023, doi: 10.1016/J.PRIME.2023.100127.

[28]   L. Zhou *et al.*, "State Estimation Models of Lithium-Ion Batteries for Battery Management System: Status, Challenges, and Future Trends," *Batteries*, vol. 9, no. 2, 2023, doi: 10.3390/batteries9020131.

[29]   M. K. Tran, S. Panchal, T. D. Khang, K. Panchal, R. Fraser, and M. Fowler, "Concept Review of a Cloud-Based Smart Battery Management System for Lithium-Ion Batteries: Feasibility, Logistics, and Functionality," *Batteries*, vol. 8, no. 2, 2022, doi: 10.3390/batteries8020019.

[30]   M. A. Hannan *et al.*, "Impact of renewable energy utilization and artificial intelligence in achieving sustainable development goals," *Energy Reports*, vol. 7, pp. 5359–5373, Nov. 2021, doi: 10.1016/J.EGYR.2021.08.172.

[31]   Y. Kang *et al.*, "A comparative study of fault diagnostic methods for lithium-ion batteries based on a standardized fault feature comparison method," *J. Clean. Prod.*, vol. 278, p. 123424, 2021, doi: 10.1016/j.jclepro.2020.123424.

[32]   A. Masias, J. Marcicki, and W. A. Paxton, "Opportunities and Challenges of Lithium Ion Batteries in Automotive Applications," *ACS Energy Lett.*, vol. 6, no. 2, pp. 621–630, 2021, doi: 10.1021/acsenergylett.0c02584.

[33]   J. Edge, S. O'Kane, R. Prosser, … N. K.-P. C., and undefined 2021, "Lithium ion battery degradation: what you need to know," *pubs.rsc.org*.

[34]   S. E. J. O'Kane *et al.*, "Lithium-ion battery degradation: how to model it," *Phys. Chem. Chem. Phys.*, vol. 24, no. 13, pp. 7909–7922, 2022, doi: 10.1039/D2CP00417H.

[35]   W. Li, N. Sengupta, P. Dechent, D. Howey, A. Annaswamy, and D. U. Sauer, "One-shot battery degradation trajectory prediction with deep learning," *J. Power Sources*, vol. 506, 2021, doi: 10.1016/j.jpowsour.2021.230024.

[36]   R. Rajasegar, C. M. Mitsingas, E. K. Mayhew, Q. Liu, T. Lee, and J. Yoo,

"Development and Characterization of Additive-Manufactured Mesoscale Combustor Array," *J. Energy Eng.*, vol. 144, no. 3, 2018, doi: 10.1061/(asce)ey.1943-7897.0000527.

[37] A. Mallik, M. A. Arman, and S. K. Pal, "Solar Based Micro Hybridized Auto-Rickshaw and its Feasibility Analysis for Bangladesh," *Proc. Int. Conf. Mech. Eng. Renew. Energy 2017*, vol. 2017, pp. 201–206, 2017.

[38] D. Bhattacharjee, T. Ghosh, P. Bhola, K. Martinsen, and P. Dan, *Ecodesigning and improving performance of plugin hybrid electric vehicle in rolling terrain through multi-criteria optimisation of powertrain*, vol. 236, no. 5. 2022. doi: 10.1177/09544070211027531.

[39] J. Li *et al.*, "The state-of-charge predication of lithium-ion battery energy storage system using data-driven machine learning," *Sustain. Energy, Grids Networks*, vol. 34, Jun. 2023, doi: 10.1016/j.segan.2023.101020.

[40] J. I. Galan and J. A. Zuñiga-Vicente, "Discovering the key factors behind multi-stakeholder partnerships for contributing to the achievement of sustainable development goals: Insights around the electric vehicle in Spain," *Corp. Soc. Responsib. Environ. Manag.*, vol. 30, no. 2, pp. 829–845, 2023, doi: 10.1002/csr.2391.

[41] R. Vinuesa *et al.*, "The role of artificial intelligence in achieving the Sustainable Development Goals," *Nat. Commun.*, vol. 11, no. 1, pp. 1–10, 2020, doi: 10.1038/s41467-019-14108-y.

[42] Y. Liang, X. Fei, J. Li, X. He, and H. Gu, "Location of Electric Vehicle Charging Piles Based on Set Coverage Model," *World Electr. Veh. J.*, vol. 13, no. 5, pp. 1–14, 2022, doi: 10.3390/wevj13050077.

[43] S. Mishra *et al.*, "A comprehensive review on developments in electric vehicle charging station infrastructure and present scenario of India," *Sustain.*, vol. 13, no. 4, pp. 1–20, 2021, doi: 10.3390/su13042396.

[44] B. Gürel, "Thermal performance evaluation for solidification process of latent heat thermal energy storage in a corrugated plate heat exchanger," *Appl. Therm. Eng.*, p. 115312, 2020, doi: 10.1016/j.applthermaleng.2020.115312.

[45] O. N. The and P. To, "Emerging Issues and Challenges in Integrating Solar with the Distribution System On the Path to SunShot : Emerging Issues and Challenges in Integrating Solar with the Distribution System," no. May, 2016.

[46] S. Hemavathi and A. Shinisha, "A study on trends and developments in electric vehicle charging technologies," *J. Energy Storage*, vol. 52, no. PC, p. 105013, 2022, doi: 10.1016/j.est.2022.105013.

[47] T. G. T. A. Bandara, J. C. Viera, and M. González, "The next generation of fast charging methods for Lithium-ion batteries: The natural current-absorption methods," *Renew. Sustain. Energy Rev.*, vol. 162, p. 112338, Jul. 2022, doi: 10.1016/J.RSER.2022.112338.

[48] P. Khumprom and N. Yodo, "A data-driven predictive prognostic model for lithium-ion batteries based on a deep learning algorithm," *Energies*, vol. 12, no. 4, 2019, doi: 10.3390/en12040660.

[49] R. Gauthier *et al.*, "How do Depth of Discharge, C-rate and Calendar Age Affect Capacity Retention, Impedance Growth, the Electrodes, and the Electrolyte in Li-Ion Cells?," *J. Electrochem. Soc.*, 2022, doi: 10.1149/1945-7111/ac4b82.

[50] X. Li, C. Yuan, and Z. Wang, "Multi-time-scale framework for prognostic health condition of lithium battery using modified Gaussian process regression and nonlinear regression," *J. Power Sources*, vol. 467, Aug. 2020.

[51] M. S. H. Lipu *et al.*, "Intelligent algorithms and control strategies for battery management system in electric vehicles: Progress, challenges and future outlook," *J. Clean. Prod.*, vol. 292, p. 126044, 2021, doi: 10.1016/J.JCLEPRO.2021.126044.

[52] L. C. Casals, M. Etxandi-Santolaya, P. A. Bibiloni-Mulet, C. Corchero, and L. Trilla, "Electric Vehicle Battery Health Expected at End of Life in the Upcoming Years Based on UK Data," *Batteries*, vol. 8, no. 10, 2022, doi: 10.3390/batteries8100164.

[53] N. P. Lutsey, "Update on the global transition to electric vehicles through 2020." 2021. [Online]. Available: https://www.gov.ca.gov/2020/09/23/governor-newsom-announces-california-will-phase-out-gasoline-

[54] R. N. Charette, "The EV Transition Explained: Charger Infrastructure," *IEEE Spectr.*, 2022, [Online]. Available: https://spectrum.ieee.org/the-ev-transition-explained-2658463735

[55] https://ourworldindata.org/grapher/energy-consumption-by-source and country?time=2007..latest, "Energy consumption by source, World," *https://ourworldindata.org/*. 2023.

[56] F. Xiao, C. Li, Y. Fan, G. Yang, and X. Tang, "State of charge estimation for lithium-ion battery based on Gaussian process regression with deep recurrent kernel," *Int. J. Electr. Power Energy Syst.*, vol. 124, 2021, doi: 10.1016/j.ijepes.2020.106369.

[57] Y. Hua *et al.*, "A comprehensive review on inconsistency and equalization technology of lithium-ion battery for electric vehicles," *Int. J. Energy Res.*,

vol. 44, no. 14, pp. 11059–11087, 2020, doi: 10.1002/er.5683.

[58] Y. Zhang, Y. Liu, J. Wang, and T. Zhang, "State-of-health estimation for lithium-ion batteries by combining model-based incremental capacity analysis with support vector regression," *Energy*, vol. 239, p. 121986, 2022, doi: 10.1016/J.ENERGY.2021.121986.

[59] Y. Che, Z. Deng, X. Tang, X. Lin, X. Nie, and X. Hu, "Lifetime and Aging Degradation Prognostics for Lithium-ion Battery Packs Based on a Cell to Pack Method," *Chinese J. Mech. Eng. (English Ed.*, vol. 35, no. 1, pp. 1–16, Dec. 2022, doi: 10.1186/S10033-021-00668-Y/TABLES/5.

[60] M. Kreimeier, A. Mondorf, and E. Stumpf, "Market volume estimation of thin-haul on-demand air mobility services in Germany," in *17th AIAA Aviation Technology, Integration, and Operations Conference, 2017*, American Institute of Aeronautics and Astronautics Inc, AIAA, 2017. doi: 10.2514/6.2017-3282.

[61] A. M. Khalid, "Socially Responsible Consumption and Marketing in Practice," *Soc. Responsible Consum. Mark. Pract.*, no. March, 2022, doi: 10.1007/978-981-16-6433-5.

[62] J. Fleischmann *et al.*, "Battery 2030: Resilient, sustainable, and circular."

[63] K. Das, R. Kumar, and A. Krishna, "Analyzing electric vehicle battery health performance using supervised machine learning," *Renew. Sustain. Energy Rev.*, vol. 189, p. 113967, 2024.

[64] A. Alzwayi and M. C. Paul, "Heat transfer enhancement of a lithium-ion battery cell using vertical and spiral cooling fins," *Therm. Sci. Eng. Prog.*, vol. 47, p. 102304, 2024, doi: 10.1016/J.TSEP.2023.102304.

[65] R. Kumar, A. Kumar, M. K. Gupta, J. Yadav, and A. Jain, "Solar tree-based water pumping for assured irrigation in sustainable Indian agriculture environment," *Sustain. Prod. Consum.*, vol. 33, pp. 15–27, 2022, doi: 10.1016/j.spc.2022.06.013.

[66] A. C. Olivieri and G. M. Escandar, "Analytical Figures of Merit," *Pract. Three-w. Calibration*, pp. 93–107, 2014, doi: 10.1016/B978-0-12-410408-2.00006-5.

[67] R. Baduel, J.-M. Bruel, I. Ober, and E. Doba, "DEFINITION OF STATES AND MODES AS GENERAL CONCEPTS FOR SYSTEM DESIGN AND VALIDATION," 2018, [Online]. Available: http://oatao.univ-toulouse.fr/24780

[68] S. Park *et al.*, "Review of state-of-the-art battery state estimation technologies for battery management systems of stationary energy storage

systems," *J. Power Electron.*, vol. 20, no. 6, pp. 1526–1540, 2020, doi: 10.1007/s43236-020-00122-7.

[69] A. Barragán-Moreno, E. Schaltz, A. Gismero, and D. I. Stroe, "Capacity State-of-Health Estimation of Electric Vehicle Batteries Using Machine Learning and Impedance Measurements," *Electron.*, vol. 11, no. 9, 2022, doi: 10.3390/electronics11091414.

[70] I. B. Espedal, A. Jinasena, O. S. Burheim, and J. J. Lamb, "Current trends for state-of-charge (SoC) estimation in lithium-ion battery electric vehicles," *Energies*, vol. 14, no. 11, 2021, doi: 10.3390/en14113284.

[71] S. Guo and L. Ma, "A comparative study of different deep learning algorithms for lithium-ion batteries on state-of-charge estimation," *Energy*, vol. 263, 2023, doi: 10.1016/j.energy.2022.125872.

[72] Z. Yang *et al.*, "High power density & energy density Li-ion battery with aluminum foam enhanced electrode: Fabrication and simulation," *J. Power Sources*, vol. 524, p. 230977, 2022, doi: 10.1016/J.JPOWSOUR.2022.230977.

[73] K. M. B. P. & M. D. Tomasov M., "Overview of Battery Models for Sustainable Power and Transport Applications," *Transp. Res. Procedia, 40, 548-555.*, vol. 388, pp. 539–547, 2018.

[74] X. Lai *et al.*, "Critical review of life cycle assessment of lithium-ion batteries for electric vehicles: A lifespan perspective," *eTransportation*, vol. 12, p. 100169, 2022, doi: 10.1016/J.ETRAN.2022.100169.

[75] D. P. Finegan and S. J. Cooper, "Battery Safety: Data-Driven Prediction of Failure," *Joule*, vol. 3, no. 11, pp. 2599–2601, 2019, doi: 10.1016/j.joule.2019.10.013.

[76] Y. Zhang, M. Jiang, Y. Zhou, S. Zhao, and Y. Yuan, "Towards High-Safety Lithium-Ion Battery Diagnosis Methods," 2023.

[77] U. H. Kim, S. B. Lee, N. Y. Park, S. J. Kim, C. S. Yoon, and Y. K. Sun, "High-Energy-Density Li-Ion Battery Reaching Full Charge in 12 min," *ACS Energy Lett.*, vol. 7, no. 11, pp. 3880–3888, 2022, doi: 10.1021/acsenergylett.2c02032.

[78] H. Zhou, F. Zhou, L. Xu, J. Kong, and QingxinYang, "Thermal performance of cylindrical Lithium-ion battery thermal management system based on air distribution pipe," *Int. J. Heat Mass Transf.*, vol. 131, pp. 984–998, 2019, doi: 10.1016/j.ijheatmasstransfer.2018.11.116.

[79] A. García, J. Monsalve-Serrano, R. L. Sari, and S. Martínez-Boggio, "Thermal runaway evaluation and thermal performance enhancement of a

lithium-ion battery coupling cooling system and battery sub-models," *Appl. Therm. Eng.*, vol. 202, p. 117884, Feb. 2022, doi: 10.1016/J.APPLTHERMALENG.2021.117884.

[80] H. You *et al.*, "Nonlinear health evaluation for lithium-ion battery within full-lifespan," *J. Energy Chem.*, 2022.

[81] R. Kumar, N. Gupta, D. Bharadwaj, D. Dutt, and A. Joshi, "Design and development of electronic clutch control unit for manual transmission," *Mater. Today Proc.*, no. xxxx, 2022, doi: 10.1016/j.matpr.2022.08.470.

[82] R. Kumar, M. Kumar Gupta, A. Kumar, P. Sharma, and R. Deorari, "Analysis of electronic clutch control unit for manual transmission vehicle oriented toward safety," *Mater. Today Proc.*, no. xxxx, 2022, doi: 10.1016/j.matpr.2022.08.473.

[83] Y. Chu, J. Li, J. Gu, and Y. Qiang, "Parameter identification and SOC estimation of lithium-ion batteries based on AGCOA-ASRCKF," *J. Power Electron.*, 2022, doi: 10.1007/S43236-022-00525-8.

[84] N. Jiang and H. Pang, "Study on Co-Estimation of SoC and SoH for Second-Use Lithium-Ion Power Batteries," *Electron.*, vol. 11, no. 11, pp. 1–15, 2022, doi: 10.3390/electronics11111789.

[85] J. Hong, Z. Wang, W. Chen, L. Y. Wang, and C. Qu, "Online joint-prediction of multi-forward-step battery SOC using LSTM neural networks and multiple linear regression for real-world electric vehicles," *J. Energy Storage*, vol. 30, pp. 1–21, 2020, doi: 10.1016/j.est.2020.101459.

[86] D. Teets and K. Whitehead, "The Discovery of Ceres: How Gauss Became Famous 12:46," vol. 72, no. 2. pp. 83–93, 1999.

[87] R. Tubb, "BATTERY-DRIVEN ELECTRIC VEHICLES."

[88] S. B. Sarmah *et al.*, "A Review of State of Health Estimation of Energy Storage Systems: Challenges and Possible Solutions for Futuristic Applications of Li-Ion Battery Packs in Electric Vehicles," *J. Electrochem. Energy Convers. Storage*, vol. 16, no. 4, 2019, doi: 10.1115/1.4042987.

[89] C. Wu *et al.*, "Current status and future directions of all-solid-state batteries with lithium metal anodes, sulfide electrolytes, and layered transition metal oxide cathodes," *Nano Energy*, vol. 87, p. 106081, 2021, doi: 10.1016/j.nanoen.2021.106081.

[90] R. Xiong, Y. Pan, W. Shen, H. Li, and F. Sun, "Lithium-ion battery aging mechanisms and diagnosis method for automotive applications: Recent advances and perspectives," *Renew. Sustain. Energy Rev.*, vol. 131, no. 5, p. 110048, 2020, doi: 10.1016/j.rser.2020.110048.

[91] Y. Surace *et al.*, "Evidence for stepwise formation of solid electrolyte interphase in a Li-ion battery," *Energy Storage Mater.*, vol. 44, pp. 156–167, 2022, doi: 10.1016/J.ENSM.2021.10.013.

[92] S. K. Heiskanen, J. Kim, and B. L. Lucht, "Generation and Evolution of the Solid Electrolyte Interphase of Lithium-Ion Batteries," *Joule*, vol. 3, no. 10, pp. 2322–2333, 2019, doi: 10.1016/j.joule.2019.08.018.

[93] A. Friesen *et al.*, "Impact of cycling at low temperatures on the safety behavior of 18650-type lithium ion cells: Combined study of mechanical and thermal abuse testing accompanied by post-mortem analysis," *J. Power Sources*, vol. 334, pp. 1–11, 2016, doi: 10.1016/j.jpowsour.2016.09.120.

[94] D. I. Stroe, M. Swierczynski, S. K. Kær, and R. Teodorescu, "Degradation Behavior of Lithium-Ion Batteries During Calendar Ageing - The Case of the Internal Resistance Increase," *IEEE Trans. Ind. Appl.*, vol. 54, no. 1, pp. 517–525, 2018, doi: 10.1109/TIA.2017.2756026.

[95] M. Kumar and A. Kumar, "Performance assessment and degradation analysis of solar photovoltaic technologies : A review," *Renew. Sustain. Energy Rev.*, vol. 78, no. May, pp. 554–587, 2017, doi: 10.1016/j.rser.2017.04.083.

[96] X. Hu, K. Zhang, K. Liu, X. Lin, S. Dey, and S. Onori, "Advanced Fault Diagnosis for Lithium-Ion Battery Systems: A Review of Fault Mechanisms, Fault Features, and Diagnosis Procedures," *IEEE Ind. Electron. Mag.*, vol. 14, no. 3, pp. 65–91, 2020, doi: 10.1109/MIE.2020.2964814.

[97] I. Baskin and Y. Ein-Eli, "Electrochemoinformatics as an Emerging Scientific Field for Designing Materials and Electrochemical Energy Storage and Conversion Devices—An Application in Battery Science and Technology," *Adv. Energy Mater.*, vol. 12, no. 48, 2022, doi: 10.1002/aenm.202202380.

[98] M. Li, J. Lu, Z. Chen, and K. Amine, "30 Years of Lithium-Ion Batteries," *Adv. Mater.*, vol. 30, no. 33, pp. 1–24, 2018, doi: 10.1002/adma.201800561.

[99] X. Shen *et al.*, "Advanced Electrode Materials in Lithium Batteries: Retrospect and Prospect," *Energy Mater. Adv.*, vol. 2021, 2021, doi: 10.34133/2021/1205324.

[100] C. R. Birkl, M. R. Roberts, E. McTurk, P. G. Bruce, and D. A. Howey, "Degradation diagnostics for lithium ion cells," *J. Power Sources*, vol. 341, pp. 373–386, 2017, doi: 10.1016/j.jpowsour.2016.12.011.

[101] C. Pastor-Fernández, T. F. Yu, W. D. Widanage, and J. Marco, "Critical review of non-invasive diagnosis techniques for quantification of degradation modes in lithium-ion batteries," *Renew. Sustain. Energy Rev.*,

vol. 109, no. March, pp. 138–159, 2019, doi: 10.1016/j.rser.2019.03.060.

[102] H. Popp, M. Koller, M. Jahn, and A. Bergmann, "Mechanical methods for state determination of Lithium-Ion secondary batteries: A review," *Journal of Energy Storage*, vol. 32. 2020. doi: 10.1016/j.est.2020.101859.

[103] W. Li, Z. Jiao, L. Du, W. Fan, and Y. Zhu, "An indirect RUL prognosis for lithium-ion battery under vibration stress using Elman neural network," *Int. J. Hydrogen Energy*, vol. 44, no. 23, pp. 12270–12276, 2019, doi: 10.1016/j.ijhydene.2019.03.101.

[104] M. M. Thackeray, C. Wolverton, and E. D. Isaacs, "Electrical energy storage for transportation - Approaching the limits of, and going beyond, lithium-ion batteries," *Energy and Environmental Science*, vol. 5, no. 7. Royal Society of Chemistry, pp. 7854–7863, 2012. doi: 10.1039/c2ee21892e.

[105] Q. Meng, Z. An, X. Yu, N. Wang, D. Bai, and S. Liu, "The Influence of Temperature on the Secondary Use of Lithium Iron Phosphate Power Battery," *IOP Conf. Ser. Earth Environ. Sci.*, vol. 791, no. 1, p. 12129, 2021, doi: 10.1088/1755-1315/791/1/012129.

[106] S. Link, C. Neef, and T. Wicke, "Trends in Automotive Battery Cell Design: A Statistical Analysis of Empirical Data," *Batteries*, vol. 9, no. 5, pp. 1–23, 2023, doi: 10.3390/batteries9050261.

[107] Y. Hong and C. W. Lee, "Pareto fronts for multiobjective optimal design of the lithium-ion battery cell," *J. Energy Storage*, vol. 17, no. April, pp. 507–514, 2018, doi: 10.1016/j.est.2018.04.003.

[108] K. Das and R. Kumar, "Assessment of Electric Two-Wheeler Ecosystem Using Novel Pareto Optimality and TOPSIS Methods for an Ideal Design Solution," *World Electr. Veh. J.*, vol. 14, no. 8, p. 215, 2023.

[109] L. Hu *et al.*, "Performance evaluation strategy for battery pack of electric vehicles: Online estimation and offline evaluation," *Energy Reports*, vol. 8, pp. 774–784, 2022, doi: 10.1016/j.egyr.2022.02.026.

[110] C.-H. Chen, F. B. Planella, K. O'Regan, D. Gastol, W. D. Widanage, and E. Kendrick, "Development of Experimental Techniques for Parameterization of Multi-scale Lithium-ion Battery Models," *J. Electrochem. Soc.*, vol. 167, no. 8, p. 80534, 2020, doi: 10.1149/1945-7111/AB9050.

[111] J. Tian, R. Xiong, J. Lu, C. Chen, and W. Shen, "Battery state-of-charge estimation amid dynamic usage with physics-informed deep learning," *Energy Storage Mater.*, vol. 50, pp. 718–729, 2022, doi: 10.1016/J.ENSM.2022.06.007.

[112] S. Khaleghi, Y. Firouz, J. Van Mierlo, and P. Van den Bossche, "Developing

a real-time data-driven battery health diagnosis method, using time and frequency domain condition indicators," *Appl. Energy*, vol. 255, no. April, p. 113813, 2019, doi: 10.1016/j.apenergy.2019.113813.

[113] J. Jenis, J. Ondriga, S. Hrcek, F. Brumercik, M. Cuchor, and E. Sadovsky, "Engineering Applications of Artificial Intelligence in Mechanical Design and Optimization," *Machines*, vol. 11, no. 6. MDPI, Sep. 2023. doi: 10.3390/machines11060577.

[114] Z. Amiri, A. Heidari, and N. J. Navimipour, "Comprehensive survey of artificial intelligence techniques and strategies for climate change mitigation," *Energy*, vol. 308, p. 132827, Sep. 2024, doi: 10.1016/J.ENERGY.2024.132827.

[115] K. Das, R. Kumar, and A. Krishna, "Supervised learning and data intensive methods for the prediction of capacity fade of lithium-ion batteries under diverse operating and environmental conditions," *Water Energy Int.*, vol. 66, no. 1, pp. 53–59, 2023.

[116] J. Park, K. Kim, S. Park, J. Baek, and J. Kim, "Complementary cooperative SOC/capacity estimator based on the discrete variational derivative combined with the DEKF for electric power applications," *Energy*, vol. 232, p. 121023, 2021, doi: 10.1016/j.energy.2021.121023.

[117] S. Akhtar *et al.*, "Short-Term Load Forecasting Models: A Review of Challenges, Progress, and the Road Ahead," *Energies*, vol. 16, no. 10. MDPI, Sep. 2023. doi: 10.3390/en16104060.

[118] L. Wang, Y. Fang, L. Wang, F. Yun, J. Wang, and S. Lu, "Understanding Discharge Voltage Inconsistency in Lithium-Ion Cells via Statistical Characteristics and Numerical Analysis," *IEEE Access*, vol. 8, pp. 84821–84836, 2020, doi: 10.1109/ACCESS.2020.2992206.

[119] D. Thiruvonasundari and K. Deepa, "Electric vehicle battery modelling methods based on state of charge– review," *J. Green Eng.*, vol. 10, no. 1, pp. 24–61, 2020.

[120] S. Rahimifard, R. Ahmed, and S. Habibi, "Interacting Multiple Model Strategy for Electric Vehicle Batteries State of Charge/Health/ Power Estimation," *IEEE Access*, vol. 9, pp. 109875–109888, 2021, doi: 10.1109/ACCESS.2021.3102607.

[121] C. J. Lee, B. K. Kim, M. K. Kwon, K. Nam, and S. W. Kang, "Real-time prediction of capacity fade and remaining useful life of lithium-ion batteries based on charge/discharge characteristics," *Electron.*, vol. 10, no. 7, 2021, doi: 10.3390/electronics10070846.

[122] R. Li *et al.*, "State of charge prediction algorithm of lithium-ion battery based

on PSO-SVR cross validation," *IEEE Access*, vol. 8, pp. 10234–10242, 2020, doi: 10.1109/ACCESS.2020.2964852.

[123] L. Ma and T. Zhang, "Deep learning-based battery state of charge estimation: Enhancing estimation performance with unlabelled training samples," *J. Energy Chem.*, vol. 80, pp. 48–57, 2023, doi: 10.1016/j.jechem.2023.01.036.

[124] A. Manoharan, K. M. Begam, V. R. Aparow, and D. Sooriamoorthy, "Artificial Neural Networks, Gradient Boosting and Support Vector Machines for electric vehicle battery state estimation: A review," *J. Energy Storage*, vol. 55, 2022, doi: 10.1016/j.est.2022.105384.

[125] C. Vidal, P. Malysz, P. Kollmeyer, and A. Emadi, "Machine Learning Applied to Electrified Vehicle Battery State of Charge and State of Health Estimation: State-of-the-Art," *IEEE Access*, vol. 8, pp. 52796–52814, 2020, doi: 10.1109/ACCESS.2020.2980961.

[126] P. S. Madhukar and L. B. Prasad, "State Estimation using Extended Kalman Filter and Unscented Kalman Filter," *Proc. - 2020 Int. Conf. Emerg. Trends Commun. Control Comput. ICONC3 2020*, 2020, doi: 10.1109/ICONC345789.2020.9117536.

[127] X. Xu, D. Wu, L. Yang, H. Zhang, and G. Liu, "State Estimation of Lithium Batteries for Energy Storage Based on Dual Extended Kalman Filter," *Math. Probl. Eng.*, vol. 2020, 2020, doi: 10.1155/2020/6096834.

[128] Y. Li, B. Xiong, D. M. Vilathgamuwa, Z. Wei, C. Xie, and C. Zou, "Constrained Ensemble Kalman Filter for Distributed Electrochemical State Estimation of Lithium-Ion Batteries," *IEEE Trans. Ind. Informatics*, vol. 17, no. 1, pp. 240–250, 2021, doi: 10.1109/TII.2020.2974907.

[129] D. Liu, L. Li, Y. Song, L. Wu, and Y. Peng, "Hybrid state of charge estimation for lithium-ion battery under dynamic operating conditions," *Int. J. Electr. Power Energy Syst.*, vol. 110, pp. 48–61, 2019, doi: 10.1016/J.IJEPES.2019.02.046.

[130] Y. Zhang, Z. Peng, Y. Guan, and L. Wu, "Prognostics of battery cycle life in the early-cycle stage based on hybrid model," *Energy*, vol. 221, p. 119901, 2021, doi: 10.1016/J.ENERGY.2021.119901.

[131] J. Jiang, X. Cong, S. Li, C. Zhang, W. Zhang, and Y. Jiang, "A Hybrid Signal-Based Fault Diagnosis Method for Lithium-Ion Batteries in Electric Vehicles," *IEEE Access*, vol. 9, pp. 19175–19186, 2021, doi: 10.1109/ACCESS.2021.3052866.

[132] Y. Preger *et al.*, "Degradation of Commercial Lithium-Ion Cells as a Function of Chemistry and Cycling Conditions," *J. Electrochem. Soc.*, vol.

167, no. 12, p. 120532, 2020, doi: 10.1149/1945-7111/abae37.

[133] M. Stighezza, V. Bianchi, and I. De Munari, "FPGA Implementation of an Ant Colony Optimization Based SVM Algorithm for State of Charge Estimation in Li-Ion Batteries," *Energies*, vol. 14, no. 21, 2021, doi: 10.3390/en14217064.

[134] J. Ouyang, D. Xiang, and J. Li, "State-of-function evaluation for lithium-ion power battery pack based on fuzzy logic control algorithm," pp. 822–826, 2020, doi: 10.1109/ITAIC49862.2020.9339149.

[135] S. Song, C. Fei, and H. Xia, "Lithium-ion battery SOH estimation based on XGBoost algorithm with accuracy correction," *Energies*, vol. 13, no. 4, 2020, doi: 10.3390/en13040812.

[136] G. C. Y. Peng *et al.*, "Multiscale modeling meets machine learning: What can we learn?," *Arch. Comput. Methods Eng.*, vol. 28, pp. 1017–1037, 2021.

[137] J. zhen Kong, F. Yang, X. Zhang, E. Pan, Z. Peng, and D. Wang, "Voltage-temperature health feature extraction to improve prognostics and health management of lithium-ion batteries," *Energy*, vol. 223, p. 120114, 2021, doi: 10.1016/J.ENERGY.2021.120114.

[138] A. A. Franco, "Multiscale modelling and numerical simulation of rechargeable lithium ion batteries: Concepts, methods and challenges," *RSC Adv.*, vol. 3, no. 32, pp. 13027–13058, 2013, doi: 10.1039/c3ra23502e.

[139] C. Han, P. Zhang, D. Bluestein, G. Cong, and Y. Deng, "Artificial intelligence for accelerating time integrations in multiscale modeling," *J. Comput. Phys.*, vol. 427, p. 110053, 2021, doi: 10.1016/j.jcp.2020.110053.

[140] M. S. H. Lipu *et al.*, "Deep learning enabled state of charge, state of health and remaining useful life estimation for smart battery management system: Methods, implementations, issues and prospects," *J. Energy Storage*, vol. 55, no. September, 2022, doi: 10.1016/j.est.2022.105752.

[141] D. Zhou, Z. Li, J. Zhu, H. Zhang, and L. Hou, "State of Health Monitoring and Remaining Useful Life Prediction of Lithium-Ion Batteries Based on Temporal Convolutional Network," *IEEE Access*, vol. 8, pp. 53307–53320, 2020, doi: 10.1109/ACCESS.2020.2981261.

[142] K. A. Severson *et al.*, "Data-driven prediction of battery cycle life before capacity degradation," *Nat. Energy*, vol. 4, no. 5, pp. 383–391, 2019, doi: 10.1038/s41560-019-0356-8.

[143] T. Ouyang, P. Xu, J. Chen, J. Lu, and N. Chen, "An Online Prediction of Capacity and Remaining Useful Life of Lithium-Ion Batteries Based on Simultaneous Input and State Estimation Algorithm," *IEEE Trans. Power*

Electron., vol. 36, no. 7, pp. 8102–8113, 2021, doi: 10.1109/TPEL.2020.3044725.

[144] D. Galatro, C. Da Silva, D. A. Romero, O. Trescases, and C. H. Amon, "Challenges in data-based degradation models for lithium-ion batteries," *Int. J. Energy Res.*, vol. 44, no. 5, pp. 3954–3975, 2020, doi: 10.1002/er.5196.

[145] W. Diao, C. Kulkarni, and M. Pecht, "Development of an informative lithium-ion battery datasheet," *Energies*, vol. 14, no. 17, pp. 1–19, 2021, doi: 10.3390/en14175434.

[146] X. Shu, G. Li, J. Shen, Z. Lei, Z. Chen, and Y. Liu, "A uniform estimation framework for state of health of lithium-ion batteries considering feature extraction and parameters optimization," *Energy*, vol. 204, p. 117957, 2020, doi: 10.1016/J.ENERGY.2020.117957.

[147] S. Greenbank and D. Howey, "Automated Feature Extraction and Selection for Data-Driven Models of Rapid Battery Capacity Fade and End of Life," *IEEE Trans. Ind. Informatics*, vol. 18, no. 5, pp. 2965–2973, 2022, doi: 10.1109/TII.2021.3106593.

[148] J. Yu, B. Mo, D. Tang, J. Yang, J. Wan, and J. Liu, "Indirect state-of-health estimation for lithium-ion batteries under randomized use," *Energies*, vol. 10, no. 12, pp. 1–19, 2017, doi: 10.3390/en10122012.

[149] D. Lu and Z. Chen, "State of Health Estimation of Lithium-Ion Batteries Based on Dual Charging State," *Shanghai Jiaotong Daxue Xuebao/Journal Shanghai Jiaotong Univ.*, vol. 56, no. 3, pp. 342–352, 2022, doi: 10.16183/j.cnki.jsjtu.2021.027.

[150] J. Jia, J. Liang, Y. Shi, J. Wen, X. Pang, and J. Zeng, "SOH and RUL prediction of lithium-ion batteries based on Gaussian process regression with indirect health indicators," *Energies*, vol. 13, no. 2, 2020, doi: 10.3390/en13020375.

[151] H. Pan, Z. Lü, H. Wang, H. Wei, and L. Chen, "Novel battery state-of-health online estimation method using multiple health indicators and an extreme learning machine," *Energy*, vol. 160, pp. 466–477, 2018, doi: 10.1016/j.energy.2018.06.220.

[152] Z. Yu, "SOH Estimation Method for Lithium-ion Battery Based on Discharge Characteristics," *Int. J. Electrochem. Sci.*, vol. 17, p. ArticleID:220725, 2022, doi: 10.20964/2022.07.38.

[153] B. Gou, Y. Xu, and X. Feng, "State-of-Health Estimation and Remaining-Useful-Life Prediction for Lithium-Ion Battery Using a Hybrid Data-Driven Method," *IEEE Trans. Veh. Technol.*, vol. 69, no. 10, pp. 10854–10867, Oct. 2020, doi: 10.1109/TVT.2020.3014932.

[154] Y. Wang *et al.*, "A comprehensive review of battery modeling and state estimation approaches for advanced battery management systems," *Renew. Sustain. Energy Rev.*, vol. 131, p. 110015, 2020, doi: 10.1016/J.RSER.2020.110015.

[155] T. Zhang *et al.*, "A systematic framework for state of charge, state of health and state of power co-estimation of lithium-ion battery in electric vehicles," *Sustain.*, vol. 13, no. 9, 2021, doi: 10.3390/su13095166.

[156] C. Liu, M. Hu, G. Jin, Y. Xu, and J. Zhai, "State of power estimation of lithium-ion battery based on fractional-order equivalent circuit model," *J. Energy Storage*, vol. 41, 2021.

[157] X. Liu, C. Zheng, J. Wu, J. Meng, D.-I. Stroe, and J. Chen, "An Improved State of Charge and State of Power Estimation Method Based on Genetic Particle Filter for Lithium-ion Batteries," *Energies 2020, Vol. 13, Page 478*, vol. 13, no. 2, p. 478, 2020, doi: 10.3390/EN13020478.

[158] S. Zhang and X. Zhang, "A novel non-experiment-based reconstruction method for the relationship between open-circuit-voltage and state-of-charge/state-of-energy of lithium-ion battery," *Electrochim. Acta*, vol. 403, p. 139637, 2022, doi: 10.1016/J.ELECTACTA.2021.139637.

[159] X. Li, T. Long, J. Tian, and Y. Tian, "Multi-state joint estimation for a lithium-ion hybrid capacitor over a wide temperature range," *J. Power Sources*, vol. 479, no. July, p. 228677, 2020, doi: 10.1016/j.jpowsour.2020.228677.

[160] Z. B. Omariba, L. Zhang, H. Kang, and D. Sun, "Parameter identification and state estimation of lithium-ion batteries for electric vehicles with vibration and temperature dynamics," *World Electr. Veh. J.*, vol. 11, no. 3, 2020, doi: 10.3390/WEVJ11030050.

[161] C. Lu, Z. J. Gu, and Y. Yan, "RUL Prediction of Lithium Ion Battery Based on ARIMA Time Series Algorithm," *Mater. Sci. Forum*, vol. 999, pp. 117–128, 2020, doi: 10.4028/WWW.SCIENTIFIC.NET/MSF.999.117.

[162] S. Wang, S. Jin, D. Deng, and C. Fernandez, "A Critical Review of Online Battery Remaining Useful Lifetime Prediction Methods," *Front. Mech. Eng.*, vol. 7, 2021, doi: 10.3389/FMECH.2021.719718.

[163] V. L. Deringer, "Modelling and understanding battery materials with machine-learning-driven atomistic simulations," *JPhys Energy*, vol. 2, no. 4, 2020, doi: 10.1088/2515-7655/abb011.

[164] C. Hu, L. Ma, S. Guo, G. Guo, and Z. Han, "Deep learning enabled state-of-charge estimation of LiFePO4 batteries: A systematic validation on state-of-the-art charging protocols," *Energy*, vol. 246, p. 123404, 2022, doi:

10.1016/J.ENERGY.2022.123404.

[165] M. S. Hosen, J. Jaguemont, J. Van Mierlo, and M. Berecibar, "Battery lifetime prediction and performance assessment of different modeling approaches," *iScience*, vol. 24, no. 2, p. 102060, 2021, doi: 10.1016/j.isci.2021.102060.

[166] J. Wei and C. Chen, "A multi-timescale framework for state monitoring and lifetime prognosis of lithium-ion batteries," *Energy*, vol. 229, Aug. 2021.

[167] C. Zhang, Y. Jiang, J. Jiang, G. Cheng, W. Diao, and W. Zhang, "Study on battery pack consistency evolutions and equilibrium diagnosis for serial-connected lithium-ion batteries," *Appl. Energy*, vol. 207, pp. 510–519, 2017, doi: 10.1016/j.apenergy.2017.05.176.

[168] M. Zhang, K. Wang, and Y. T. Zhou, "Online state of charge estimation of lithium-ion cells using particle filter-based hybrid filtering approach," *Complexity*, vol. 2020, 2020, doi: 10.1155/2020/8231243.

[169] M. S. H. Lipu *et al.*, "Review of electric vehicle converter configurations, control schemes and optimizations: Challenges and suggestions," *Electron.*, vol. 10, no. 4, pp. 1–37, 2021, doi: 10.3390/electronics10040477.

[170] S. Wang, S. Jin, D. Deng, and C. Fernandez, "A Critical Review of Online Battery Remaining Useful Lifetime Prediction Methods," *Front. Mech. Eng.*, vol. 0, p. 71, 2021, doi: 10.3389/FMECH.2021.719718.

[171] R. Zhu, B. Duan, J. Zhang, Q. Zhang, and C. Zhang, "Co-estimation of model parameters and state-of-charge for lithium-ion batteries with recursive restricted total least squares and unscented Kalman filter," *Appl. Energy*, vol. 277, no. July, p. 115494, 2020, doi: 10.1016/j.apenergy.2020.115494.

[172] A. A. H. Akinlabi and D. Solyali, "Configuration, design, and optimization of air-cooled battery thermal management system for electric vehicles: A review," *Renew. Sustain. Energy Rev.*, vol. 125, no. February, p. 109815, 2020, doi: 10.1016/j.rser.2020.109815.

[173] T. Mamo and F. K. Wang, "Long short-term memory with attention mechanism for state of charge estimation of lithium-ion batteries," *IEEE Access*, vol. 8, pp. 94140–94151, 2020, doi: 10.1109/ACCESS.2020.2995656.

[174] C. Q. Du, J. B. Shao, D. M. Wu, Z. Ren, Z. Y. Wu, and W. Q. Ren, "Research on Co-Estimation Algorithm of SOC and SOH for Lithium-Ion Batteries in Electric Vehicles," *Electron.*, vol. 11, no. 2, 2022, doi: 10.3390/electronics11020181.

[175] G. Zhao, Y. Liu, G. Liu, S. Jiang, and W. Hao, "State-of-charge state-

of-health estimation for lithium-ion battery using the direct wave signals of guided wave," *J. Energy Storage*, vol. 39, no. July 2020, p. 102657, 2021, doi: 10.1016/j.est.2021.102657.

[176] Y. Che, Y. Liu, Z. Cheng, and J. Zhang, "SOC and SOH Identification Method of Li-Ion Battery Based on SWPSO-DRNN," *IEEE J. Emerg. Sel. Top. Power Electron.*, vol. 9, no. 4, pp. 4050–4061, 2021, doi: 10.1109/JESTPE.2020.3004972.

[177] M. S. Hassan *et al.*, "Machine Learning and Artificial Intelligence-Driven Multi-Scale Modeling for High Burnup Accident-Tolerant Fuels for Light Water-Based SMR Applications," 2022, doi: 10.1007/978-3-030-72322-4_149-1.

[178] M. R. Wahid, B. A. Budiman, E. Joelianto, and M. Aziz, "A review on drive train technologies for passenger electric vehicles," *Energies*, vol. 14, no. 20, pp. 1–24, 2021, doi: 10.3390/en14206742.

[179] S. Tamilselvi *et al.*, "A review on battery modelling techniques," *Sustain.*, vol. 13, no. 18, pp. 1–26, 2021, doi: 10.3390/su131810042.

[180] M. V Reddy, A. Mauger, C. M. Julien, A. Paolella, and K. Zaghib, "Brief history of early lithium-battery development," *Materials (Basel).*, vol. 13, no. 8, 2020, doi: 10.3390/MA13081884.

[181] D. Guyornard and J.-M. Tarascon, "ADVANCED MATERIALS Rocking-Chair or Li thium-Ion Rechargeable Lithium Batteries."

[182] P. A. Johnson and A. L. Babb, "Liquid diffu-sion of non-electrolytes," *Z. Physik. Chem*, vol. 56, no. 2. Interscience, p. 643, 1960.

[183] G. V. S. Rao and J. C. Tsang, "Electrolysis method of intercalation of layered transition metal dichalcogenides," *Mater. Res. Bull.*, vol. 9, no. 7, pp. 921–926, 1974, doi: 10.1016/0025-5408(74)90171-8.

[184] M. S. Whittingham, "Electrical energy storage and intercalation chemistry," *Science (80-.).*, vol. 192, no. 4244, pp. 1126–1127, 1976, doi: 10.1126/science.192.4244.1126.

[185] Y. Li, R. C. Massé, E. Uchaker, and G. Cao, "Revitalized interest in vanadium pentoxide as cathode material for lithium-ion batteries and beyond." 2017.

[186] M. Thingvad, L. Calearo, A. Thingvad, R. Viskinde, and M. Marinelli, "Characterization of NMC Lithium-ion Battery Degradation for Improved Online State Estimation," *UPEC 2020 - 2020 55th Int. Univ. Power Eng. Conf. Proc.*, 2020, doi: 10.1109/UPEC49904.2020.9209879.

[187] E. Schaltz, D. I. Stroe, K. Norregaard, L. S. Ingvardsen, and A. Christensen,

"Incremental Capacity Analysis Applied on Electric Vehicles for Battery State-of-Health Estimation," *IEEE Trans. Ind. Appl.*, vol. 57, no. 2, pp. 1810–1817, 2021, doi: 10.1109/TIA.2021.3052454.

[188] B. Epding, B. Rumberg, H. Jahnke, I. Stradtmann, and A. Kwade, "Investigation of significant capacity recovery effects due to long rest periods during high current cyclic aging tests in automotive lithium ion cells and their influence on lifetime," *J. Energy Storage*, vol. 22, no. December 2018, pp. 249–256, 2019, doi: 10.1016/j.est.2019.02.015.

[189] J. B and M. K. Shobana, "Enhanced cathode materials for advanced lithium-ion batteries using nickel-rich and lithium/manganese-rich LiNixMnyCozO2," *J. Energy Storage*, vol. 54, p. 105353, 2022, doi: 10.1016/J.EST.2022.105353.

[190] M. Zhang *et al.*, "A Review of SOH Prediction of Li-Ion Batteries Based on Data-Driven Algorithms," *Energies*, vol. 16, no. 7, 2023, doi: 10.3390/en16073167.

[191] M. C. Schulze and N. R. Neale, "Half-Cell Cumulative Efficiency Forecasts Full-Cell Capacity Retention in Lithium-Ion Batteries," *ACS Energy Lett.*, vol. 6, no. 3, pp. 1082–1086, 2021, doi: 10.1021/acsenergylett.1c00173.

[192] R. Kumar, R. K. Pachauri, P. Badoni, D. Bharadwaj, U. Mittal, and A. Bisht, "Investigation on parallel hybrid electric bicycle along with issuer management system for mountainous region," *J. Clean. Prod.*, vol. 362, p. 132430, 2022, doi: 10.1016/J.JCLEPRO.2022.132430.

[193] V. V. Krishnan and B. I. Koshy, "Evaluating the factors influencing purchase intention of electric vehicles in households owning conventional vehicles," *Case Stud. Transp. Policy*, vol. 9, no. 3, pp. 1122–1129, 2021, doi: 10.1016/j.cstp.2021.05.013.

[194] M. F. Ge, Y. Liu, X. Jiang, and J. Liu, "A review on state of health estimations and remaining useful life prognostics of lithium-ion batteries," *Meas. J. Int. Meas. Confed.*, vol. 174, no. December 2020, p. 109057, 2021, doi: 10.1016/j.measurement.2021.109057.

[195] H. Yang *et al.*, "Remaining useful life prediction based on denoising technique and deep neural network for lithium-ion capacitors," *eTransportation*, vol. 5, p. 100078, 2020, doi: 10.1016/J.ETRAN.2020.100078.

[196] J. Duan *et al.*, *Building Safe Lithium-Ion Batteries for Electric Vehicles: A Review*, vol. 3, no. 1. Springer Singapore, 2020. doi: 10.1007/s41918-019-00060-4.

[197] W. Chen, J. Liang, Z. Yang, and G. Li, "A review of lithium-ion battery for

electric vehicle applications and beyond," *Energy Procedia*, vol. 158, pp. 4363–4368, 2019, doi: 10.1016/j.egypro.2019.01.783.

[198] D. P. Finegan *et al.*, "The Application of Data-Driven Methods and Physics-Based Learning for Improving Battery Safety," *Joule*, vol. 5, no. 2, pp. 316–329, 2021, doi: 10.1016/j.joule.2020.11.018.

[199] P. J. Swornowski, "Destruction mechanism of the internal structure in Lithium-ion batteries used in aviation industry," *Energy*, vol. 122, pp. 779–786, 2017, doi: 10.1016/j.energy.2017.01.121.

[200] J. Y. Gao, Y. F. Yang, X. K. Zhang, S. L. Li, P. Hu, and J. S. Wang, "A review on recent progress of thermionic cathode," *Tungsten*, vol. 2, no. 3, pp. 289–300, 2020, doi: 10.1007/s42864-020-00059-1.

[201] F. H. Gandoman *et al.*, "Concept of reliability and safety assessment of lithium-ion batteries in electric vehicles: Basics, progress, and challenges," *Appl. Energy*, vol. 251, no. January, p. 113343, 2019, doi: 10.1016/j.apenergy.2019.113343.

[202] Z. Cui, L. Wang, Q. Li, and K. Wang, "A comprehensive review on the state of charge estimation for lithium-ion battery based on neural network," *Int. J. Energy Res.*, vol. 46, no. 5, pp. 5423–5440, 2022, doi: 10.1002/ER.7545.

[203] M. K. Tran and M. Fowler, "A review of lithium-ion battery fault diagnostic algorithms: Current progress and future challenges," *Algorithms*, vol. 13, no. 3, 2020, doi: 10.3390/a13030062.

[204] R. He *et al.*, "Towards interactional management for power batteries of electric vehicles," *RSC Advances*, vol. 13, no. 3. Royal Society of Chemistry, pp. 2036–2056, 2023. doi: 10.1039/d2ra06004c.

[205] C. S. Huang, Z. Cheng, and M. Y. Chow, "A Robust and Efficient State-of-Charge Estimation Methodology for Serial-Connected Battery Packs: Most Significant Cell Methodology," *IEEE Access*, vol. 9, pp. 74360–74369, 2021, doi: 10.1109/ACCESS.2021.3081619.

[206] L. H. Saw *et al.*, "Novel thermal management system using mist cooling for lithium-ion battery packs," *Appl. Energy*, vol. 223, no. April, pp. 146–158, 2018, doi: 10.1016/j.apenergy.2018.04.042.

[207] K. Saqli *et al.*, "Battery Pack Thermal Modeling , Simulation and electric model Identification To cite this version : HAL Id : hal-02486438 Battery Pack Thermal Modeling , Simulation and," 2020.

[208] C. Zhang, G. Cheng, Q. Ju, W. Zhang, J. Jiang, and L. Zhang, "Study on Battery Pack Consistency Evolutions during Electric Vehicle Operation with Statistical Method," *Energy Procedia*, vol. 105, pp. 3551–3556, 2017, doi:

10.1016/j.egypro.2017.03.816.

[209] L. Hu *et al.*, "Performance evaluation strategy for battery pack of electric vehicles: Online estimation and offline evaluation," *Energy Reports*, vol. 8, pp. 774–784, 2022, doi: 10.1016/J.EGYR.2022.02.026.

[210] B. Balagopal, C. S. Huang, and M. Y. Chow, "Sensitivity Analysis of Lithium Ion Battery Parameters to Degradation of Anode Lithium Ion Concentration," *IECON Proc. (Industrial Electron. Conf.*, vol. 2019-Octob, pp. 4543–4548, 2019, doi: 10.1109/IECON.2019.8926969.

[211] D. Burow *et al.*, "Inhomogeneous degradation of graphite anodes in automotive lithium ion batteries under low-temperature pulse cycling conditions," *J. Power Sources*, vol. 307, pp. 806–814, 2016, doi: 10.1016/j.jpowsour.2016.01.033.

[212] G. Zhang *et al.*, "Lithium plating on the anode for lithium-ion batteries during long-term low temperature cycling," *J. Power Sources*, vol. 484, no. November 2020, p. 229312, 2021, doi: 10.1016/j.jpowsour.2020.229312.

[213] L. Wang *et al.*, "Insights for understanding multiscale degradation of LiFePO4 cathodes," *eScience*, vol. 2, no. 2, pp. 125–137, 2022, doi: 10.1016/j.esci.2022.03.006.

[214] C. Zhang, Y. Wang, Y. Gao, F. Wang, B. Mu, and W. Zhang, "Accelerated fading recognition for lithium-ion batteries with Nickel-Cobalt-Manganese cathode using quantile regression method," *Appl. Energy*, vol. 256, no. August, p. 113841, 2019, doi: 10.1016/j.apenergy.2019.113841.

[215] X. Wu, D. Ruan, S. Tan, M. Feng, B. Li, and G. Hu, "Effect of stirring environment humidity on electrochemical performance of nickel-rich cathode materials as lithium ion batteries," *Ionics (Kiel).*, vol. 26, no. 11, pp. 5427–5434, 2020, doi: 10.1007/s11581-020-03708-0.

[216] B. Dixon, A. Mason, and E. Sahraei, "Effects of electrolyte, loading rate and location of indentation on mechanical integrity of li-ion pouch cells," *J. Power Sources*, vol. 396, no. June, pp. 412–420, 2018, doi: 10.1016/j.jpowsour.2018.06.042.

[217] Q. Li, Y. Yang, X. Yu, and H. Li, "A 700 W·h·kg−1 Rechargeable Pouch Type Lithium Battery," *Chinese Phys. Lett.*, vol. 40, no. 4, 2023, doi: 10.1088/0256-307X/40/4/048201.

[218] X. Zhong *et al.*, "Binding mechanisms of PVDF in lithium ion batteries," *Appl. Surf. Sci.*, vol. 553, p. 149564, 2021, doi: 10.1016/J.APSUSC.2021.149564.

[219] D. L. Wood, J. Li, and S. J. An, "Formation Challenges of Lithium-Ion

Battery Manufacturing," *Joule*, vol. 3, no. 12, pp. 2884–2888, 2019, doi: 10.1016/j.joule.2019.11.002.

[220] et al. Che, "Lifetime and Aging Degradation Prognostics for Lithium-ion Battery Packs Based on a Cell to Pack Method," *Chinese J. Mech. Eng.*, 2022.

[221] D. Juarez-Robles, A. A. Vyas, C. Fear, J. A. Jeevarajan, and P. P. Mukherjee, "Overdischarge and Aging Analytics of Li-Ion Cells," *J. Electrochem. Soc.*, vol. 167, no. 9, p. 090558, 2020, doi: 10.1149/1945-7111/aba00a.

[222] J.-Y. Bae, "Electrical Modeling and Impedance Spectra of Lithium-Ion Batteries and Supercapacitors," *Batteries*, vol. 9, no. 3, p. 160, 2023, doi: 10.3390/batteries9030160.

[223] N. Kirkaldy, M. A. Samieian, G. J. Offer, M. Marinescu, and Y. Patel, "Lithium-Ion Battery Degradation: Measuring Rapid Loss of Active Silicon in Silicon-Graphite Composite Electrodes," *ACS Appl. Energy Mater.*, vol. 5, no. 11, pp. 13367–13376, 2022, doi: 10.1021/acsaem.2c02047.

[224] W. Li, H. Zhang, B. van Vlijmen, P. Dechent, and D. U. Sauer, "Forecasting battery capacity and power degradation with multi-task learning," *Energy Storage Mater.*, vol. 53, pp. 453–466, 2022, doi: 10.1016/j.ensm.2022.09.013.

[225] M. Johnen, S. Pitzen, U. Kamps, M. Kateri, P. Dechent, and D. U. Sauer, "Modeling long-term capacity degradation of lithium-ion batteries," *J. Energy Storage*, vol. 34, pp. 1–15, 2021, doi: 10.1016/j.est.2020.102011.

[226] M. Raissi, P. Perdikaris, and G. E. Karniadakis, "Physics-informed neural networks: A deep learning framework for solving forward and inverse problems involving nonlinear partial differential equations," *J. Comput. Phys.*, vol. 378, pp. 686–707, Sep. 2019, doi: 10.1016/J.JCP.2018.10.045.

[227] A. Mondal, A. Routray, and S. Puravankara, "Parameter identification and co-estimation of state-of-charge of Li-ion battery in real-time on Internet-of-Things platform," *J. Energy Storage*, vol. 51, no. June, p. 104370, 2022, doi: 10.1016/j.est.2022.104370.

[228] P. Nian, Z. Shuzhi, and Z. Xiongwen, "Co-estimation for capacity and state of charge for lithium-ion batteries using improved adaptive extended Kalman filter," *J. Energy Storage*, vol. 40, no. May, p. 102559, 2021, doi: 10.1016/j.est.2021.102559.

[229] J. Shen *et al.*, "Alternative combined co-estimation of state of charge and capacity for lithium-ion batteries in wide temperature scope," *Energy*, vol. 244, no. January, 2022, doi: 10.1016/j.energy.2022.123236.

[230] M. U. Ali *et al.*, "A Hybrid Data-Driven Approach for Multistep Ahead Prediction of State of Health and Remaining Useful Life of Lithium-Ion Batteries," *Comput. Intell. Neurosci.*, vol. 2022, 2022, doi: 10.1155/2022/1575303.

[231] Y. Shi *et al.*, "The optimization of state of charge and state of health estimation for lithium-ions battery using combined deep learning and Kalman filter methods," *Int. J. Energy Res.*, vol. 45, no. 7, pp. 11206–11230, 2021, doi: 10.1002/er.6601.

[232] X. Lai *et al.*, "Co-Estimation of State-of-Charge and State-of-Health for Lithium-Ion Batteries Considering Temperature and Ageing," 2022.

[233] F. Feng *et al.*, "Co-estimation of lithium-ion battery state of charge and state of temperature based on a hybrid electrochemical-thermal-neural-network model," *J. Power Sources*, vol. 455, p. 227935, Apr. 2020, doi: 10.1016/j.jpowsour.2020.227935.

[234] W. Li *et al.*, "Physics-informed neural networks for electrode-level state estimation in lithium-ion batteries," *J. Power Sources*, vol. 506, no. June, 2021, doi: 10.1016/j.jpowsour.2021.230034.

[235] S. Khaleghi *et al.*, "Online health diagnosis of lithium-ion batteries based on nonlinear autoregressive neural network," *Appl. Energy*, vol. 282, no. PA, p. 116159, 2021, doi: 10.1016/j.apenergy.2020.116159.

[236] Y. Wu, B. Sicard, and S. A. Gadsden, "A Review of Physics-Informed Machine Learning Methods with Applications to Condition Monitoring and Anomaly Detection," Sep. 2024, [Online]. Available: http://arxiv.org/abs/2401.11860

[237] Z. Liu, J. Zhao, H. Wang, and C. Yang, "A new lithium-ion battery SOH estimation method based on an indirect enhanced health indicator and support vector regression in PHMs," *Energies*, vol. 13, no. 4, 2020, doi: 10.3390/en13040830.

[238] P. M. Attia *et al.*, "Review—"Knees" in Lithium-Ion Battery Aging Trajectories," *J. Electrochem. Soc.*, 2022, doi: 10.1149/1945-7111/ac6d13.

[239] A. Fly, B. Wimarshana, I. Bin-mat-arishad, and M. Sarmiento-Carnevali, "Temperature dependency of diagnostic methods in lithium-ion batteries," *J. Energy Storage*, vol. 52, no. PA, p. 104721, 2022, doi: 10.1016/j.est.2022.104721.

[240] Z. Deng, X. Lin, J. Cai, and X. Hu, "Battery health estimation with degradation pattern recognition and transfer learning," *J. Power Sources*, vol. 525, no. 51741707, 2022, doi: 10.1016/j.jpowsour.2022.231027.

[241] H. Ruan, J. Chen, W. Ai, and B. Wu, "Generalised diagnostic framework for rapid battery degradation quantification with deep learning," *Energy AI*, vol. 9, no. May, p. 100158, 2022, doi: 10.1016/j.egyai.2022.100158.

[242] G. Jiang, L. Zhuang, Q. Hu, Z. Liu, and J. Huang, "An investigation of heat transfer and capacity fade in a prismatic Li-ion battery based on an electrochemical-thermal coupling model," *Appl. Therm. Eng.*, vol. 171, p. 115080, 2020, doi: 10.1016/j.applthermaleng.2020.115080.

[243] S. Atalay, M. Sheikh, A. Mariani, Y. Merla, E. Bower, and W. D. Widanage, "Theory of battery ageing in a lithium-ion battery: Capacity fade, nonlinear ageing and lifetime prediction," *J. Power Sources*, vol. 478, 2020, doi: 10.1016/j.jpowsour.2020.229026.

[244] S. Greenbank and D. Howey, "Automated feature extaction and selection for data-driven models of rapid battery capacity fade and end of life," *IEEE Trans. Ind. Informatics*, pp. 1–9, 2021, doi: 10.1109/TII.2021.3106593.

[245] M. Lu, X. Zhang, J. Ji, X. Xu, and Y. Zhang, "Research progress on power battery cooling technology for electric vehicles," *J. Energy Storage*, vol. 27, no. December 2019, p. 101155, 2020, doi: 10.1016/j.est.2019.101155.

[246] X. Li and Z. Wang, "A novel fault diagnosis method for lithium-Ion battery packs of electric vehicles," *Meas. J. Int. Meas. Confed.*, vol. 116, no. November 2017, pp. 402–411, 2018, doi: 10.1016/j.measurement.2017.11.034.

[247] B. C. Barnes, J. K. Brennan, E. F. C. Byrd, S. Izvekov, J. P. Larentzos, and B. M. Rice, *Multiscale Modeling Approach for Energetic Materials*. Springer International Publishing, 2019. doi: 10.1007/978-3-030-05600-1.

[248] M. Bracconi, "Intensification of catalytic reactors: A synergic effort of Multiscale Modeling, Machine Learning and Additive Manufacturing," *Chem. Eng. Process. - Process Intensif.*, vol. 181, p. 109148, 2022, doi: 10.1016/J.CEP.2022.109148.

[249] R. Radhakrishnan, "A survey of multiscale modeling: Foundations, historical milestones, current status, and future prospects," *AIChE J.*, vol. 67, no. 3, pp. 1–21, 2021, doi: 10.1002/aic.17026.

[250] Y. Che, S. B. Vilsen, J. Meng, X. Sui, and R. Teodorescu, "Battery health prognostic with sensor-free differential temperature voltammetry reconstruction and capacity estimation based on multi-domain adaptation," *eTransportation*, vol. 17, no. September 2022, 2023, doi: 10.1016/j.etran.2023.100245.

[251] Y. Li, H. Sheng, Y. Cheng, D. I. Stroe, and R. Teodorescu, "State-of-health estimation of lithium-ion batteries based on semi-supervised transfer

component analysis," *Appl. Energy*, vol. 277, no. February, p. 115504, 2020, doi: 10.1016/j.apenergy.2020.115504.

[252] R. Zhou, S. Fu, and W. Peng, "A Review of State-of-health Estimation of Lithiumion Batteries: Experiments and Data," *2020 Asia-Pacific Int. Symp. Adv. Reliab. Maint. Model. APARM 2020*, 2020, doi: 10.1109/APARM49247.2020.9209548.

[253] U. Moralı, "Computational modeling and statistical evaluation of thermal behavior of cylindrical lithium-ion battery," *J. Energy Storage*, vol. 55, p. 105376, 2022, doi: 10.1016/J.EST.2022.105376.

[254] C. Cortes, V. Vapnik, and L. Saitta, "Support-Vector Networks Editor," *Machine Leaming*, vol. 20. Kluwer Academic Publishers, pp. 273–297, 1995.

[255] A. Botchkarev, "Performance Metrics (Error Measures) in Machine Learning Regression, Forecasting and Prognostics: Properties and Typology."

[256] K. Liu, T. R. Ashwin, X. Hu, M. Lucu, and W. D. Widanage, "An evaluation study of different modelling techniques for calendar ageing prediction of lithium-ion batteries," *Renew. Sustain. Energy Rev.*, vol. 131, p. 110017, 2020, doi: 10.1016/J.RSER.2020.110017.

[257] S. Wang, F. Wu, P. Takyi-Aninakwa, C. Fernandez, D. I. Stroe, and Q. Huang, "Improved singular filtering-Gaussian process regression-long short-term memory model for whole-life-cycle remaining capacity estimation of lithium-ion batteries adaptive to fast aging and multi-current variations," *Energy*, vol. 284, p. 128677, 2023, doi: 10.1016/J.ENERGY.2023.128677.

[258] C. Zhang, H. Wang, and L. Wu, "Life prediction model for lithium-ion battery considering fast-charging protocol," *Energy*, vol. 263, p. 126109, 2023, doi: 10.1016/J.ENERGY.2022.126109.

[259] "perrycollins,+7_v49n3_Davis (1)".

[260] L. Cai, J. Lin, and X. Liao, "A data-driven method for state of health prediction of lithium-ion batteries in a unified framework," *J. Energy Storage*, vol. 51, p. 104371, 2022.

[261] V. Sulzer *et al.*, "The challenge and opportunity of battery lifetime prediction from field data," *Joule*, vol. 5, no. 8, pp. 1934–1955, 2021.

SNL_18650_NMC_15C_0-100_0.5-2C_

Cycle_Index	Start_Time	End_Time	Test_Time (s)	Cycle Time (s)	Min_Curre	Max_Curre	Min_Volta	Max_Volta	Charge_Ca	Discharge_Capacity (Ah)	Capacity_Loss (Ah)	Charge_En	Discharge	Energy Loss (Wh)
1	11:29.0	17:29.1	14770.085	14770.085	-1.5	1.499	1.999	4.2	2.582	2.724	-0.142	10.092	9.551	0.541
2	17:29.1	29:02.7	29863.699	15093.614	-1.5	1.499	1.999	4.2	2.731	2.732	-0.001	10.584	9.587	0.997
3	29:02.9	40:26.0	44947.034	15083.335	-1.5	1.499	1.999	4.2	2.731	2.727	0.004	10.581	9.575	1.006
4	40:26.0	08:00.5	64601.545	19654.511	-6	1.499	1.999	4.2	5.436	5.414	0.022	21.061	17.261	3.8
5	10:00.6	45:51.9	74072.87	9471.325	-5.999	1.499	1.999	4.2	2.698	2.689	0.009	10.439	8.575	1.864
6	47:51.9	23:11.7	83512.706	9439.836	-5.999	1.499	1.999	4.2	2.688	2.679	0.009	10.401	8.547	1.854
7	25:11.8	00:09.6	92930.614	9417.908	-5.999	1.499	1.998	4.2	2.683	2.674	0.009	10.386	8.544	1.842
8	02:09.7	36:41.8	102322.792	9392.178	-5.999	1.499	1.999	4.2	2.671	2.664	0.007	10.34	8.516	1.824
9	38:41.8	12:53.1	111694.087	9371.295	-5.999	1.499	1.999	4.2	2.664	2.657	0.007	10.313	8.505	1.808
10	14:53.1	48:47.0	121048.038	9353.951	-5.999	1.499	1.998	4.2	2.657	2.651	0.006	10.289	8.496	1.793
11	50:47.1	24:24.7	130385.713	9337.675	-5.999	1.499	1.999	4.2	2.651	2.646	0.005	10.267	8.486	1.781
12	26:24.8	59:46.2	139707.195	9321.482	-5.999	1.499	1.999	4.2	2.646	2.641	0.005	10.246	8.478	1.768
13	01:46.2	34:53.6	149014.611	9307.416	-5.999	1.499	1.999	4.2	2.64	2.635	0.005	10.226	8.469	1.757
14	36:53.7	09:45.8	158306.789	9292.178	-5.999	1.499	1.999	4.2	2.635	2.63	0.005	10.206	8.459	1.747
15	11:45.8	44:23.3	167584.349	9277.56	-5.999	1.499	1.999	4.2	2.63	2.625	0.005	10.187	8.45	1.737
16	46:23.4	18:45.6	176846.569	9262.22	-5.999	1.499	1.999	4.2	2.625	2.62	0.005	10.169	8.441	1.728
17	20:45.6	52:53.5	186094.479	9247.91	-5.999	1.499	1.998	4.2	2.619	2.616	0.003	10.149	8.431	1.718
18	54:53.5	26:48.3	195329.348	9234.869	-5.999	1.499	1.997	4.2	2.615	2.611	0.004	10.132	8.42	1.712
19	28:48.4	00:27.8	204548.803	9219.455	-5.998	1.499	1.997	4.2	2.609	2.606	0.003	10.113	8.408	1.705
20	02:27.9	33:54.1	213755.096	9206.293	-5.998	1.499	1.999	4.2	2.605	2.601	0.004	10.096	8.397	1.699
21	35:54.1	07:06.5	222947.497	9192.401	-5.999	1.499	1.999	4.2	2.6	2.596	0.004	10.078	8.386	1.692
22	09:06.5	40:05.1	232126.103	9178.606	-5.999	1.499	1.999	4.2	2.595	2.592	0.003	10.061	8.376	1.685
23	42:05.2	12:50.8	241291.829	9165.726	-5.999	1.499	1.997	4.2	2.591	2.587	0.004	10.044	8.364	1.68
24	14:50.9	45:23.4	250444.449	9152.62	-5.999	1.499	1.998	4.2	2.586	2.583	0.003	10.027	8.353	1.674
25	47:23.5	17:42.9	259583.939	9139.49	-5.999	1.499	1.998	4.2	2.582	2.579	0.003	10.011	8.342	1.669
26	19:43.0	49:51.0	268711.97	9128.031	-5.999	1.499	1.997	4.2	2.578	2.575	0.003	9.996	8.332	1.664
27	51:51.0	21:47.3	277828.263	9116.293	-5.999	1.499	1.999	4.2	2.574	2.571	0.003	9.982	8.323	1.659
28	23:47.3	53:31.3	286932.318	9104.055	-5.999	1.499	1.999	4.2	2.569	2.566	0.003	9.966	8.311	1.655
29	55:31.4	25:03.1	296024.119	9091.801	-5.999	1.499	1.999	4.2	2.565	2.562	0.003	9.95	8.3	1.65
30	27:03.2	56:21.7	305102.677	9078.558	-5.999	1.499	1.997	4.2	2.56	2.558	0.002	9.934	8.288	1.646
31	58:21.7	27:29.4	314170.383	9067.706	-5.998	1.499	1.998	4.2	2.556	2.554	0.002	9.919	8.276	1.643
32	29:29.4	58:24.3	323225.347	9054.964	-5.998	1.499	1.998	4.2	2.552	2.55	0.002	9.904	8.266	1.638
33	00:24.4	29:08.5	332269.46	9044.113	-5.998	1.499	1.999	4.2	2.548	2.546	0.002	9.89	8.255	1.635
34	31:08.5	59:41.1	341302.069	9032.609	-5.998	1.499	1.998	4.2	2.545	2.542	0.003	9.877	8.245	1.632
35	01:41.1	30:02.1	350323.057	9020.988	-5.999	1.499	1.998	4.2	2.541	2.539	0.002	9.865	8.235	1.63
36	32:02.1	00:11.2	359332.177	9009.12	-5.999	1.499	1.998	4.2	2.538	2.535	0.003	9.852	8.226	1.626
37	02:11.2	30:17.9	368338.912	9006.735	-5.999	1.499	1.997	4.2	2.537	2.534	0.003	9.849	8.225	1.624
38	32:17.9	00:11.7	377332.663	8993.751	-5.999	1.499	1.999	4.2	2.533	2.531	0.002	9.837	8.215	1.622
39	02:11.7	29:51.7	386312.692	8980.029	-5.999	1.499	1.997	4.2	2.529	2.527	0.002	9.823	8.204	1.619
40	31:51.8	59:20.4	395281.351	8968.659	-5.999	1.499	1.997	4.2	2.526	2.523	0.003	9.81	8.194	1.616
41	01:20.4	28:36.0	404237.002	8955.651	-5.999	1.499	1.999	4.2	2.521	2.519	0.002	9.795	8.183	1.612
42	30:36.1	57:40.1	413181.126	8944.124	-5.999	1.499	1.999	4.2	2.517	2.515	0.002	9.777	8.169	1.608
43	59:40.2	26:32.1	422113.117	8931.991	-6	1.499	1.997	4.2	2.512	2.51	0.002	9.759	8.155	1.604
44	28:32.2	55:14.4	431035.371	8922.254	-6	1.499	1.996	4.2	2.508	2.506	0.002	9.744	8.143	1.601
45	57:14.4	23:43.5	439944.534	8909.163	-6	1.499	1.997	4.2	2.504	2.5	0.004	9.729	8.124	1.605
46	25:43.6	52:00.6	448841.608	8897.074	-6	1.499	1.997	4.2	2.499	2.498	0.001	9.713	8.117	1.596
47	54:00.7	20:09.0	457730.026	8888.418	-6	1.499	1.997	4.2	2.496	2.494	0.002	9.702	8.105	1.597
48	22:09.1	48:07.3	466608.318	8878.292	-6	1.499	1.999	4.2	2.493	2.491	0.002	9.69	8.093	1.597
49	50:07.4	15:54.6	475475.623	8867.305	-5.999	1.499	1.997	4.2	2.489	2.487	0.002	9.676	8.081	1.595
50	17:54.7	43:31.8	484332.793	8857.17	-5.999	1.499	1.996	4.2	2.486	2.484	0.002	9.663	8.071	1.592
51	45:31.8	10:58.0	493179.011	8846.218	-5.999	1.499	1.997	4.2	2.482	2.48	0.002	9.65	8.06	1.59
52	12:58.1	38:15.5	502016.462	8837.451	-5.999	1.499	1.997	4.2	2.479	2.477	0.002	9.639	8.05	1.589
53	40:15.5	05:22.9	510843.897	8827.435	-5.999	1.499	1.999	4.2	2.476	2.473	0.003	9.627	8.04	1.587
54	07:23.0	32:21.6	519662.635	8818.738	-6	1.499	1.999	4.2	2.473	2.471	0.002	9.617	8.031	1.586
55	34:21.7	59:09.4	528470.442	8807.807	-5.999	1.499	1.996	4.2	2.469	2.467	0.002	9.604	8.021	1.583
56	01:09.5	25:51.3	537272.326	8801.884	-5.999	1.499	1.997	4.2	2.466	2.464	0.002	9.595	8.011	1.584
57	27:51.4	52:22.8	546063.789	8791.463	-5.999	1.499	1.998	4.2	2.463	2.461	0.002	9.584	8.003	1.581
58	54:22.8	18:41.1	554842.089	8778.3	-5.999	1.499	1.998	4.2	2.46	2.458	0.002	9.573	7.993	1.58
59	20:41.1	44:45.6	563606.634	8764.545	-5.999	1.499	1.998	4.2	2.456	2.454	0.002	9.559	7.982	1.577
60	46:45.7	10:39.3	572360.289	8753.655	-5.999	1.499	1.996	4.2	2.452	2.45	0.002	9.544	7.97	1.574
61	12:39.3	36:23.0	581104.037	8743.748	-5.999	1.499	1.997	4.2	2.448	2.446	0.002	9.528	7.956	1.572
62	38:23.1	01:55.4	589836.397	8732.36	-6	1.499	1.997	4.2	2.444	2.442	0.002	9.512	7.944	1.568
63	03:55.4	27:18.5	598559.539	8723.142	-6	1.499	1.997	4.2	2.44	2.438	0.002	9.498	7.93	1.568
64	29:18.6	52:31.8	607272.76	8713.221	-6	1.499	1.996	4.2	2.437	2.435	0.002	9.487	7.919	1.568
65	54:31.8	17:35.4	615976.42	8703.66	-6	1.499	1.999	4.2	2.434	2.431	0.003	9.475	7.908	1.567
66	19:35.5	42:29.5	624670.489	8694.069	-5.999	1.499	1.998	4.2	2.43	2.428	0.002	9.462	7.897	1.565
67	44:29.5	07:12.5	633353.507	8683.018	-5.999	1.499	1.999	4.2	2.427	2.424	0.003	9.449	7.885	1.564
68	09:12.6	31:46.2	642027.203	8673.696	-5.999	1.499	1.999	4.2	2.423	2.421	0.002	9.437	7.874	1.563
69	33:46.3	56:09.6	650690.622	8663.419	-5.999	1.499	1.999	4.2	2.42	2.418	0.002	9.425	7.864	1.561
70	58:09.7	20:25.2	659346.16	8655.538	-5.999	1.499	1.999	4.2	2.417	2.415	0.002	9.414	7.854	1.56
71	22:25.2	44:32.0	667992.98	8646.82	-5.999	1.499	1.999	4.2	2.414	2.412	0.002	9.403	7.845	1.558
72	46:32.0	08:32.1	676633.062	8640.082	-5.999	1.499	1.998	4.2	2.411	2.409	0.002	9.395	7.836	1.559
73	10:32.1	32:22.5	685263.526	8630.464	-5.999	1.499	1.999	4.2	2.409	2.406	0.003	9.385	7.828	1.557
74	34:22.6	56:00.4	693881.409	8617.883	-5.999	1.499	1.997	4.2	2.406	2.403	0.003	9.375	7.819	1.556
75	58:00.5	19:25.4	702486.366	8604.957	-5.999	1.499	1.997	4.2	2.402	2.4	0.002	9.363	7.808	1.555
76	21:25.4	42:40.8	711081.809	8595.443	-5.999	1.499	1.998	4.2	2.398	2.396	0.002	9.347	7.794	1.553
77	44:40.9	05:44.6	719665.61	8583.801	-6	1.499	1.995	4.2	2.393	2.391	0.002	9.327	7.779	1.548
78	07:44.7	28:38.4	728239.384	8573.774	-6	1.499	1.997	4.2	2.389	2.387	0.002	9.312	7.766	1.546
79	30:38.4	51:21.2	736802.186	8562.802	-6	1.499	1.999	4.2	2.385	2.383	0.002	9.299	7.753	1.546
80	53:21.3	13:54.2	745355.197	8553.011	-6	1.499	1.999	4.2	2.382	2.38	0.002	9.287	7.74	1.547
81	15:54.3	36:17.3	753898.292	8543.095	-5.999	1.499	1.995	4.2	2.379	2.377	0.002	9.275	7.729	1.546
82	38:17.4	58:31.5	762432.533	8534.241	-5.999	1.499	1.997	4.2	2.376	2.373	0.003	9.264	7.719	1.545
83	00:31.6	20:35.0	770955.953	8523.42	-5.999	1.499	1.996	4.2	2.372	2.37	0.002	9.251	7.708	1.543
84	22:35.0	42:29.4	779470.392	8514.439	-5.999	1.499	1.997	4.2	2.369	2.367	0.002	9.24	7.697	1.543
85	44:29.5	04:15.6	787976.606	8506.214	-5.999	1.499	1.996	4.2	2.366	2.364	0.002	9.228	7.687	1.541
86	06:15.6	25:53.6	796474.573	8497.967	-5.999	1.499	1.995	4.2	2.363	2.361	0.002	9.218	7.677	1.541
87	27:53.6	47:25.0	804965.963	8491.39	-5.999	1.499	1.998	4.2	2.36	2.358	0.002	9.209	7.668	1.541
88	49:25.0	08:42.5	813443.493	8477.53	-5.999	1.499	1.999	4.2	2.357	2.355	0.002	9.197	7.657	1.54
89	10:42.6	29:46.9	821907.949	8464.456	-5.999	1.499	1.999	4.2	2.354	2.352	0.002	9.186	7.647	1.539
90	31:47.0	50:38.7	830359.722	8451.773	-5.999	1.499	1.998	4.2	2.35	2.347	0.003	9.17	7.634	1.536

91	52:38.8	11:21.0	838802.02	8442.298	-5.999	1.499	1.995	4.2	2.345	2.343	0.002	9.153	7.62	1.533
92	13:21.1	31:52.6	847233.623	8431.603	-6	1.499	1.996	4.2	2.341	2.339	0.002	9.136	7.605	1.531
93	33:52.7	52:14.7	855655.742	8422.119	-6	1.499	1.994	4.2	2.337	2.335	0.002	9.124	7.594	1.53
94	54:14.8	12:26.8	864067.751	8412.009	-6	1.499	1.997	4.2	2.334	2.332	0.002	9.112	7.581	1.531
95	14:26.8	32:29.7	872470.681	8402.93	-6	1.499	1.995	4.2	2.331	2.329	0.002	9.1	7.569	1.531
96	34:29.7	52:23.0	880864.035	8393.354	-5.999	1.499	1.994	4.2	2.328	2.326	0.002	9.088	7.558	1.53
97	54:23.1	12:06.9	889247.877	8383.842	-5.999	1.499	1.999	4.2	2.324	2.322	0.002	9.076	7.546	1.53
98	14:06.9	31:40.3	897621.266	8373.389	-5.999	1.499	1.996	4.2	2.321	2.319	0.002	9.063	7.536	1.527
99	33:40.3	51:05.6	905986.61	8365.344	-5.999	1.499	1.995	4.2	2.318	2.316	0.002	9.052	7.525	1.527
100	53:05.7	10:22.9	914343.887	8357.277	-5.999	1.499	1.996	4.2	2.315	2.313	0.002	9.042	7.515	1.527
101	12:23.0	29:33.3	922694.299	8350.412	-5.999	1.499	1.996	4.2	2.312	2.31	0.002	9.033	7.506	1.527
102	31:33.3	48:33.4	931034.39	8340.091	-5.999	1.499	1.994	4.2	2.31	2.308	0.002	9.026	7.499	1.527
103	50:33.5	07:20.8	939361.849	8327.459	-5.999	1.499	1.997	4.2	2.307	2.305	0.002	9.015	7.49	1.525
104	09:20.9	25:55.7	947676.65	8314.801	-5.999	1.499	1.998	4.2	2.303	2.301	0.002	9	7.477	1.523
105	27:55.7	44:19.5	955980.473	8303.823	-5.999	1.499	1.994	4.2	2.298	2.296	0.002	8.983	7.463	1.52
106	46:19.5	02:34.1	964275.05	8294.577	-6	1.499	1.997	4.2	2.294	2.292	0.002	8.966	7.448	1.518
107	04:34.1	20:37.4	972558.439	8283.389	-6	1.499	1.996	4.2	2.29	2.288	0.002	8.951	7.435	1.516
108	22:37.5	38:34.0	980834.951	8276.512	-6	1.499	1.995	4.2	2.288	2.286	0.002	8.942	7.424	1.518
109	40:34.0	56:19.6	989100.624	8265.673	-6	1.499	1.994	4.2	2.284	2.282	0.002	8.929	7.411	1.518
110	58:19.7	13:55.8	997356.83	8256.206	-5.999	1.499	1.994	4.2	2.281	2.279	0.002	8.917	7.401	1.516
111	15:55.9	31:23.5	1005604.481	8247.651	-5.999	1.499	1.996	4.2	2.278	2.276	0.002	8.905	7.389	1.516
112	33:23.5	48:41.1	1013842.136	8237.655	-5.999	1.499	1.997	4.2	2.275	2.272	0.003	8.893	7.378	1.515
113	50:41.2	05:50.5	1022071.487	8229.351	-5.999	1.499	1.997	4.2	2.272	2.27	0.002	8.883	7.368	1.515
114	07:50.5	22:54.2	1030295.184	8223.697	-6	1.499	1.997	4.2	2.27	2.268	0.002	8.878	7.363	1.515
115	24:54.2	39:49.7	1038510.71	8215.526	-5.999	1.499	1.996	4.2	2.267	2.265	0.002	8.869	7.354	1.515
116	41:49.7	56:36.6	1046717.623	8206.913	-5.999	1.499	1.994	4.2	2.265	2.263	0.002	8.86	7.346	1.514
117	58:36.7	13:11.2	1054912.213	8194.59	-5.999	1.499	1.996	4.2	2.262	2.26	0.002	8.85	7.336	1.514
118	15:11.3	29:33.9	1063094.868	8182.655	-5.999	1.499	1.998	4.2	2.258	2.256	0.002	8.836	7.326	1.51
119	31:34.0	45:47.2	1071268.177	8173.309	-5.999	1.499	1.996	4.201	2.254	2.252	0.002	8.82	7.312	1.508
120	47:47.2	01:49.8	1079430.827	8162.65	-6	1.499	1.996	4.2	2.25	2.248	0.002	8.803	7.298	1.505
121	03:49.9	17:44.1	1087585.096	8154.269	-6	1.499	1.994	4.2	2.247	2.245	0.002	8.791	7.286	1.505
122	19:44.1	33:29.1	1095730.056	8144.96	-6	1.499	1.998	4.2	2.244	2.242	0.002	8.78	7.274	1.506
123	35:29.1	49:05.7	1103866.659	8136.603	-6	1.499	1.995	4.2	2.241	2.239	0.002	8.77	7.264	1.506
124	51:05.7	04:34.2	1111995.204	8128.545	-6	1.499	1.997	4.2	2.238	2.236	0.002	8.759	7.253	1.506
125	06:34.2	19:53.7	1120114.675	8119.471	-6	1.5	1.997	4.2	2.235	2.233	0.002	8.748	7.244	1.504
126	21:53.7	35:04.9	1128225.921	8111.246	-6	1.499	1.996	4.2	2.232	2.23	0.002	8.737	7.234	1.503
127	37:05.0	50:09.0	1136330.019	8104.098	-6	1.499	1.998	4.2	2.229	2.228	0.001	8.727	7.224	1.503
128	52:09.1	05:06.9	1144427.923	8097.904	-6	1.499	1.999	4.2	2.227	2.225	0.002	8.718	7.215	1.503
129	07:07.0	19:59.3	1152520.281	8092.358	-5.999	1.499	1.993	4.2	2.225	2.223	0.002	8.711	7.209	1.502
130	21:59.3	34:41.7	1160602.731	8082.45	-5.999	1.499	1.994	4.2	2.223	2.221	0.002	8.704	7.192	1.502
131	36:41.8	49:12.6	1168673.582	8070.851	-5.999	1.499	1.997	4.2	2.22	2.218	0.002	8.692	7.192	1.5
132	51:12.6	03:33.3	1176734.296	8060.714	-5.999	1.499	1.993	4.2	2.216	2.214	0.002	8.679	7.181	1.498
133	05:33.3	17:44.8	1184785.784	8051.488	-5.999	1.499	1.995	4.2	2.212	2.21	0.002	8.663	7.167	1.496
134	19:44.8	31:48.0	1192828.983	8043.199	-6	1.499	1.997	4.2	2.208	2.207	0.001	8.649	7.156	1.493
135	33:48.0	45:43.4	1200864.395	8035.412	-6	1.499	1.997	4.2	2.206	2.204	0.002	8.639	7.145	1.494
136	47:43.5	59:29.9	1208890.903	8026.508	-6	1.499	1.999	4.2	2.203	2.201	0.002	8.628	7.134	1.494
137	01:30.0	13:08.8	1216909.828	8018.925	-6	1.499	1.995	4.2	2.2	2.198	0.002	8.618	7.122	1.496
138	15:08.9	26:39.7	1224920.721	8010.893	-6	1.499	1.998	4.2	2.197	2.195	0.002	8.607	7.113	1.494
139	28:39.8	40:03.5	1232924.532	8003.811	-5.999	1.499	1.998	4.2	2.194	2.193	0.001	8.597	7.104	1.493
140	42:03.6	53:20.5	1240921.465	7996.933	-5.999	1.499	1.998	4.2	2.192	2.191	0.001	8.588	7.096	1.492
141	55:20.5	06:31.7	1248912.665	7991.2	-5.999	1.499	1.996	4.2	2.19	2.189	0.001	8.581	7.09	1.491
142	08:31.7	19:38.2	1256899.192	7986.527	-5.999	1.499	1.999	4.2	2.188	2.187	0.001	8.575	7.083	1.492
143	21:38.2	32:35.7	1264876.722	7977.53	-5.999	1.499	1.994	4.2	2.186	2.185	0.001	8.567	7.076	1.491
144	34:35.8	45:23.4	1272844.382	7967.66	-5.999	1.499	1.995	4.2	2.184	2.182	0.002	8.558	7.068	1.49
145	47:23.4	58:02.0	1280802.956	7958.574	-5.999	1.499	1.999	4.2	2.181	2.179	0.002	8.548	7.059	1.489
146	00:02.0	10:31.9	1288752.948	7949.992	-5.999	1.499	1.997	4.2	2.177	2.176	0.001	8.534	7.048	1.486
147	12:32.0	22:53.0	1296693.962	7941.014	-6	1.499	1.997	4.2	2.174	2.173	0.001	8.521	7.036	1.485
148	24:53.0	35:08.3	1304629.319	7935.357	-6	1.499	1.997	4.2	2.171	2.17	0.001	8.512	7.027	1.485
149	37:08.4	47:15.4	1312556.447	7927.128	-6	1.499	1.998	4.2	2.169	2.167	0.002	8.5	7.015	1.485
150	49:15.5	59:15.4	1320476.417	7919.97	-6	1.499	1.993	4.2	2.166	2.165	0.001	8.49	7.006	1.484
151	01:15.5	11:08.4	1328389.372	7912.955	-5.999	1.499	1.997	4.2	2.163	2.162	0.001	8.48	6.997	1.483
152	13:08.4	22:56.2	1336297.208	7907.836	-5.999	1.499	1.996	4.2	2.161	2.16	0.001	8.473	6.989	1.484
153	24:56.3	34:36.9	1344197.917	7900.709	-5.999	1.499	1.998	4.2	2.159	2.158	0.001	8.465	6.981	1.484
154	36:37.0	46:13.3	1352094.305	7896.388	-5.999	1.499	1.993	4.2	2.157	2.156	0.001	8.458	6.975	1.483
155	48:13.3	57:46.1	1359987.125	7892.82	-5.999	1.499	1.996	4.2	2.156	2.155	0.001	8.453	6.97	1.483
156	59:46.2	09:10.8	1367871.811	7884.686	-5.999	1.499	1.998	4.2	2.154	2.153	0.001	8.449	6.964	1.485
157	11:10.9	20:26.7	1375747.713	7875.902	-6	1.499	1.995	4.2	2.152	2.151	0.001	8.441	6.957	1.484
158	22:26.8	31:35.2	1383616.156	7868.443	-5.999	1.499	1.998	4.2	2.15	2.149	0.001	8.432	6.95	1.482
159	33:35.2	42:37.3	1391478.347	7862.191	-5.999	1.499	1.993	4.2	2.147	2.146	0.001	8.42	6.94	1.48
160	44:37.4	53:32.3	1399333.273	7854.926	-6	1.499	1.997	4.2	2.144	2.143	0.001	8.409	6.929	1.48
161	55:32.3	04:19.7	1407180.729	7847.456	-6	1.499	1.998	4.2	2.141	2.141	0	8.399	6.921	1.478
162	06:19.8	15:01.0	1415021.951	7841.222	-6	1.499	1.994	4.2	2.139	2.138	0.001	8.392	6.911	1.481
163	17:01.0	25:35.6	1422856.553	7834.602	-6	1.499	1.998	4.2	2.137	2.136	0.001	8.382	6.903	1.479
164	27:35.6	36:05.3	1430686.343	7829.79	-5.999	1.499	1.999	4.2	2.135	2.134	0.001	8.375	6.896	1.479
165	38:05.4	46:29.8	1438510.786	7824.443	-6	1.499	1.994	4.2	2.133	2.132	0.001	8.368	6.889	1.479
166	48:29.8	56:50.5	1446331.508	7820.722	-5.999	1.499	1.998	4.2	2.132	2.131	0.001	8.363	6.884	1.479
167	58:50.6	07:06.4	1454147.419	7815.911	-5.999	1.499	1.994	4.2	2.13	2.129	0.001	8.357	6.877	1.48
168	09:06.5	17:19.3	1461960.336	7812.917	-5.999	1.499	1.994	4.2	2.129	2.128	0.001	8.353	6.874	1.479
169	19:19.4	27:25.6	1469766.574	7806.238	-5.999	1.499	1.999	4.2	2.128	2.127	0.001	8.349	6.869	1.48
170	29:25.6	37:22.9	1477563.862	7797.288	-5.999	1.499	1.995	4.2	2.126	2.125	0.001	8.34	6.863	1.477
171	39:22.9	47:15.5	1485356.503	7792.504	-5.999	1.499	1.999	4.2	2.123	2.123	0	8.333	6.856	1.477
172	49:15.6	57:01.3	1493142.305	7785.802	-6	1.499	1.994	4.2	2.12	2.12	0	8.319	6.845	1.474
173	59:01.4	06:42.2	1500923.227	7780.922	-6	1.499	1.997	4.2	2.118	2.117	0.001	8.311	6.836	1.475
174	08:42.3	16:17.0	1508697.951	7774.724	-6	1.499	1.994	4.2	2.116	2.116	0	8.305	6.83	1.475
175	18:17.0	25:47.3	1516468.253	7770.302	-6	1.499	1.997	4.2	2.115	2.114	0.001	8.3	6.823	1.477
176	27:47.4	35:11.4	1524232.447	7764.194	-5.999	1.499	1.997	4.2	2.113	2.112	0.001	8.292	6.816	1.476
177	37:11.5	44:30.7	1531991.735	7759.288	-5.999	1.499	1.994	4.2	2.111	2.11	0.001	8.283	6.808	1.475
178	46:30.8	53:45.7	1539746.712	7754.977	-6	1.499	1.997	4.2	2.109	2.108	0.001	8.276	6.802	1.474
179	55:45.8	02:58.3	1547499.262	7752.55	-6	1.499	1.997	4.2	2.108	2.107	0.001	8.273	6.798	1.475
180	04:58.3	12:09.9	1555250.906	7751.644	-5.999	1.499	1.997	4.2	2.107	2.107	0	8.271	6.795	1.476
181	14:09.9	21:13.9	1562994.906	7744	-5.999	1.499	1.995	4.2	2.106	2.105	0.001	8.266	6.789	1.477

182	23:14.0	30:09.4	1570730.431	7735.525	-5.999	1.499	1.998	4.201	2.104	2.104	0	8.259	6.783	1.476
183	32:09.5	38:59.2	1578460.216	7729.785	-6	1.499	1.995	4.2	2.102	2.101	0.001	8.25	6.776	1.474
184	40:59.3	47:44.6	1586185.576	7725.36	-5.999	1.499	1.996	4.2	2.099	2.098	0.001	8.239	6.766	1.473
185	49:44.6	56:25.4	1593906.385	7720.809	-6	1.499	1.997	4.2	2.096	2.096	0	8.229	6.758	1.471
186	58:25.4	05:03.0	1601623.958	7717.573	-6	1.499	1.998	4.2	2.095	2.095	0	8.225	6.751	1.474
187	07:03.0	13:34.8	1609335.828	7711.87	-6	1.499	1.996	4.2	2.094	2.093	0.001	8.219	6.744	1.475
188	15:34.8	22:01.0	1617042.023	7706.195	-5.999	1.499	1.999	4.2	2.092	2.092	0	8.213	6.738	1.475
189	24:01.0	30:22.3	1624743.288	7701.265	-5.999	1.499	1.998	4.2	2.09	2.09	0	8.207	6.733	1.474
190	32:22.4	38:40.1	1632441.097	7697.809	-5.999	1.499	1.999	4.2	2.089	2.089	0	8.2	6.727	1.473
191	40:40.2	46:54.1	1640135.145	7694.048	-6	1.499	1.996	4.2	2.087	2.087	0	8.195	6.721	1.474
192	48:54.2	55:06.1	1647827.099	7691.954	-5.999	1.499	1.998	4.2	2.086	2.086	0	8.191	6.718	1.473
193	57:06.1	03:14.6	1655515.628	7688.529	-5.999	1.499	1.996	4.2	2.086	2.085	0.001	8.19	6.715	1.475
194	05:14.7	11:14.2	1663195.227	7679.599	-5.999	1.499	1.997	4.2	2.084	2.084	0	8.182	6.708	1.474
195	13:14.3	19:06.9	1670867.939	7672.712	-5.999	1.499	1.997	4.2	2.082	2.081	0.001	8.174	6.699	1.475
196	21:07.0	26:55.5	1678536.477	7668.538	-5.999	1.499	1.997	4.2	2.079	2.079	0	8.165	6.693	1.472
197	28:55.5	34:39.4	1686200.392	7663.915	-6	1.499	1.999	4.2	2.077	2.077	0	8.156	6.685	1.471
198	36:39.4	42:19.4	1693860.434	7660.042	-6	1.499	1.994	4.2	2.076	2.076	0	8.151	6.679	1.472
199	44:19.4	49:57.7	1701518.726	7658.292	-6	1.499	1.997	4.2	2.075	2.075	0	8.148	6.674	1.474
200	51:57.8	57:31.6	1709172.624	7653.898	-6	1.499	1.993	4.2	2.074	2.073	0.001	8.142	6.668	1.474
201	59:31.7	05:01.4	1716822.441	7649.817	-5.999	1.499	1.995	4.2	2.073	2.073	0	8.139	6.664	1.475
202	07:01.5	12:27.2	1724468.184	7645.743	-5.999	1.499	1.994	4.2	2.071	2.071	0	8.134	6.66	1.474
203	14:27.3	19:50.7	1732111.737	7643.553	-6	1.499	1.993	4.2	2.07	2.07	0	8.13	6.657	1.473
204	21:50.7	27:12.0	1739752.994	7641.257	-5.999	1.499	1.997	4.2	2.069	2.069	0	8.126	6.652	1.474
205	29:12.1	34:30.6	1747391.564	7638.57	-6	1.499	1.994	4.2	2.068	2.068	0	8.122	6.648	1.474
206	36:30.7	41:42.5	1755023.509	7631.945	-5.999	1.499	1.993	4.2	2.067	2.067	0	8.118	6.645	1.473
207	43:42.5	48:47.0	1762648.003	7624.494	-6	1.499	1.997	4.2	2.065	2.066	-0.001	8.112	6.639	1.473
208	50:47.1	55:49.0	1770269.986	7621.983	-5.999	1.499	1.997	4.2	2.063	2.063	0	8.104	6.632	1.472
209	57:49.1	02:46.7	1777887.746	7617.76	-6	1.499	1.997	4.2	2.061	2.061	0	8.096	6.625	1.471
210	04:46.8	09:41.1	1785502.071	7614.325	-6	1.499	1.997	4.2	2.06	2.06	0	8.09	6.62	1.47
211	11:41.2	16:31.3	1793112.31	7610.239	-6	1.499	1.994	4.2	2.059	2.059	0	8.085	6.613	1.472
212	18:31.3	23:18.2	1800719.206	7606.896	-6	1.499	1.999	4.2	2.057	2.057	0	8.08	6.605	1.475
213	25:18.3	30:01.4	1808322.359	7603.153	-5.999	1.499	1.994	4.2	2.056	2.056	0	8.076	6.603	1.473
214	32:01.4	36:43.9	1815924.918	7602.559	-5.999	1.499	1.998	4.2	2.056	2.056	0	8.074	6.601	1.474
215	38:44.0	43:25.0	1823525.98	7601.062	-5.999	1.499	1.996	4.2	2.056	2.056	0	8.074	6.6	1.474
216	45:25.0	50:01.9	1831122.941	7596.961	-5.999	1.499	1.999	4.2	2.054	2.054	0	8.069	6.596	1.473
217	52:02.0	56:37.0	1838717.961	7595.02	-5.999	1.499	1.997	4.2	2.053	2.053	0	8.066	6.592	1.474
218	58:37.1	03:06.9	1846307.922	7589.961	-5.999	1.499	1.998	4.2	2.052	2.052	0	8.062	6.588	1.474
219	05:07.0	09:30.0	1853891.037	7583.115	-5.999	1.499	1.995	4.2	2.051	2.051	0	8.057	6.583	1.474
220	11:30.1	15:48.4	1861469.425	7578.388	-5.999	1.499	1.999	4.2	2.049	2.049	0	8.05	6.579	1.471
221	17:48.5	22:02.8	1869043.842	7574.417	-6	1.499	1.994	4.2	2.047	2.047	0	8.041	6.572	1.469
222	24:02.9	28:14.6	1876615.641	7571.799	-6	1.499	1.996	4.2	2.045	2.045	0	8.034	6.564	1.47
223	30:14.7	34:22.7	1884183.704	7568.063	-6	1.499	1.996	4.2	2.044	2.044	0	8.03	6.559	1.471
224	36:22.8	40:28.9	1891749.919	7566.215	-6	1.499	1.996	4.2	2.044	2.043	0.001	8.028	6.554	1.474
225	42:28.9	46:31.6	1899312.611	7562.692	-5.999	1.5	1.996	4.2	2.043	2.043	0	8.024	6.552	1.472
226	48:31.6	52:32.4	1906873.391	7560.78	-5.999	1.499	1.998	4.2	2.042	2.042	0	8.021	6.548	1.473
227	54:32.5	58:31.3	1914432.336	7558.945	-5.999	1.499	1.999	4.2	2.041	2.041	0	8.018	6.545	1.473
228	00:31.4	04:30.0	1921991.034	7558.698	-5.999	1.499	1.993	4.2	2.04	2.041	-0.001	8.016	6.543	1.473
229	06:30.1	10:28.3	1929549.295	7558.261	-5.999	1.499	1.997	4.2	2.04	2.04	0	8.015	6.541	1.474
230	12:28.4	16:20.8	1937101.754	7552.459	-5.999	1.499	1.996	4.2	2.04	2.04	0	8.014	6.539	1.475
231	18:20.8	22:05.6	1944646.559	7544.805	-6	1.499	1.993	4.2	2.038	2.038	0	8.001	6.535	1.473
232	24:05.6	27:46.1	1952187.08	7540.521	-6	1.499	1.999	4.2	2.036	2.036	0	8.001	6.528	1.473
233	29:46.1	33:22.3	1959723.288	7536.208	-5.999	1.499	1.994	4.2	2.034	2.034	0	7.991	6.52	1.471
234	35:22.4	38:55.6	1967256.599	7533.311	-6	1.499	1.998	4.2	2.032	2.032	0	7.983	6.515	1.468
235	40:55.6	44:26.9	1974787.929	7531.33	-6	1.499	1.997	4.2	2.031	2.032	-0.001	7.981	6.51	1.471
236	46:26.9	49:55.9	1982316.919	7528.99	-6	1.499	1.996	4.2	2.031	2.031	0	7.979	6.506	1.473
237	51:55.9	55:20.7	1989841.708	7524.789	-5.999	1.499	1.996	4.2	2.03	2.03	0	7.974	6.5	1.474
238	57:20.7	00:43.5	1997364.463	7522.755	-5.999	1.499	1.999	4.2	2.029	2.029	0	7.97	6.497	1.473
239	02:43.6	06:05.2	2004886.169	7521.706	-5.999	1.499	1.995	4.2	2.028	2.028	0	7.968	6.495	1.473
240	08:05.2	11:26.2	2012407.167	7520.998	-5.999	1.499	1.996	4.2	2.028	2.028	0	7.967	6.495	1.472
241	13:26.3	16:47.5	2019928.546	7521.379	-6	1.499	1.994	4.2	2.028	2.028	0	7.967	6.493	1.474
242	18:47.6	22:03.9	2027444.857	7516.311	-5.999	1.499	1.997	4.2	2.027	2.027	0	7.965	6.491	1.474
243	24:04.0	27:15.1	2034956.067	7511.21	-5.999	1.499	1.996	4.2	2.026	2.026	0	7.962	6.489	1.473
244	29:15.1	32:22.6	2042463.555	7507.488	-6	1.499	1.995	4.2	2.025	2.025	0	7.958	6.485	1.473
245	34:22.6	37:26.7	2049967.737	7504.182	-5.999	1.499	1.996	4.2	2.023	2.024	-0.001	7.951	6.481	1.47
246	39:26.8	42:26.0	2057467.025	7499.288	-6	1.499	1.996	4.2	2.021	2.022	-0.001	7.943	6.473	1.47
247	44:26.1	47:22.7	2064963.674	7496.649	-6	1.499	1.995	4.2	2.02	2.02	0	7.938	6.468	1.47
248	49:22.8	52:16.7	2072457.729	7494.055	-6	1.499	1.994	4.2	2.019	2.019	0	7.934	6.462	1.472
249	54:16.8	57:08.4	2079949.423	7491.694	-6	1.499	1.998	4.2	2.018	2.018	0	7.931	6.458	1.473
250	59:08.5	01:58.0	2087438.992	7489.569	-5.999	1.499	1.997	4.2	2.017	2.018	-0.001	7.927	6.455	1.472
251	03:58.0	06:45.0	2094925.984	7486.992	-6	1.499	1.998	4.2	2.016	2.016	0	7.923	6.45	1.473
252	08:45.0	11:30.6	2102411.571	7485.587	-6	1.499	1.997	4.2	2.016	2.016	0	7.921	6.449	1.472
253	11:30.6	27:29.7	2114170.672	7405.587	-1.5	1.499	1.997	4.2	2.015	2.034	-0.019	7.92	7.245	0.675
254	27:29.7	44:50.5	2126011.533	7385.587	-1.5	1.499	1.999	4.2	2.044	2.043	0.001	8.05	7.294	0.756
255	44:50.7	02:15.7	2137856.687	7445.587	-1.5	1.499	1.998	4.2	2.044	2.044	0	8.049	7.299	0.75
256	02:15.7	03:15.8	2137916.822	7332.587	-1.5	1.499	1.998	4.2	2.044	2.044	0	8.049	7.299	0.75
258	53:12.0	08:42.3	2149657.116	7400.587	-1.5	1.499	1.998	4.2	2.002	2.023	-0.021	7.934	7.179	0.755
259	08:42.3	24:32.9	2161407.75	7289.587	-1.5	1.499	1.998	4.2	2.028	2.025	0.003	8.003	7.187	0.816
260	24:33.0	40:05.9	2173140.758	7435.587	-1.5	1.499	1.998	4.2	2.023	2.021	0.002	7.981	7.176	0.805
261	40:05.9	58:49.2	2188664.059	7555.587	-5.999	1.499	1.995	4.2	2.023	2.021	0.002	15.892	7.176	8.716
262	00:49.3	03:06.4	2196121.218	7457.159	-5.999	1.499	1.993	4.2	2.01	2.009	0.001	7.911	6.346	1.565
263	05:06.5	07:26.5	2203581.277	7460.059	-5.999	1.499	1.997	4.2	2.011	2.01	0.001	7.914	6.357	1.557
264	09:26.5	11:47.5	2211042.304	7461.027	-5.999	1.499	1.993	4.2	2.011	2.01	0.001	7.912	6.366	1.546
265	13:47.5	16:10.9	2218505.768	7463.464	-5.999	1.499	1.998	4.2	2.011	2.011	0	7.914	6.375	1.539
266	18:11.0	20:35.7	2225970.54	7464.772	-5.999	1.499	1.996	4.2	2.011	2.011	0	7.913	6.382	1.531
267	22:35.8	25:03.0	2233437.866	7467.326	-5.999	1.499	1.998	4.2	2.012	2.012	0	7.914	6.391	1.523
268	27:03.1	29:30.7	2240905.475	7467.609	-5.999	1.499	1.993	4.2	2.012	2.012	0	7.913	6.397	1.516
269	31:30.7	33:59.1	2248373.958	7468.483	-5.999	1.499	1.999	4.2	2.012	2.012	0	7.913	6.401	1.512
270	35:59.2	38:27.5	2255842.285	7468.327	-5.999	1.499	1.999	4.2	2.012	2.012	0	7.911	6.406	1.505
271	40:27.5	42:55.9	2263310.738	7468.453	-5.999	1.499	1.994	4.2	2.012	2.012	0	7.91	6.409	1.501
272	44:56.0	47:23.7	2270778.543	7467.805	-5.999	1.499	1.993	4.2	2.011	2.011	0	7.908	6.41	1.498
273	49:23.8	51:50.2	2278245	7466.457	-5.999	1.499	1.996	4.2	2.01	2.01	0	7.905	6.409	1.496

274	53:50.2	56:14.1	2285708.931	7463.931	-5.999	1.499	1.995	4.2	2.01	2.01	0	7.902	6.41	1.492
275	58:14.2	00:37.1	2293171.966	7463.035	-5.999	1.499	1.999	4.2	2.009	2.009	0	7.9	6.408	1.492
276	02:37.2	04:57.5	2300632.297	7460.331	-5.999	1.499	1.998	4.2	2.008	2.009	-0.001	7.896	6.408	1.488
277	06:57.5	09:17.1	2308091.911	7459.614	-5.999	1.499	1.997	4.2	2.008	2.008	0	7.895	6.405	1.49
278	11:17.1	13:35.0	2315549.815	7457.904	-5.999	1.499	1.995	4.2	2.007	2.008	-0.001	7.892	6.406	1.486
279	15:35.1	17:50.3	2323005.155	7455.34	-5.999	1.499	1.995	4.2	2.007	2.007	0	7.889	6.404	1.485
280	19:50.4	22:02.9	2330457.771	7452.616	-5.999	1.499	1.996	4.2	2.006	2.006	0	7.887	6.402	1.485
281	24:03.0	26:13.4	2337908.259	7450.488	-5.999	1.499	1.993	4.2	2.005	2.005	0	7.882	6.398	1.484
282	28:13.5	30:21.1	2345355.885	7447.626	-5.999	1.499	1.995	4.2	2.004	2.004	0	7.876	6.393	1.483
283	32:21.1	34:25.8	2352800.626	7444.741	-5.999	1.499	1.993	4.2	2.003	2.003	0	7.873	6.391	1.482
284	36:25.9	38:27.5	2360242.311	7441.685	-5.999	1.499	1.996	4.2	2.002	2.002	0	7.869	6.387	1.482
285	40:27.5	42:25.9	2367680.745	7438.434	-5.999	1.499	1.997	4.2	2.001	2.001	0	7.865	6.384	1.481
286	44:26.0	46:21.8	2375116.612	7435.867	-5.999	1.499	1.996	4.2	2	2	0	7.862	6.381	1.481
287	48:21.8	50:14.9	2382549.767	7433.155	-5.999	1.499	1.999	4.2	1.999	1.999	0	7.858	6.379	1.479
288	52:15.0	54:05.1	2389979.971	7430.204	-5.999	1.499	1.995	4.2	1.998	1.998	0	7.855	6.374	1.481
289	56:05.2	57:52.7	2397407.499	7427.528	-5.999	1.499	1.998	4.2	1.997	1.998	-0.001	7.851	6.372	1.479
290	59:52.7	01:37.9	2404832.744	7425.245	-5.999	1.499	1.997	4.2	1.996	1.997	-0.001	7.848	6.368	1.48
291	03:38.0	05:19.6	2412254.38	7421.636	-5.999	1.499	1.996	4.2	1.995	1.996	-0.001	7.844	6.364	1.48
292	07:19.6	08:59.7	2419674.5	7420.12	-5.999	1.499	1.997	4.2	1.994	1.995	-0.001	7.841	6.362	1.479
293	10:59.7	12:36.5	2427091.371	7416.871	-5.999	1.499	1.998	4.2	1.993	1.993	0	7.836	6.357	1.479
294	14:36.6	16:10.5	2434505.347	7413.976	-5.999	1.499	1.999	4.2	1.992	1.992	0	7.832	6.353	1.479
295	18:10.6	19:40.2	2441915.032	7409.685	-5.999	1.499	1.997	4.2	1.991	1.991	0	7.827	6.348	1.479
296	21:40.3	23:08.1	2449322.905	7407.873	-5.999	1.499	1.997	4.2	1.99	1.99	0	7.823	6.344	1.479
297	25:08.1	26:33.5	2456728.356	7405.451	-5.999	1.499	1.993	4.2	1.989	1.99	-0.001	7.819	6.342	1.477
298	28:33.6	29:56.2	2464130.996	7402.64	-5.999	1.499	1.995	4.2	1.988	1.988	0	7.816	6.336	1.48
299	31:56.2	33:15.3	2471530.086	7399.09	-5.999	1.499	1.999	4.2	1.987	1.987	0	7.811	6.332	1.479
300	35:15.3	36:32.1	2478926.935	7396.849	-5.999	1.499	1.997	4.2	1.986	1.987	-0.001	7.809	6.329	1.48
301	38:32.2	39:45.8	2486320.666	7393.731	-5.999	1.499	1.993	4.2	1.985	1.986	-0.001	7.804	6.326	1.478
302	41:45.9	42:57.5	2493712.321	7391.655	-5.999	1.499	1.997	4.2	1.984	1.985	-0.001	7.802	6.322	1.48
303	44:57.6	46:06.0	2501100.794	7388.473	-5.999	1.499	1.995	4.2	1.983	1.984	-0.001	7.797	6.32	1.477
304	48:06.0	49:12.3	2508487.157	7386.363	-5.999	1.499	1.995	4.2	1.982	1.982	0	7.793	6.315	1.478
305	51:12.4	52:14.9	2515869.738	7382.581	-5.999	1.499	1.999	4.2	1.98	1.981	-0.001	7.787	6.309	1.478
306	54:15.0	55:14.8	2523249.639	7379.901	-5.999	1.499	1.995	4.2	1.98	1.98	0	7.784	6.306	1.478
307	57:14.9	58:12.4	2530627.252	7377.613	-5.999	1.499	1.994	4.2	1.978	1.979	-0.001	7.78	6.302	1.478
308	00:12.5	01:07.1	2538001.964	7374.712	-5.999	1.499	1.995	4.2	1.978	1.978	0	7.777	6.299	1.478
309	03:07.2	03:58.5	2545373.352	7371.388	-5.999	1.499	1.996	4.2	1.977	1.977	0	7.773	6.294	1.479
310	05:58.6	06:46.3	2552741.142	7367.79	-5.999	1.499	1.994	4.2	1.975	1.976	-0.001	7.768	6.289	1.479
311	08:46.4	09:31.4	2560106.19	7365.048	-5.999	1.499	1.999	4.2	1.974	1.975	-0.001	7.764	6.284	1.48
312	11:31.4	12:13.6	2567468.412	7362.222	-5.999	1.499	1.996	4.2	1.974	1.974	0	7.761	6.283	1.478
313	14:13.6	14:52.6	2574827.415	7359.003	-5.999	1.499	1.994	4.2	1.972	1.973	-0.001	7.757	6.278	1.479
314	16:52.6	17:29.3	2582184.089	7356.674	-5.999	1.499	1.998	4.2	1.972	1.972	0	7.753	6.275	1.478
315	19:29.3	20:02.1	2589536.881	7352.792	-5.999	1.499	1.994	4.2	1.97	1.971	-0.001	7.749	6.271	1.478
316	22:02.1	22:33.2	2596888.052	7351.171	-5.999	1.499	1.994	4.2	1.97	1.97	0	7.746	6.268	1.478
317	24:33.3	25:01.1	2604235.965	7347.913	-5.999	1.499	1.997	4.2	1.969	1.969	0	7.742	6.264	1.478
318	27:01.2	27:26.0	2611580.849	7344.884	-5.999	1.499	1.994	4.2	1.968	1.968	0	7.738	6.259	1.479
319	29:26.1	29:48.6	2618923.405	7342.556	-5.999	1.499	1.998	4.2	1.967	1.967	0	7.735	6.255	1.48
320	31:48.6	32:07.9	2626262.77	7339.365	-5.999	1.499	1.999	4.2	1.966	1.966	0	7.731	6.252	1.479
321	34:08.0	34:23.9	2633598.768	7335.998	-5.999	1.499	1.999	4.2	1.965	1.965	0	7.727	6.248	1.479
322	36:24.0	36:37.3	2640932.096	7333.328	-5.999	1.499	1.997	4.2	1.964	1.964	0	7.724	6.244	1.48
323	38:37.3	38:47.8	2648262.602	7330.506	-5.999	1.499	1.994	4.2	1.963	1.964	-0.001	7.719	6.241	1.478
324	40:47.8	40:56.0	2655590.856	7328.254	-5.999	1.499	1.995	4.2	1.962	1.963	-0.001	7.716	6.239	1.477
325	42:56.1	42:49.5	2662904.357	7313.501	-5.999	1.499	1.995	4.2	1.958	1.958	0	7.699	6.21	1.489
326	44:49.6	44:42.1	2670216.96	7312.603	-5.999	1.499	1.995	4.2	1.958	1.958	0	7.702	6.211	1.491
327	46:42.2	46:31.4	2677526.208	7309.248	-5.999	1.499	1.999	4.2	1.957	1.957	0	7.698	6.209	1.489
328	48:31.5	48:18.2	2684833.054	7306.846	-5.999	1.499	1.997	4.2	1.956	1.956	0	7.693	6.203	1.49
329	50:18.3	50:03.5	2692138.295	7305.241	-5.999	1.499	1.995	4.2	1.955	1.956	-0.001	7.692	6.202	1.49
330	52:03.5	51:45.8	2699440.636	7302.341	-5.999	1.499	1.996	4.2	1.954	1.955	-0.001	7.688	6.199	1.489
331	53:45.9	53:26.4	2706741.249	7300.613	-5.999	1.499	1.994	4.2	1.953	1.954	-0.001	7.685	6.197	1.488
332	55:26.5	55:07.9	2714042.756	7301.507	-5.999	1.499	1.996	4.2	1.953	1.954	-0.001	7.685	6.195	1.49
333	57:08.0	56:50.9	2721345.693	7302.937	-5.999	1.499	1.996	4.2	1.954	1.954	0	7.686	6.195	1.491
334	58:50.9	58:32.0	2728646.872	7301.179	-5.999	1.499	1.998	4.2	1.954	1.954	0	7.687	6.196	1.491
335	00:32.1	00:07.3	2735942.084	7295.212	-5.999	1.499	1.999	4.2	1.953	1.954	-0.001	7.684	6.194	1.49
336	02:07.3	01:37.5	2743232.356	7290.272	-5.999	1.499	1.999	4.2	1.952	1.952	0	7.678	6.189	1.489
337	03:37.6	03:04.0	2750518.788	7286.432	-5.999	1.499	1.995	4.2	1.95	1.95	-0.001	7.669	6.185	1.484
338	05:04.0	04:28.4	2757803.266	7284.478	-6	1.499	1.995	4.2	1.948	1.949	-0.001	7.664	6.181	1.483
339	06:28.5	05:50.7	2765085.494	7282.228	-6	1.499	1.999	4.2	1.947	1.948	-0.001	7.66	6.174	1.486
340	07:50.7	07:11.5	2772366.301	7280.807	-6	1.499	1.995	4.2	1.946	1.947	-0.001	7.657	6.17	1.487
341	09:11.5	08:30.6	2779645.428	7279.127	-5.999	1.499	1.997	4.2	1.946	1.946	0	7.656	6.168	1.488
342	10:30.7	09:47.7	2786922.518	7277.09	-5.999	1.499	1.999	4.2	1.945	1.946	-0.001	7.653	6.167	1.486
343	11:47.8	11:06.0	2794200.785	7278.267	-5.999	1.499	1.997	4.2	1.945	1.946	-0.001	7.653	6.166	1.487
344	13:06.0	12:23.6	2801478.45	7277.665	-5.999	1.499	1.997	4.2	1.945	1.946	-0.001	7.653	6.167	1.486
345	14:23.7	13:38.9	2808753.754	7275.304	-5.999	1.499	1.994	4.2	1.945	1.946	-0.001	7.655	6.166	1.489
346	15:39.0	14:45.9	2816020.728	7266.974	-5.999	1.499	1.997	4.2	1.944	1.945	-0.001	7.649	6.163	1.486
347	16:46.0	15:49.8	2823284.589	7263.861	-5.999	1.499	1.995	4.2	1.942	1.943	-0.001	7.641	6.158	1.483
348	17:49.8	16:50.5	2830545.315	7260.726	-6	1.499	1.998	4.2	1.94	1.941	-0.001	7.632	6.151	1.481
349	18:50.5	17:49.8	2837804.638	7259.323	-6	1.499	1.999	4.2	1.939	1.94	-0.001	7.629	6.147	1.482
350	19:49.9	18:47.3	2845062.078	7257.44	-6	1.499	1.997	4.2	1.938	1.939	-0.001	7.627	6.142	1.485
351	20:47.3	19:42.3	2852317.154	7255.076	-5.999	1.499	1.998	4.2	1.938	1.938	0	7.624	6.138	1.486
352	21:42.4	20:35.9	2859570.726	7253.572	-5.999	1.499	1.998	4.2	1.937	1.938	-0.001	7.622	6.137	1.485
353	22:35.9	21:28.7	2866823.476	7252.75	-5.999	1.499	1.997	4.2	1.937	1.937	0	7.62	6.135	1.485
354	23:28.7	22:23.1	2874077.904	7254.428	-5.999	1.499	1.998	4.2	1.937	1.937	0	7.621	6.134	1.487
355	24:23.1	23:15.1	2881329.882	7251.978	-5.999	1.499	1.998	4.2	1.936	1.937	-0.001	7.62	6.133	1.487
356	25:15.1	24:00.9	2888575.73	7245.848	-5.999	1.499	1.997	4.2	1.936	1.937	-0.001	7.619	6.132	1.487
357	26:01.0	24:41.6	2895816.41	7240.68	-5.999	1.499	1.997	4.2	1.935	1.935	0	7.613	6.129	1.484
358	26:41.7	25:18.5	2903053.274	7236.864	-5.999	1.499	1.997	4.2	1.932	1.933	-0.001	7.604	6.121	1.483
359	27:18.5	25:51.9	2910286.701	7233.427	-6	1.499	1.999	4.2	1.93	1.931	-0.001	7.596	6.116	1.48
360	27:51.9	26:24.9	2917519.675	7232.974	-6	1.499	1.998	4.2	1.93	1.931	-0.001	7.595	6.112	1.483
361	28:24.9	26:55.3	2924750.126	7230.451	-6	1.499	1.997	4.2	1.929	1.93	-0.001	7.589	6.106	1.486
362	28:55.4	27:23.3	2931978.162	7228.036	-5.999	1.499	1.998	4.2	1.929	1.929	0	7.589	6.102	1.487
363	29:23.4	27:48.7	2939203.546	7225.384	-5.999	1.499	1.995	4.2	1.928	1.928	0	7.585	6.1	1.485
364	29:48.7	28:14.0	2946428.834	7225.288	-5.999	1.499	1.995	4.2	1.927	1.928	-0.001	7.585	6.098	1.487

365	30:14.1	28:39.6	2953654.398	7225.564	-5.999	1.499	1.998	4.2	1.927	1.928	-0.001	7.584	6.097	1.487
366	30:39.6	29:05.6	2960880.428	7226.03	-5.999	1.499	1.994	4.2	1.928	1.928	0	7.586	6.099	1.487
367	31:05.7	29:26.0	2968100.816	7220.388	-5.999	1.499	1.997	4.2	1.927	1.928	-0.001	7.586	6.097	1.489
368	31:26.0	29:38.9	2975313.74	7212.924	-5.999	1.499	1.996	4.2	1.926	1.927	-0.001	7.58	6.093	1.487
369	31:39.0	29:49.6	2982524.424	7210.684	-5.999	1.499	1.997	4.2	1.924	1.925	-0.001	7.573	6.087	1.486
370	31:49.7	29:57.7	2989732.509	7208.085	-5.999	1.499	1.998	4.2	1.922	1.923	-0.001	7.565	6.082	1.483
371	31:57.8	30:02.6	2996937.429	7204.92	-6	1.499	1.994	4.2	1.921	1.922	-0.001	7.559	6.078	1.481
372	32:02.6	30:06.3	3004141.085	7203.656	-6	1.499	1.994	4.2	1.92	1.921	-0.001	7.558	6.071	1.487
373	32:06.3	30:08.5	3011343.278	7202.193	-5.998	1.499	1.998	4.2	1.92	1.92	0	7.557	6.069	1.488
374	32:08.5	30:07.4	3018542.214	7198.936	-5.998	1.499	1.995	4.2	1.919	1.92	-0.001	7.552	6.065	1.487
375	32:07.5	30:06.7	3025741.505	7199.291	-5.999	1.499	1.996	4.2	1.919	1.919	0	7.552	6.065	1.487
376	32:06.7	30:05.1	3032939.965	7198.46	-5.999	1.499	1.996	4.2	1.918	1.919	-0.001	7.549	6.063	1.486
377	32:05.2	30:04.3	3040139.09	7199.125	-5.999	1.499	1.995	4.2	1.918	1.919	-0.001	7.55	6.062	1.488
378	32:04.3	30:02.8	3047337.632	7198.542	-5.999	1.499	1.997	4.2	1.918	1.919	-0.001	7.55	6.062	1.488
379	32:02.9	29:55.9	3054530.697	7193.065	-5.999	1.499	1.997	4.2	1.918	1.918	0	7.55	6.06	1.49
380	31:55.9	29:43.1	3061717.97	7187.273	-5.999	1.499	1.995	4.2	1.916	1.917	-0.001	7.544	6.056	1.488
381	31:43.2	29:27.5	3068902.329	7184.359	-5.999	1.499	1.997	4.2	1.915	1.916	-0.001	7.538	6.051	1.487
382	31:27.5	29:09.2	3076084.072	7181.743	-5.999	1.499	1.999	4.2	1.913	1.913	0	7.529	6.045	1.484
383	31:09.3	28:48.3	3083263.083	7179.011	-6	1.499	1.996	4.2	1.911	1.912	-0.001	7.524	6.041	1.483
384	30:48.3	28:26.3	3090441.13	7178.047	-6	1.499	1.997	4.2	1.911	1.912	-0.001	7.522	6.037	1.485
385	30:26.3	27:58.7	3097613.476	7172.346	-6	1.499	1.994	4.2	1.909	1.91	-0.001	7.515	6.028	1.487
386	27:58.7	35:36.6	3108871.455	11257.979	-1.5	1.499	1.994	4.2	1.909	1.93	-0.021	7.513	6.853	0.66
387	35:36.7	44:24.0	3120198.833	11327.378	-1.5	1.499	1.999	4.2	1.936	1.936	0	7.641	6.885	0.756
388	44:24.0	53:02.6	3131517.421	11318.588	-1.5	1.499	1.998	4.2	1.932	1.933	-0.001	7.624	6.878	0.746
389	53:02.6	54:02.8	3131577.577	60.156	0	0	0	2.797	0	0	0	0	0	0

SNL_18650_NMC_25C_0-100_0.5-2C_

Cycle_Index	Start_Time	End_Time	Test_Time	Min_Current	Max_Current	Min_Voltage	Max_Voltage	Charge_Capacity (Ah)	Discharge_Capacity (Ah)	Capacity Loss (Ah)	Charge_Energy (Wh)	Discharge_Energy (Wh)	Energy Loss (Wh)
1	12:57.0	38:44.5	15957.47	-1.5	1.499	1.999	4.2	2.83	2.929	-0.099	10.942	10.437	0.505
2	38:44.5	07:34.4	32087.37	-1.5	1.5	1.999	4.2	2.926	2.924	0.002	11.242	10.428	0.814
3	07:34.4	35:51.4	48187.08	-1.5	1.5	1.999	4.2	2.92	2.916	0.004	11.217	10.409	0.808
4	35:54.1	24:59.8	69132.76	-6.001	1.499	1.998	4.2	5.796	5.767	0.029	22.286	19.076	3.21
5	26:59.8	13:23.3	79236.32	-6.001	1.499	1.999	4.2	2.875	2.868	0.007	11.047	9.501	1.546
6	15:23.4	01:24.4	89317.44	-6.001	1.5	1.999	4.2	2.865	2.86	0.005	11.012	9.486	1.526
7	03:24.5	49:07.1	99380.09	-6.001	1.499	1.999	4.2	2.857	2.852	0.005	10.982	9.473	1.509
8	51:07.1	36:35.1	109428.1	-6.001	1.499	1.998	4.2	2.849	2.845	0.004	10.955	9.459	1.496
9	38:35.2	23:47.5	119460.5	-6.001	1.499	1.997	4.2	2.842	2.838	0.004	10.928	9.447	1.481
10	25:47.6	10:42.3	129475.3	-6.001	1.499	1.998	4.2	2.835	2.832	0.003	10.902	9.432	1.47
11	12:42.3	57:19.3	139472.3	-6.001	1.499	1.999	4.2	2.828	2.825	0.003	10.877	9.416	1.461
12	59:19.3	43:39.1	149452.1	-6.001	1.499	1.999	4.2	2.821	2.818	0.003	10.853	9.4	1.453
13	45:39.1	29:40.7	159413.7	-6.001	1.499	1.999	4.2	2.815	2.812	0.003	10.829	9.384	1.445
14	31:40.7	15:25.2	169358.2	-6.001	1.499	1.998	4.2	2.808	2.806	0.002	10.806	9.368	1.438
15	17:25.3	00:52.7	179285.7	-6.001	1.499	1.999	4.2	2.802	2.801	0.001	10.785	9.355	1.43
16	02:52.7	46:04.7	189197.7	-6.001	1.5	1.997	4.2	2.797	2.796	0.001	10.766	9.343	1.423
17	48:04.7	31:04.5	199097.5	-6.001	1.499	1.999	4.2	2.792	2.79	0.002	10.749	9.331	1.418
18	33:04.6	15:50.0	208983	-6.001	1.499	1.998	4.2	2.787	2.786	0.001	10.73	9.319	1.411
19	17:50.0	00:22.2	218855.2	-6.001	1.5	1.998	4.2	2.782	2.781	0.001	10.712	9.306	1.406
20	02:22.3	44:43.7	228716.7	-6.001	1.499	1.999	4.2	2.777	2.776	0.001	10.695	9.294	1.401
21	46:43.7	28:50.8	238563.8	-6.001	1.5	1.999	4.2	2.772	2.772	0	10.679	9.282	1.397
22	30:50.9	12:45.4	248398.4	-6.001	1.499	1.998	4.2	2.768	2.767	0.001	10.662	9.271	1.391
23	14:45.5	56:17.0	258210	-6.001	1.499	1.998	4.2	2.763	2.762	0.001	10.645	9.248	1.397
24	58:17.0	39:33.7	268006.7	-6.001	1.499	1.998	4.2	2.758	2.758	0	10.63	9.235	1.395
25	41:33.7	22:37.9	277790.9	-6.001	1.5	1.999	4.2	2.754	2.754	0	10.614	9.224	1.39
26	24:38.0	05:32.8	287565.8	-6.001	1.499	1.999	4.2	2.75	2.751	-0.001	10.602	9.216	1.386
27	07:32.9	48:15.9	297328.9	-6.001	1.5	1.999	4.2	2.747	2.747	0	10.589	9.205	1.384
28	50:15.9	30:49.7	307082.7	-6.001	1.5	1.998	4.2	2.743	2.744	-0.001	10.576	9.196	1.38
29	32:49.8	13:12.6	316825.6	-6.001	1.499	1.996	4.2	2.74	2.74	0	10.564	9.186	1.378
30	15:12.6	55:25.8	326558.8	-6.001	1.499	1.998	4.2	2.736	2.737	-0.001	10.551	9.176	1.375
31	57:25.9	37:29.1	336282.1	-6.001	1.5	1.996	4.2	2.733	2.733	0	10.539	9.167	1.372
32	39:29.2	19:22.1	345995.1	-6.001	1.499	1.996	4.2	2.73	2.73	0	10.528	9.157	1.371
33	21:22.2	01:05.4	355698.4	-6.001	1.499	1.998	4.2	2.726	2.727	-0.001	10.516	9.149	1.367
34	03:05.4	42:39.4	365392.4	-6.001	1.5	1.997	4.2	2.723	2.724	-0.001	10.505	9.14	1.365
35	44:39.5	24:03.8	375076.8	-6.001	1.5	1.999	4.2	2.72	2.721	-0.001	10.494	9.131	1.363
36	26:03.9	05:19.5	384752.5	-6.001	1.5	1.996	4.2	2.717	2.718	-0.001	10.483	9.124	1.359
37	07:19.6	46:27.5	394420.5	-6.001	1.499	1.999	4.2	2.714	2.715	-0.001	10.473	9.115	1.358
38	48:27.5	27:26.0	404079	-6.001	1.499	1.998	4.2	2.711	2.713	-0.002	10.462	9.108	1.354
39	29:26.0	08:16.4	413729.4	-6.001	1.499	1.997	4.2	2.709	2.71	-0.001	10.453	9.101	1.352
40	10:16.4	48:56.9	423369.9	-6.001	1.5	1.996	4.2	2.706	2.707	-0.001	10.443	9.093	1.35
41	50:56.9	29:32.6	433005.6	-6.001	1.499	1.999	4.2	2.703	2.705	-0.002	10.434	9.085	1.349
42	31:32.7	10:00.8	442633.8	-6.001	1.499	1.997	4.2	2.701	2.702	-0.001	10.425	9.078	1.347
43	12:00.9	50:19.2	452252.2	-6.001	1.499	1.998	4.201	2.698	2.7	-0.002	10.416	9.071	1.345
44	52:19.3	30:29.7	461862.7	-6.001	1.499	1.998	4.2	2.696	2.697	-0.001	10.407	9.063	1.344
45	32:29.7	10:33.9	471466.9	-6.001	1.5	1.998	4.2	2.693	2.695	-0.002	10.398	9.057	1.341
46	12:34.0	50:31.3	481064.3	-6.001	1.5	1.999	4.2	2.691	2.692	-0.001	10.39	9.049	1.341
47	52:31.3	30:18.5	490651.5	-6.001	1.5	1.998	4.2	2.688	2.69	-0.002	10.381	9.043	1.338
48	32:18.6	10:01.2	500234.2	-6.001	1.499	1.998	4.2	2.686	2.688	-0.002	10.374	9.036	1.338
49	12:01.3	49:36.9	509809.9	-6.001	1.5	1.999	4.2	2.684	2.686	-0.002	10.365	9.03	1.335
50	51:37.0	29:06.5	519379.5	-6.001	1.499	1.996	4.2	2.682	2.684	-0.002	10.358	9.024	1.334
51	31:06.5	08:29.5	528942.5	-6.001	1.5	1.997	4.2	2.68	2.682	-0.002	10.35	9.017	1.333
52	10:29.6	47:44.9	538497.9	-6.001	1.5	1.996	4.2	2.677	2.679	-0.002	10.342	9.011	1.331
53	49:44.9	26:53.8	548046.8	-6.001	1.5	1.999	4.2	2.676	2.677	-0.001	10.335	9.006	1.329
54	28:53.9	05:54.5	557587.5	-6.001	1.5	1.998	4.2	2.673	2.675	-0.002	10.328	9	1.328
55	07:54.6	44:50.7	567123.7	-6.001	1.499	1.998	4.2	2.672	2.674	-0.002	10.321	8.994	1.327
56	46:50.7	23:42.6	576655.6	-6.001	1.5	1.999	4.2	2.67	2.672	-0.002	10.314	8.989	1.325
57	25:42.6	02:28.6	586181.6	-6.001	1.5	1.997	4.2	2.668	2.67	-0.002	10.307	8.984	1.323
58	04:28.7	41:10.5	595703.5	-6.001	1.5	1.996	4.2	2.666	2.668	-0.002	10.301	8.979	1.322
59	43:10.6	19:46.5	605219.5	-6.001	1.499	1.999	4.2	2.664	2.666	-0.002	10.294	8.973	1.321
60	21:46.5	58:18.3	614731.3	-6.001	1.499	1.997	4.2	2.662	2.665	-0.003	10.288	8.969	1.319
61	00:18.3	36:44.0	624237	-6.001	1.499	1.998	4.2	2.661	2.663	-0.002	10.282	8.965	1.317
62	38:44.1	15:05.6	633738.6	-6.001	1.5	1.999	4.2	2.659	2.661	-0.002	10.276	8.961	1.315
63	17:05.7	53:22.8	643235.8	-6.001	1.5	1.999	4.2	2.658	2.66	-0.002	10.271	8.957	1.314
64	55:22.9	31:34.7	652727.7	-6.001	1.499	1.995	4.2	2.656	2.658	-0.002	10.264	8.951	1.313
65	33:34.7	09:42.9	662215.9	-6.001	1.499	1.999	4.2	2.654	2.657	-0.003	10.259	8.946	1.313
66	11:43.0	47:46.1	671699.1	-6.001	1.499	1.995	4.2	2.653	2.655	-0.002	10.252	8.943	1.309
67	49:46.1	25:45.9	681178.9	-6.001	1.5	1.999	4.2	2.651	2.653	-0.002	10.248	8.938	1.31
68	27:46.0	03:38.8	690651.8	-6.001	1.499	1.998	4.2	2.649	2.652	-0.003	10.241	8.933	1.308
69	05:38.9	41:26.5	700119.5	-6.001	1.499	1.997	4.2	2.648	2.65	-0.002	10.235	8.929	1.306
70	43:26.6	19:09.1	709582.1	-6.001	1.499	1.997	4.2	2.647	2.649	-0.002	10.231	8.925	1.306
71	21:09.2	56:46.1	719039.1	-6.001	1.5	1.998	4.2	2.645	2.647	-0.002	10.225	8.92	1.305
72	58:46.1	34:18.9	728491.9	-6.001	1.499	1.998	4.2	2.643	2.646	-0.003	10.22	8.917	1.303
73	36:19.0	11:49.2	737942.2	-6.001	1.5	1.997	4.2	2.642	2.645	-0.003	10.215	8.912	1.303
74	13:49.3	49:15.0	747388	-6.001	1.5	1.997	4.2	2.641	2.643	-0.002	10.21	8.909	1.301
75	51:15.0	26:36.2	756829.2	-6.001	1.499	1.999	4.2	2.639	2.642	-0.003	10.205	8.904	1.301
76	28:36.3	03:53.8	766266.8	-6.001	1.5	1.998	4.2	2.638	2.641	-0.003	10.2	8.9	1.3
77	05:53.9	40:52.7	775685.7	-6.001	1.499	1.997	4.2	2.636	2.638	-0.002	10.192	8.88	1.312
78	42:52.7	17:43.1	785096.1	-6.001	1.5	1.999	4.2	2.634	2.636	-0.002	10.186	8.872	1.314
79	19:43.2	54:28.0	794501	-6.001	1.499	1.997	4.2	2.632	2.635	-0.003	10.182	8.867	1.315
80	56:28.0	31:05.6	803898.6	-6.001	1.5	1.995	4.2	2.63	2.634	-0.004	10.172	8.862	1.31
81	33:05.7	07:39.5	813292.5	-6.001	1.499	1.996	4.2	2.629	2.632	-0.003	10.172	8.857	1.315
82	09:39.5	44:10.6	822683.6	-6.001	1.499	1.996	4.2	2.628	2.631	-0.003	10.167	8.854	1.313
83	46:10.7	20:38.0	832071	-6.001	1.499	1.997	4.2	2.627	2.629	-0.002	10.162	8.849	1.313
84	22:38.1	57:00.9	841453.9	-6.001	1.499	1.995	4.2	2.626	2.628	-0.002	10.158	8.846	1.312
85	59:00.9	33:20.3	850833.3	-6.001	1.499	1.999	4.2	2.624	2.627	-0.003	10.154	8.843	1.311
86	35:20.3	09:37.0	860210	-6.001	1.499	1.997	4.2	2.623	2.626	-0.003	10.149	8.839	1.31
87	11:37.1	45:47.7	869580.7	-6.001	1.5	1.998	4.2	2.622	2.625	-0.003	10.144	8.835	1.309
88	47:47.8	21:56.4	878949.4	-6.001	1.499	1.995	4.2	2.621	2.624	-0.003	10.14	8.832	1.308
89	23:56.4	58:02.6	888315.6	-6.001	1.499	1.999	4.2	2.62	2.622	-0.002	10.137	8.829	1.308
90	00:02.6	34:02.6	897675.6	-6.001	1.499	1.995	4.2	2.618	2.621	-0.003	10.132	8.826	1.306

91	36:02.6	09:59.3	907032.3	-6.001	1.499	1.999	4.2	2.617	2.62	-0.003	10.128	8.822	1.306
92	11:59.3	45:53.2	916386.2	-6.001	1.499	1.997	4.2	2.616	2.619	-0.003	10.123	8.818	1.305
93	47:53.2	21:45.1	925738.1	-6.001	1.5	1.996	4.2	2.615	2.618	-0.003	10.119	8.815	1.304
94	23:45.2	57:34.5	935087.5	-6.001	1.499	1.996	4.2	2.614	2.617	-0.003	10.116	8.812	1.304
95	59:34.6	33:17.4	944430.4	-6.001	1.5	1.998	4.2	2.613	2.616	-0.003	10.111	8.809	1.302
96	35:17.4	08:58.3	953771.3	-6.001	1.499	1.999	4.2	2.612	2.615	-0.003	10.107	8.806	1.301
97	10:58.4	44:36.5	963109.5	-6.001	1.499	1.995	4.2	2.611	2.614	-0.003	10.103	8.803	1.3
98	46:36.5	20:10.4	972443.4	-6.001	1.5	1.996	4.2	2.61	2.613	-0.003	10.1	8.8	1.3
99	22:10.5	55:41.0	981774	-6.001	1.5	1.995	4.2	2.609	2.611	-0.002	10.096	8.796	1.3
100	57:41.0	31:09.0	991102	-6.001	1.5	1.996	4.2	2.608	2.61	-0.002	10.092	8.793	1.299
101	33:09.0	06:33.2	1000426	-6.001	1.499	1.997	4.2	2.606	2.609	-0.003	10.088	8.79	1.298
102	08:33.3	41:54.3	1009747	-6.001	1.499	1.999	4.2	2.605	2.608	-0.003	10.085	8.787	1.298
103	43:54.3	17:13.4	1019066	-6.001	1.499	1.999	4.2	2.604	2.607	-0.003	10.081	8.784	1.297
104	19:13.5	52:29.5	1028383	-6.001	1.499	1.995	4.2	2.603	2.606	-0.003	10.077	8.781	1.296
105	54:29.6	27:43.5	1037696	-6.001	1.5	1.999	4.2	2.603	2.605	-0.002	10.074	8.777	1.297
106	29:43.6	02:51.9	1047005	-6.001	1.499	1.999	4.2	2.601	2.604	-0.003	10.069	8.774	1.295
107	04:51.9	37:56.4	1056309	-6.001	1.499	1.998	4.2	2.6	2.603	-0.003	10.066	8.771	1.295
108	39:56.4	12:57.0	1065610	-6.001	1.499	1.995	4.2	2.599	2.602	-0.003	10.062	8.767	1.295
109	14:57.1	47:54.9	1074908	-6.001	1.499	1.996	4.2	2.598	2.601	-0.003	10.059	8.764	1.295
110	49:54.9	22:49.3	1084202	-6.001	1.499	1.997	4.2	2.597	2.6	-0.003	10.055	8.761	1.294
111	24:49.3	57:41.6	1093495	-6.001	1.499	1.997	4.2	2.596	2.599	-0.003	10.052	8.758	1.294
112	59:41.7	32:31.1	1102784	-6.001	1.5	1.996	4.2	2.595	2.598	-0.003	10.048	8.755	1.293
113	34:31.2	07:16.1	1112069	-6.001	1.499	1.995	4.2	2.594	2.597	-0.003	10.045	8.751	1.294
114	09:16.2	41:56.4	1121349	-6.001	1.499	1.998	4.2	2.593	2.596	-0.003	10.041	8.746	1.295
115	43:56.4	16:33.1	1130626	-6.001	1.499	1.996	4.2	2.592	2.595	-0.003	10.037	8.743	1.294
116	18:33.2	51:05.6	1139899	-6.001	1.5	1.995	4.2	2.591	2.594	-0.003	10.034	8.739	1.295
117	53:05.7	25:36.5	1149169	-6.001	1.499	1.998	4.2	2.59	2.593	-0.003	10.031	8.736	1.295
118	27:36.6	00:04.6	1158438	-6.001	1.499	1.997	4.2	2.589	2.592	-0.003	10.027	8.733	1.294
119	02:04.6	34:29.7	1167703	-6.001	1.499	1.998	4.2	2.588	2.591	-0.003	10.024	8.73	1.294
120	36:29.7	08:51.0	1176964	-6.001	1.499	1.998	4.2	2.588	2.591	-0.003	10.021	8.727	1.294
121	10:51.0	43:09.1	1186222	-6.001	1.499	1.997	4.2	2.587	2.59	-0.003	10.017	8.724	1.293
122	45:09.1	17:25.1	1195478	-6.001	1.499	1.996	4.2	2.586	2.589	-0.003	10.014	8.722	1.292
123	19:25.1	51:39.8	1204733	-6.001	1.499	1.994	4.2	2.585	2.588	-0.003	10.012	8.72	1.292
124	53:39.9	25:53.2	1213986	-6.001	1.499	1.996	4.2	2.584	2.587	-0.003	10.009	8.717	1.292
125	27:53.2	00:03.3	1223236	-6.001	1.499	1.996	4.2	2.583	2.587	-0.004	10.006	8.714	1.292
126	02:03.3	34:08.0	1232481	-6.001	1.499	1.999	4.2	2.582	2.585	-0.003	10.002	8.711	1.291
127	36:08.0	08:11.7	1241725	-6.001	1.5	1.997	4.2	2.582	2.585	-0.003	9.999	8.709	1.29
128	10:11.7	42:11.4	1250964	-6.001	1.499	1.999	4.2	2.581	2.584	-0.003	9.996	8.706	1.29
129	42:11.4	44:42.0	1265515	-1.5	1.5	1.999	4.2	2.58	2.61	-0.03	9.993	9.466	0.527
130	44:42.0	48:08.5	1280121	-1.5	1.499	1.999	4.2	2.605	2.609	-0.004	10.094	9.466	0.628
131	48:08.5	51:27.3	1294720	-1.5	1.5	1.999	4.2	2.604	2.607	-0.003	10.089	9.462	0.627
132	51:27.3	52:27.4	1294780	0	0	2.775	2.787	2.604	2.607	-0.003	10.089	9.462	0.627
134	16:45.0	18:28.3	1309294	-1.5	1.499	1.999	4.2	2.581	2.604	-0.023	10.051	9.421	0.63
135	18:28.4	20:17.2	1323803	-1.5	1.5	1.998	4.2	2.603	2.602	0.001	10.099	9.415	0.684
136	20:17.3	21:48.7	1338294	-1.5	1.5	1.999	4.2	2.598	2.599	-0.001	10.081	9.407	0.674
137	21:48.7	36:57.9	1357203	-6.001	1.499	1.997	4.2	2.598	2.599	-0.001	10.081	9.407	0.674
138	38:58.0	08:44.4	1366310	-6.001	1.499	1.996	4.2	2.567	2.568	-0.001	9.961	8.537	1.424
139	10:44.5	40:22.1	1375407	-6.001	1.499	1.996	4.2	2.564	2.566	-0.002	9.951	8.529	1.422
140	42:22.1	11:55.1	1384500	-6.001	1.499	1.997	4.2	2.562	2.564	-0.002	9.944	8.526	1.418
141	13:55.2	43:25.4	1393591	-6.001	1.499	1.999	4.2	2.561	2.563	-0.002	9.938	8.525	1.413
142	45:25.4	14:54.0	1402679	-6.001	1.499	1.996	4.2	2.56	2.562	-0.002	9.934	8.526	1.408
143	16:54.1	46:21.5	1411767	-6.001	1.499	1.998	4.2	2.559	2.561	-0.002	9.93	8.525	1.405
144	48:21.6	17:47.0	1420852	-6.001	1.499	1.995	4.2	2.558	2.56	-0.002	9.926	8.525	1.401
145	19:47.1	49:12.4	1429938	-6.001	1.499	1.998	4.2	2.557	2.56	-0.003	9.923	8.525	1.398
146	51:12.4	20:37.8	1439023	-6.001	1.499	1.999	4.2	2.556	2.559	-0.003	9.921	8.525	1.396
147	22:37.9	51:59.9	1448105	-6.001	1.499	1.997	4.2	2.555	2.558	-0.003	9.917	8.524	1.393
148	54:00.0	23:21.2	1457187	-6.001	1.499	1.995	4.2	2.554	2.557	-0.003	9.913	8.523	1.39
149	25:21.2	54:41.0	1466266	-6.001	1.499	1.999	4.2	2.554	2.556	-0.002	9.911	8.522	1.389
150	56:41.0	25:59.1	1475344	-6.001	1.5	1.994	4.2	2.553	2.556	-0.003	9.908	8.521	1.387
151	27:59.1	57:17.1	1484422	-6.001	1.5	1.995	4.2	2.552	2.555	-0.003	9.906	8.52	1.386
152	59:17.1	28:32.2	1493498	-6.001	1.499	1.996	4.2	2.552	2.554	-0.002	9.902	8.519	1.383
153	30:32.2	59:45.4	1502571	-6.001	1.499	1.999	4.2	2.551	2.554	-0.003	9.899	8.519	1.38
154	01:45.5	30:59.7	1511645	-6.001	1.499	1.997	4.2	2.55	2.553	-0.003	9.897	8.519	1.378
155	32:59.7	02:13.3	1520719	-6.001	1.499	1.995	4.2	2.55	2.553	-0.003	9.895	8.52	1.375
156	04:13.3	33:27.3	1529793	-6.001	1.499	1.995	4.2	2.549	2.552	-0.003	9.893	8.521	1.372
157	35:27.3	04:35.6	1538861	-6.001	1.499	1.997	4.2	2.548	2.551	-0.003	9.888	8.485	1.403
158	06:35.6	35:10.1	1547896	-6.001	1.5	1.997	4.2	2.543	2.546	-0.003	9.874	8.464	1.41
159	37:10.2	05:42.6	1556928	-6.001	1.499	1.996	4.2	2.542	2.545	-0.003	9.871	8.463	1.408
160	07:42.7	36:06.8	1565952	-6.001	1.5	1.997	4.2	2.541	2.543	-0.002	9.865	8.454	1.411
161	38:06.8	06:33.9	1574979	-6.001	1.499	1.996	4.2	2.541	2.544	-0.003	9.866	8.459	1.407
162	08:33.9	37:01.2	1584007	-6.001	1.5	1.998	4.2	2.54	2.543	-0.003	9.864	8.461	1.403
163	39:01.2	07:27.7	1593033	-6.001	1.499	1.999	4.2	2.54	2.543	-0.003	9.861	8.461	1.4
164	09:27.7	37:55.2	1602061	-6.001	1.5	1.999	4.201	2.539	2.542	-0.003	9.86	8.462	1.398
165	39:55.3	08:22.0	1611087	-6.001	1.499	1.996	4.2	2.539	2.542	-0.003	9.858	8.463	1.395
166	10:22.1	38:43.2	1620109	-6.001	1.499	1.996	4.2	2.537	2.541	-0.004	9.853	8.455	1.398
167	40:43.2	09:06.7	1629132	-6.001	1.499	1.996	4.2	2.538	2.541	-0.003	9.853	8.459	1.394
168	11:06.8	39:29.8	1638155	-6.001	1.499	1.997	4.2	2.537	2.54	-0.003	9.851	8.46	1.391
169	41:29.9	09:54.0	1647179	-6.001	1.499	1.994	4.2	2.537	2.54	-0.003	9.85	8.46	1.39
170	11:54.1	40:18.2	1656204	-6.001	1.499	1.994	4.2	2.536	2.539	-0.003	9.848	8.46	1.388
171	42:18.2	10:41.5	1665227	-6.001	1.499	1.995	4.2	2.536	2.539	-0.003	9.846	8.461	1.385
172	12:41.6	41:03.6	1674249	-6.001	1.499	1.997	4.2	2.535	2.539	-0.004	9.844	8.46	1.384
173	43:03.7	11:23.8	1683269	-6.001	1.5	1.997	4.2	2.535	2.538	-0.003	9.841	8.459	1.382
174	13:23.8	41:43.1	1692289	-6.001	1.499	1.999	4.2	2.534	2.538	-0.004	9.84	8.458	1.382
175	43:43.2	12:00.6	1701306	-6.001	1.5	1.999	4.2	2.534	2.537	-0.003	9.837	8.457	1.38
176	14:00.7	42:17.4	1710323	-6.001	1.499	1.998	4.2	2.533	2.536	-0.003	9.835	8.456	1.379
177	44:17.5	12:33.8	1719339	-6.001	1.499	1.995	4.2	2.533	2.536	-0.003	9.833	8.456	1.377
178	14:33.9	42:12.3	1728318	-6.001	1.5	1.995	4.2	2.517	2.533	-0.016	9.77	8.405	1.365
179	44:12.4	11:28.5	1737274	-6.001	1.5	1.997	4.2	2.522	2.525	-0.003	9.803	8.365	1.438
180	13:28.5	40:42.1	1746228	-6.001	1.5	1.996	4.2	2.522	2.525	-0.003	9.8	8.367	1.433
181	42:42.2	09:58.2	1755184	-6.001	1.5	1.998	4.2	2.522	2.525	-0.003	9.8	8.372	1.428
182	11:58.2	39:16.2	1764142	-6.001	1.5	1.996	4.2	2.522	2.525	-0.003	9.799	8.376	1.423

183	41:16.3	08:35.9	1773101	-6.001	1.5	1.998	4.2	2.522	2.525	-0.003	9.798	8.38	1.418
184	10:36.0	37:57.6	1782063	-6.001	1.5	1.994	4.2	2.522	2.525	-0.003	9.798	8.384	1.414
185	39:57.6	07:21.0	1791026	-6.001	1.499	1.996	4.2	2.522	2.525	-0.003	9.797	8.387	1.41
186	09:21.0	36:47.1	1799992	-6.001	1.5	1.997	4.2	2.522	2.525	-0.003	9.797	8.391	1.406
187	38:47.1	06:13.5	1808959	-6.001	1.499	1.998	4.2	2.521	2.524	-0.003	9.796	8.392	1.404
188	08:13.6	35:39.8	1817925	-6.001	1.499	1.995	4.2	2.521	2.525	-0.004	9.795	8.395	1.4
189	37:39.9	05:08.0	1826893	-6.001	1.499	1.998	4.2	2.521	2.524	-0.003	9.794	8.397	1.397
190	07:08.0	34:36.8	1835862	-6.001	1.499	1.999	4.2	2.521	2.524	-0.003	9.793	8.398	1.395
191	36:36.9	04:04.7	1844830	-6.001	1.499	1.995	4.2	2.521	2.524	-0.003	9.791	8.398	1.393
192	06:04.7	33:32.8	1853798	-6.001	1.499	1.998	4.2	2.52	2.523	-0.003	9.79	8.398	1.392
193	35:32.9	02:59.0	1862765	-6.001	1.499	1.995	4.2	2.52	2.523	-0.003	9.788	8.398	1.39
194	04:59.9	32:26.0	1871731	-6.001	1.499	1.998	4.2	2.519	2.523	-0.004	9.786	8.398	1.388
195	34:26.1	01:51.0	1880696	-6.001	1.499	1.997	4.2	2.519	2.522	-0.003	9.784	8.397	1.387
196	03:51.1	31:16.8	1889662	-6.001	1.499	1.996	4.2	2.518	2.522	-0.004	9.783	8.396	1.387
197	33:16.9	00:42.4	1898628	-6.001	1.499	1.995	4.2	2.518	2.521	-0.003	9.781	8.397	1.384
198	02:42.4	30:03.6	1907589	-6.001	1.499	1.994	4.2	2.517	2.521	-0.004	9.778	8.395	1.383
199	32:03.7	59:26.7	1916552	-6.001	1.499	1.997	4.2	2.517	2.52	-0.003	9.778	8.395	1.383
200	01:26.7	28:48.2	1925514	-6.001	1.5	1.998	4.2	2.517	2.52	-0.003	9.776	8.394	1.382
201	30:48.3	58:06.5	1934472	-6.001	1.5	1.999	4.2	2.516	2.519	-0.003	9.773	8.391	1.382
202	00:06.6	27:23.8	1943429	-6.001	1.499	1.996	4.2	2.515	2.518	-0.003	9.77	8.388	1.382
203	29:23.8	56:38.3	1952384	-6.001	1.499	1.994	4.2	2.514	2.518	-0.004	9.767	8.385	1.382
204	58:38.3	25:51.2	1961337	-6.001	1.5	1.996	4.2	2.514	2.517	-0.003	9.765	8.384	1.381
205	27:51.2	55:02.1	1970287	-6.001	1.499	1.999	4.2	2.513	2.516	-0.003	9.762	8.381	1.381
206	57:02.1	24:10.3	1979236	-6.001	1.499	1.996	4.2	2.512	2.516	-0.004	9.759	8.379	1.38
207	26:10.4	53:17.0	1988182	-6.001	1.499	1.995	4.2	2.512	2.515	-0.003	9.758	8.378	1.38
208	55:17.1	22:23.2	1997129	-6.001	1.5	1.998	4.2	2.511	2.515	-0.004	9.756	8.376	1.38
209	24:23.3	51:27.8	2006073	-6.001	1.499	1.999	4.2	2.511	2.514	-0.003	9.754	8.375	1.379
210	53:27.8	20:31.1	2015017	-6.001	1.499	1.995	4.2	2.51	2.514	-0.004	9.752	8.374	1.378
211	22:31.2	49:34.2	2023960	-6.001	1.499	1.996	4.2	2.51	2.513	-0.003	9.751	8.373	1.378
212	51:34.3	18:34.8	2032900	-6.001	1.499	1.996	4.2	2.509	2.513	-0.004	9.749	8.371	1.378
213	20:34.9	47:34.5	2041840	-6.001	1.499	1.996	4.2	2.509	2.512	-0.003	9.747	8.37	1.377
214	49:34.5	16:35.6	2050781	-6.001	1.499	1.999	4.2	2.509	2.512	-0.003	9.746	8.37	1.376
215	18:35.6	45:33.0	2059718	-6.001	1.499	1.997	4.2	2.508	2.511	-0.003	9.744	8.368	1.376
216	47:33.0	14:27.7	2068653	-6.001	1.499	1.999	4.2	2.507	2.511	-0.004	9.741	8.366	1.375
217	16:27.8	43:21.4	2077587	-6.001	1.499	1.994	4.2	2.507	2.51	-0.003	9.739	8.365	1.374
218	45:21.4	12:14.0	2086519	-6.001	1.499	1.996	4.2	2.506	2.51	-0.004	9.738	8.364	1.374
219	14:14.0	41:04.1	2095450	-6.001	1.499	1.997	4.2	2.506	2.509	-0.003	9.735	8.361	1.374
220	43:04.2	09:55.0	2104380	-6.001	1.499	1.998	4.2	2.505	2.509	-0.004	9.733	8.361	1.372
221	11:55.1	38:44.6	2113310	-6.001	1.499	1.994	4.2	2.505	2.508	-0.003	9.732	8.359	1.373
222	40:44.6	07:33.2	2122239	-6.001	1.499	1.997	4.2	2.504	2.508	-0.004	9.73	8.358	1.372
223	09:33.2	53:03.1	2132168	-6.001	1.499	1.999	4.229	2.557	2.548	0.009	9.953	8.494	1.459
224	55:03.1	21:27.3	2141073	-6.001	1.499	1.996	4.2	2.495	2.502	-0.007	9.697	8.334	1.363
225	23:27.4	06:30.2	2150976	-6.001	1.499	1.995	4.218	2.549	2.536	0.013	9.922	8.378	1.544
226	08:30.3	33:11.7	2159777	-6.001	1.499	1.994	4.2	2.473	2.479	-0.006	9.625	8.162	1.463
227	35:11.7	59:45.7	2168571	-6.001	1.5	1.999	4.2	2.473	2.477	-0.004	9.626	8.149	1.477
228	01:45.8	26:13.7	2177359	-6.001	1.499	1.994	4.2	2.472	2.477	-0.005	9.624	8.144	1.48
229	28:13.7	52:35.3	2186141	-6.001	1.5	1.999	4.2	2.471	2.475	-0.004	9.621	8.122	1.499
230	54:35.4	18:42.8	2194908	-6.001	1.499	1.996	4.2	2.468	2.472	-0.004	9.611	8.099	1.512
231	20:42.8	44:44.3	2203670	-6.001	1.499	1.998	4.2	2.466	2.47	-0.004	9.607	8.085	1.522
232	46:44.4	10:39.6	2212425	-6.001	1.499	1.999	4.2	2.465	2.469	-0.004	9.603	8.071	1.532
233	12:39.7	36:28.8	2221174	-6.001	1.5	1.995	4.2	2.463	2.467	-0.004	9.598	8.061	1.537
234	38:28.9	02:14.6	2229920	-6.001	1.499	1.997	4.2	2.462	2.466	-0.004	9.595	8.055	1.54
235	04:14.7	27:58.4	2238664	-6.001	1.499	1.995	4.2	2.462	2.466	-0.004	9.593	8.053	1.54
236	29:58.5	53:40.6	2247406	-6.001	1.499	1.999	4.2	2.461	2.465	-0.004	9.591	8.04	1.551
237	55:40.6	19:14.4	2256140	-6.001	1.499	1.996	4.2	2.459	2.463	-0.004	9.584	8.026	1.558
238	21:14.4	44:44.4	2264870	-6.001	1.499	1.996	4.2	2.458	2.462	-0.004	9.582	8.021	1.561
239	46:44.5	10:13.5	2273599	-6.001	1.499	1.996	4.2	2.458	2.462	-0.004	9.581	8.021	1.56
240	12:13.5	35:41.8	2282327	-6.001	1.5	1.999	4.2	2.458	2.462	-0.004	9.58	8.024	1.556
241	37:41.9	01:13.1	2291059	-6.001	1.499	1.997	4.2	2.458	2.462	-0.004	9.581	8.025	1.556
242	03:13.2	26:41.5	2299787	-6.001	1.499	1.995	4.2	2.458	2.461	-0.003	9.579	8.017	1.562
243	28:41.5	52:02.7	2308508	-6.001	1.499	1.998	4.2	2.456	2.46	-0.004	9.573	8.004	1.569
244	54:02.7	17:20.9	2317226	-6.001	1.499	1.997	4.2	2.455	2.459	-0.004	9.57	8	1.57
245	19:21.0	42:37.2	2325943	-6.001	1.499	1.999	4.2	2.455	2.458	-0.003	9.568	7.994	1.574
246	44:37.2	07:48.7	2334654	-6.001	1.499	1.995	4.2	2.453	2.457	-0.004	9.564	7.987	1.577
247	09:48.8	32:59.6	2343365	-6.001	1.499	1.997	4.2	2.453	2.456	-0.003	9.563	7.984	1.579
248	34:59.6	58:06.2	2352072	-6.001	1.499	1.998	4.2	2.452	2.455	-0.003	9.559	7.976	1.583
249	00:06.3	23:12.4	2360778	-6.001	1.499	1.999	4.2	2.451	2.455	-0.004	9.558	7.98	1.578
250	25:12.4	48:21.6	2369487	-6.001	1.499	1.995	4.2	2.452	2.456	-0.004	9.56	7.987	1.573
251	50:21.7	13:27.4	2378193	-6.001	1.499	1.995	4.2	2.451	2.455	-0.004	9.556	7.975	1.581
252	15:27.4	38:24.9	2386890	-6.001	1.499	1.997	4.2	2.449	2.453	-0.004	9.549	7.963	1.586
253	40:25.0	03:23.4	2395589	-6.001	1.499	1.996	4.2	2.449	2.453	-0.004	9.549	7.954	1.595
254	05:23.4	28:12.8	2404278	-6.001	1.499	1.996	4.2	2.447	2.45	-0.003	9.541	7.944	1.597
255	30:12.9	53:06.9	2412972	-6.001	1.5	1.998	4.2	2.448	2.451	-0.003	9.544	7.951	1.593
256	55:06.9	17:59.0	2421664	-6.001	1.499	1.999	4.2	2.447	2.451	-0.004	9.542	7.951	1.591
257	19:59.0	42:53.6	2430359	-6.001	1.5	1.997	4.2	2.447	2.451	-0.004	9.543	7.963	1.58
258	44:53.6	07:56.7	2439062	-6.001	1.499	1.997	4.2	2.45	2.453	-0.003	9.549	7.98	1.569
259	09:56.8	32:57.8	2447763	-6.001	1.499	1.996	4.2	2.449	2.453	-0.004	9.547	7.979	1.568
260	34:57.9	58:01.0	2456466	-6.001	1.499	1.996	4.2	2.449	2.453	-0.004	9.548	7.984	1.564
261	00:01.1	23:04.3	2465170	-6.001	1.499	1.999	4.2	2.449	2.453	-0.004	9.547	7.984	1.563
262	23:04.3	12:41.1	2478947	-1.5	1.5	1.999	4.2	2.449	2.478	-0.029	9.547	8.928	0.619
263	12:41.1	03:12.2	2492778	-1.5	1.499	1.999	4.2	2.472	2.478	-0.006	9.64	8.931	0.709
264	03:12.2	53:45.3	2506611	-1.5	1.5	1.998	4.2	2.473	2.478	-0.005	9.642	8.952	0.69
265	53:45.3	54:45.4	2506671	-1.5	1.5	1.998	4.2	2.473	2.478	-0.005	9.642	8.952	0.69
266	12:45.0	57:05.7	2520141	-1.5	1.5	1.999	4.2	2.378	2.411	-0.033	9.346	8.574	0.772
267	57:05.8	42:09.1	2533645	-1.5	1.5	1.999	4.2	2.413	2.413	0	9.455	8.584	0.871
268	42:09.2	27:03.2	2547139	-1.5	1.5	1.999	4.2	2.41	2.412	-0.002	9.442	8.582	0.86
269	27:03.2	22:33.3	2564869	-6.001	1.499	1.996	4.2	2.41	2.412	-0.002	9.442	8.582	0.86
270	24:33.3	45:55.0	2573471	-6.001	1.499	1.996	4.2	2.423	2.424	-0.001	9.469	7.739	1.73
271	47:55.1	09:02.7	2582058	-6.001	1.499	1.997	4.2	2.419	2.421	-0.002	9.453	7.73	1.723
272	11:02.7	32:05.7	2590641	-6.001	1.499	1.999	4.2	2.417	2.419	-0.002	9.448	7.724	1.724
273	34:05.7	55:15.0	2599231	-6.001	1.499	1.999	4.2	2.419	2.421	-0.002	9.453	7.737	1.716

274	57:15.0	18:27.5	2607823	-6.001	1.5	1.997	4.2	2.42	2.422	-0.002	9.454	7.736	1.718
275	20:27.6	41:42.2	2616418	-6.001	1.499	1.995	4.2	2.42	2.423	-0.003	9.455	7.762	1.693
276	43:42.2	05:06.6	2625022	-6.001	1.5	1.999	4.2	2.423	2.426	-0.003	9.464	7.782	1.682
277	07:06.7	28:42.1	2633638	-6.001	1.499	1.995	4.2	2.426	2.429	-0.003	9.473	7.807	1.666
278	30:42.1	52:30.6	2642266	-6.001	1.5	1.998	4.2	2.43	2.433	-0.003	9.485	7.832	1.653
279	54:30.7	16:23.1	2650899	-6.001	1.499	1.998	4.2	2.43	2.434	-0.004	9.487	7.844	1.643
280	18:23.2	40:14.1	2659530	-6.001	1.499	1.996	4.2	2.43	2.433	-0.003	9.485	7.843	1.642
281	42:14.1	04:08.2	2668164	-6.001	1.499	1.999	4.2	2.431	2.434	-0.003	9.488	7.851	1.637
282	06:08.2	28:03.8	2676800	-6.001	1.499	1.995	4.2	2.431	2.434	-0.003	9.488	7.855	1.633
283	30:03.8	52:01.4	2685437	-6.001	1.499	1.998	4.2	2.431	2.435	-0.004	9.487	7.864	1.623
284	54:01.5	16:02.2	2694078	-6.001	1.499	1.999	4.2	2.432	2.435	-0.003	9.491	7.866	1.625
285	18:02.3	40:04.8	2702721	-6.001	1.499	1.996	4.2	2.432	2.436	-0.004	9.491	7.871	1.62
286	42:04.8	04:06.7	2711362	-6.001	1.499	1.996	4.2	2.432	2.436	-0.004	9.49	7.875	1.615
287	06:06.7	28:10.4	2720006	-6.001	1.499	1.995	4.2	2.432	2.436	-0.004	9.491	7.88	1.611
288	30:10.4	52:15.8	2728652	-6.001	1.499	1.999	4.2	2.433	2.436	-0.003	9.492	7.888	1.604
289	54:15.8	16:22.9	2737299	-6.001	1.499	1.999	4.2	2.433	2.436	-0.003	9.492	7.892	1.6
290	18:23.0	40:32.7	2745948	-6.001	1.499	1.998	4.2	2.434	2.437	-0.003	9.494	7.897	1.597
291	42:32.7	04:44.5	2754600	-6.001	1.499	1.997	4.2	2.434	2.438	-0.004	9.495	7.903	1.592
292	06:44.6	28:59.4	2763255	-6.001	1.499	1.996	4.2	2.435	2.438	-0.003	9.497	7.909	1.588
293	30:59.4	53:15.6	2771911	-6.001	1.499	1.996	4.2	2.435	2.438	-0.003	9.497	7.914	1.583
294	55:15.7	17:32.3	2780568	-6.001	1.499	1.995	4.2	2.435	2.438	-0.003	9.497	7.92	1.577
295	19:32.4	41:50.2	2789226	-6.001	1.499	1.995	4.2	2.435	2.439	-0.004	9.497	7.924	1.573
296	43:50.2	06:10.0	2797886	-6.001	1.499	1.999	4.2	2.435	2.439	-0.004	9.498	7.926	1.572
297	08:10.1	30:27.4	2806543	-6.001	1.499	1.995	4.2	2.435	2.438	-0.003	9.495	7.926	1.569
298	32:27.5	54:43.6	2815199	-6.001	1.499	1.997	4.2	2.434	2.438	-0.004	9.494	7.923	1.571
299	56:43.7	19:00.7	2823857	-6.001	1.499	1.995	4.2	2.434	2.438	-0.004	9.494	7.921	1.573
300	21:00.8	43:16.8	2832513	-6.001	1.499	1.995	4.2	2.434	2.437	-0.003	9.492	7.921	1.571
301	45:16.9	07:33.1	2841169	-6.001	1.499	1.999	4.2	2.434	2.437	-0.003	9.492	7.922	1.57
302	09:33.1	31:49.4	2849825	-6.001	1.499	1.997	4.2	2.434	2.437	-0.003	9.491	7.922	1.569
303	33:49.4	56:05.1	2858481	-6.001	1.5	1.997	4.2	2.433	2.437	-0.004	9.49	7.92	1.57
304	58:05.1	20:18.7	2867134	-6.001	1.5	1.995	4.2	2.433	2.436	-0.003	9.487	7.918	1.569
305	22:18.7	44:32.5	2875788	-6.001	1.499	1.999	4.2	2.433	2.436	-0.003	9.486	7.918	1.568
306	46:32.5	08:44.9	2884441	-6.001	1.5	1.996	4.2	2.432	2.436	-0.004	9.485	7.917	1.568
307	10:44.9	32:57.0	2893093	-6.001	1.5	1.995	4.2	2.432	2.435	-0.003	9.484	7.919	1.565
308	34:57.0	57:09.5	2901745	-6.001	1.499	1.995	4.2	2.432	2.435	-0.003	9.484	7.921	1.563
309	59:09.5	21:21.6	2910397	-6.001	1.499	1.997	4.2	2.432	2.435	-0.003	9.483	7.918	1.565
310	23:21.7	45:29.5	2919045	-6.001	1.499	1.995	4.2	2.431	2.434	-0.003	9.478	7.911	1.567
311	47:29.5	09:34.6	2927690	-6.001	1.5	1.994	4.2	2.43	2.433	-0.003	9.476	7.904	1.572
312	11:34.6	33:36.3	2936332	-6.001	1.499	1.996	4.2	2.429	2.432	-0.003	9.472	7.9	1.572
313	35:36.4	57:38.9	2944975	-6.001	1.499	1.999	4.2	2.429	2.432	-0.003	9.471	7.902	1.569
314	59:39.0	21:38.1	2953614	-6.001	1.499	1.995	4.2	2.428	2.432	-0.004	9.468	7.9	1.568
315	23:38.2	45:35.5	2962251	-6.001	1.499	1.997	4.2	2.427	2.43	-0.003	9.466	7.894	1.572
316	47:35.5	09:31.1	2970887	-6.001	1.499	1.995	4.2	2.426	2.43	-0.004	9.464	7.892	1.572
317	11:31.2	33:22.0	2979518	-6.001	1.499	1.997	4.2	2.425	2.429	-0.004	9.46	7.886	1.574
318	35:22.1	57:11.6	2988147	-6.001	1.499	1.998	4.2	2.425	2.428	-0.003	9.458	7.886	1.572
319	59:11.6	21:02.3	2996778	-6.001	1.499	1.996	4.2	2.425	2.429	-0.004	9.458	7.892	1.566
320	23:02.4	44:50.2	3005406	-6.001	1.499	1.997	4.2	2.424	2.427	-0.003	9.455	7.881	1.574
321	46:50.2	08:30.0	3014026	-6.001	1.499	1.998	4.2	2.422	2.425	-0.003	9.448	7.865	1.583
322	10:30.0	32:00.1	3022636	-6.001	1.499	1.995	4.2	2.419	2.423	-0.004	9.439	7.85	1.589
323	34:00.1	55:22.7	3031238	-6.001	1.499	1.996	4.2	2.417	2.42	-0.003	9.432	7.838	1.594
324	57:22.7	18:35.5	3039831	-6.001	1.499	1.995	4.2	2.414	2.418	-0.004	9.423	7.825	1.598
325	20:35.5	41:41.9	3048418	-6.001	1.499	1.996	4.2	2.412	2.416	-0.004	9.417	7.815	1.602
326	43:41.9	04:36.9	3056993	-6.001	1.499	1.998	4.2	2.409	2.413	-0.004	9.407	7.808	1.599
327	06:36.9	27:34.3	3065570	-6.001	1.499	1.999	4.2	2.41	2.413	-0.003	9.408	7.802	1.606
328	29:34.3	50:19.4	3074135	-6.001	1.499	1.996	4.2	2.406	2.41	-0.004	9.396	7.78	1.616
329	52:19.4	12:59.1	3082695	-6.001	1.499	1.997	4.2	2.405	2.408	-0.003	9.391	7.772	1.619
330	14:59.1	35:31.6	3091247	-6.001	1.499	1.996	4.2	2.402	2.406	-0.004	9.383	7.764	1.619
331	37:31.6	58:00.9	3099797	-6.001	1.499	1.998	4.2	2.401	2.405	-0.004	9.38	7.758	1.622
332	00:00.9	20:25.8	3108342	-6.001	1.499	1.996	4.2	2.4	2.403	-0.003	9.375	7.742	1.633
333	22:25.8	42:38.8	3116875	-6.001	1.499	1.998	4.2	2.397	2.4	-0.003	9.363	7.725	1.638
334	44:38.8	04:46.1	3125402	-6.001	1.499	1.998	4.2	2.395	2.398	-0.003	9.357	7.708	1.649
335	06:46.1	26:50.7	3133927	-6.001	1.499	1.999	4.2	2.394	2.397	-0.003	9.355	7.699	1.656
336	28:50.7	49:00.1	3142456	-6.001	1.499	1.997	4.2	2.395	2.399	-0.004	9.359	7.701	1.658
337	51:00.1	11:16.2	3150992	-6.001	1.499	1.995	4.2	2.397	2.401	-0.004	9.365	7.703	1.662
338	13:16.2	33:28.8	3159525	-6.001	1.499	1.998	4.2	2.396	2.399	-0.003	9.359	7.693	1.666
339	35:28.8	55:38.9	3168055	-6.001	1.499	1.996	4.2	2.395	2.399	-0.004	9.357	7.688	1.669
340	57:39.0	17:42.8	3176579	-6.001	1.499	1.998	4.2	2.393	2.396	-0.003	9.351	7.675	1.676
341	19:42.8	39:35.6	3185091	-6.001	1.499	1.996	4.2	2.389	2.393	-0.004	9.338	7.685	1.653
342	41:35.6	01:36.1	3193612	-6.001	1.499	1.996	4.2	2.392	2.396	-0.004	9.348	7.695	1.653
343	03:36.1	23:42.6	3202138	-6.001	1.499	1.999	4.2	2.394	2.397	-0.003	9.353	7.69	1.663
344	25:42.6	45:32.8	3210649	-6.001	1.499	1.995	4.2	2.389	2.392	-0.003	9.334	7.662	1.672
345	47:32.8	07:14.6	3219150	-6.001	1.499	1.999	4.2	2.386	2.389	-0.003	9.325	7.627	1.698
346	09:14.7	29:04.5	3227660	-6.001	1.499	1.997	4.2	2.388	2.392	-0.004	9.334	7.644	1.69
347	31:04.5	50:53.4	3236169	-6.001	1.499	1.999	4.2	2.388	2.392	-0.004	9.332	7.627	1.705
348	52:53.4	13:46.1	3244742	-6.001	1.499	1.999	4.2	2.406	2.41	-0.004	9.391	7.712	1.679
349	15:46.1	36:55.4	3253331	-6.001	1.499	1.999	4.2	2.41	2.414	-0.004	9.404	7.753	1.651
350	38:55.5	59:34.1	3261890	-6.001	1.499	1.999	4.2	2.402	2.406	-0.004	9.378	7.689	1.689
351	01:34.1	22:23.7	3270459	-6.001	1.499	1.999	4.2	2.405	2.409	-0.004	9.387	7.706	1.681
352	24:23.7	45:11.6	3279027	-6.001	1.499	1.998	4.2	2.404	2.408	-0.004	9.385	7.719	1.666
353	47:11.6	07:41.2	3287577	-6.001	1.499	1.998	4.2	2.399	2.403	-0.004	9.369	7.67	1.699
354	09:41.2	30:05.9	3296122	-6.001	1.499	1.999	4.2	2.398	2.401	-0.003	9.363	7.674	1.689
355	32:05.9	52:36.3	3304672	-6.001	1.5	1.999	4.2	2.399	2.403	-0.004	9.368	7.657	1.711
356	54:36.3	15:27.5	3313243	-6.001	1.499	1.998	4.2	2.405	2.408	-0.003	9.384	7.71	1.674
357	17:27.5	38:24.0	3321820	-6.001	1.499	1.998	4.2	2.406	2.409	-0.003	9.388	7.692	1.696
358	40:24.0	01:33.3	3330409	-6.001	1.499	1.997	4.2	2.409	2.414	-0.005	9.399	7.756	1.643
359	03:33.3	24:58.4	3339014	-6.001	1.499	1.997	4.2	2.413	2.417	-0.004	9.412	7.779	1.633
360	26:58.4	48:34.6	3347630	-6.001	1.499	1.997	4.2	2.416	2.42	-0.004	9.419	7.846	1.573
361	50:34.7	12:13.9	3356250	-6.001	1.499	1.998	4.2	2.417	2.419	-0.002	9.422	7.805	1.617
362	14:13.9	35:52.3	3364868	-6.001	1.499	1.997	4.2	2.416	2.421	-0.005	9.419	7.871	1.548
363	37:52.3	59:35.5	3373491	-6.001	1.499	1.999	4.2	2.418	2.42	-0.002	9.424	7.839	1.585
364	01:35.6	23:13.0	3382109	-6.001	1.499	1.994	4.2	2.416	2.419	-0.003	9.419	7.799	1.62

365	25:13.0	46:51.0	3390727	-6.001	1.499	1.999	4.2	2.416	2.419	-0.003	9.418	7.803	1.615
366	48:51.0	10:20.6	3399336	-6.001	1.499	1.999	4.2	2.413	2.417	-0.004	9.411	7.827	1.584
367	12:20.6	33:51.5	3407947	-6.001	1.499	1.995	4.2	2.414	2.417	-0.003	9.412	7.82	1.592
368	35:51.6	57:11.7	3416548	-6.001	1.499	1.995	4.2	2.411	2.414	-0.003	9.403	7.784	1.619
369	59:11.8	20:24.9	3425141	-6.001	1.499	1.997	4.2	2.409	2.412	-0.003	9.396	7.765	1.631
370	22:24.9	43:31.7	3433728	-6.001	1.499	1.998	4.2	2.407	2.411	-0.004	9.391	7.745	1.646
371	45:31.7	06:41.2	3442317	-6.001	1.499	1.998	4.2	2.408	2.412	-0.004	9.393	7.804	1.589
372	08:41.2	29:52.3	3450908	-6.001	1.499	1.996	4.2	2.408	2.412	-0.004	9.393	7.764	1.629
373	31:52.3	52:58.0	3459494	-6.001	1.499	1.997	4.2	2.407	2.41	-0.003	9.389	7.768	1.621
374	54:58.1	16:03.4	3468079	-6.001	1.499	1.997	4.2	2.407	2.41	-0.003	9.388	7.749	1.639
375	18:03.4	39:00.5	3476656	-6.001	1.5	1.996	4.2	2.404	2.408	-0.004	9.38	7.738	1.642
376	41:00.6	01:58.0	3485234	-6.001	1.499	1.997	4.2	2.404	2.408	-0.004	9.38	7.744	1.636
377	03:58.0	24:45.0	3493801	-6.001	1.499	1.996	4.2	2.402	2.405	-0.003	9.372	7.718	1.654
378	26:45.0	47:30.3	3502366	-6.001	1.5	1.998	4.2	2.401	2.405	-0.004	9.37	7.706	1.664
379	49:30.4	10:18.1	3510934	-6.001	1.499	1.997	4.2	2.402	2.405	-0.003	9.371	7.707	1.664
380	12:18.1	32:55.5	3519491	-6.001	1.499	1.997	4.2	2.399	2.402	-0.003	9.362	7.682	1.68
381	34:55.6	55:28.9	3528045	-6.001	1.499	1.999	4.2	2.398	2.401	-0.003	9.359	7.671	1.688
382	57:28.9	18:07.3	3536603	-6.001	1.499	1.994	4.2	2.399	2.402	-0.003	9.361	7.677	1.684
383	20:07.3	40:42.2	3545158	-6.001	1.499	1.995	4.2	2.398	2.402	-0.004	9.358	7.669	1.689
384	42:42.3	03:16.3	3553712	-6.001	1.499	1.999	4.2	2.397	2.401	-0.004	9.357	7.668	1.689
385	05:16.4	25:49.7	3562265	-6.001	1.499	1.995	4.2	2.397	2.401	-0.004	9.354	7.68	1.674
386	27:49.7	48:25.1	3570821	-6.001	1.5	1.997	4.2	2.398	2.401	-0.003	9.357	7.67	1.687
387	50:25.2	10:55.5	3579371	-6.001	1.5	1.995	4.2	2.396	2.4	-0.004	9.353	7.675	1.678
388	12:55.5	33:26.2	3587922	-6.001	1.499	1.995	4.2	2.396	2.399	-0.003	9.353	7.649	1.704
389	35:26.2	55:43.2	3596458	-6.001	1.499	1.998	4.2	2.392	2.396	-0.004	9.339	7.622	1.717
390	57:42.3	18:03.6	3604999	-6.001	1.499	1.998	4.2	2.394	2.396	-0.002	9.343	7.614	1.729
391	20:03.6	40:23.8	3613540	-6.001	1.5	1.998	4.2	2.393	2.397	-0.004	9.34	7.618	1.722
392	42:23.8	02:59.4	3622095	-6.001	1.499	1.997	4.2	2.397	2.4	-0.003	9.353	7.701	1.652
393	04:59.4	25:55.4	3630671	-6.001	1.499	1.995	4.2	2.401	2.406	-0.005	9.367	7.794	1.573
394	25:55.4	11:46.0	3644222	-1.5	1.5	1.995	4.2	2.4	2.428	-0.028	9.363	8.753	0.61
395	11:46.1	58:30.5	3657826	-1.5	1.5	1.999	4.2	2.422	2.428	-0.006	9.453	8.757	0.696
396	58:30.5	45:16.7	3671432	-1.5	1.5	1.999	4.2	2.423	2.428	-0.005	9.456	8.757	0.699
397	45:16.7	46:16.7	3671493	-1.5	1.5	1.999	4.2	2.423	2.428	-0.005	9.456	8.757	0.699
398	23:30.0	11:04.7	3685157	-1.5	1.5	1.999	4.2	2.417	2.436	-0.019	9.457	8.78	0.677
399	11:04.8	58:30.8	3698803	-1.5	1.5	1.999	4.2	2.433	2.434	-0.001	9.494	8.777	0.717
400	58:30.9	45:46.7	3712439	-1.5	1.5	1.998	4.2	2.43	2.433	-0.003	9.483	8.773	0.71
401	45:46.7	42:55.5	3730268	-6.001	1.5	1.998	4.2	2.43	2.433	-0.003	9.483	8.773	0.71
402	44:55.5	05:56.7	3738849	-6.001	1.5	1.999	4.2	2.405	2.405	0	9.382	7.739	1.643
403	07:56.8	29:09.0	3747441	-6.001	1.5	1.999	4.2	2.406	2.409	-0.003	9.385	7.823	1.562
404	31:09.0	52:01.0	3756014	-6.001	1.499	1.999	4.2	2.406	2.411	-0.005	9.366	7.79	1.576
405	54:01.1	15:22.0	3764615	-6.001	1.5	1.996	4.2	2.408	2.411	-0.003	9.389	7.85	1.539
406	17:22.1	38:30.6	3773203	-6.001	1.5	1.998	4.2	2.406	2.407	-0.001	9.38	7.792	1.588
407	40:30.6	01:23.9	3781776	-6.001	1.499	1.998	4.2	2.401	2.404	-0.003	9.366	7.792	1.574
408	03:23.9	24:19.4	3790352	-6.001	1.499	1.999	4.2	2.401	2.404	-0.003	9.365	7.809	1.556
409	26:19.5	46:59.9	3798912	-6.001	1.499	1.999	4.2	2.397	2.401	-0.004	9.352	7.701	1.651
410	48:59.9	09:48.4	3807481	-6.001	1.499	1.995	4.2	2.399	2.403	-0.004	9.356	7.843	1.513
411	11:48.5	32:43.3	3816056	-6.001	1.5	1.999	4.2	2.401	2.402	-0.001	9.363	7.725	1.638
412	34:43.4	55:18.0	3824611	-6.001	1.5	1.999	4.2	2.395	2.398	-0.003	9.344	7.741	1.603
413	57:18.1	17:47.5	3833160	-6.001	1.5	1.994	4.2	2.393	2.396	-0.003	9.339	7.754	1.585
414	19:47.6	40:24.6	3841717	-6.001	1.499	1.996	4.2	2.394	2.401	-0.007	9.34	7.847	1.493
415	42:24.6	03:15.3	3850288	-6.001	1.499	1.997	4.2	2.399	2.399	0	9.357	7.774	1.583
416	05:15.3	25:32.7	3858825	-6.001	1.499	1.999	4.2	2.389	2.395	-0.006	9.326	7.705	1.621
417	27:32.8	48:12.0	3867384	-6.001	1.499	1.998	4.2	2.395	2.4	-0.005	9.344	7.841	1.503
418	50:12.0	10:59.6	3875952	-6.001	1.499	1.996	4.2	2.398	2.4	-0.002	9.352	7.708	1.644
419	12:59.6	33:29.8	3884502	-6.001	1.5	1.994	4.2	2.393	2.399	-0.006	9.335	7.853	1.482
420	35:29.8	56:23.6	3893076	-6.001	1.499	1.998	4.2	2.399	2.402	-0.003	9.355	7.821	1.534
421	58:23.6	18:59.9	3901632	-6.001	1.499	1.999	4.2	2.395	2.397	-0.002	9.34	7.772	1.568
422	21:00.0	41:27.4	3910180	-6.001	1.5	1.999	4.2	2.392	2.395	-0.003	9.332	7.663	1.669
423	43:27.4	03:38.7	3918711	-6.001	1.5	1.999	4.2	2.388	2.391	-0.003	9.317	7.754	1.563
424	05:38.8	25:46.8	3927239	-6.001	1.499	1.996	4.2	2.387	2.39	-0.003	9.313	7.684	1.629
425	27:46.9	47:54.2	3935767	-6.001	1.499	1.996	4.2	2.386	2.389	-0.003	9.312	7.752	1.56
426	49:54.3	10:07.3	3944300	-6.001	1.5	1.998	4.2	2.386	2.394	-0.008	9.311	7.699	1.612
427	12:07.3	33:18.9	3952891	-6.001	1.5	1.998	4.2	2.401	2.405	-0.004	9.357	7.923	1.434
428	35:18.9	56:23.9	3961476	-6.001	1.5	1.995	4.2	2.4	2.403	-0.003	9.352	7.897	1.455
429	58:24.0	19:18.5	3970051	-6.001	1.499	1.999	4.2	2.397	2.4	-0.003	9.344	7.869	1.475
430	21:18.6	42:07.9	3978620	-6.001	1.5	1.998	4.2	2.395	2.399	-0.004	9.338	7.85	1.488
431	44:08.0	04:50.9	3987183	-6.001	1.5	1.994	4.2	2.394	2.397	-0.003	9.334	7.833	1.501
432	06:50.9	27:32.5	3995745	-6.001	1.499	1.995	4.2	2.394	2.397	-0.003	9.333	7.822	1.511
433	29:32.6	50:17.5	4004310	-6.001	1.499	1.995	4.2	2.395	2.398	-0.003	9.336	7.82	1.516
434	52:17.5	12:57.0	4012870	-6.001	1.499	1.996	4.2	2.393	2.396	-0.003	9.33	7.806	1.524
435	14:57.1	35:38.4	4021431	-6.001	1.5	1.999	4.2	2.393	2.397	-0.004	9.331	7.809	1.522
436	37:38.5	58:15.5	4029988	-6.001	1.499	1.995	4.2	2.392	2.396	-0.004	9.328	7.799	1.529
437	00:15.6	20:59.6	4038552	-6.001	1.5	1.998	4.2	2.394	2.397	-0.003	9.332	7.819	1.513
438	22:59.7	43:43.1	4047116	-6.001	1.5	1.999	4.2	2.394	2.397	-0.003	9.331	7.833	1.498
439	45:43.2	06:27.8	4055680	-6.001	1.5	1.999	4.2	2.394	2.397	-0.003	9.331	7.816	1.515
440	08:27.8	29:06.6	4064239	-6.001	1.499	1.999	4.2	2.392	2.395	-0.003	9.326	7.805	1.521
441	31:06.7	51:44.9	4072797	-6.001	1.499	1.997	4.2	2.392	2.395	-0.003	9.325	7.805	1.52
442	53:44.9	14:28.2	4081361	-6.001	1.499	1.995	4.2	2.393	2.396	-0.003	9.328	7.804	1.524
443	16:28.3	37:02.4	4089915	-6.001	1.499	1.998	4.2	2.39	2.394	-0.004	9.32	7.801	1.519
444	39:02.5	59:49.7	4098482	-6.001	1.499	1.999	4.2	2.393	2.398	-0.005	9.329	7.892	1.437
445	01:49.8	22:48.1	4107061	-6.001	1.5	1.998	4.2	2.396	2.399	-0.003	9.337	7.869	1.468
446	24:48.1	45:35.4	4115628	-6.001	1.499	1.995	4.2	2.394	2.394	0	9.33	7.709	1.621
447	47:35.5	08:02.7	4124175	-6.001	1.5	1.999	4.2	2.387	2.394	-0.007	9.31	7.902	1.408
448	10:02.7	31:11.1	4132764	-6.001	1.499	1.994	4.201	2.398	2.401	-0.003	9.341	7.928	1.413
449	33:11.1	54:20.1	4141353	-6.001	1.499	1.996	4.2	2.397	2.401	-0.004	9.34	7.922	1.418
450	56:20.1	17:24.2	4149937	-6.001	1.5	1.995	4.2	2.396	2.4	-0.004	9.336	7.914	1.422
451	19:24.2	40:24.4	4158517	-6.001	1.5	1.996	4.2	2.395	2.399	-0.004	9.333	7.904	1.429
452	42:24.4	03:19.7	4167092	-6.001	1.499	1.995	4.2	2.394	2.397	-0.003	9.329	7.891	1.438
453	05:19.7	26:08.7	4175661	-6.001	1.499	1.999	4.2	2.392	2.396	-0.004	9.323	7.872	1.451
454	28:08.8	48:48.0	4184221	-6.001	1.499	1.998	4.2	2.39	2.393	-0.003	9.316	7.843	1.473
455	50:48.0	11:16.5	4192769	-6.001	1.499	1.996	4.2	2.387	2.39	-0.003	9.307	7.805	1.502

456	13:16.5	33:43.8	4201316	-6.001	1.499	1.995	4.2	2.386	2.389	-0.003	9.304	7.835	1.469
457	35:43.9	55:57.5	4209850	-6.001	1.499	1.997	4.2	2.383	2.385	-0.002	9.293	7.751	1.542
458	57:57.5	18:05.6	4218378	-6.001	1.499	1.995	4.2	2.38	2.388	-0.008	9.284	7.877	1.407
459	20:05.6	41:00.0	4226953	-6.001	1.5	1.998	4.2	2.392	2.396	-0.004	9.32	7.909	1.411
460	43:00.1	03:53.3	4235526	-6.001	1.499	1.998	4.2	2.392	2.395	-0.003	9.32	7.903	1.417
461	05:53.3	26:44.8	4244097	-6.001	1.499	1.999	4.2	2.392	2.395	-0.003	9.319	7.895	1.424
462	28:44.8	49:31.9	4252664	-6.001	1.499	1.997	4.2	2.391	2.394	-0.003	9.315	7.88	1.435
463	51:31.9	12:12.2	4261225	-6.001	1.499	1.996	4.2	2.39	2.389	0.001	9.312	7.823	1.489
464	14:12.2	34:11.5	4269744	-6.001	1.499	1.994	4.2	2.378	2.386	-0.008	9.276	7.867	1.409
465	36:11.5	57:00.7	4278313	-6.001	1.499	1.999	4.2	2.391	2.394	-0.003	9.315	7.897	1.418
466	59:00.7	19:47.3	4286880	-6.001	1.499	1.997	4.2	2.39	2.393	-0.003	9.312	7.894	1.418
467	21:47.4	42:32.9	4295445	-6.001	1.499	1.995	4.2	2.39	2.393	-0.003	9.311	7.888	1.423
468	44:33.0	05:14.8	4304007	-6.001	1.499	1.999	4.2	2.389	2.392	-0.003	9.307	7.879	1.428
469	07:14.8	27:53.4	4312566	-6.001	1.499	1.995	4.2	2.388	2.391	-0.003	9.304	7.862	1.442
470	29:53.5	50:10.7	4321103	-6.001	1.499	1.997	4.2	2.383	2.386	-0.003	9.289	7.723	1.566
471	52:10.7	12:31.1	4329644	-6.001	1.5	1.993	4.2	2.383	2.388	-0.005	9.29	7.885	1.405
472	14:31.1	35:14.1	4338207	-6.001	1.499	1.997	4.2	2.388	2.392	-0.004	9.306	7.899	1.407
473	37:14.1	57:57.2	4346770	-6.001	1.499	1.993	4.2	2.388	2.391	-0.003	9.304	7.894	1.41
474	59:57.2	20:37.1	4355330	-6.001	1.499	1.996	4.2	2.387	2.39	-0.003	9.301	7.882	1.419
475	22:37.1	43:10.0	4363883	-6.001	1.499	1.999	4.2	2.385	2.389	-0.004	9.296	7.864	1.432
476	45:10.0	05:34.7	4372427	-6.001	1.5	1.998	4.2	2.384	2.387	-0.003	9.291	7.837	1.454
477	07:34.8	27:41.9	4380954	-6.001	1.499	1.997	4.2	2.38	2.381	-0.001	9.279	7.647	1.632
478	29:42.0	49:30.6	4389463	-6.001	1.499	1.994	4.2	2.374	2.381	-0.007	9.26	7.859	1.401
479	51:30.7	12:03.3	4398016	-6.001	1.499	1.993	4.2	2.385	2.388	-0.003	9.294	7.89	1.404
480	14:03.3	34:34.4	4406567	-6.001	1.499	1.995	4.2	2.385	2.388	-0.003	9.292	7.885	1.407
481	36:34.5	57:03.1	4415116	-6.001	1.499	1.998	4.2	2.384	2.387	-0.003	9.289	7.877	1.412
482	59:03.1	19:27.0	4423660	-6.001	1.499	1.995	4.2	2.383	2.386	-0.003	9.284	7.866	1.418
483	21:27.1	41:46.5	4432199	-6.001	1.5	1.998	4.2	2.381	2.383	-0.002	9.28	7.834	1.446
484	43:46.6	03:27.2	4440700	-6.001	1.499	1.999	4.2	2.372	2.373	-0.001	9.251	7.599	1.652
485	05:27.3	25:02.7	4449195	-6.001	1.499	1.995	4.2	2.369	2.376	-0.007	9.242	7.829	1.413
486	27:02.7	47:16.1	4457729	-6.001	1.499	1.998	4.2	2.379	2.382	-0.003	9.273	7.852	1.421
487	49:16.1	09:29.7	4466262	-6.001	1.5	1.995	4.2	2.379	2.382	-0.003	9.273	7.844	1.429
488	11:29.8	31:39.6	4474792	-6.001	1.499	1.995	4.2	2.378	2.381	-0.003	9.271	7.823	1.448
489	33:39.7	53:39.6	4483312	-6.001	1.499	1.994	4.2	2.376	2.379	-0.003	9.264	7.787	1.477
490	55:39.7	15:23.8	4491816	-6.001	1.499	1.999	4.2	2.373	2.373	0	9.253	7.684	1.569
491	17:23.8	36:56.5	4500309	-6.001	1.5	1.993	4.2	2.368	2.375	-0.007	9.239	7.831	1.408
492	38:56.6	59:06.7	4508839	-6.001	1.5	1.994	4.2	2.378	2.381	-0.003	9.269	7.855	1.414
493	01:06.7	21:18.9	4517371	-6.001	1.5	1.995	4.2	2.378	2.382	-0.004	9.269	7.855	1.414
494	23:19.0	43:29.5	4525902	-6.001	1.499	1.995	4.2	2.378	2.381	-0.003	9.267	7.851	1.416
495	45:29.6	05:37.4	4534430	-6.001	1.499	1.995	4.2	2.377	2.38	-0.003	9.265	7.844	1.421
496	07:37.5	27:45.5	4542958	-6.001	1.5	1.997	4.2	2.377	2.38	-0.003	9.264	7.836	1.428
497	29:45.5	49:43.7	4551476	-6.001	1.499	1.995	4.2	2.374	2.378	-0.004	9.257	7.809	1.448
498	51:43.8	11:32.4	4559985	-6.001	1.499	1.996	4.2	2.372	2.375	-0.003	9.25	7.775	1.475
499	13:32.5	33:09.9	4568482	-6.001	1.5	1.994	4.2	2.369	2.372	-0.003	9.241	7.724	1.517
500	35:10.0	54:36.7	4576969	-6.001	1.499	1.999	4.2	2.367	2.368	-0.001	9.233	7.704	1.529
501	56:36.8	15:55.8	4585448	-6.001	1.499	1.994	4.2	2.364	2.37	-0.006	9.222	7.788	1.434
502	17:55.8	37:38.5	4593951	-6.001	1.499	1.996	4.2	2.37	2.373	-0.003	9.243	7.765	1.478
503	39:38.6	59:11.3	4602444	-6.001	1.5	1.995	4.2	2.367	2.373	-0.006	9.233	7.794	1.439
504	01:11.3	22:19.8	4611032	-6.001	1.499	1.998	4.2	2.387	2.391	-0.004	9.294	7.98	1.314
505	24:19.9	45:28.0	4619620	-6.001	1.499	1.993	4.2	2.387	2.391	-0.004	9.292	7.981	1.311
506	47:28.0	08:36.4	4628209	-6.001	1.499	1.996	4.2	2.387	2.39	-0.003	9.292	7.981	1.311
507	10:36.4	31:43.1	4636796	-6.001	1.5	1.998	4.2	2.387	2.39	-0.003	9.29	7.98	1.31
508	33:43.2	54:49.3	4645382	-6.001	1.5	1.995	4.2	2.386	2.39	-0.004	9.289	7.98	1.309
509	56:49.3	17:54.0	4653967	-6.001	1.5	1.997	4.2	2.386	2.389	-0.003	9.287	7.978	1.309
510	19:54.1	40:57.7	4662550	-6.001	1.499	1.996	4.2	2.385	2.389	-0.004	9.285	7.976	1.309
511	42:57.8	04:00.8	4671133	-6.001	1.499	1.993	4.2	2.385	2.388	-0.003	9.283	7.975	1.308
512	06:00.8	27:01.7	4679714	-6.001	1.499	1.995	4.2	2.384	2.388	-0.004	9.282	7.973	1.309
513	29:01.8	50:01.6	4688294	-6.001	1.499	1.993	4.2	2.384	2.387	-0.003	9.28	7.953	1.327
514	52:01.7	12:37.6	4696850	-6.001	1.499	1.993	4.2	2.379	2.383	-0.004	9.272	7.92	1.352
515	14:37.7	34:55.6	4705388	-6.001	1.499	1.997	4.2	2.375	2.378	-0.003	9.253	7.863	1.39
516	36:55.6	56:45.6	4713898	-6.001	1.499	1.999	4.2	2.369	2.373	-0.004	9.235	7.844	1.391
517	58:45.6	18:32.4	4722405	-6.001	1.5	1.996	4.2	2.369	2.372	-0.003	9.233	7.841	1.392
518	20:32.5	40:15.9	4730908	-6.001	1.499	1.997	4.2	2.368	2.371	-0.003	9.229	7.84	1.389
519	42:15.9	01:59.0	4739411	-6.001	1.499	1.999	4.2	2.367	2.37	-0.003	9.227	7.841	1.386
520	03:59.0	23:42.4	4747915	-6.001	1.499	1.997	4.2	2.367	2.37	-0.003	9.226	7.844	1.382
521	25:42.5	45:25.6	4756418	-6.001	1.499	1.998	4.2	2.367	2.37	-0.003	9.225	7.843	1.382
522	47:25.6	07:07.9	4764920	-6.001	1.499	1.998	4.2	2.366	2.37	-0.004	9.224	7.845	1.379
523	09:07.9	28:48.0	4773421	-6.001	1.5	1.998	4.2	2.366	2.369	-0.003	9.221	7.841	1.38
524	30:48.1	50:27.6	4781920	-6.001	1.499	1.999	4.2	2.365	2.369	-0.004	9.22	7.843	1.377
525	52:27.7	12:07.4	4790420	-6.001	1.499	1.997	4.2	2.365	2.368	-0.003	9.219	7.844	1.375
526	12:07.4	55:33.6	4803826	-1.5	1.5	1.997	4.201	2.365	2.386	-0.021	8.638	8.638	0.58
527	55:33.7	39:36.7	4817269	-1.5	1.5	1.998	4.2	2.381	2.387	-0.006	9.288	8.64	0.648
528	39:36.7	23:40.1	4830713	-1.5	1.5	1.998	4.2	2.382	2.386	-0.004	9.291	8.638	0.653
529	23:40.1	24:40.2	4830773	-1.5	1.5	1.998	4.2	2.382	2.386	-0.004	9.291	8.638	0.653
530	09:49.0	50:06.1	4844000	-1.501	1.5	1.999	4.2	2.322	2.352	-0.03	9.137	8.446	0.691
531	50:06.2	31:16.2	4857270	-1.5	1.5	1.998	4.201	2.357	2.356	0.001	9.223	8.466	0.757
532	31:16.2	12:26.2	4870540	-1.501	1.5	1.999	4.2	2.355	2.356	-0.001	9.214	8.473	0.741
533	12:26.2	02:57.9	4887972	-6.001	1.5	1.996	4.2	2.355	2.356	-0.001	9.214	8.473	0.741
534	04:57.9	23:05.5	4896379	-6.001	1.5	1.998	4.2	2.345	2.346	-0.001	9.16	7.651	1.509
535	25:05.5	43:05.7	4904779	-6.001	1.499	1.993	4.2	2.343	2.344	-0.001	9.15	7.647	1.503
536	45:05.7	03:19.1	4913193	-6.001	1.499	1.997	4.2	2.346	2.347	-0.001	9.159	7.667	1.492
537	05:19.2	23:27.7	4921601	-6.001	1.5	1.999	4.2	2.344	2.346	-0.002	9.153	7.663	1.49
538	25:27.8	43:43.0	4930017	-6.001	1.5	1.995	4.2	2.345	2.347	-0.002	9.156	7.676	1.48
539	45:43.0	04:02.4	4938436	-6.001	1.499	1.995	4.2	2.346	2.348	-0.002	9.156	7.685	1.471
540	06:02.5	24:24.9	4946859	-6.001	1.499	1.994	4.201	2.346	2.348	-0.002	9.157	7.694	1.463
541	26:24.9	44:48.2	4955282	-6.001	1.499	1.997	4.2	2.346	2.348	-0.002	9.156	7.699	1.457
542	46:48.2	05:14.0	4963708	-6.001	1.499	1.997	4.2	2.346	2.349	-0.003	9.158	7.707	1.451
543	07:14.1	25:41.3	4972135	-6.001	1.499	1.994	4.2	2.347	2.349	-0.002	9.158	7.712	1.446
544	27:41.4	46:10.5	4980564	-6.001	1.499	1.993	4.2	2.347	2.35	-0.003	9.158	7.716	1.442
545	48:10.5	06:32.6	4988986	-6.001	1.499	1.995	4.201	2.345	2.347	-0.002	9.15	7.706	1.444
546	08:32.6	26:57.6	4997411	-6.001	1.499	1.994	4.2	2.345	2.348	-0.003	9.152	7.712	1.44

547	28:57.7	47:19.1	5005833	-6.001	1.5	1.995	4.2	2.344	2.347	-0.003	9.148	7.711	1.437
548	49:19.1	07:44.7	5014258	-6.001	1.5	1.993	4.2	2.345	2.348	-0.003	9.149	7.716	1.433
549	09:44.7	28:09.9	5022684	-6.001	1.499	1.997	4.2	2.345	2.347	-0.002	9.148	7.718	1.43
550	30:09.9	48:34.7	5031108	-6.001	1.5	1.999	4.2	2.344	2.347	-0.003	9.147	7.722	1.425
551	50:34.7	08:59.7	5039533	-6.001	1.5	1.995	4.2	2.344	2.347	-0.003	9.146	7.722	1.424
552	10:59.7	29:23.8	5047958	-6.001	1.5	1.996	4.2	2.344	2.347	-0.003	9.144	7.724	1.42
553	31:23.9	49:48.3	5056382	-6.001	1.499	1.998	4.2	2.343	2.346	-0.003	9.143	7.725	1.418
554	51:48.3	10:12.6	5064806	-6.001	1.5	1.998	4.2	2.343	2.346	-0.003	9.142	7.726	1.416
555	12:12.7	30:36.6	5073230	-6.001	1.5	1.993	4.2	2.343	2.346	-0.003	9.14	7.727	1.413
556	32:36.7	50:59.8	5081654	-6.001	1.5	1.998	4.2	2.342	2.345	-0.003	9.138	7.727	1.411
557	52:59.8	11:22.3	5090076	-6.001	1.499	1.993	4.2	2.342	2.345	-0.003	9.136	7.727	1.409
558	13:22.3	31:43.7	5098497	-6.001	1.499	1.995	4.2	2.342	2.344	-0.002	9.135	7.727	1.408
559	33:43.8	52:04.4	5106918	-6.001	1.499	1.995	4.2	2.341	2.344	-0.003	9.133	7.727	1.406
560	54:04.5	12:25.2	5115339	-6.001	1.499	1.997	4.2	2.341	2.344	-0.003	9.132	7.727	1.405
561	14:25.2	32:43.6	5123757	-6.001	1.499	1.999	4.2	2.34	2.343	-0.003	9.129	7.725	1.404
562	34:43.7	53:01.5	5132175	-6.001	1.499	1.995	4.2	2.34	2.343	-0.003	9.127	7.726	1.401
563	55:01.6	13:19.1	5140593	-6.001	1.499	1.995	4.2	2.339	2.342	-0.003	9.126	7.726	1.4
564	15:19.2	33:35.4	5149009	-6.001	1.499	1.992	4.2	2.339	2.342	-0.003	9.125	7.727	1.398
565	35:35.5	53:51.7	5157425	-6.001	1.499	1.999	4.2	2.339	2.342	-0.003	9.124	7.727	1.397
566	55:51.7	14:06.0	5165840	-6.001	1.499	1.994	4.2	2.338	2.341	-0.003	9.121	7.725	1.396
567	16:06.0	34:19.5	5174253	-6.001	1.499	1.997	4.2	2.338	2.341	-0.003	9.119	7.725	1.394
568	36:19.5	54:31.3	5182665	-6.001	1.499	1.999	4.2	2.337	2.34	-0.003	9.117	7.724	1.393
569	56:31.4	14:40.3	5191074	-6.001	1.499	1.995	4.2	2.336	2.339	-0.003	9.114	7.721	1.393
570	16:40.4	34:47.1	5199481	-6.001	1.499	1.999	4.2	2.335	2.338	-0.003	9.111	7.718	1.393
571	36:47.1	54:52.3	5207886	-6.001	1.5	1.999	4.2	2.335	2.338	-0.003	9.109	7.716	1.393
572	56:52.4	14:55.2	5216289	-6.001	1.5	1.995	4.2	2.334	2.337	-0.003	9.106	7.715	1.391
573	16:55.3	34:57.9	5224692	-6.001	1.499	1.998	4.2	2.334	2.336	-0.002	9.104	7.712	1.392
574	36:57.9	54:58.4	5233092	-6.001	1.499	1.999	4.2	2.333	2.336	-0.003	9.102	7.711	1.391
575	56:58.4	14:57.7	5241491	-6.001	1.5	1.994	4.2	2.332	2.335	-0.003	9.1	7.711	1.389
576	16:57.7	34:55.8	5249890	-6.001	1.5	1.998	4.201	2.332	2.335	-0.003	9.098	7.709	1.389
577	36:55.9	54:52.2	5258286	-6.001	1.5	1.995	4.2	2.331	2.334	-0.003	9.095	7.709	1.386
578	56:52.3	14:46.0	5266680	-6.001	1.499	1.999	4.2	2.331	2.334	-0.003	9.093	7.707	1.386
579	16:46.1	34:40.0	5275074	-6.001	1.5	1.993	4.2	2.33	2.333	-0.003	9.091	7.707	1.384
580	36:40.1	54:32.6	5283466	-6.001	1.5	1.999	4.201	2.33	2.333	-0.003	9.089	7.705	1.384
581	56:32.6	14:23.8	5291857	-6.001	1.5	1.992	4.2	2.329	2.332	-0.003	9.086	7.704	1.382
582	16:23.8	34:14.2	5300248	-6.001	1.499	1.996	4.2	2.329	2.332	-0.003	9.085	7.703	1.382
583	36:14.3	54:03.9	5308638	-6.001	1.499	1.992	4.201	2.328	2.331	-0.003	9.083	7.703	1.38
584	56:04.0	13:52.0	5317026	-6.001	1.499	1.999	4.2	2.328	2.33	-0.002	9.081	7.701	1.38
585	15:52.0	33:39.5	5325413	-6.001	1.499	1.991	4.201	2.327	2.33	-0.003	9.079	7.702	1.377
586	35:39.6	53:24.9	5333799	-6.001	1.5	1.993	4.2	2.327	2.33	-0.003	9.078	7.7	1.378
587	55:24.9	13:09.2	5342183	-6.001	1.5	1.992	4.2	2.326	2.329	-0.003	9.076	7.7	1.376
588	15:09.2	32:51.7	5350565	-6.001	1.5	1.999	4.201	2.326	2.328	-0.002	9.073	7.697	1.376
589	34:51.7	52:30.9	5358945	-6.001	1.499	1.998	4.2	2.325	2.328	-0.003	9.069	7.695	1.374
590	54:31.0	12:09.2	5367323	-6.001	1.499	1.999	4.2	2.324	2.327	-0.003	9.067	7.694	1.373
591	14:09.2	31:45.6	5375699	-6.001	1.499	1.995	4.2	2.323	2.326	-0.003	9.064	7.692	1.372
592	33:45.7	51:20.4	5384074	-6.001	1.499	1.997	4.2	2.323	2.326	-0.003	9.062	7.691	1.371
593	53:20.4	10:53.9	5392448	-6.001	1.499	1.993	4.2	2.322	2.325	-0.003	9.06	7.69	1.37
594	12:53.9	30:26.3	5400820	-6.001	1.499	1.994	4.2	2.322	2.325	-0.003	9.058	7.687	1.371
595	32:26.4	49:56.8	5409191	-6.001	1.499	1.994	4.2	2.321	2.324	-0.003	9.055	7.686	1.369
596	51:56.9	09:25.7	5417559	-6.001	1.499	1.996	4.2	2.32	2.323	-0.003	9.053	7.684	1.369
597	11:25.7	28:52.2	5425926	-6.001	1.499	1.994	4.2	2.32	2.323	-0.003	9.05	7.682	1.368
598	30:52.3	48:16.3	5434290	-6.001	1.499	1.993	4.2	2.319	2.322	-0.003	9.047	7.68	1.367
599	50:16.4	07:38.7	5442652	-6.001	1.499	1.995	4.2	2.318	2.321	-0.003	9.045	7.678	1.367
600	09:38.7	27:00.7	5451014	-6.001	1.5	1.992	4.2	2.318	2.321	-0.003	9.043	7.676	1.367
601	29:00.8	46:21.8	5459376	-6.001	1.499	1.995	4.2	2.317	2.32	-0.003	9.041	7.674	1.367
602	48:21.9	05:41.3	5467735	-6.001	1.499	1.992	4.2	2.317	2.32	-0.003	9.038	7.673	1.365
603	07:41.4	24:58.6	5476092	-6.001	1.499	1.993	4.2	2.316	2.319	-0.003	9.037	7.671	1.366
604	26:58.7	44:14.6	5484448	-6.001	1.5	1.994	4.2	2.316	2.319	-0.003	9.035	7.67	1.365
605	46:14.6	03:30.1	5492804	-6.001	1.499	1.993	4.2	2.315	2.318	-0.003	9.033	7.669	1.364
606	05:30.1	22:43.5	5501157	-6.001	1.499	1.998	4.2	2.314	2.317	-0.003	9.031	7.667	1.364
607	24:43.6	41:54.7	5509508	-6.001	1.499	1.993	4.2	2.314	2.317	-0.003	9.028	7.665	1.363
608	43:54.8	01:03.7	5517857	-6.001	1.499	1.995	4.201	2.313	2.316	-0.003	9.027	7.663	1.364
609	03:03.7	20:10.8	5526204	-6.001	1.499	1.996	4.2	2.313	2.316	-0.003	9.024	7.662	1.362
610	22:10.8	39:04.6	5534538	-6.001	1.499	1.993	4.2	2.309	2.312	-0.003	9.012	7.639	1.373
611	41:04.6	58:01.5	5542875	-6.001	1.499	1.994	4.2	2.31	2.313	-0.003	9.014	7.643	1.371
612	00:01.5	16:56.8	5551210	-6.001	1.499	1.998	4.2	2.309	2.312	-0.003	9.011	7.642	1.369
613	18:56.8	35:47.9	5559542	-6.001	1.499	1.996	4.2	2.308	2.311	-0.003	9.008	7.64	1.368
614	37:48.0	54:40.2	5567874	-6.001	1.499	1.995	4.2	2.308	2.311	-0.003	9.007	7.639	1.368
615	56:40.2	13:31.1	5576205	-6.001	1.499	1.998	4.2	2.307	2.31	-0.003	9.005	7.637	1.368
616	15:31.2	32:19.5	5584533	-6.001	1.499	1.995	4.2	2.307	2.31	-0.003	9.002	7.635	1.367
617	34:19.6	50:52.3	5592846	-6.001	1.499	1.995	4.2	2.303	2.305	-0.002	8.988	7.605	1.383
618	52:52.3	09:26.4	5601160	-6.001	1.499	1.996	4.2	2.303	2.306	-0.003	8.989	7.609	1.38
619	11:26.4	27:59.7	5609473	-6.001	1.499	1.993	4.2	2.302	2.305	-0.003	8.988	7.609	1.379
620	29:59.8	46:32.4	5617786	-6.001	1.499	1.997	4.2	2.302	2.305	-0.003	8.986	7.608	1.378
621	48:32.4	05:03.1	5626097	-6.001	1.499	1.995	4.2	2.301	2.304	-0.003	8.983	7.608	1.375
622	07:03.2	23:33.1	5634407	-6.001	1.499	1.996	4.2	2.301	2.304	-0.003	8.982	7.607	1.375
623	25:33.2	42:01.6	5642715	-6.001	1.499	1.997	4.2	2.3	2.303	-0.003	8.98	7.605	1.375
624	44:01.6	00:27.8	5651021	-6.001	1.5	1.995	4.2	2.3	2.302	-0.002	8.977	7.602	1.375
625	02:27.8	18:52.5	5659326	-6.001	1.499	1.996	4.2	2.299	2.302	-0.003	8.975	7.6	1.375
626	20:52.6	37:14.5	5667628	-6.001	1.499	1.996	4.201	2.298	2.301	-0.003	8.972	7.597	1.375
627	39:14.5	55:34.5	5675928	-6.001	1.499	1.993	4.2	2.298	2.301	-0.003	8.969	7.595	1.374
628	57:34.6	13:50.7	5684224	-6.001	1.499	1.996	4.2	2.297	2.298	-0.001	8.967	7.575	1.392
629	15:50.7	30:25.4	5692419	-6.001	1.499	1.995	4.2	2.27	2.272	-0.002	8.881	7.369	1.512
630	32:25.4	47:06.7	5700620	-6.001	1.499	1.999	4.2	2.272	2.275	-0.003	8.888	7.362	1.526
631	49:06.8	03:53.2	5708827	-6.001	1.499	1.998	4.2	2.273	2.276	-0.003	8.891	7.352	1.539
632	05:53.3	20:36.2	5717030	-6.001	1.499	1.999	4.2	2.272	2.275	-0.003	8.886	7.347	1.539
633	22:36.2	37:15.6	5725229	-6.001	1.499	1.996	4.2	2.27	2.273	-0.003	8.882	7.347	1.535
634	39:15.7	53:50.2	5733424	-6.001	1.499	1.993	4.2	2.269	2.272	-0.003	8.876	7.339	1.537
635	55:50.3	10:15.9	5741610	-6.001	1.499	1.994	4.2	2.266	2.269	-0.003	8.868	7.322	1.546
636	12:16.0	26:36.5	5749790	-6.001	1.499	1.996	4.2	2.265	2.267	-0.002	8.862	7.317	1.545
637	28:36.5	42:54.8	5757969	-6.001	1.499	1.999	4.2	2.264	2.267	-0.003	8.859	7.306	1.553

638	44:54.9	59:05.7	5766139	-6.001	1.499	1.994	4.2	2.262	2.265	-0.003	8.852	7.296	1.556
639	01:05.7	15:14.9	5774309	-6.001	1.499	1.995	4.2	2.261	2.264	-0.003	8.85	7.294	1.556
640	17:15.0	31:21.5	5782475	-6.001	1.499	1.994	4.2	2.26	2.263	-0.003	8.847	7.293	1.554
641	33:21.6	47:27.8	5790642	-6.001	1.499	1.999	4.2	2.26	2.263	-0.003	8.846	7.293	1.553
642	49:27.9	03:31.4	5798805	-6.001	1.5	1.999	4.2	2.259	2.262	-0.003	8.842	7.286	1.556
643	05:31.4	19:34.3	5806968	-6.001	1.499	1.995	4.2	2.259	2.262	-0.003	8.841	7.286	1.555
644	21:34.4	35:33.5	5815127	-6.001	1.499	1.995	4.2	2.258	2.261	-0.003	8.837	7.282	1.555
645	37:33.6	51:28.7	5823282	-6.001	1.5	1.995	4.2	2.256	2.259	-0.003	8.832	7.275	1.557
646	53:28.7	07:20.5	5831434	-6.001	1.499	1.999	4.201	2.255	2.258	-0.003	8.829	7.278	1.551
647	09:20.5	23:07.8	5839581	-6.001	1.499	1.997	4.2	2.254	2.257	-0.003	8.824	7.271	1.553
648	25:07.8	38:52.5	5847726	-6.001	1.499	1.998	4.2	2.253	2.256	-0.003	8.819	7.269	1.55
649	40:52.5	54:34.8	5855869	-6.001	1.499	1.998	4.2	2.252	2.255	-0.003	8.816	7.263	1.553
650	56:34.8	10:16.6	5864010	-6.001	1.499	1.998	4.2	2.251	2.254	-0.003	8.814	7.261	1.553
651	12:16.6	25:53.7	5872147	-6.001	1.499	1.995	4.201	2.25	2.253	-0.003	8.81	7.253	1.557
652	27:53.7	41:27.8	5880282	-6.001	1.499	1.998	4.2	2.249	2.252	-0.003	8.807	7.255	1.552
653	43:27.8	57:00.3	5888414	-6.001	1.499	1.994	4.2	2.249	2.252	-0.003	8.804	7.251	1.553
654	59:00.4	12:30.8	5896544	-6.001	1.5	1.998	4.2	2.248	2.251	-0.003	8.802	7.239	1.563
655	14:30.8	27:57.0	5904671	-6.001	1.499	1.995	4.2	2.247	2.25	-0.003	8.797	7.232	1.565
656	29:57.0	43:19.5	5912793	-6.001	1.5	1.994	4.2	2.245	2.248	-0.003	8.793	7.225	1.568
657	45:19.5	58:39.8	5920914	-6.001	1.499	1.997	4.2	2.245	2.247	-0.002	8.79	7.225	1.565
658	58:39.8	31:57.8	5933712	-1.501	1.5	1.997	4.2	2.243	2.263	-0.02	8.784	8.144	0.64
659	31:57.9	05:56.4	5946550	-1.5	1.5	1.998	4.2	2.259	2.264	-0.005	8.855	8.15	0.705
660	05:56.4	39:53.1	5959387	-1.5	1.5	1.999	4.2	2.259	2.264	-0.005	8.854	8.147	0.707
661	39:53.1	40:53.2	5959447	0	0	2.774	2.786	0	0	0	0	0	0

SUMMARY OUTPUT
SNL_18650_NMC_15C_0-100_0.5-1C_a_cycle

Regression Statistics	
Multiple R	0.789261713
R Square	0.622934051
Adjusted R Square	0.622194706
Standard Error	0.203025141
Observations	512

ANOVA

	df	SS	MS	F	Significance F
Regression	1	34.7291835	34.7291835	842.5485	4.3314E-110
Residual	510	21.021796	0.041219208		
Total	511	55.7509795			

	Coefficients	Standard Error	t Stat	P-value	Lower 95%	Upper 95%	Lower 95.0%	Upper 95.0%
Intercept	2.511383315	0.01795817	139.846285	0	2.476102221	2.546664409	2.476102221	2.546664409
X Variable 1	-0.001756963	6.05292E-05	-29.02668674	4.3E-110	-0.001875881	-0.001638046	-0.001875881	-0.001638046

SNL_18650_NMC_25C_0-100_0.5-1C_a_cycle

Regression Statistics	
Multiple R	0.451260683
R Square	0.203636204
Adjusted R Square	0.202098822
Standard Error	0.278720061
Observations	520

ANOVA

	df	SS	MS	F	Significance F
Regression	1	10.28986559	10.28986559	132.4565	1.88283E-27
Residual	518	40.24076391	0.077684872		
Total	519	50.53062951			

	Coefficients	Standard Error	t Stat	P-value	Lower 95%	Upper 95%	Lower 95.0%	Upper 95.0%
Intercept	2.781920375	0.024463509	113.7171456	0	2.733860486	2.829980263	2.733860486	2.829980263
X Variable 1	-0.000934415	8.11902E-05	-11.50897436	1.88E-27	-0.001093918	-0.000774913	-0.001093918	-0.000774913

SNL_18650_NMC_35C_0-100_0.5-1C_a_cycle

Regression Statistics	
Multiple R	0.412748197
R Square	0.170361074
Adjusted R Square	0.169301509
Standard Error	0.286600473
Observations	785

ANOVA

	df	SS	MS	F	Significance F
Regression	1	13.20677611	13.20677611	160.7841	1.2069E-33
Residual	783	64.31548775	0.082139831		
Total	784	77.52226386			

	Coefficients	Standard Error	t Stat	P-value	Lower 95%	Upper 95%	Lower 95.0%	Upper 95.0%
Intercept	2.717474075	0.020478405	132.6994976	0	2.677275	2.75767315	2.677275	2.75767315
X Variable 1	-0.000571418	4.50643E-05	-12.68006574	1.21E-33	-0.00065988	-0.000482957	-0.00065988	-0.000482957

SNL_18650_NMC_15C_0-100_0.5-1C_b_cycle

Regression Statistics	
Multiple R	0.794820495
R Square	0.63173962
Adjusted R Square	0.631017541
Standard Error	0.195068034
Observations	512

ANOVA

	df	SS	MS	F	Significance F
Regression	1	33.29089793	33.29089793	874.8897	1.0392E-112
Residual	510	19.40628438	0.038051538		
Total	511	52.6971823			

	Coefficients	Standard Error	t Stat	P-value	Lower 95%	Upper 95%	Lower 95.0%	Upper 95.0%
Intercept	2.494196066	0.01725434	144.5547052	0	2.460297735	2.528094398	2.460297735	2.528094398
X Variable 1	-0.001720197	5.81569E-05	-29.57853412	1E-112	-0.001834454	-0.00160594	-0.001834454	-0.00160594

SNL_18650_NMC_25C_0-100_0.5-1C_b_cycle

Regression Statistics	
Multiple R	0.40920751
R Square	0.167450786
Adjusted R Square	0.166386145
Standard Error	0.283939506
Observations	784

ANOVA

	df	SS	MS	F	Significance F
Regression	1	12.68047943	12.68047943	157.2838	5.25798E-33
Residual	782	63.04612482	0.080621643		
Total	783	75.72660425			

	Coefficients	Standard Error	t Stat	P-value	Lower 95%	Upper 95%	Lower 95.0%	Upper 95.0%
Intercept	2.677018678	0.020301299	131.8644002	0	2.637167183	2.716870174	2.637167183	2.716870174
X Variable 1	-0.000560989	4.47314E-05	-12.54128435	5.26E-33	-0.000648796	-0.000473181	-0.000648796	-0.000473181

SNL_18650_NMC_35C_0-100_0.5-1C_b_cycle

Regression Statistics	
Multiple R	0.39060905
R Square	0.15257543
Adjusted R Square	0.151493151
Standard Error	0.284714616
Observations	785

ANOVA

	df	SS	MS	F	Significance F
Regression	1	11.42785803	11.42785803	140.976	5.14896E-30
Residual	783	63.47186885	0.081062412		
Total	784	74.89972687			

	Coefficients	Standard Error	t Stat	P-value	Lower 95%	Upper 95%	Lower 95.0%	Upper 95.0%
Intercept	2.70168824	0.020343655	132.8024975	0	2.661753679	2.741622802	2.661753679	2.741622802
X Variable 1	-0.000531543	4.47678E-05	-11.87333322	5.15E-30	-0.000619422	-0.000443664	-0.000619422	-0.000443664

CALIBRATION CERTIFICATE			Certificate No. CAL/23-24/CC/429-197	
			ULR No. CC224823000004203F	
Voltmeter			**Date of Issue** 13.09.2023	
Date of Calibration 12.09.2023	**Next Calibration Due Date** 11.09.2024		**Page No.** 1	**No. of Pages** 1

Calibrated For	M/s. Energon Solution PVT. LTD. E-11 Malegaon, M.I.D.C. Sinnar, Nashik			
Date of Receipt	12.09.2023	**Challan No.**	Onsite 12.09.2023 Electrical Testing lab	
Condition of the Instrument	Functional	**Calibrated at**		
SRF No and date	CAL/23-24/CSRF/429	**SRF Date**		
NEC ID No.	CAL/23-24/ID/429-197	**Location**		

Details of Test Instrument

Description	Voltmeter	**Make**	Digatron Ador India.	**Model**	—
Type	—	**ID. No.**	E-027	**Sr No.**	—
Range	0-20V DC	**Least Count**	1V	**Location**	Electrical Test Lab
Machine No. UBT10-020-15ME			**Calibration Procedure No.**	WI/NEC/CAL/ET/01	
Calibration Environments		**Temperature**	25 ± 4°C	**Relative Humidity**	30 to 75% RH

Reference Standard Used For Calibration (Traceable To National / International Standards)

Description	Make/Model	Sr No.	Cal.Cert No	Valid upto	Traceability
6 1/2 Digit Multimeter	Tektronix	1805210	CAL/22-23/CC/162-1	14.03.2024	NEC, Nashik

Calibration Results

Discipline:Electro-Technical

Parameter: DC Voltage @ Charge Mode

Range	Reading On UUC	Reading On Standard*	Deviation	% Deviation	(±) Expanded Uncertainty
V	V	V	V	%	%
20	6	6.0010	-0.0010	-0.017	0.0019
	12	12.0012	-0.0012	-0.010	0.0019
	14	14.0019	-0.0019	-0.014	0.0019
	18	18.0021	-0.0021	-0.012	0.0019

Parameter: DC Voltage @ Discharge Mode

Range	Reading On UUC	Reading On Standard*	Deviation	% Deviation	(±) Expanded Uncertainty
V	V	V	V	%	%
20	6	6.0011	-0.0011	-0.018	0.0019
	12	12.0014	-0.0014	-0.012	0.0019
	14	14.0015	-0.0015	-0.011	0.0019
	18	18.0023	-0.0023	-0.013	0.0019

UUC*:- Unit Under Calibration

Remarks:

1) Due date of calibration (1 Year) is mentioned in the certificate is as per customer request.
2) The calibration certifcate pertains to the above equipment calibration.
3) The calibration certifcate shall not be reproduced except in full,without written approval of the laboratory.
4) Uncertainty has been calculated for a coverage factor k=2 corresponding to approximately 95.45 % Confidence Level.
5) The Standard maintained are traceable to National / International Standard through accredited Laboratories.
6) The observations reported represent values at the time of the measurements, and under the stated conditions. they do not convey any long term stability information.
7) Measured O/P is average of 5 reading.

Prepared By
Sagar Patil
(Calibration Engineer)

Reviewed & Approved By
Rahul Golesar
(Quality Manager)

*** End of Certificate ***

QR/NEC/CC/01

CamScanner

Nashik Engineering Cluster

(Under the aegis of Department of Industrial Policy & Promotion, (DIPP),
Ministry of Commerce & Industry, Govt. of India, New Delhi)

NABL Accredited Testing & Calibration Laboratory as per ISO/IEC:17025:2017,
Test House approval from Directorate General of Aeronautical Quality Assurance
(DGAQA), Ministry of Defence, Govt. of India, New Delhi

ilac-MRA
CC-2248

" Sahastrarashmi", C-10, MIDC, Ambad, Nashik-422 010. Tel.: +91 253 6699231,32,91 TeleFax: + 91 253 6699222
E-mail : calibration@nec.org.in, quality.lab@nec.org.in, testinglab@nec.org.in, info@nec.org.in, website: www.nec.org.in

CALIBRATION CERTIFICATE		Certificate No.
		CAL/23-24/CC/429-157
		ULR No.
Ammeter		**CC224823000004163F**
		Date of Issue
		13.09.2023

Date of Calibration	Next Calibration Due Date	Page No.	No. of Pages
12.09.2023	**11.09.2024**	**1**	**1**

Calibrated For	M/s. Energon Solution PVT. LTD.		
	E-11 Malegaon, M.I.D.C. Sinnar, Nashik		

Date of Receipt	12.09.2023	Challan No.	Onsite
Condition of the Instrument	Functional	Calibrated at	
SRF No and date	CAL/23-24/CSRF/429	SRF Date	12.09.2023
NEC ID No.	CAL/23-24/ID/429-157	Location	----

Details of Test Instrument

Description	Ammeter	Make	Digatron Ador India.	Model	—
Type	—	ID. No.	E-028	Sr No.	—
Range	0-10A DC	Least Count	1A	Location	Electrical Test Lab
Machine No.	UBT10-020-15ME		Calibration Procedure No.	WI/NEC/CAL/ET/02	
Calibration Environments		Temperature	25 ± 4°C	Relative Humidity	30 to 75% RH

Reference Standard Used For Calibration (Traceable To National / International Standards)

Description	Make/Model	Sr No.	Cal.Cert No	Valid upto	Traceability
6 1/2 Digit Multimeter	Tektronix /4050	1805210	CAL/22-23/CC/162-1	14.03.2024	NEC, Nashik

Calibration Results
Discipline:Electro-Technical

Parameter: DC Current @ Charge Mode

Range	Reading On UUC	Reading On Standard*	Deviation	% Deviation	(±) Expanded Uncertainty
A	A	A	A	%	%
	0.1	0.100015	-0.000015	-0.015	0.04
10	1	0.999972	0.000028	0.003	0.04
	5	5.00045	-0.00045	-0.009	0.04
	10	10.00019	-0.00019	-0.002	0.02

Parameter: DC Current @ Discharge Mode

Range	Reading On UUC	Reading On Standard*	Deviation	% Deviation	(±) Expanded Uncertainty
A	A	A	A	%	%
	0.1	0.100011	-0.000011	-0.011	0.04
10	1	0.999959	0.000041	0.004	0.04
	5	5.00032	-0.00032	-0.006	0.04
	10	10.00015	-0.00015	-0.001	0.02

UUC*:- Unit Under Calibration

Remarks:
1) Due date of calibration (1 Year) is mentioned in the certificate is as per customer request.
2) The calibration certifcate pertains to the above equipment calibration.
3) The calibration certifcate shall not be reproduced except in full, without written approval of the laboratory.
4) Uncertainty has been calculated for a coverage factor k=2 corresponding to approximately 95.45 % Confidence Level.
5) The Standard maintained are traceable to National / International Standard through accredited Laboratories.
6) The observations reported represent values at the time of the measurements, and under the stated conditions. they do not convey any long term stability information.
7) Measured O/P is average of 5 reading.

Prepared By
Aditya Ahire
(Calibration Engineer)

Reviewed & Approved By
Rahul Golesar
(Quality Manager)

*** End of Certificate ***

QR/NEC/CC/01

Services Offered: Testing/ Calibration, CNC Machining Center, RPT, CMM, Metallurgical Lab, Electrical Testing,

175

CamScanner

Nashik Engineering Cluster

(Under the aegis of Department of Industrial Policy & Promotion, (DIPP),
Ministry of Commerce & Industry, Govt. of India, New Delhi)

NABL Accredited Testing & Calibration Laboratory as per ISO/IEC:17025:2017,
Test House approval from Directorate General of Aeronautical Quality Assurance
(DGAQA), Ministry of Defence, Govt. of India, New Delhi

ilac-MRA   CC-2248

" Sahastrarashmi", C-10, MIDC, Ambad, Nashik-422 010. Tel.: +91 253 6699231,32,91 TeleFax: + 91 253 6699222
E-mail : calibration@nec.org.in, quality.lab@nec.org.in, testinglab@nec.org.in, info@nec.org.in, website: www.nec.org.in

CALIBRATION CERTIFICATE		Certificate No.
		CAL/23-24/CC/429-199
		ULR No.
Voltmeter		**CC224823000004205F**
		Date of Issue
		13.09.2023

Date of Calibration	Next Calibration Due Date	Page No.	No. of Pages
12.09.2023	**11.09.2024**	**1**	**1**

Calibrated For	M/s. Energon Solution PVT. LTD.		
	E-11 Malegaon, M.I.D.C. Sinnar, Nashik		
Date of Receipt	12.09.2023	Challan No.	
Condition of the Instrument	Functional	Calibrated at	Onsite
SRF No and date	CAL/23-24/CSRF/429	SRF Date	12.09.2023
NEC ID No.	CAL/23-24/ID/429-199	Location	Electrical Testing lab

Details of Test Instrument

Description	Voltmeter	Make	Digatron Ador India.	Model	---
Type	—	ID. No.	E-031	Sr No.	—
Range	0-20V DC	Least Count	1V	Location	Electrical Test Lab
Machine No.	UBT10-020-15ME		Calibration Procedure No.	WI/NEC/CAL/ET/01	
Calibration Environments		Temperature	25 ± 4°C	Relative Humidity	30 to 75% RH

Reference Standard Used For Calibration (Traceable To National / International Standards)

Description	Make/Model	Sr No.	Cal.Cert No	Valid upto	Traceability
6 1/2 Digit Multimeter	Tektronix	1805210	CAL/22-23/CC/162-1	14.03.2024	NEC, Nashik

Calibration Results
Discipline:Electro-Technical

Parameter: DC Voltage @ Charge Mode

Range	Reading On UUC	Reading On Standard*	Deviation	% Deviation	(±) Expanded Uncertainty
V	V	V	V	%	%
20	6	6.0013	-0.0013	-0.022	0.0019
	12	12.0021	-0.0021	-0.018	0.0019
	14	14.0028	-0.0028	-0.020	0.0019
	18	18.0032	-0.0032	-0.018	0.0019

Parameter: DC Voltage @ Discharge Mode

Range	Reading On UUC	Reading On Standard*	Deviation	% Deviation	(±) Expanded Uncertainty
V	V	V	V	%	%
20	6	6.0011	-0.0011	-0.018	0.0019
	12	12.0022	-0.0022	-0.018	0.0019
	14	14.0027	-0.0027	-0.019	0.0019
	18	18.0031	-0.0031	-0.017	0.0019

UUC*:- Unit Under Calibration

Remarks:
1) Due date of calibration (1 Year) is mentioned in the certificate is as per customer request.
2) The calibration certifcate pertains to the above equipment calibration.
3) The calibration certifcate shall not be reproduced except in full,without written approval of the laboratory.
4) Uncertainty has been calculated for a coverage factor k=2 corresponding to approximately 95.45 % Confidence Level.
5) The Standard maintained are traceable to National / International Standard through accredited Laboratories.
6) The observations reported represent values at the time of the measurements, and under the stated conditions. they do not convey any long term stability information.
7) Measured O/P is average of 5 reading.

Prepared By
Sagar Patil
(Calibration Engineer)

*** End of Certificate ***

Reviewed & Approved By
Rahul Golesar
(Quality Manager)

QR/NEC/CC/01

Services Offered: Testing/ Calibration, CNC Machining Center, RPT, CMM, Metallurgical Lab, Electrical Testing, Environmental Testing, Heat Treatment, Seminar halls & Auditorium Etc.

Nashik Engineering Cluster

(Under the aegis of Department of Industrial Policy & Promotion, (DIPP),
Ministry of Commerce & Industry, Govt. of India, New Delhi)

NABL Accredited Testing & Calibration Laboratory as per ISO/IEC:17025:2017,
Test House approval from Directorate General of Aeronautical Quality Assurance
(DGAQA), Ministry of Defence, Govt. of India, New Delhi

ilac-MRA

CC-2248

" Sahastrarashmi", C-10, MIDC, Ambad, Nashik-422 010. Tel.: +91 253 6699231,32,91 TeleFax: + 91 253 6699222
E-mail : calibration@nec.org.in, quality.lab@nec.org.in, testinglab@nec.org.in, info@nec.org.in, website: www.nec.org.in
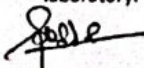
CALIBRATION CERTIFICATE		Certificate No. CAL/23-24/CC/429-159	
		ULR No. CC224823000004165F	
Ammeter		Date of Issue 13.09.2023	

Date of Calibration 12.09.2023		Next Calibration Due Date 11.09.2024		Page No. 1	No. of Pages 1

Calibrated For	M/s. Energon Solution PVT. LTD. E-11 Malegaon, M.I.D.C. Sinnar, Nashik				
Date of Receipt	12.09.2023		Challan No.		
Condition of the Instrument	Functional		Calibrated at	Onsite	
SRF No and date	CAL/23-24/CSRF/429		SRF Date	12.09.2023	
NEC ID No.	CAL/23-24/ID/429-159		Location	----	

Details of Test Instrument

Description	Ammeter		Make	Digatron Ador India.	Model	---
Type	---		ID. No.	E-032	Sr No.	---
Range	0-10A DC		Least Count	1A	Location	Electrical Test Lab
Machine No.	UBT10-020-15ME			Calibration Procedure No.	WI/NEC/CAL/ET/02	
Calibration Environments			Temperature	25 ± 4°C	Relative Humidity	30 to 75% RH

Reference Standard Used For Calibration (Traceable To National / International Standards)

Description	Make/Model	Sr No.	Cal.Cert No	Valid upto	Traceability
6 1/2 Digit Multimeter	Tektronix /4050	1805210	CAL/22-23/CC/162-1	14.03.2024	NEC, Nashik

Calibration Results
Discipline:Electro-Technical

Parameter: DC Current @ Charge Mode

Range	Reading On UUC	Reading On Standard*	Deviation	% Deviation	(±) Expanded Uncertainty
A	A	A	A	%	%
10	0.1	0.100022	-0.000022	-0.022	0.04
	1	0.999974	0.000026	0.003	0.04
	5	5.00025	-0.00025	-0.005	0.04
	10	10.00023	-0.00023	-0.002	0.02

Parameter: DC Current @ Discharge Mode

Range	Reading On UUC	Reading On Standard*	Deviation	% Deviation	(±) Expanded Uncertainty
A	A	A	A	%	%
10	0.1	0.100021	-0.000021	-0.021	0.04
	1	0.999955	0.000045	0.004	0.04
	5	5.00019	-0.00019	-0.004	0.04
	10	10.00045	-0.00045	-0.005	0.02

UUC*:- Unit Under Calibration

Remarks:
1) Due date of calibration (1 Year) is mentioned in the certificate is as per customer request.
2) The calibration certifcate pertains to the above equipment calibration.
3) The calibration certifcate shall not be reproduced except in full,without written approval of the laboratory.
4) Uncertainty has been calculated for a coverage factor k=2 corresponding to approximately 95.45 % Confidence Level.
5) The Standard maintained are traceable to National / International Standard through accredited Laboratories.
6) The observations reported represent values at the time of the measurements, and under the stated conditions. they do not convey any long term stability information.
7) Measured O/P is average of 5 reading.

Prepared By
Aditya Ahire
(Calibration Engineer)

*** End of Certificate ***

Reviewed & Approved By
Rahul Golesar
(Quality Manager)

QR/NEC/CC/01

Services Offered: Testing/ Calibration, CNC Machining Center, RPT, CMM, Metallurgical Lab, Electrical Testing, Environmental Testing, Heat Treatment, Seminar halls & Auditorium Etc.

Nashik Engineering Cluster

(Under the aegis of Department of Industrial Policy & Promotion, (DIPP),
Ministry of Commerce & Industry, Govt. of India, New Delhi)

NABL Accredited Testing & Calibration Laboratory as per ISO/IEC:17025:2017,
Test House approval from Directorate General of Aeronautical Quality Assurance
(DGAQA), Ministry of Defence, Govt. of India, New Delhi

ilac-MRA   CC-2248

" Sahastrarashmi", C-10, MIDC, Ambad, Nashik-422 010. Tel.: +91 253 6699231,32,91 TeleFax: + 91 253 6699222
E-mail : calibration@nec.org.in, quality.lab@nec.org.in, testinglab@nec.org.in, info@nec.org.in, website: www.nec.org.in

CALIBRATION CERTIFICATE		Certificate No. CAL/23-24/CC/429-200	
		ULR No. CC224823000004205F	
Voltmeter		Date of Issue 13.09.2023	
Date of Calibration 12.09.2023	Next Calibration Due Date 11.09.2024	Page No. 1	No. of Pages 1

Calibrated For	M/s. Energon Solution PVT. LTD. E-11 Malegaon, M.I.D.C. Sinnar, Nashik		
Date of Receipt	12.09.2023	Challan No.	Onsite
Condition of the Instrument	Functional	Calibrated at	12.09.2023
SRF No and date	CAL/23-24/CSRF/429	SRF Date	Electrical Testing lab
NEC ID No.	CAL/23-24/ID/429-200	Location	

Details of Test Instrument

Description	Voltmeter	Make	Digatron Ador India.	Model	---
Type	—	ID. No.	E-033	Sr No.	—
Range	0-20V DC	Least Count	1V	Location	Electrical Test Lab
Machine No.	UBT10-020-15ME		Calibration Procedure No.	WI/NEC/CAL/ET/01	
Calibration Environments		Temperature	25 ± 4°C	Relative Humidity	30 to 75% RH

Reference Standard Used For Calibration (Traceable To National / International Standards)

Description	Make/Model	Sr No.	Cal.Cert No	Valid upto	Traceability
6 1/2 Digit Multimeter	Tektronix	1805210	CAL/22-23/CC/162-1	14.03.2024	NEC, Nashik

Calibration Results

Discipline:Electro-Technical

Parameter: DC Voltage @ Charge Mode

Range	Reading On UUC	Reading On Standard*	Deviation	% Deviation	(±) Expanded Uncertainty
V	V	V	V	%	%
20	6	6.0012	-0.0012	-0.020	0.0019
	12	12.0015	-0.0015	-0.013	0.0019
	14	14.0021	-0.0021	-0.015	0.0019
	18	18.0029	-0.0029	-0.016	0.0019

Parameter: DC Voltage @ Discharge Mode

Range	Reading On UUC	Reading On Standard*	Deviation	% Deviation	(±) Expanded Uncertainty
V	V	V	V	%	%
20	6	6.0012	-0.0012	-0.020	0.0019
	12	12.0016	-0.0016	-0.013	0.0019
	14	14.0024	-0.0024	-0.017	0.0019
	18	18.0029	-0.0029	-0.016	0.0019

UUC*:- Unit Under Calibration

Remarks:
1) Due date of calibration (1 Year) is mentioned in the certificate is as per customer request.
2) The calibration certifcate pertains to the above equipment calibration.
3) The calibration certifcate shall not be reproduced except in full,without written approval of the laboratory.
4) Uncertainty has been calculated for a coverage factor k=2 corresponding to approximately 95.45 % Confidence Level.
5) The Standard maintained are traceable to National / International Standard through accredited Laboratories.
6) The observations reported represent values at the time of the measurements, and under the stated conditions. they do not convey any long term stability information.
7) Measured O/P is average of 5 reading.

Prepared By
Sagar Patil
(Calibration Engineer)

*** End of Certificate ***

Reviewed & Approved By
Rahul Golesar
(Quality Manager)

QR/NEC/CC/01

Services Offered: Testing/ Calibration, CNC Machining Center, RPT, CMM, Metallurgical Lab, Electrical Testing,
Environmental Testing, Heat Treatment, Seminar halls & Auditorium Etc.

178

NASHIK ENGINEERING CLUSTER

(Under the aegis of Department of Industrial Policy & Promotion, (DIPP),
Ministry of Commerce & Industry, Govt. of India, New Delhi)
NABL Accredited Testing & Calibration Laboratory as per ISO/IEC: 17025:2017,
Certificate No.: TC-5448 & CC-2248

CC-2248

" Sahastrarashmi", C-10, MIDC, Ambad, Nashik-422 010. Tel.: +91 253 6699231,32,91 TeleFax: + 91 253 6699222
E-mail : calibration@nec.org.in, quality.lab@nec.org.in, testinglab@nec.org.in, info@nec.org.in, website: www.nec.org.in

CALIBRATION CERTIFICATE		Certificate No. CAL/23-24/CC/038-1			
		ULR No. CC224823000001518F			
Multi-Product Calibrator		Date of Issue 19.04.2023			
Date of Calibration 16.04.2023 To 19.04.2023		Next Calibration Due Date 18.04.2024		Page No. 1	No. of Pages 29

Calibrated For	M/s. NASHIK ENGINEERING CLUSTER C-10, MIDC, AMBAD, NASHIK- 422010
Date of Receipt of Instrument	16.04.2023
Condition of the Instrument on Receipt	Functional
SRF No & Date	CAL/23-24/CSRF/038 Dated. 16.04.2023
NEC ID No.	CAL/23-24/ID/038-1
Calibrated at	In Lab
Details of Test Instrument	
Description	Multi-Product Calibrator
Make/Model	Fluke/5522A
Sr No.	5768904
ID No.	NEC/CAL/ET/03
Range	As per manual
Resolution	As per manual
Accuracy	As per manual
Calibration Procedure No.	WI/NEC/CAL/ET/01,02,03,05,06,07,08,14,15
Calibration Environments	
Temperature	25 ± 4°C
Relative Humidity	30 to 75% RH

Reference Standard Used For Calibration (Traceable To National / International Standards)

Description	Make/Model	Sr/No.	Cal. Cert No.	valid upto	Traceability
8½ digit Reference Multimeter	Fluke / 8508A	995658797	CC/ECL/1499/22-23	09.01.2024	IDEMI, Mumbai
Frequency Counter /Timer Analyser	Fluke/PM6690	996956	TSC/22-23/7959-1	19.08.2023	Transcal, Banglore
AC Measurement Standard	Fluke/5790A	9935033	NEC/22-23/AA/185-1	17.08.2023	NEC, Nashik
Programmable Auto. RCL Meter	Fluke/PM6304	995002	CC/ECL/1872/22-23	19.03.2024	IDEMI, Mumbai
6 1/2 Digit Multimeter	Tektronix	1805210	CAL/22-23/CC/162-1	14.03.2024	NEC,Nash k
Three Phase Comparator	Zera/COM 3003	050008653	CC/ECL/1075A/22-23	09.11.2023	IDEMI, Mumbai
POWER ANALYSER	HIOKI/3390	110930682	NEC/22-23/SP/027-1	31.07.2023	NEC , Nashik

Note: 1) Calibration results are enclosed on page no. 2 onwards.
2) Next calibration date (1 year) mentioned in the certificate is given as per customer request.
3) The calibration certificate pertains to the above equipment calibration.
4) The calibration certificate shall not be reproduced except in full,without written approval of the laboratory.

Calibrated By
Suvarna Patil
(Calibration Engineer)

CALIBRATION LAB

Reviewed & Approved By
Rahul Golesar
(Quality Manager)
QR/NEC/CC/01

Services Offered: Testing/ Calibration, CNC Machining Center, RPT, CMM, Metallurgical Lab, Electrical Testing, Environmental Testing, Heat Treatment, Seminar halls & Auditorium Etc.

Nashik Engineering Cluster

(Under the aegis of Department of Industrial Policy & Promotion, (DIPP), Ministry of Commerce & Industry, Govt. of India, New Delhi)

NABL Accredited Testing & Calibration Laboratory as per ISO/IEC:17025:2017,
Test House approval from Directorate General of Aeronautical Quality Assurance
(DGAQA), Ministry of Defence, Govt. of India, New Delhi

ilac-MRA   CC-2248

NASHIK ENGINEERING CLUSTER

" Sahastrarashmi", C-10, MIDC, Ambad, Nashik-422 010. Tel.: +91 253 6699231,32,91 TeleFax: + 91 253 6699222
E-mail : calibration@nec.org.in, quality.lab@nec.org.in, testinglab@nec.org.in, info@nec.org.in, website: www.nec.org.in

CALIBRATION CERTIFICATE		Certificate No. CAL/23-24/CC/999-1	
		ULR No. CC224824000001172F	
6½ Digit Precision Multimeter		Date of Issue 15.03.2024	
Date of Calibration 14.03.2024	Next Calibration Due Date 13.03.2025	Page No. 1	No. of Pages 10

Calibrated For	M/s. NASHIK ENGINEERING CLUSTER C-10, MIDC, AMBAD, NASHIK- 422010
Date of Receipt of Instrument	14.03.2024
Condition of the Instrument on Receipt	Functional
SRF No & Date	CAL/23-24/CSRF/999 Dated 14.03.2024
NEC ID No.	CAL/23-24/ID/999-1
Calibrated at	In Lab

Details of Test Instrument

Description Make/Model Serial No. ID No. Range & Accuracy Calibration Procedure No.	6½ Digit Precision Multimeter Tektronix/4050 1805210 NEC/CAL/ET/18 As per Manual WI/NEC/CAL/ET/01,02,03,04,06,08

Calibration Environments

Temperature Relative Humidity	25 ± 4°C 30 to 75% RH

Reference Standard Used For Calibration (Traceable To National / International Standards)

Description	Make/Model	Sr/No.	Cal. Cert No.	valid upto	Traceability
Multiproduct Calibrator	Fluke/5522A	5768904	CAL/23-24/CC/038-1	18.04.2024	NEC, Nashik
Multifunction Calibrator	Fluke / 5720A	9928201	CR/PCAL/52664/01	31.01.2025	ETDC , Banglore
Decade Resistance Box	Vaiseshika	6709	CC/ECL/0800/23-24	16.10.2024	IDEMI, Mumbai

Note:
1) Calibration results are enclosed on page no. 2 to 10.
2) Next calibration date (1 year) mentioned in the certificate is given as per customer request.
3) The calibration certificate pertains to the above equipment calibration.
4) The calibration certificate shall not be reproduced except in full,without written approval of the laboratory.

Calibrated By
Kanchan Phadol
(Calibration Engineer)

Reviewed & Approved By
Rahul Golesar
(Quality Manager)

QR/NEC/CC/01

Services Offered: Testing/ Calibration, CNC Machining Center, RPT, CMM, Metallurgical Lab, Electrical Testing, Environmental Testing, Heat Treatment, Seminar Halls & Auditorium Etc.

180

CALIBRATION CERTIFICATE

Work Order No.	: WO/ECL/370/23-24	Certificate No.	: CC/ECL/0800/23-24 CC-2287
Work Order Date	: 15/09/2023	Date of Calibration	: 27/09 to 17/10/2023
Date of	: 15/09/2023	Page No.	: 1 of 5
ULR No.	: CC228723100001482F	Date of Issue:	: 17/11/2023
Discipline	: Electro-Technical Calibration (Group : Direct Current)		

Calibrated for : M/s. Nashik Engineering Cluster, Sahastrarashmi, C-10, MIDC, Ambad, Nashik - 422 010.

Calibrated at : IDEMI, Mumbai.

Description and Identification of Device Under Calibration	Standards Used for Calibration
Name : Decade Resistance Box Manufacturer : M/s. Vaiseshika Condition on receipt : No visible damage Calibrated Decades : 1 MΩ (X 100 kΩ / Step), 10 MΩ (X 1 MΩ / Step), 100 MΩ (X 10 MΩ / Step), 1 GΩ (X 100 MΩ / Step), 10 GΩ (X 1 GΩ / Step), 100 GΩ (X 10 GΩ / Step), 1 TΩ (X 100 GΩ / Step) & 10 TΩ (X 1 TΩ / Step). Sr. No. : 6709 Model : 8400HV ID No. : NEC/CAL/ET-17 Accuracy : As per manual	1) Electrometer / High Resistance Meter ID No. : IDEMI/ECL/ELECT/01 Calibration Valid up to 04/11/2024 All measurement results are traceable to the International system of units (SI), ensured by comparison, directly or indirectly with National or International standards through unbroken chain of calibration

Ambient Conditions :

Temperature : 23.8 °C to 24.8 °C   Relative Humidity : 54 % to 58 %

Remarks : Please refer page 2 to 5 for Calibration Results.

1) Procedure of Calibration : Above mentioned item is calibrated as per operating procedure : OP-ECL-21.

2) The reported expanded uncertainty in measurement is stated as the combined standard uncertainty in measurement multiplied by the coverage factor $k = 2$, which for a normal distribution corresponds to a coverage probability of approximately 95 %.

3) Calibration Status : Sticker No. 800 indicating 'CAL STATUS' is affixed on instrument.

4) Our NABL Accreditation Certificate No. is CC - 2287, Valid up to 30/08/2025.

NISHANT NARESH PAWASKAR
Digitally signed by NISHANT NARESH PAWASKAR
Date: 2023.11.17 12:33:23 +05'30'

AUTHORISED SIGNATORY

Note:
1. This certificate refers only to the particular item(s), submitted for calibration. The certificate should not be reproduced expect in full without the prior permission from the Principal Director, IDEMI, Mumbai - 400 022.
2. This is computer generated certificate and may not contain signature. Where send by email, this is signed with digital signature of authorized signatory, approved by NABL. For any queries, please quote work order number mentioned in this certificate

वैद्युतिक मापन उपयंत्र अभिकल्प संस्थान, मुंबई
INSTITUTE FOR DESIGN OF ELECTRICAL MEASURING INSTRUMENTS, MUMBAI
भारत सरकार की सोसायटी
सूक्ष्म लघु एवं मध्यम उद्यम मंत्रालय
Government of India Society
Ministry of Micro Small & medium Enterprises
स्वातंत्र्यवीर सात्या टोपे मार्ग चुनाभट्टी सायन साकपर मुंबई
Swatantryaveer Tatya Tope Marg, Chunabhatti, Sion, P.O. Mumbai - 400 022

FF-LAB-003 Rev. 01

DecisionTreeRegressor

Decision Trees work by recursively splitting the dataset into subsets based on the most significant features that reduce a specific loss function (such as Mean Squared Error for regression or Gini Impurity for classification). At each node, the tree chooses a feature and a threshold to split the data in a way that results in the most homogeneous subgroups. This process continues until the tree reaches a maximum depth or no further meaningful splits can be made, leading to predictions based on the average value of the outcomes in the final leaf nodes.

The Decision Tree Regressor is best applied in situations where the data has non-linear relationships and complex interactions between features, yet interpretability is important.

Syntax:

class **sklearn.tree.DecisionTreeRegressor(***, *criterion*='squared_error'**,** *splitter*='best'**,** *max_depth*=None**,** *min_samples_split*=2**,** *min_samples_leaf*=1**,** *min_weight_fraction_leaf*=0.0**,** *max_features*=None**,** *random_state*=None**,** *max_leaf_nodes*=None**,** *min_impurity_decrease*=0.0**,** *ccp_alpha*=0.0**,** *monotonic_cst*=None**)**

Hyperparameters used or tested

Criterion: {"squared_error"}

Specifies the function to measure the quality of a split. Mean squared error is typically used in regression.

Splitter: {"best"}

The strategy used to choose the split at each node. Supported strategies are "best" to choose the best split and "random" to choose the best random split.

max_depthint, default=None

Limits the maximum depth of the tree. Prevents overfitting by restricting the number of splits, ensuring that the model doesn't become overly complex.

Min_samples_split, default=2

Specifies the minimum number of samples required to split a node. Higher values prevent splitting small nodes and can reduce overfitting.

min_samples_leaf, default=1

The minimum number of samples required to be at a leaf node. A split point at any depth will only be considered if it leaves at least min_samples_leaf training samples in each of the left and right branches. This may have the effect of smoothing the model, especially in regression**.**

RandomForestRegressor

The Random Forest Regressor works by constructing multiple decision trees on different subsets of the dataset and averaging their predictions to improve accuracy and reduce overfitting. Each tree is trained on a random sample of the data with random subsets of features, which helps in capturing complex patterns while being robust against noise. This ensemble method leverages the diversity of individual trees to enhance overall performance.

The best use cases for Random Forest Regressor include predicting complex, non-linear relationships, where high accuracy and robustness are essential.

Syntax

class **sklearn.ensemble.RandomForestRegressor(***n_estimators=100*, **,*
criterion='squared_error', *max_depth=None*, *min_samples_split=2*,
min_samples_leaf=1, *min_weight_fraction_leaf=0.0*, *max_features=1.0*,
max_leaf_nodes=None, *min_impurity_decrease=0.0*, *bootstrap=True*,
oob_score=False, *n_jobs=None*, *random_state=None*, *verbose=0*,
warm_start=False, *ccp_alpha=0.0*, *max_samples=None*, *monotonic_cst=None*)

n_estimators, default=100

The number of trees in the forest. A higher number of trees generally improves performance but increases computational cost.

Criterion, {"squared_error"}

The function to measure the quality of a split.

max_depth, default=None

The maximum depth of the tree. Controls overfitting by preventing trees from growing too complex.

min_samples_split, default=2

The minimum number of samples required to split an internal node: Larger values reduce overfitting by preventing the model from creating small splits.

min_samples_leaf, default=1

The minimum number of samples required to be at a leaf node. Higher values help create more generalized trees, reducing the chance of overfitting.

Bootstrap bool, default=True

Whether bootstrap samples are used when building trees. If False, the whole dataset is used to build each tree.

KNeighborsClassifier

The **KNeighbors Regressor** works by predicting the value of a data point based on the average (or weighted average) of its nearest neighbors in the feature space. It uses a distance metric (like Euclidean distance) to identify the k closest data points and then combines their values to make a prediction. This method is non-parametric and can capture local patterns in the data, making it flexible but sensitive to the choice of k and the distance metric.

The best use cases for KNeighbors Regressor include scenarios with small to medium-sized datasets where the relationship between variables is complex but the data is relatively smooth.

Syntax

class **sklearn.neighbors.KNeighborsRegressor(***n_neighbors*=5, *, *weights*='uniform', *algorithm*='auto', *leaf_size*=30, *p*=2, *metric*='minkowski', *metric_params*=None, *n_jobs*=None**)**

Parameters:

n_neighborsint, default=5

Number of neighbors to use by default for **kneighbors** queries.

weights{'uniform', 'distance'}, callable or None, default='uniform'

Weight function used in prediction. Possible values:

- 'uniform' : uniform weights. All points in each neighborhood are weighted equally.

- 'distance' : weight points by the inverse of their distance. in this case, closer neighbors of a query point will have a greater influence than neighbors which are further away.

LinearRegression

class **sklearn.linear_model.LinearRegression(***, *fit_intercept=True*, *copy_X=True*, *n_jobs=None*, *positive=False***)**

Linear Regression works by modeling the relationship between a dependent variable and one or more independent variables using a linear equation. It aims to find the best-fitting line or hyperplane that minimizes the difference between predicted and actual values, typically using methods like Ordinary Least Squares (OLS). This straightforward approach makes it easy to interpret and understand the relationship between variables.

Best use cases for linear regression include scenarios where the relationship between variables is expected to be linear. It's ideal for problems with a clear, linear relationship and when interpretability is important.

Attributes:

coef_array of shape (n_features,) or (n_targets, n_features)

Estimated coefficients for the linear regression problem. If multiple targets are passed during the fit (y 2D), this is a 2D array of shape (n_targets, n_features), while if only one target is passed, this is a 1D array of length n_features.

rank_int

Rank of matrix X. Only available when X is dense.

singular_array of shape (min(X, y),)

Singular values of X. Only available when X is dense.

intercept_float or array of shape (n_targets,)

Independent term in the linear model. Set to 0.0 if fit_intercept = False.

n_features_in_int

Number of features seen during fit.

GRID SEARCH CV

GridSearchCV is the process of performing hyperparameter tuning in order to determine the optimal values for a given model. Doing this manually could take a considerable amount of time and resources and thus we use GridSearchCV to automate the tuning of hyperparameters.

Parameters

1.**estimator**: Pass the model instance for which you want to check the hyperparameters.

2.**params_grid**: the dictionary object that holds the hyperparameters you want to try

3.**scoring**: evaluation metric that you want to use, you can simply pass a valid string/ object of evaluation metric

4.**cv**: number of cross-validation you have to try for each selected set of hyperparameters

5.**verbose**: you can set it to 1 to get the detailed print out while you fit the data to GridSearchCV

Working

1. Grid Definition: You define a grid of possible hyperparameter values for the model.
2. 2. Exhaustive Search: `GridSearchCV` tries every possible combination of these hyperparameters and evaluates the model using cross-validation on the training data.

3. Performance Evaluation: For each combination, the model is evaluated using the specified scoring metric (e.g., accuracy, mean squared error). The cross-validation ensures that the model is assessed on different subsets of data, reducing the risk of overfitting to a particular train-test split.

4. Best Model Selection: After completing the search, `GridSearchCV` returns the best combination of hyperparameters based on the scoring metric.

5. Refitting: The model can be refit on the entire training set using the best hyperparameters, providing a final model ready for deployment.

Example code snippet for Decision Tree Regressor

```python
from sklearn.tree import DecisionTreeRegressor

from sklearn.model_selection import GridSearchCV

from sklearn.datasets import load_boston

from sklearn.model_selection import train_test_split


# Load the dataset (use your own dataset here)

data = load_boston()

X, y = data.data, data.target


# Split the data into training and testing sets

X_train, X_test, y_train, y_test = train_test_split(X, y, test_size=0.2, random_state=42)


# Define the model

dt = DecisionTreeRegressor()


# Define the parameter grid

param_grid = {

    'max_depth': [None, 10, 20, 30],

    'min_samples_split': [2, 5, 10],

    'min_samples_leaf': [1, 2, 4],

    'max_features': [None, 'sqrt', 'log2']

}


# Initialize GridSearchCV

grid_search = GridSearchCV(estimator=dt, param_grid=param_grid, cv=5,
scoring='neg_mean_squared_error', n_jobs=-1)
```

```python
# Fit the model
grid_search.fit(X_train, y_train)


# Get the best parameters
print("Best hyperparameters:", grid_search.best_params_)


# Evaluate the best model on the test set
best_model = grid_search.best_estimator_
test_score = best_model.score(X_test, y_test)
print("Test set score:", test_score)
```

PUBLICATION

During the course of this scientific work, the following research papers have been published:

SCIENTIFIC JOURNALS

[1]. Das, Kaushik, Roushan Kumar, and Anurup Krishna. **"Analyzing electric vehicle battery health performance using supervised machine learning."** Renewable and Sustainable Energy Reviews 189 (2024): 113967. Publisher: Elsevier, Online ISSN: 1879-0690 Print ISSN: 1364-0321. http://dx.doi.org/10.1016/j.rser.2023.113967 indexed in SCI (IF: 15.9).

[2]. Kumar, Roushan, Kaushik Das, and Anurup Krishna. **"Comparative analysis of data-driven electric vehicle battery health models across different operating conditions."** *Energy* 309 (2024): 133155. https://doi.org/10.1016/j.energy.2024.133155. indexed in SCI (IF: 9.0).

[3]. Kumar, Roushan, and Kaushik Das. **"Lithium battery prognostics and health management for electric vehicle application–A perspective review."** Sustainable Energy Technologies and Assessments 65 (2024): 103766. Publisher: Elsevier Online ISSN: 2213-1396 Linking ISSN: 2213-1388. https://doi.org/10.1016/j.seta.2024.103766 indexed in SCI (IF: 8.0).

[4]. Das, Kaushik, and Roushan Kumar. **"Electric vehicle battery capacity degradation and health estimation using machine-learning techniques: a review."** Clean Energy 7.6 (2023): 1268-1281. Publisher: Oxford University Press, Online ISSN 2515-396X Print ISSN 2515-4230. https://doi.org/10.1093/ce/zkad054 indexed in SCI (IF: 2.3).

[5]. Das, Kaushik, and Roushan Kumar. **"Assessment of electric two-wheeler ecosystem using novel pareto optimality and TOPSIS methods for an ideal design solution."** World Electric Vehicle Journal 14.8 (2023): 215. Publisher: MDPI, Online ISSN: 2032-6653. https://doi.org/10.3390/wevj14080215 indexed in SCI (IF: 2.3).

[6]. Das, Kaushik, and Roushan Kumar. **"A Comprehensive Review of Categorization and Perspectives on State-of-Charge Estimation Using Deep Learning Methods for Electric Transportation."** Wireless Personal Communications (2024): 1-20. Publisher:

Springer Science+ Business Media ISSN: 0929-6212 (print); 1572-834X (web). https://doi.org/10.1007/s11277-023-10830-5 indexed in SCI (IF: 2.22).

[7]. Das, Kaushik, Roushan Kumar, and Anurup Krishna. **"Supervised learning and data intensive methods for the prediction of capacity fade of lithium-ion batteries under diverse operating and environmental conditions."** Water and Energy International 66.1 (2023): 53-59. Publisher: Central Board of Irrigation and Power, Print ISSN: 0974-4207 Online ISSN: 0974-4711. Indexed in SCOPUS. (IF: 2.63).

CONFERENCE PAPER

[1]. **"Co-Estimation of State of Charge, State of Health, and Remaining Useful Life Prediction for Lithium Ion Battery in Electrified Vehicle using Machine Learning Methods: A Comprehensive Review"** 5th International Conference on Intelligent Communication, Control and Devices Dehradun, India. Publisher: River Publishers Series in Proceedings. e-ISBN: 9788770228299.

[2]. **"Lithium Ion Based E-Mobility Battery's State Co-Estimation Methods and Its Significance in Monitoring, Diagnostics and Prognostics"** ICMME-2023 jointly organized by Department of Mechanical Engineering, GLA University, Mathura (India) and UFRGS, Porto Alegre (Brazil) held on 13th – 14th October 2023.

REVISION SUBMITTED

1. **"Lithium-ion Battery Progress in Surface Transportation: Status, Challenges, and Future Directions"**, submitted in Multimedia Tools and Applications (IF 3.6).

Kaushik Das

✉: kaydas@gmail.com
☎: +91 9999005237

An accomplished business leader, researcher and technologist specializing in various types of battery technologies. Proven expertise in hybrid methodologies, e-mobility, battery assessment, and renewable energy innovations, quest to leverage technical and academic skills for cutting-edge advancements in battery health optimization and energy systems.

1. Personal Competencies

- Critical thinking & problem solving.
- Capable of working on own initiative.
- Excellent decision -making, leadership & conflict resolution capabilities.
- Good negotiation skills.
- Adaptability to stressful situations & ability to tolerate stress.
- Good communication skills, self-motivated and comfortable working with teams and independently as well as with strong personalities.
- Comfortable translating technical information into Business Speak.
- Good organizational skills.
- Demonstrated learning agility in ambiguous and unfamiliar situations.
- Good knowledge of various engineering standards (International/ Indian) & its implementation in product development.
- Data analytics and reporting.

2. Engineering, Management & General Software Competencies

- *Battery related*: JIS C 8702, IEC 60896-21 & 22, IRS S 93/96A, IS 15549, IS 1651 etc.
- *Engineering:* Proficient in various engineering & general software like SAP/ CRM, AutoCAD, MS Office etc.
- *Project*: Proficient in various planning & monitoring software like PERT, GANTT Chart, MS Project, Freedcamp.

3. Job Profile

A. As Head- Stationary Battery for Energon Solutions Pvt Ltd from 2024 to till date.
- Part of Gulf Oil Lubricants joined this startup and developed all techno- commercial credentials, like ISO 9001:2015, ISO 14001:2015, ISO/ IEC 17025:2017 certifications, battery testing standards, product quality standards, developed OEM and Govt business from scratch.
- Complete P&L responsibility with developing team and business domain to newer territory.

B. As Head- Lithium & VRLA for Ned Energy Ltd from June 2021 to till 2023.
- Segment head for VRLA (12V & 2V) & T Gel batteries (2V & 1V) for all Govt. business through GeM, IREPS, E Procurement & other state Govt.
- Certifications for VRLA (JIS C 8702, IEC 60896-21 & 22, IS 15549, CE) & Lithium-ion battery.

- Development of battery for new applications like solar, communication & special applications.
- Instrumented in transforming channel & OEM dependent business model.

C. As **Head- Operations** for JLNPhenix Energy Pvt Ltd (Lithium Ion Battery Assembly plant) from Dec 2019 till June 2021.

- *As part of initial startup team*, formulated customer specific product planning & implementation strategies.
- Selection of proper man- Machine- Material for effective execution of prototype, sample & final product.
- Development of various product line- 2W & 3W battery packs, ESS, Solar Batteries, Drone batteries etc. withright selection of cell, BMS & BOS for its life, reliability along with optimum performance.
- Active in product development into 2W & 3W(e-mobility), Mechanical design.
- Capturing the Voice of Customer and translating it into product requirement document.
- Part of design & development team of 38.4 KWh in stationery (ESS), several 2W & 3W (e-mobility)- differentdesigns.

D. As **Head- North** for Artheon Electronics/ Artheon Battery Co, from Nov 2014 to Dec 2019.

- Instrumented in creating some of the finest technical & financial credentials to make the product and companyeligible for various pre- qualifications for Government and OEM sector business.
- Instrumented in diversifying into other related products through partnership with our OEM for betterbusiness reach, bonding and achieving a higher turnover and margin.

   5. Activities

- Towards Management – day to day on all relevant information regarding company's business operations, develop and present alternatives and recommend courses of action.
- Strategic and Operational Planning – formulate and recommend annual/ monthly business Plan & identifiesissues to address to realize the future vision and sets short, medium and long -term objectives and strategies.
- Corporate Organization – authority and delegated responsibilities to team.
- Financial Management – develop an annual/ monthly budget.
- Leadership of Human Resources – lead staff in their achievement of business objectives with integrity, fairnessand transparency.
- Resource Acquisition, Allocation and Utilization – control, monitoring and performance.
- Operations –identify opportunities and propose new methods of improving existing operations.
- Decisions –to meet the challenges presented by new trends and developments in the market.

- Communications – effective communication strategies, objectives and performances.

6. Early Career

- **TROPICANA ENTERPRISES PVT LTD** as Head -North & East (Launched Tropicana Batteries in Indian market) from Oct 2010 to Nov 2014.
- **ARTHEON BATTERY COMPANY PVT LIMITED** as Regional Manager-North (Part of initial product launching team) from Apr 2008 to Oct 2010, in-charge of sales & business development & certifications (JIS C 8702, ICE 60896 etc).
- **EXIDE INDUSTRIES LIMITED** as Associate Manager -Industrial (In-charge of Industrial batteries (2V- VRLA, Plante & Flooded Tubular) from Jan 2003 to Apr 2008 in Power sector at Delhi RO & earlier for 2V & 12V batteries at BO, Lucknow.
- **RAAJ UNOCAL LUBRICANTS LIMITED** as Area Manager from Jul 1995 to Jun 2001.

7. Education

- Presuing PhD (Engineering) from UPES, Dehradun.
- 1st Class Graduate Engineer (Mech.) from National Institute of Technology, Jamshedpur in 1993.
- Affiliations & Memberships: Chartered Engineer (I), MIE, AMIE.
- Trained auditor for ISO/ IEC 17025:2017, ISO 9001:2015, and ISO 14001:2015.

Thesis_Final

PRIMARY SOURCES

1 Sandeep Rawat, Sushabhan Choudhury, Devender Kumar Saini, Yogesh Chandra Gupta. "Advancements and Current Developments in Integrated System Architectures of Lithium-Ion Batteries for Electric Mobility", World Electric Vehicle Journal, 2024
Publication

1%

2 Kaushik Das, Roushan Kumar, Anurup Krishna. "Analyzing electric vehicle battery health performance using supervised machine learning", Renewable and Sustainable Energy Reviews, 2024
Publication

1%

3 www.mdpi.com
Internet Source

1%

4 pluginhighway.ca
Internet Source

1%

5 academic.oup.com
Internet Source

<1%